Lattice Walks in Cones: Combinatorial and Probabilistic Aspects

by

Amélie Trotignon

M.Sc., Université de Tours, France, 2016
B.Sc., Université de Tours, France, 2014

Thesis Submitted in Partial Fulfillment of the
Requirements for the Joint Degree (cotutelle)

Doctor of Philosophy in the Department of Mathematics
Faculty of Science at Simon Fraser University (Canada)
-and-
Docteure en Mathématiques
Faculté des Sciences de l'Université de Tours (France)

SIMON FRASER UNIVERSITY
UNIVERSITÉ DE TOURS
Fall 2019

Approval

Name: **Amélie Trotignon**

Degree: **Doctor of Philosophy (Mathematics)**

Title: **Lattice Walks in Cones:**
Combinatorial and Probabilistic Aspects

Examining Committee:

Chair: Cédric Lecouvey
Professor, Université de Tours

Marni Mishna
Senior Supervisor
Professor, Simon Fraser University

Kilian Raschel
Co-Supervisor
CNRS researcher, Université de Tours

Nils Bruin
Supervisor
Professor, Simon Fraser University

Frédéric Chyzak
External Examiner
INRIA researcher, Saclay

Wolfgang Woess
External Examiner
Professor, Graz University of Technology

Mireille Bousquet-Mélou
External Examiner
CNRS Senior researcher, Université de Bordeaux

Irina Kurkova
External Examiner
Professor, Sorbonne Université, Paris

Cédric Lecouvey
External Examiner
Professor, Université de Tours

Date Defended: **December 6, 2019**

Abstract

Lattice walks in cones have many applications in combinatorics and probability theory. While walks restricted to the first quadrant have been well studied, the case of non-convex cones and three-dimensional walks has been systematically approached recently. In this thesis, we extend the analytic method of the study of walks and its discrete harmonic functions in the quarter plane to the three-quarter plane applying the strategy of splitting the domain into two symmetric convex cones. This method is composed of three main steps: write a system of functional equations satisfied by the generating function, which may be simplified into one single equation under symmetry conditions; transform the functional equation into a boundary value problem; and solve this problem using conformal mappings. We obtain explicit expressions for the generating functions of walks and its associated harmonic functions. The advantage of this method is the uniform treatment of models corresponding to different step sets. In a second part of this thesis, we explore the asymptotic enumeration of three-dimensional excursions confined to the positive octant. The critical exponent is related to the smallest eigenvalue of a Dirichlet problem in a spherical triangle. Combinatorial properties of the step set are related to geometric and analytic properties of the associate spherical triangle.

Keywords: Enumerative combinatorics; Lattice walks in cones; Discrete harmonic functions; Generating functions; Boundary value problem; Conformal mapping.

Résumé

Les marches sur des réseaux dans des cônes ont de nombreuses applications en combinatoire et en probabilités. Tandis que les marches restreintes au quart de plan ont été très étudiées, le cas des cônes non convexes et des marches en trois dimensions n'a été systématiquement approché que récemment. Dans cette thèse, nous étendons la méthode analytique à l'étude des marches et ses fonctions harmoniques discrètes dans le quart de plan au trois quarts de plan en appliquant la stratégie de couper le domaine en deux cônes symétriques convexes. Cette méthode est composée de trois parties : écrire un système d'équations fonctionnelles satisfait par la fonction génératrice, qui peut être réduit à une seule équation sous des conditions de symétrie ; transformer cette équation fonctionnelle en problème frontière ; et finalement résoudre ce problème à l'aide de transformations conformes. Nous obtenons des expressions explicites pour la fonction génératrice des marches et ses fonctions harmoniques associées. L'avantage de cette méthode est un traitement uniforme des modèles correspondant à des ensembles de pas différents. Dans la deuxième partie de la thèse, nous explorons l'asymptotique de l'énumération des excursions tridimensionnelles dans l'octant positif. L'exposant critique est relié à la plus petite valeur propre d'un problème de Dirichlet dans un triangle sphérique. Les propriétés combinatoires de l'ensemble de pas peuvent être reliées aux propriétés géométriques et analytiques du triangle sphérique associé.

Mots clés : Combinatoire énumérative ; Marches sur des réseaux dans des cônes ; Fonctions harmoniques discrètes ; Fonctions génératrices ; Problème frontière ; Transformation conforme.

Acknowledgements – Remerciements

Just like my *cotutelle* between France and Canada, I have chosen here to write bilingual acknowledgements so that each person mentioned can understand my gratitude to her or him. The PhD, as well as the studies before, is a long and (sometimes) difficult journey, thus I would like to thank all of those who contributed to this achievement. I sincerely hope that I have not forgotten anyone, and if that is the case, I deeply apologize.

À l'image de ma cotutelle entre la France et le Canada, j'ai choisi ici de rédiger des remerciements bilingues, afin que chaque personne mentionnée puisse comprendre la phrase qui lui est adressée. Le doctorat, tout comme le parcours pour y accéder, est un chemin long et (parfois) difficile ainsi je souhaite ici remercier l'ensemble des personnes ayant contribué à cet accomplissement. J'espère sincèrement n'avoir oublié personne, et si tel est le cas, je m'en excuse profondément.

Je souhaite remercier en premier lieu ma directrice Marni Mishna et mon directeur Kilian Raschel d'avoir rendu mon projet de thèse possible. Ces trois riches années ont confirmé mon opinion déjà positive et enthousiaste sur les bienfaits et avantages d'une cotutelle internationale. Je vous suis extrêment reconnaissante pour votre soutien tout au long de la thèse et pour le temps pris pour relire ce manuscrit. Enfin, merci pour votre gentillesse et votre profonde humanité.

Merci beaucoup Marni pour tes conseils et ta bonne humeur. Merci pour ton engagement, ta bienveillance et toutes les opportunités que tu m'as données. Cette expérience au Canada m'aura été très profitable, autant mathématiquement que personnellement.

Un grand merci Kilian pour m'avoir encouragée et soutenue dans mes projets, mes doutes, mes réussites et ce, depuis six ans déjà. Merci pour ton temps, ton engagement et ta patience. Je ressortais toujours extrêmement motivée et enthousiaste de nos entretiens.

Je remercie vivement mes rapporteurs Frédéric Chyzak et Wolfgang Woess pour le temps consacré à la relecture attentive de cette thèse et à leur transmission de commentaires constructifs et pertinents. Je remercie chaleureusement Mireille Bousquet-Mélou, Nils Bruin, Irina Kurkova et Cédric Lecouvey d'avoir accepté de faire partie de mon jury de thèse.

Merci à l'Institut Denis Poisson et sa direction, l'école doctorale MIPTIS et le département de mathématiques de SFU de m'avoir accueillie pendant ces trois années de thèse. Je remercie

également la région Centre-Val de Loire ainsi que l'ensemble des institutions et organismes ayant financé mon contrat doctoral et mes divers déplacements professionels.

Je n'ai pas choisi d'aller à Tours, mais j'ai choisi d'y rester. Je pense que seule cette phrase pourrait suffire à résumer mes sentiments sur ces dernières années tourangelles. Je remercie vivement les membres de l'équipe SPACE Tours, en particulier Olivier Durieu, Jean-Baptiste Gouéré, Jérémie Guilhot, Cédric Lecouvey, Florent Malrieu et Marc Peigné pour leur accueil chaleureux. Je remercie aussi l'ensemble de l'équipe pédagogique des départements de mathématiques de Tours et d'Orléans qui m'a confortée dans mon choix de continuer à étudier les mathématiques. En particulier, je souhaite en premier lieu remercier Natacha Sandier pour sa patience et sa gentillesse à répondre à mes (*nombreuses*) questions et de m'avoir très tôt encouragée au doctorat. J'ajoute aussi un merci à Jean Fabbri et Christine Georgelin pour leur bienveillance et leur aide pour mes questions administratives en rapport avec l'agrégation.

I have always wanted to go to Canada, wish granted with this joint PhD. In the view of the size of the country (or even the one of British Columbia), I can only say that I know pretty well Vancouver and surrounding areas. From its montain, SFU campus is the perfect place to focus on research and escape from the hustle and bustle of city life and its overwhelming buildings. I will miss Stanley Park as well as the academic quadrangle's pond and its seagull, faithful companion on its rock, some of my favorite spots to take a break. I would like to thank the members of the mathematic department at SFU, in particular Cédric Chauve, Nathan Ilten, Jonathan Jedwab, and also David Muraki for our interesting and helpful discussions in the Spring of 2018.

I am very grateful to Brenda Davison and Jamie Mulholland for their time, advices, and educational conversations. Merci aussi à Emmanuel Chasseigne avec qui j'ai pu avoir des échanges très intéressants sur l'enseignement à l'université et la pédagogie.

Je souhaite également remercier Élodie Demoussis, Anouchka Lepine, Laeticia Portier et Sandrine Renard-Riccetti pour leur aide, parfois à distance, et leur bonne humeur. I would also like to thank Casey Bell, Christie Carlson, JoAnne Hennessey and Sofia Leposavic for their help and precious advice.

Les conférences et séminaires sont des moments privilégiés de rencontres, d'échanges, et je tiens à remercier l'ensemble des chercheurs et chercheuses qui ont manifestés de l'intérêt à mes travaux. En particulier, merci à Alin Bostan et Thomas Dreyfus pour les discussions instructives et les conseils bienveillants.

Finally, because a PhD is not an end in itself but the beginning of a wonderful journey, I would like to thank Manuel Kauers for hiring me for a post doc at the Institut for Algebra of Johannes Kepler University.

J'ai une pensée pour mes collègues et amis doctorants/docteurs de l'Institut Denis Poisson ou d'ailleurs. En particulier, merci à mes camarades de bureau Abraham, Florestan, Frédéric, Ha, et

Jean-David pour cette ambiance studieuse et conviviale. Merci également à Adrien, Ayman, Cam, Guillaume, Gwladys, Salam, Sandro, Shouman, Thomas N., Thomas R., Vivien et Xavier. A big thanks to my SFU mates Allie, Sam and Stefan. I really spend good times with you (specially at CanaDAM 2019). Thanks to Sasha for our working afternoons on algebra assignments during the Fall 2017. Enfin, merci à Thomas W. pour nos pauses déjeuner à la française (dont le traditionnel restaurant coréen du vendredi), nos longues discussions et notre soutien mutuel à l'autre bout du monde (sans oublier ta brillante victoire dans la bataille du moustique ;-)).

Un grand merci à Inès pour sa présence depuis la L3 (notre meilleure année je crois !). C'est avec le temps et la distance qu'on découvre les vrais amis, et tu en fais définitivement partie. Marion et Lucie, merci pour ces grandes discussions, ces pauses déjeuner et ces moments de partage. Nous avons pu nous soutenir ensemble dans cette grande aventure qu'est la fin de thèse. J'ai eu beaucoup de chance de vous rencontrer et je suis certaine que cette récente et immédiate amitié va perdurer. Enfin, j'ai une pensée amicale pour Dianne, Geneviève A., Geneviève L., Jean-Christophe, Marie-Claude, Philippe, Sophie et Sylvie, membres d'un merveilleux groupe de conversation anglaise du mercredi soir dont j'ai eu le plaisir de faire partie.

L'écriture de ces remerciements est aussi l'occasion de faire le bilan du chemin parcouru. J'ai eu la chance d'avoir pu bénéficier tout au long de ma scolarité d'un environnement privilégié et propice à l'apprentissage. Certains professeurs et leurs leçons m'ont particulièrement marqués ; je citerai ici Madame Chappat pour m'avoir appris à écrire, Madame Jayez pour qui le respect et la rigueur sont des valeurs fondamentales, Madame Guyot pour m'avoir donné le goût des mathématiques et Madame Pillet pour m'avoir réconciliée avec la langue anglaise.

Merci également à mon oncle Laurent et à mon cousin Nicolas pour leurs encouragements et toute l'attention qu'ils portent à mes études et mes projets.

Je remercie ma famille, et particulièrement mes parents, qui ont toujours fait de l'éducation une priorité. Merci pour leur soutien, leur compréhension et leur présence. Je suis certaine que mon frère et ma sœur se joignent à ma reconnaissance pour tous les sacrifices que vous avez fait pour nous et de la chance que vous nous avez donnée. Merci Clémence et Henri pour votre patience et votre écoute qui m'ont permis de devenir la (*redoutable*) grande sœur que je suis aujourd'hui. Enfin, j'ai une dernière pensée pour Hepsy, dont je n'aurais jamais pensé qu'il prendrait autant de place dans mon cœur.

Contents

List of Tables

List of Figures

Chapter 1

Introduction

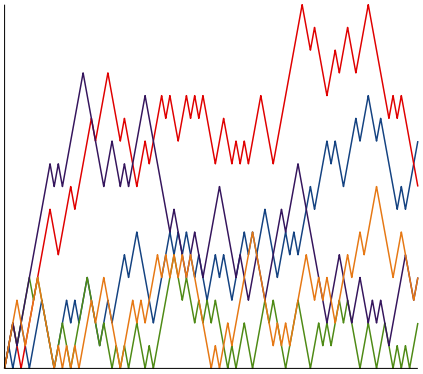

Five trajectories of Dyck 100 step walk

In this thesis we are interested in combinatorial and probabilistic aspects of walks restricted to cones. From a combinatorial point of view we present results on the enumeration of walks in three-quarter plane and positive walks in dimension three. From a probabilistic viewpoint, we are interested in discrete harmonic functions associated to random walks in the three-quarter plane. As we shall see, random walks and harmonic functions are complementary topics and enrich one another. We present in this introduction main questions and topics in the study of lattice walks and discrete harmonic functions. This chapter also includes a list of our original contributions and a presentation of the main structure of the thesis.

1.1 Lattice walks

Consider the D-dimensional integer lattice $\mathbb{Z}^D$ and a finite set $\mathcal{S} \subset \mathbb{Z}^D$. A walk is a sequence of incremental jumps from a given step set $\mathcal{S}$. A walk of length n can be encoded by $W = W_1 W_2 \dots W_n$ with $W_i \in \mathcal{S}$. The walk is with *small steps* when $\mathcal{S} \subset \{-1, 0, 1\}^D$, and is said to be with *large* or *big steps* otherwise. In dimension 1, the only non-trivial small step walks have jumps in $\mathcal{S} = \{-1, +1\}$

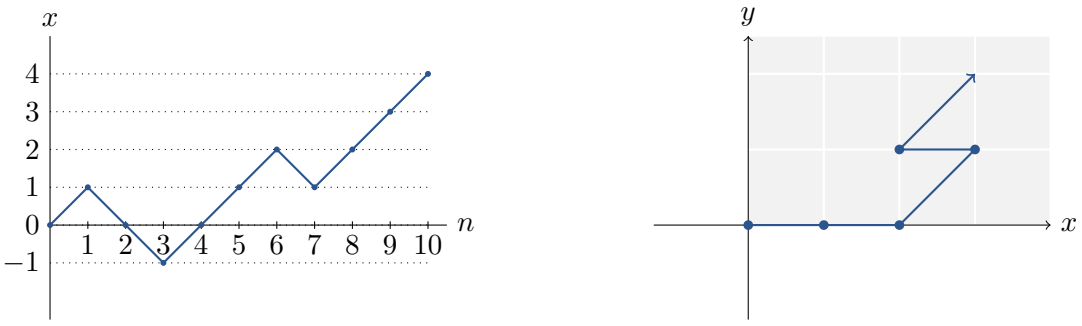

(a) Walk in $\mathbb{Z}$;
$W = (1, -1, -1, 1, 1, 1, -1, 1, 1, 1)$

(b) Walk in $\mathbb{N}^2$;
$W = \big((1,0), (1,0), (1,1), (-1,0), (1,1)\big)$

Figure 1.1 – Walks in various cones

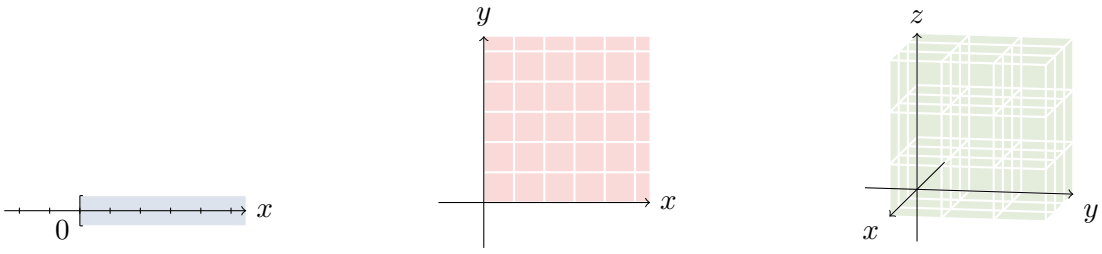

(a) $\mathbb{N}$ (b) $\mathbb{N}^2$ (c) $\mathbb{N}^3$

Figure 1.2 – Some cones of restriction

(see Figure 1.1a). When they are positive, these walks are called Dyck paths and are widely studied in combinatorics. In two dimensions, we can depict the step set with an arrow diagram: for example the North direction $(0, 1)$ is denoted by $\uparrow$, whereas the South-West step $(-1, -1)$ is represented as $\swarrow$. Some of two dimensional step sets have names, which we will use within this thesis. We summarize all of this terminology in Table 2.1. A walk model is a set of allowable steps $\mathcal{S}$ together with a region to which the walk is confined (usually a cone). For example, in dimension one, a walk can be restricted to the positive axis, in dimension two to the quarter plane, in dimension three to the positive octant (see Figure 1.2).

Enumeration of lattice walks in cones is a central problem in combinatorics and probability theory. One of the first uses of lattice paths was the study of the ballot problem [19, 4] where an election is held between two candidates A and B. We suppose that the candidate A wins the election with a votes and that the candidate B receives $b < a$ votes. An interesting problem is the probability that the candidate A will be strictly ahead of B throughout the counting. This question can be translated into lattice path enumeration: we are interested in the number of Dyck paths which never touch the x-axis, where the step $(1, 1)$ models a vote for the candidate A and $(1, -1)$ a vote in favor of the candidate B. Many other discrete Markov chains can be modeled by random walks, as for instance the famous gambler ruin problem (see Section 1.2). Random walks can also

model biology populations [24, 47] such as the Galton-Watson process (which was introduced to investigate the extinction of family names) and birth-and-death processes (which can be related to Dyck paths where the step $+1$ stands for the birth and -1 for the death), queues [50, 81, 80, 102] (see Section 3.4.1) or Markov order-book in finance [51]. Random walks can be linked to representation theory [20, 22, 21, 23, 59] and potential theory [98, 91, 35]. Numerous combinatorial objects can be encoded by walks: maps [16], graphs [126], Young tableaux [86], partitions [97], permutations [2, 70]. This variety of examples and applications justifies the profuse interest given to walks in cones.

Many studies have been done on small step lattice paths restricted to a quadrant with various methods and techniques: combinatorics [109, 41, 106, 107], complex analysis [72, 99, 113, 74, 100, 101], probability theory [58], computer algebra [31, 29], Galois theory of difference equations [62, 61, 63, 60]. Each of these approaches reinforces the other in many ways. Three main topics are developed:

1. *Exact expressions for the generating function of the number of walks.* The generating function can be expressed as infinite series [109], positive part extractions of diagonals [41], contour integrals on quartics [74, 113], integrals of hypergeometric functions [29];

2. *Asymptotic behavior of the number of excursions.* Let $q_{i,j}^{\mathcal{S}}(n)$ be the number of n-steps excursions joining $(0,0)$ to (i,j) with step set $\mathcal{S}$ within the quadrant. When n goes to infinity, the behavior of $q_{i,j}^{\mathcal{S}}(n)$ is known [41, 74, 58, 34]. Although the full picture is still incomplete, the asymptotics of the total number of walks is also obtained in several cases [41, 74, 58, 66, 29];

3. *Nature of the trivariate generating function.* A complete classification has been done for some convex cones. In the quarter plane, the generating function is D-finite (that is, satisfies a linear differential equation with polynomial coefficients) if and only if a certain group of birational transformations is finite [41, 31, 100].

In the whole plane, the half-plane [10] and the quarter plane (intersection of two half planes), walks are well understood and their structure have been deeply explored. Recently, some variations of such walks have been developed: walks with larger steps [28] or inhomogeneous walks [12, 127, 45]. Another natural generalization is to consider other domains of restriction and determine how the framework of walks is different from the quarter plane in this new region.

1.2 Harmonic functions

At first sight, the topic of discrete harmonic functions could seem disjoint from the enumeration of walks in Section 1.1, but as we shall see, they are strongly related.

A continuous harmonic function is a function for which the standard Laplacien Δf is zero. For example, in dimension two, if f is a harmonic function on an open set $\mathcal{U} \subset \mathbb{R}^2$, then f is twice

$\mathbb{R}$-differentiable and

$$\Delta f = \frac{\partial^2 f}{\partial x^2} + \frac{\partial^2 f}{\partial y^2} = 0.$$

Continuous harmonic functions are important functions in analysis, in particular in the resolution of partial differential equations. These functions are strongly related to holomorphic functions and are in particular infinitely differentiable in open sets. They satisfy interesting properties such as, for example, the maximum principle, the mean value property and in the case of non-negative harmonic functions, Harnack's inequalities.

What about discrete harmonic functions? The simplest discrete Laplacian in dimension two is defined by

$$\Delta f(x,y) = f(x-1,y) + f(x+1,y) + f(x,y-1) + f(x,y+1) - 4f(x,y). \tag{1.1}$$

Discrete harmonic functions have, in particular, first been studied in the mid 20th century by Ferrand [76] and Duffin [65]. After some decades, because of their applications in discrete complex analysis, probability of absorption at absorbing states of Markov chains or the Ising model, mathematicians like Smirnov [119] have been interested in discrete harmonic functions. Let us add that discrete harmonic functions satisfy multivariate linear recurrence relations [42], which are ubiquitous in combinatorics.

Let $(X_n)_{n\geq 0}$ be a Markov chain. If P is the probability matrix which describes the transitions of $(X_n)_{n\geq 0}$, then an associated harmonic function is defined by

$$Pf = f.$$

To give an elementary example, let $(X_n)_{n\geq 0}$ be a positive random walk with small steps. We denote by $p \in (0,1)$ the probability to perform a right move and $q = 1-p$ a left move (see Figure 1.3). By definition, the associated discrete harmonic function f which vanishes at 0 satisfies $Pf = f$, where

$$P = \begin{pmatrix} \ddots & \ddots & \ddots & & \\ \ddots & 0 & p & 0 & \\ \ddots & q & 0 & p & \ddots \\ & 0 & q & 0 & \ddots \\ & & \ddots & \ddots & \ddots \end{pmatrix}.$$

Thus

$$\begin{cases} f(i) &= pf(i+1) + qf(i-1), \quad \forall i \geq 1 \\ f(0) &= 0. \end{cases}$$

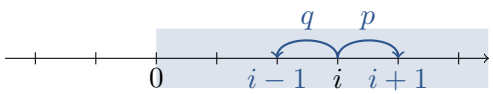

Figure 1.3 – Step probability for a random walk in $\mathbb{N}$

The characteristic polynomial of this induction is $px^2 - x + q = 0$, with roots 1 and q/p. There are two different cases:

(i) $\frac{q}{p} \neq 1$. The roots are distinct and

$$\begin{cases} f(i) &= a + b\left(\frac{q}{p}\right)^i, \quad \forall i \geq 1, \\ f(0) &= a + b = 0 \end{cases} \qquad a, b \in \mathbb{R}.$$

Then for all $i \geq 0$, $f(i) = a\left(1 - \left(\frac{q}{p}\right)^i\right)$, $a \in \mathbb{R}$.

(ii) $\frac{q}{p} = 1$. Then 1 is a root of degree two and

$$\begin{cases} f(i) &= a + bi, \quad i \geq 1, \\ f(0) &= a = 0 \end{cases} \qquad a, b \in \mathbb{R}.$$

Then for all $i \geq 0$, $f(i) = bi$, $b \in \mathbb{R}$.

Harmonic functions are computed up to a multiplicative constant.

Consider the simple random walk restricted to $\mathbb{N}^2$. The probabilities to make a right, up, left, down move are all equal to 1/4. Associated discrete harmonics function are defined by

$$\forall (i, j) \in \mathbb{N}^2, \quad f(i, j) = cij,\ c \in \mathbb{R},$$

and we can easily check that such functions satisfy the discrete Laplacian defined in (1.1). Heuristically, we can consider that the simple random walk in $\mathbb{N}^2$ is the cartesian product of two simple random walks in $\mathbb{N}$ [112] whose structure emerges as well in the product form of the harmonic function expression.

Discrete harmonic functions appear in the computation of probability of absorption at absorbing states of Markov chains as well. Consider a gambler with initial fortune of i gold coins[1]. At every step, the gambler bets 1 gold coin and wins with probability p and loses with probability $q = 1 - p$. Let S_n be the fortune of the gambler at time n. We have

$$\begin{cases} S_n &= i + \sum_{k=1}^n X_k, & \text{if } S_{n-1} > 0 \\ S_n &= 0 & \text{otherwise,} \end{cases}$$

[1] one can pick her or his favorite currency!

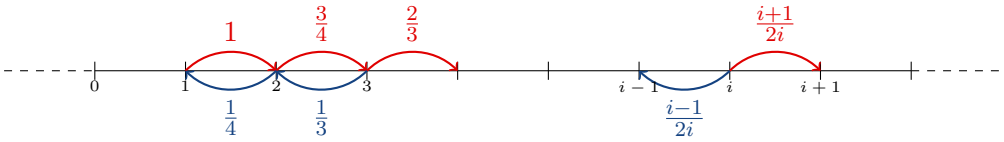

Figure 1.4 – Random walk $(T_n)_{n\in\mathbb{N}}$. This is a Doob transform of a simple random walk over $\mathbb{N}$

where X_k are the random variables defined by

$$X_k = \begin{cases} 1 & \text{with probability } p; \\ -1 & \text{with probability } q. \end{cases}$$

In other words, $(S_n)_{n\in\mathbb{N}}$ is a random walk starting at $i > 0$ absorbed at 0. Let

$$h_i = \mathbb{P}_i[\exists n \geq 0 : S_n = 0]$$

be the probability for the gambler to be ruined in a finite time, or with a random walk point of view, the probability for the walk to be absorbed at 0 starting from i. Because $(S_n)_{n\geq 0}$ is a Markov chain, for $i \geq 1$ we have

$$\begin{aligned} h_i =& \mathbb{P}_i[\exists n \geq 0 : S_n = 0] \\ =& \mathbb{P}_i[\exists n \geq 0 : S_n = 0 | X_1 = 1]\mathbb{P}[X_1 = 1] \\ &+ \mathbb{P}_i[\exists n \geq 0 : S_n = 0 | X_1 = -1]\mathbb{P}[X_1 = -1] \\ =& p\mathbb{P}_{i+1}[\exists n \geq 0 : S_n = 0] + q\mathbb{P}_{i-1}[\exists n \geq 0 : S_n = 0] \\ =& ph_{i+1} + qh_{i-1}, \end{aligned}$$

and

$$h_0 = \mathbb{P}_0[\exists n \geq 0 : S_n = 0] = 1.$$

Notice that the transition matrix of $(S_n)_{n\geq 0}$ is defined by

$$P = (P(i,j))_{i,j\in\mathbb{N}} = \begin{pmatrix} 1 & 0 & 0 & \cdots & \cdots & \cdots \\ q & 0 & p & 0 & \cdots & \cdots \\ 0 & q & 0 & p & 0 & \cdots \\ \vdots & \ddots & \ddots & \ddots & \ddots & \ddots \end{pmatrix},$$

and $h = (h_i)_{i\geq 0}$ satisfies $Ph = h$. Then h is a harmonic function associated to $(S_n)_{n\geq 0}$.

Harmonic functions are also a main object in Doob transformations, which are a standard procedure in probability. From a Markov process and an associated harmonic function we can define a new random process. For example, let $(S_n)_{n\in\mathbb{N}}$ be a simple random walk over $\mathbb{Z}$. The function V defined by $V(i) = i$ ($i \in \mathbb{N}$) is a discrete harmonic function for $(S_n)_{n\geq 0}$, for the same reason as for (ii) above. We define $(T_n)_{n\in\mathbb{N}}$ from $(S_n)_{n\in\mathbb{N}}$ by

$$\begin{cases} \mathbb{P}\left[T_{n+1} = i+1 \mid T_n = i\right] &= \frac{V(i+1)}{2V(i)} &= \frac{i+1}{2i}, \\ \mathbb{P}\left[T_{n+1} = i-1 \mid T_n = i\right] &= \frac{V(i-1)}{2V(i)} &= \frac{i-1}{2i}. \end{cases}$$

The process $(T_n)_{n\in\mathbb{N}}$ is a random walk over $\mathbb{N}^*$. From a simple non-constrained random walk (S_n), we get a constrained random walk (T_n). However, this new random walk is not spatially homogeneous (the transition probabilities depend on the space position of the random walk), see Figure 1.4.

In general, finding (positive) harmonic functions is a difficult problem, as hard as solving a multivariate recurrence. Explicit expressions for positive harmonic functions of random walks in the quarter plane are given in [114]. In Chapter 4, we obtain an algebraic explicit expression for harmonic functions associated to random walks avoiding a quadrant.

1.3 Structure of the thesis

The structure of this thesis is schematically summarized in Figure 1.5.

Chapter 2 can be seen as an introductory guide for the other chapters. We present tools and techniques used in the study of enumeration of walks together with results for walks restricted in a quadrant. One of the main objects, called the kernel of the walks, is a bivariate polynomial of degree two which encodes the step set of the walks and appears in various functional equations. The kernel is central in the analytical method for the resolution of walks via boundary value problems. We finally recall the notion of group of the walks and review the nature of generating functions of lattice paths.

Chapter 3 presents original results on walks avoiding a quadrant with an analytic approach. The advantage of this method is the uniform treatment of models corresponding to different step sets. After splitting the three quadrants into two symmetric convex cones, the method is composed of three main steps: write a system of functional equations satisfied by the counting generating function, which may be simplified into one single equation under symmetry conditions; transform the functional equation into a boundary value problem; and finally solve this problem, using a new concept of anti-Tutte's invariant. The result is a contour-integral expression for the generating function. Such systems of functional equations also appear in queueing theory, namely, in the Join-the-Shortest-Queue model (still open in the non-symmetric case), or in the study of walks with large steps [75, 28].

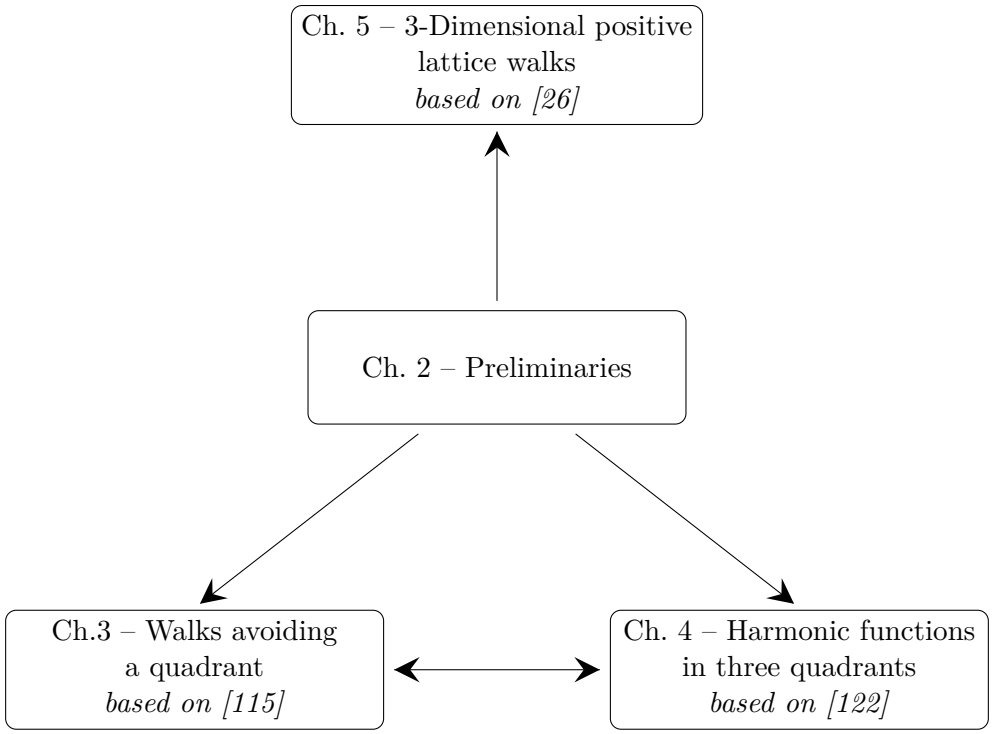

Figure 1.5 – Chapter 2 introduces essential materials for the other chapters of this document. Chapter 3 and Chapter 4 present related ideas and techniques on walks in the three-quarter plane and can somehow be linked. Chapter 5 on walks in dimension three is independent of Chapters 3 and 4

Chapter 4 presents original results on positive discrete harmonic functions with Dirichlet conditions in three quadrants. We extend the method in the quarter plane – resolution of a functional equation via boundary value problem using conformal gluing function – to the three quarter plane applying the strategy of splitting the domain into two symmetric convex cones. We obtain an explicit simple expression for the harmonic functions of random walks avoiding a quadrant.

Chapter 5 presents original results on the critical exponent of the asymptotic enumeration of three-dimensional excursions confined to the positive octant. In $\mathbb{N}^3$, the number of models to consider is huge: more than 11 million. The same natural topics for walks in quarter the plane extend to walks in $\mathbb{N}^3$: exact expression for the generating function of walks, nature of this generating function and asymptotic behavior. We first review the group classification, the Hadamard factorization and recall some asymptotic results. The critical exponent can be expressed as a function of the smallest eigenvalue of a Dirichlet problem in a spherical triangle. Combinatorial properties of the step set are related to geometric and analytic properties of the associated spherical triangle.

1.4 Contributions

Chapters 3, 4 and 5 are based on original contributions. We itemize them in order of appearance in this thesis.

- **On walks avoiding a quadrant**, with K. Raschel.
  The Electronic Journal of Combinatorics, 26(P3.31):1–34, 2019;
  arXiv:1807.08610:1-32
  In this article we develop an analytic approach for the enumeration of walks avoiding a quadrant and obtain contour-integral expression for the generating function of walks.

- **Discrete harmonic functions in the three-quarter plane**.
  arXiv:1906.08082:1-26, 2019.
  In this article we obtain an explicit algebraic expression for the generating function of harmonic functions associated to random walks avoiding a quadrant.

- **3D positive lattice walks and spherical triangles**, with B. Bogosel, V. Perrollaz and K. Raschel.
  arXiv:1804.06245:1-41, 2018.
  The critical exponent can be related to the smallest eigenvalue of a Dirichlet problem in a spherical triangle. In this article, we link combinatorial properties of the step set to geometric and analytic properties of the associated spherical triangle.

Chapter 2

Preliminaries

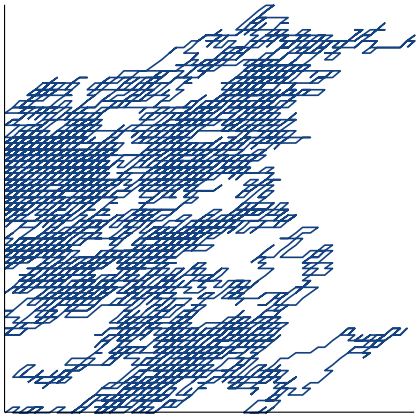

A Gessel 10,000 step walk in the quarter plane

As we have seen in Chapter 1, the study of lattice walks can be divided into three principal questions 1, 2 and 3. We present in this chapter tools and techniques which answer them. Unless explicitly mentioned, all walks will have small steps, i.e., jumps in $\{-1,0,1\}^2 \setminus (0,0)$. *A priori*, there are $2^8 = 256$ step sets (see Table 2.1 for some examples). In the whole plane or the half-plane [10], walks are well understood. In the quarter plane

$$\mathcal{Q} = \Big\{(i,j) \in \mathbb{Z}^2 : i \geq 0 \text{ and } j \geq 0\Big\} = \mathbb{N}^2, \tag{2.1}$$

see Figure 1.2b, Bousquet-Mélou and Mishna [41] have reduced this number to 79, removing the empty walk and models equivalent to walks in the half-plane, then identifying isomorphic models as symmetric models for example.

Consider walks with step set $\mathcal{S}$. We denote by $q_{i,j}(n)$ the number of paths within $\mathcal{Q}$ of length n, starting at $(0,0)$ and ending at (i,j). The generating function of walks restricted to a quadrant

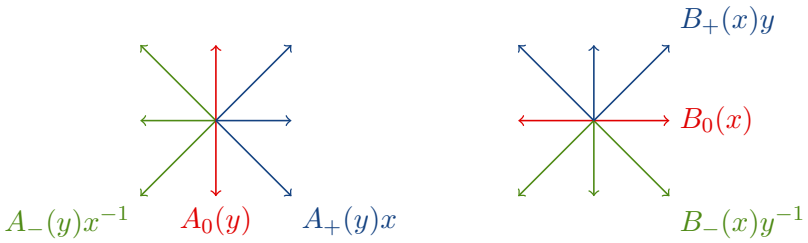

Figure 2.1 – Decomposition of the inventory polynomial (2.4)

$Q(x,y)$ is defined by

$$Q(x,y) = \sum_{n\geq 0} \sum_{(i,j)\in\mathbb{N}^2} q_{i,j}(n) x^i y^j t^n, \tag{2.2}$$

with $0 < t < 1/|\mathcal{S}|$ to ensure series convergence when the formal power series are interpreted as functions.

2.1 Exact expressions for the generating functions of the walk

2.1.1 Functional equations

In most of the methods, the starting point is to reduce the (enumerating or probabilistic) problem to the resolution of a functional equation. Classically, a functional equation is derived from the construction of a walk by adding a new step at the end of the walk at each stage.

We introduce the inventory Laurent polynomial for the step set $\mathcal{S}$ defined by

$$S(x,y) = \sum_{(i,j)\in\mathcal{S}} x^i y^j. \tag{2.3}$$

Examples of two-dimensional inventory polynomials are given in Table 2.1. Let us write[1]

$$S(x,y) = A_-(y)x^{-1} + A_0(y) + A_+(y)x = B_-(x)y^{-1} + B_0(x) + B_+(x)y. \tag{2.4}$$

The term $A_-(y)x^{-1}$ (resp. $B_-(x)y^{-1}$) represents the steps in the negative x-direction (resp. y-direction), $A_0(y)$ (resp. $B_0(x)$) is for steps without x-direction (resp. y-direction) and $A_+(y)x$ (resp. $B_+(x)y$) stands for steps with positive x-direction (resp. y-direction), see Figure 2.1.

Plane case. Let $P(x,y)$ be the generating function of walks in the plane $\mathbb{Z}^2$. Walks in $\mathbb{Z}^2$ can be empty, with generating function 1, or can be composed of a walk in $\mathbb{Z}^2$ added with a new step from

[1]Note that the notations are slightly different from those in [41]. For more consistence between the walks in two dimensions in Chapters 2 and 3 and walks in three dimensions in Chapter 5, we rather use in the whole thesis the notations of [27].

#	Name of the model	Arrow diagram	Inventory $S(x,y)$
1.1	Simple		$x+y+x^{-1}+y^{-1}$
1.2	Diagonal		$xy+x^{-1}y+x^{-1}y^{-1}+xy^{-1}$
1.4	King		$x+xy+y+x^{-1}y+x^{-1}+x^{-1}y^{-1}+y^{-1}+xy^{-1}$
2.1	Tandem		$x+x^{-1}y+y^{-1}$
2.3	Kreweras		$xy+x^{-1}+y^{-1}$
2.4	Reverse Kreweras		$x+y+x^{-1}y^{-1}$
2.5	Double Kreweras		$x+xy+y+x^{-1}+x^{-1}y^{-1}+y^{-1}$
3.1	Gessel		$x+xy+x^{-1}+x^{-1}y^{-1}$
3.2	Gouyou-Beauchamps		$x+x^{-1}y^{-1}+x^{-1}+xy^{-1}$

Table 2.1 – Terminology of some two-dimensional walks. We follow the numbering from [41].

the step set, that is $tS(x,y)P(x,y)$. The functional equation of walks in the plane is then

$$P(x,y) = 1 + tS(x,y)P(x,y). \tag{2.5}$$

The plane case, and more generally the unconstrained case in $\mathbb{Z}^D$, is definitely the simplest case: an expression of $P(x,y)$ can directly be derived from the functional equation (2.5). For example, for the simple step set (see model 1.1 in Table 2.1), $P(x,y) = \frac{1}{1-t(x+x^{-1}+y+y^{-1})}$.

Half-plane case. Consider now walks restricted in the half-plane $\mathbb{Z}\times\mathbb{N}$ with generating function $G(x,y)$. A walk ending in the upper half-plane can be empty, with generating function 1, can be composed of a half-plane walk added with a new step giving $tS(x,y)G(x,y)$ and walks going out of the cone $tB_-(x)y^{-1}G(x,0)$ need to be removed. The functional equation of walks restricted to the upper half-plane can be written as

$$G(x,y) = 1 + tS(x,y)G(x,y) - tB_-(x)y^{-1}G(x,0). \tag{2.6}$$

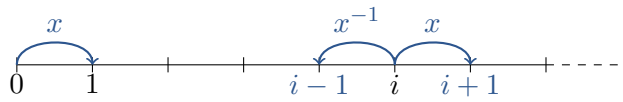

Figure 2.2 – Positive walk in dimension one

This equation is slightly more complex than the plane case (2.5). However, because the positive constraint is on only one axis, walks in the a half-plane can be related to walks in $\mathbb{N}$ (see Figure 1.2a). Let us point out that even if both problems have a one-dimensional constraint, generating functions of walks in the half-plane have three variables x, y and t (unlike the one dimensional case with two variables x and t) and is therefore a slightly more complicated problem. Let us present here a resolution of one-dimensional constraint walk.

We consider the walk with step inventory $S(x) = x + x^{-1}$ over the positive half-line. Let $q_i(n)$ be the number of walks starting at the position i, of length n and $Q(x)$ its generating function defined by

$$Q(x) = \sum_{i,n\geq 0} q_i(n) x^i t^n.$$

By a step by step construction (see Figure 2.2), we can write the following functional equation

$$Q(x) = 1 + t(x + x^{-1})Q(x) - tx^{-1}Q(0),$$

which can be rewritten as

$$Q(x)K(x) = -x + tQ(0), \tag{2.7}$$

with the kernel defined by $K(x) = tx^2 - x + t$ which vanishes at $x = x_1$ and $x = x_2$ defined by

$$x_1 = \frac{1 - \sqrt{1 - 4t^2}}{2t} = t + t^3 + 2\,t^5 + O\left(t^7\right),$$
$$x_2 = \frac{1 + \sqrt{1 - 4t^2}}{2t} = t^{-1} - t - t^3 - 2\,t^5 + O\left(t^6\right).$$

We evaluate the functional equation (2.7) at $x = x_1$ and we get[2] $Q(0) = x_1/t$. Finally

$$Q(x) = -\frac{x - x_1}{K(x)} = \frac{1 - 2\,xt - \sqrt{1 - 4\,t^2}}{(2\,x^2 + 2)\,t^2 - 2\,xt} = 1 + xt + (1 + x^2)t^2 + (2x + x^3)t^3 + O\left(t^4\right).$$

Quadrant case. We derive a functional equation for $Q(x, y)$ defined in (2.2) by taking into account all possible endpoints in the quadrant. We illustrate this construction with Figure 2.3 in the particular case of the king walk. The empty walk 1 ends in the quadrant. Then, we may add

[2]Being a power series, $Q(0)$ can not be expressed in terms of x_2.

a step from $\mathcal{S}$ to walks ending in the quadrant, yielding in (2.8) the term $tS(x,y)Q(x,y)$, see the third picture in Figure 2.3. Walks going out of the quadrant need to be removed, giving rise in (2.8) to the terms $tB_-(x)y^{-1}Q(x,0)$ (positive x-axis) and $tA_-(y)x^{-1}Q(0,y)$, see the fourth and the fifth pictures in Figure 2.3. We finally add the term $t\delta_{-1,-1}x^{-1}y^{-1}Q(0,0)$ which was subtracted twice, corresponding to the rightmost picture in Figure 2.3. In the general case, for a step set $\mathcal{S}$ we end up with the functional equation (where $\delta_{-1,-1}=1$ if $(-1,-1)\in\mathcal{S}$ and 0 otherwise):

$$Q(x,y) = 1 + tS(x,y)Q(x,y) - tB_-(x)y^{-1}Q(x,0) - tA_-(y)x^{-1}Q(0,y) + t\delta_{-1,-1}x^{-1}y^{-1}Q(0,0). \quad (2.8)$$

Unlike the half-plane case (2.6), the functional equation in the quadrant case (2.8) involves both $Q(x,0)$ and $Q(0,y)$ sections. This functional equation can be solved with various methods, each of them giving a different expression for the generating function of walks, see references in topic 1 of Section 1.1. We present in Section 2.1.2 an analytic method to solve the functional equation of walks in the quadrant (2.8) and get explicit integral expressions for the generating function $Q(x,y)$.

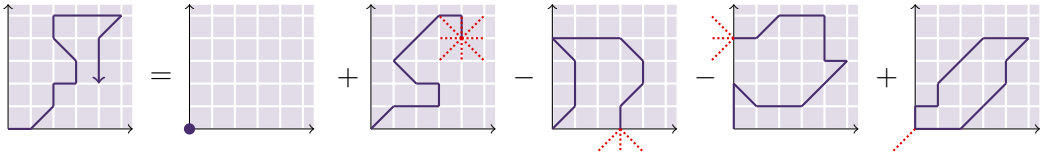

Figure 2.3 – Illustration of the functional equation (2.8) for the example of the king walk. We construct a walk by adding a new step (in dotted red) at each stage. The right-hand side describes the different ways to end in the positive quadrant making sure to remove the walks going out of quadrant

The large step case is more complicated and involves more terms (see [28, Sec. 2]). In dimension two, where $Q(x,y)$ is the generating function of walks in the quadrant, $x^iQ_{i,-}(y)$ (resp. $y^jQ_{-,j}$) counts walks ending at abscissa i (resp. ordinate j), and $Q_{i,j}$ the length generating function of walks ending at (i,j), the functional equation can be written as[3]

$$Q(x,y) = 1 + tS(x,y)Q(x,y) - t\sum_{(k,l)\in\mathcal{S}} x^ky^l\left(\sum_{0\le i<-k} x^iQ_{i,-}(y) + \sum_{0\le j<-l} y^jQ_{-,j}(x) - \sum_{\substack{0\le i<-k\\0\le j<-l}} x^iy^jQ_{i,j}\right). \quad (2.9)$$

Three-quadrant case. The construction of the functional equation of the generating function of walks in the three-quadrant $C(x,y)$ (see (3.1)) is similar to the previous cases. We illustrate this construction with Figure 2.4 in the particular case of the king walk. Let $\delta_{-1,-1}=1$ if $(-1,-1)\in\mathcal{S}$

[3]In this thesis we take the convention $K(x,y) = -xy\widetilde{K}(x,y)$, where $\widetilde{K}(x,y)$ is the kernel defined in [28, Sec. 2].

and 0 otherwise. The empty walk 1 ends in the three-quadrant, see the first picture in Figure 2.4 as well as walks in the three-quadrant to which we add a step from $\mathcal{S}$ with generating function $tS(x,y)Q(x,y)$, see the second picture in Figure 2.4. Walks going out of the three-quadrant $tB_-(x)y^{-1}C_{-0}(x^{-1})$ and $tA_-(y)x^{-1}C_{0-}(y^{-1})$ need to be removed, see the third and the fourth pictures in Figure 2.4. We finally add the term $t\delta_{-1,-1}x^{-1}y^{-1}Q(0,0)$ which was subtracted twice, corresponding to the rightmost picture in Figure 2.4. This gives the following formal functional equation

$$C(x,y) = 1 + tS(x,y)C(x,y) - tB_-(x)y^{-1}C_{-0}(x^{-1}) - tA_-(y)x^{-1}C_{0-}(y^{-1}) + t\delta_{-1,-1}x^{-1}y^{-1}C(0,0). \quad (2.10)$$

Due to convergence issues when the formal power series are interpreted as functions, the three-quadrant case is however more complicated and therefore more difficult to work with. Walks in three-quadrant are developed in Chapter 3.

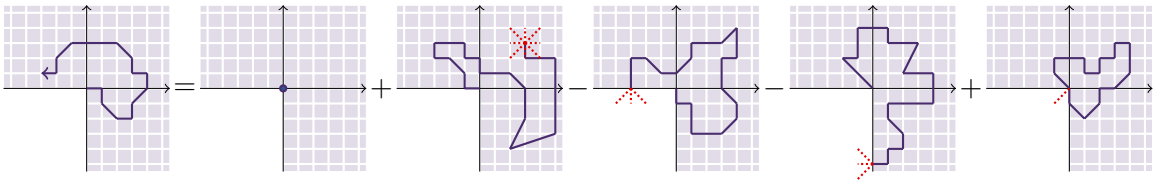

Figure 2.4 – Different ways to end in the three-quadrant (example of the king walk)
Illustration of the functional equation (2.10) for the example of the king walk. The right-hand side describes the different ways to end in the three-quadrant making sure to remove the walks going out of the three-quadrant

2.1.2 Analytic method in the quadrant case

We present here the analytic approach of [113] which consists in transforming the functional equation (2.8) into a boundary value problem on a curve depending on the step set. The result is a contour-integral expression for the generating function. In the 70's Malyshev in Russia then Fayolle and Iasnogorodski in France first used an analytic method via boundary value problem to solve a functional equation satisfied by generating functions of stationary probability of random walks [72].

The kernel of the model (2.12) is a main object we can use to transform a functional equation into a boundary value problem. We are interested in the Riemann surface of the zeros of the polynomial $K(x,y)$. The zeros of the kernel are defined by two algebraic functions (2.16), one over the complex plane $\mathcal{C}_x$ and the other over $\mathcal{C}_y$. Each of these functions has branches which, when they are evaluated between two branch points, define the curves of the boundary value problem. More details on this method can be found in [72, 113].

Kernel and functional equation. We start from the functional equation (2.8). After multiplication by xy, we get

$$K(x,y)Q(x,y) = -xy + tB_-(x)xQ(x,0) + tA_-(y)yQ(0,y) - t\delta_{-1,-1}Q(0,0), \tag{2.11}$$

where the polynomial on the left-hand side

$$K(x,y) = xy\,[tS(x,y) - 1] \tag{2.12}$$

is called the kernel of the walk. It encodes the elements of $\mathcal{S}$ (the steps of the walks). In the 2D small step case, $K(x,y)$ is a polynomial of degree two in x and y. We can rewrite it as:

$$K(x,y) = \widetilde{a}(y)x^2 + \widetilde{b}(y)x + \widetilde{c}(y) = a(x)y^2 + b(x)y + c(x), \tag{2.13}$$

where[4]:

$$\begin{cases} a(x) = tx\sum_{(i,1)\in\mathcal{S}} x^i; & b(x) = tx\sum_{(i,0)\in\mathcal{S}} x^i - x; & c(x) = tx\sum_{(i,-1)\in\mathcal{S}} x^i; \\ \widetilde{a}(y) = ty\sum_{(1,j)\in\mathcal{S}} y^j; & \widetilde{b}(y) = ty\sum_{(0,j)\in\mathcal{S}} y^j - y; & \widetilde{c}(y) = ty\sum_{(-1,j)\in\mathcal{S}} y^j. \end{cases} \tag{2.14}$$

We also define the discriminants in x and y of the kernel (2.12):

$$\widetilde{d}(y) = \widetilde{b}(y)^2 - 4\widetilde{a}(y)\widetilde{c}(y) \qquad \text{and} \qquad d(x) = b(x)^2 - 4a(x)c(x). \tag{2.15}$$

The discriminant $d(x)$ (resp. $\widetilde{d}(y)$) in (2.15) is a polynomial of degree three or four. Hence it admits three or four roots (also called branch points) x_1, x_2, x_3, x_4 (resp. y_1, y_2, y_3, y_4), with $x_4 = \infty$ (resp. $y_4 = \infty$) when $d(x)$ (resp. $\widetilde{d}(y)$) is of degree 3.

Lemma 1 (Sec. 3.2 in [113])**.** *Let $t \in (0, 1/|\mathcal{S}|)$. The branch points x_i, which depend on t, are real and distinct. Two of them (say x_1 and x_2) are in the open unit disc, with $x_1 < x_2$ and $x_2 > 0$. The other two (say x_3 and x_4) are outside the closed unit disc, with $x_3 > 0$ and $x_3 < x_4$ if $x_4 > 0$. The discriminant $d(x)$ is negative on (x_1, x_2) and (x_3, x_4), where if $x_4 < 0$, the set (x_3, x_4) stands for the union of intervals $(x_3, \infty) \cup (-\infty, x_4)$. Symmetric results hold for the branch points y_i.*

[4]The kernel $K(x,y)$ coefficients and the inventory polynomial $S(x,y)$ coefficients are simply related:

$$a(x) = txB_+(x), \quad b(x) = tB_0(x) - x, \quad c(x) = txB_-(x).$$

Similar equalities hold for $\widetilde{a}(y), A_+(y), \widetilde{b}(y), A_0(y), \widetilde{c}(y)$ and $A_-(y)$.

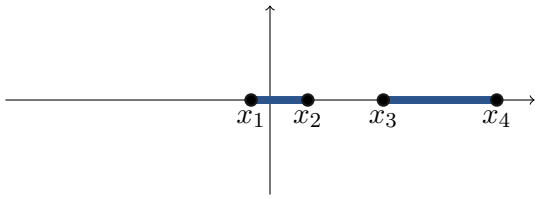

(a) Cut plane $\mathbb{C} \setminus ([x_1, x_2] \cup [x_3, x_4])$, with $x_4 > 0$. Model with step set $\{\mathsf{E}, \mathsf{NE}, \mathsf{NW}, \mathsf{SW}, \mathsf{S}\}$, $t = 1/6$

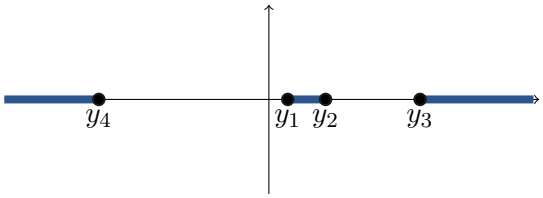

(b) Cut plane $\mathbb{C} \setminus ([y_1, y_2] \cup [y_3, y_4])$, with $y_4 < 0$. Model with step set $\{\mathsf{E}, \mathsf{NE}, \mathsf{NW}, \mathsf{SW}, \mathsf{S}\}$, $t = 1/6$

Figure 2.5 – The functions $X_0(y)$ and $X_1(y)$ are meromorphic on $\mathbb{C} \setminus ([y_1, y_2] \cup [y_3, y_4])$;
The functions $Y_0(x)$ and $Y_1(x)$ are meromorphic on $\mathbb{C} \setminus ([x_1, x_2] \cup [x_3, x_4])$

Let $Y(x)$ (resp. $X(y)$) be the algebraic function defined by the relation $K(x, Y(x)) = 0$ (resp. $K(X(y), y) = 0$). Obviously with (2.13) and (2.15) we have

$$Y(x) = \frac{-b(x) \pm \sqrt{d(x)}}{2a(x)} \qquad \text{and} \qquad X(y) = \frac{-\widetilde{b}(y) \pm \sqrt{\widetilde{d}(y)}}{2\widetilde{a}(y)}. \tag{2.16}$$

The function Y has two branches Y_0 and Y_1, which are meromorphic on the cut plane $\mathbb{C} \setminus ([x_1, x_2] \cup [x_3, x_4])$ (see Figure 2.5). On the cuts $[x_1, x_2]$ and $[x_3, x_4]$, the two branches still exist and are complex conjugate (but possibly infinite at $x_1 = 0$, as discussed in Lemma 2). At the branch points x_i, we have $Y_0(x_i) = Y_1(x_i)$ (when finite), and we denote this common value by $Y(x_i)$.

Fix the notation of the branches by choosing $Y_0 = Y_-$ and $Y_1 = Y_+$ in (2.16). We further fix the determination of the logarithm so as to have $\sqrt{d(x)} > 0$ on (x_2, x_3). Then [72, Eq. (5.3.8)] we have

$$|Y_0| \leq |Y_1| \tag{2.17}$$

on (x_2, x_3), and as proved in [72, Thm 5.3.3], the inequality (2.17) holds true on the whole complex plane and is strict, except on the cuts, where Y_0 and Y_1 are complex conjugate.

A key object is the curve $\mathcal{L}$ defined by

$$\mathcal{L} = Y_0([x_1, x_2]) \cup Y_1([x_1, x_2]) = \{y \in \mathbb{C} : K(x, y) = 0 \text{ and } x \in [x_1, x_2]\}. \tag{2.18}$$

By construction, it is symmetric with respect to the real axis. We denote by $\mathcal{G}_{\mathcal{L}}$ the open domain delimited by $\mathcal{L}$ and avoiding the real point at $+\infty$. See Figure 2.6 for some examples. Furthermore,

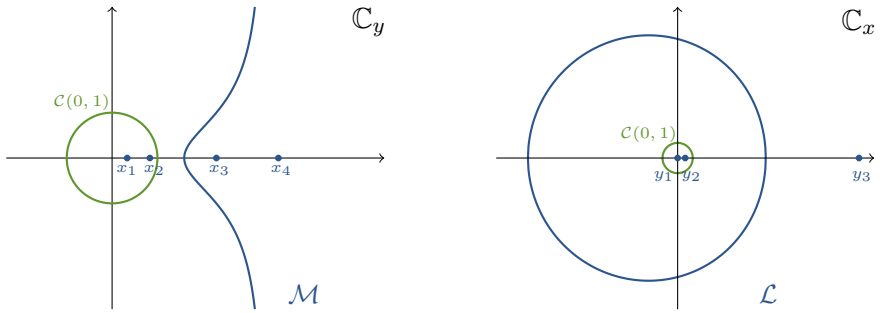

(a) Gessel's model ($t = 1/8$)

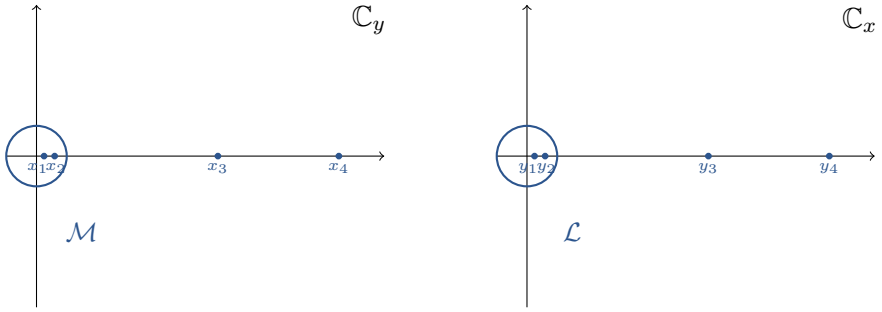

(b) Simple model ($t \in (0, 1/4)$)

Figure 2.6 – The curves $\mathcal{L}$ and $\mathcal{M}$ for two models

let $\mathcal{L}_0$ (resp. $\mathcal{L}_1$) be the upper (resp. lower) half of $\mathcal{L}$, i.e., the part of $\mathcal{L}$ with non-negative (resp. non-positive) imaginary part. Likewise, we define $\mathcal{M} = X_0([y_1, y_2]) \cup X_1([y_1, y_2])$.

Lemma 2 (Lem. 18 in [17]). *The curve $\mathcal{L}$ in (2.18) is symmetric with respect to the real axis. It intersects this axis at $Y(x_2) > 0$.*

If $\mathcal{L}$ is unbounded, $Y(x_2)$ is the only intersection point. This occurs if and only if neither $(-1, 1)$ nor $(-1, 0)$ belong to $\mathcal{S}$. In this case, $x_1 = 0$ and the only point of $[x_1, x_2]$ where at least one branch $Y_i(x)$ is infinite is x_1 (and then both branches are infinite there). Otherwise, the curve $\mathcal{L}$ goes through a second real point, namely $Y(x_1) \leq 0$.

Consequently, the point 0 is either in the domain $\mathcal{G}_\mathcal{L}$ or on the curve $\mathcal{L}$. The domain $\mathcal{G}_\mathcal{L}$ also contains the (real) branch points y_1 and y_2, of modulus less than 1. The other two branch points, y_3 and y_4, are in the complement of $\mathcal{G}_\mathcal{L} \cup \mathcal{L}$.

Remark 3. When the walk is symmetric (i.e., when $S(x, y) = S(y, x)$) the curves $\mathcal{L}$ and $\mathcal{M}$ are the same. Furthermore, for any model satisfying $S(x, y) = S(x^{-1}, y) = S(y, x)$ (such as the simple step set), the curves $\mathcal{L}$ and $\mathcal{M}$ are the unit circle $\mathcal{C}(0, 1)$ for all $t \in (0, 1/4)$ (see Figure 2.6b).

Lemma 4 (Cor. 5.3.5 in [72]). *We have the following automorphism relations:*

$$X_0 : \mathcal{G}_\mathcal{L} \setminus [y_1, y_2] \to \mathcal{G}_\mathcal{M} \setminus [x_1, x_2] \qquad \text{and} \qquad Y_0 : \mathcal{G}_\mathcal{M} \setminus [x_1, x_2] \to \mathcal{G}_\mathcal{L} \setminus [y_1, y_2]$$

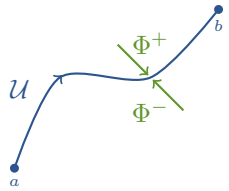

Figure 2.7 – Left and right limits on the open contour $\mathcal{U}$

are conformal and inverse of one another.

Let us apply the properties of the kernel (2.12) to the functional equation (2.11). The function $c(x)Q(x,0)$ can be holomorphically continued from the open unit disc $\mathcal{D}$ to the domain $\mathcal{G}_{\mathcal{M}} \cup \mathcal{D}$ [113, Thm 5]. Then, we evaluate the functional equation (2.11) at $x = X_0(y)$ for y close to $[y_1, y_2]$:

$$X_0(y)y - c(X_0(y))Q(X_0(y),0) - \widetilde{c}(y)Q(0,y) + t\delta_{-1,-1}Q(0,0) = 0.$$

Letting y go to any point y^* of $[y_1, y_2]$ with a positive (resp. negative) imaginary part, we obtain two new equations with $x = \lim X_0(y)$ when $y \to y^* + i0^+$, $x \in \mathcal{M}$,

$$\begin{aligned} xY_0(x) - c(x)Q(x,0) - \widetilde{c}(Y_0(x))Q(0,Y_0(x)) + t\delta_{-1,-1}Q(0,0) = 0,\\ \bar{x}Y_0(\bar{x}) - c(\bar{x})Q(\bar{x},0) - \widetilde{c}(Y_0(\bar{x}))Q(0,Y_0(\bar{x})) + t\delta_{-1,-1}Q(0,0) = 0. \end{aligned}$$

Taking the difference of the two equations and using the automorphism relation of Lemma 4 we obtain

$$c(x)Q(x,0) - c(\bar{x})Q(\bar{x},0) = Y_0(x)(x - \bar{x}), \quad x \in \mathcal{M}. \tag{2.19}$$

With the regularity condition of $c(x)Q(x,0)$ and the boundary condition (2.19), we say that the function $c(x)Q(x,0)$ satisfies a boundary value problem. This kind of boundary problem is also called a Riemann boundary value problem with a shift of the variable (in our case (2.19), the shift $\overline{x}$ denotes the complex conjugate of x).

Riemann boundary value problem. In this paragraph we present the main formulas used to solve a Riemann boundary value problem[5]. Our main references are the books of Gakhov [83, Chap. 2] and Lu [104, Chap. 4].

Suppose that $\mathcal{U}$ is an open, smooth, non-intersecting, oriented curve from a to b, see Figure 2.7 for an example. Throughout, for $z \in \mathcal{U}$, we will denote by $\Phi^+(z)$ (resp. $\Phi^-(z)$) the limit of a function Φ as $y \to z$ from the left (resp. right) of $\mathcal{U}$, see again Figure 2.7.

Definition 5 (Riemann BVP)**.** Let $\mathcal{U}$ be as above. A function Φ satisfies a BVP on $\mathcal{U}$ if:

[5]Boundary Value Problem is abbreviated as BVP.

- Φ is sectionally analytic, i.e., analytic in $\mathbb{C} \setminus \mathcal{U}$;
- Φ has finite degree at ∞ (the only singularity at ∞ is a pole of finite order), and Φ is bounded in the vicinity of the extremities a and b;
- Φ has left limits Φ^+ and right limits Φ^- on $\mathcal{U}$;
- Φ satisfies the following boundary condition

$$\Phi^+(z) = G(z)\Phi^-(z) + g(z), \quad z \in \mathcal{U}, \tag{2.20}$$

  where G and g are Hölder functions[6] on $\mathcal{U}$, and G does not vanish on $\mathcal{U}$.

Let us recall the so-called Sokhotski-Plemelj formulas, which represent a crucial tool to solve the BVP of Definition 5.

Proposition 6 (Sokhotski-Plemelj formulas)**.** *Let $\mathcal{U}$ be as above, and let f be a Hölder function on $\mathcal{U}$. The contour integral*

$$F(z) = \frac{1}{2i\pi} \int_{\mathcal{U}} \frac{f(u)}{u - z} \, \mathrm{d}u$$

is sectionally analytic on $\mathbb{C} \setminus \mathcal{U}$. It admits left and right limits values F^+ and F^-, which are Hölder functions on $\mathcal{U}$ and satisfy, for $z \in \mathcal{U}$,

$$F^{\pm}(z) = \pm \frac{1}{2} f(z) + \frac{1}{2i\pi} \int_{\mathcal{U}} \frac{f(u)}{u - z} \, \mathrm{d}u,$$

where the very last integral is understood in the sense of Cauchy-principal value, see [83, Chap. 1, Sec. 12]. This is equivalent to the following equations on $\mathcal{U}$:

$$\begin{cases} F^+(z) - F^-(z) = f(z), \\ F^+(z) + F^-(z) = \dfrac{1}{i\pi} \displaystyle\int_{\mathcal{L}} \frac{f(u)}{u - z} \, \mathrm{d}u. \end{cases} \tag{2.21}$$

We also define the following important quantity:

Definition 7 (Index)**.** Let $\mathcal{U}$ be as above and let G be the function (continuous on $\mathcal{U}$) as in (2.20). The index χ of the BVP of Definition 5 is

$$\chi = \mathrm{ind}_{\mathcal{U}} G = \frac{1}{2\pi} [\arg G]_{\mathcal{U}} = \frac{1}{2i\pi} [\log G]_{\mathcal{U}} = \frac{1}{2i\pi} \int_{\mathcal{U}} \frac{G'(u)}{G(u)} \, \mathrm{d}u.$$

[6] A function f satisfies the Hölder condition on a curve $\mathcal{U}$ if there exists positive constants μ and M such that for any two points t_1, t_2 of $\mathcal{U}$, $|f(t_2) - f(t_1)| \leq M|t_2 - t_1|^{\mu}$.

Plainly, χ represents the variation of argument of $G(u)$ when u moves along the contour $\mathcal{U}$ in the positive direction.

The main result is the following, see [104, Chap. 4, Thm 2.1.2]:

Theorem 8 (Solution of Riemann BVP)**.** *Let $\mathcal{U}$ and χ be as above. Define also*

$$\left\{\begin{array}{rcl} \Gamma(z) & = & \dfrac{1}{2i\pi}\displaystyle\int_{\mathcal{U}} \frac{\log G(u)}{u-z}\,\mathrm{d}u, \\ X(z) & = & (z-b)^{-\chi}\exp\Gamma(z), \\ \psi(z) & = & \dfrac{1}{2i\pi}\displaystyle\int_{\mathcal{U}} \frac{g(u)}{X^+(u)(u-z)}\,\mathrm{d}u, \end{array}\right.$$

where the left limits X^+, Γ^+ of X, Γ are related by

$$X^+(z) = (z-b)^{-\chi}\exp\Gamma^+(z),$$

and Γ^+ can be computed with the help of Sokhotski-Plemelj formulas, see Proposition 6. Three cases must be distinguished:

(a) if $\chi \geq 0$. The solution of the BVP of Definition 5 is given by, for $z \notin \mathcal{U}$,

$$X(z)\psi(z) + X(z)P_\chi(z), \tag{2.22a}$$

where P_χ is an arbitrary polynomial of degree χ.

(b) if $\chi = -1$. The solution of the BVP of Definition 5 is given by, for $z \notin \mathcal{U}$,

$$X(z)\psi(z). \tag{2.22b}$$

(c) if $\chi < -1$ and the following solvability conditions hold

$$\frac{1}{2i\pi}\int_{\mathcal{U}} \frac{g(u)u^{k-1}}{X^+(u)}\,\mathrm{d}u = 0, \quad k = 1, \ldots, -\chi - 1.$$

The solution of the BVP of Definition 5 is given by, for $z \notin \mathcal{U}$,

$$X(z)\psi(z). \tag{2.22c}$$

Our boundary condition (2.19) with shift on a closed contour does not look like the boundary condition (2.20) on an open contour. The key to get back to this type of boundary condition is to introduce a particular conformal mapping for $\mathcal{G}_\mathcal{M}$.

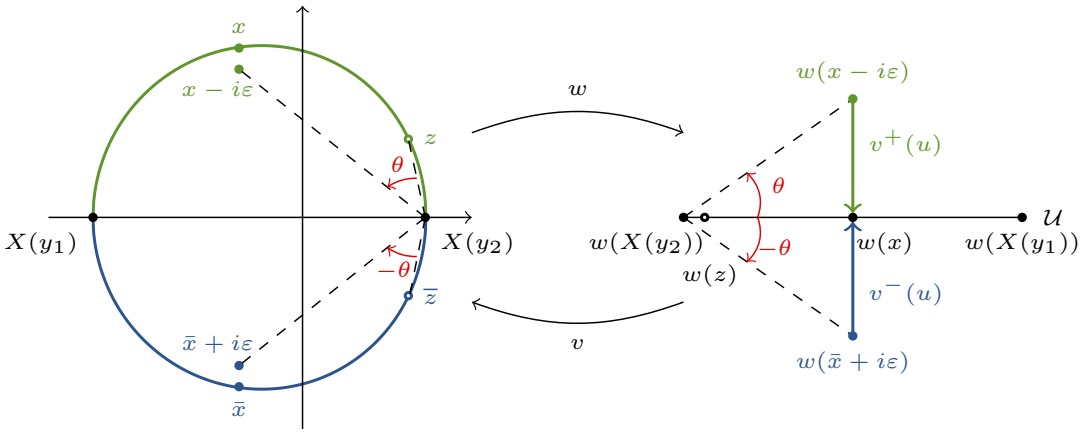

Figure 2.8 – Conformal gluing function from $\mathcal{G}_\mathcal{M}$ to $\mathbb{C} \setminus \mathcal{U}$

Definition 9 (Conformal gluing function)**.** A function w is said to be a conformal gluing function for the set $\mathcal{G}_\mathcal{M}$ if:

- w is meromorphic in $\mathcal{G}_\mathcal{M}$ and admits finite limits on $\mathcal{M}$;
- w is bijective on $\mathcal{G}_\mathcal{M}$ to the cut plane $\mathbb{C} \setminus \mathcal{U}$;
- for all x on $\mathcal{M}$, $w(x) = w(\overline{x})$.

Respectively, we define $\widetilde{w}$ to be a conformal gluing function for the set $\mathcal{G}_\mathcal{L}$.

Let w be a conformal gluing function for the set $\mathcal{G}_\mathcal{M}$ in the sense of Definition 9, and let $\mathcal{U}$ denote the real segment

$$\mathcal{U} = w(\mathcal{M}).$$

(With this notation, w is a conformal map from $\mathcal{G}_\mathcal{M}$ onto the cut plane $\mathbb{C} \setminus \mathcal{U}$.) The segment $\mathcal{U}$ is oriented such that the positive direction is from $w(X(y_2))$ to $w(X(y_1))$, see Figure 2.8.

Define v as the inverse function of w. The latter is meromorphic on $\mathbb{C} \setminus \mathcal{U}$. Following the previous notation and [72], we denote by v^+ and v^- the left and right limits of v on $\mathcal{U}$. The quantities v^+ and v^- are complex conjugate on $\mathcal{U}$, and more precisely, since w preserves angles[7], we have for $u \in \mathcal{U}$ and $x \in \mathcal{M}_0$ [8],

$$\begin{cases} v^+(u) &= v^+(w(x)) &= x, \\ v^-(u) &= v^-(w(x)) &= \overline{x}, \end{cases}$$

see Figure 2.8 for an illustration of the above properties.

[7] As a conformal function w preserves orientations (and in particular angles, see Figure 2.8)

[8] $\mathcal{M}_0$ is the upper half of the curve $\mathcal{M}$ i.e., the part above the real axis.

With the conformal mapping defined in Definition 9, we can transform the Riemann boundary value problem (2.19) on the countour $\mathcal{M}$ into a Riemann boundary value problem on a segment $\mathcal{U}$, see Figure 2.8. We have

$$c\left(v^+(u)\right) Q\left(v^+(u),0\right) = c\left(v^-(u)\right) Q\left(v^-(u),0\right) + Y_0(v^+(u))\left(v^+(u)-v^-(u)\right), \quad u \in \mathcal{U}. \tag{2.23}$$

Finding w or $\widetilde{w}$ is generally not an easy problem. It is as difficult as finding a conformal map of a given domain. Kurkova and Raschel in [99] and Raschel in [113] found explicit expressions of w and $\widetilde{w}$. In the small step case, the curves $\mathcal{M}$ and $\mathcal{L}$ are quartic plane curves and this structure allows to get expressions of w and $\widetilde{w}$ involving elliptic Weierstrass functions. For some models, it degenerates into a rational expression (for example for the simple walks we can take $w(x) = x + \frac{1}{x}$), whereas for the Gessel's walks, the function w is more complicated but algebraic. In the case of an infinite group, w is non-D-finite [113].

Contour-integral expression. From Theorem 8, solving (2.23) yields to a contour-integral expression of $c(x)Q(x,0)$. Up to an additive function of t, we have for $u \in \mathcal{U}$:

$$c(v(u))Q(v(u),0) = \frac{1}{2i\pi}\int_{\mathcal{U}} \frac{v^+(s)Y_0(v^+(s)) - v^-(s)Y_0(v^-(s))}{s-u}\,\mathrm{d}u. \tag{2.24}$$

With the change of variable $s = w(x)$, up to an additive function of t, we have for $x \in \mathcal{G}_{\mathcal{M}}$:

$$c(x)Q(x,0) = \frac{1}{2i\pi}\int_{\mathcal{M}} zY_0(z)\frac{w'(z)}{w(z)-w(x)}\,\mathrm{d}z. \tag{2.25}$$

We deduce the following theorem:

Theorem 10. *Consider walks with small steps restricted to the quarter plane. The generating function $Q(x,y)$ has the explicit expression:*

$$Q(x,y) = \frac{c(x)Q(x,0) - \widetilde{c}(y)Q(0,y) - t\delta_{-1,-1}Q(0,0) - xy}{K(x,y)}, \tag{2.26}$$

where:

1. *For $x \in \mathcal{G}_{\mathcal{M}}$, $y \in \mathcal{G}_{\mathcal{L}}$,*

$$c(x)Q(x,0) - c(0)Q(0,0) = \frac{1}{2i\pi}\int_{\mathcal{M}} zY_0(z)\left[\frac{w'(z)}{w(z)-w(x)} - \frac{w'(z)}{w(z)-w(0)}\right]\mathrm{d}z \tag{2.27}$$

$$\widetilde{c}(y)Q(0,y) - \widetilde{c}(0)Q(0,0) = \frac{1}{2i\pi}\int_{\mathcal{L}} zX_0(z)\left[\frac{\widetilde{w}'(z)}{\widetilde{w}(z)-\widetilde{w}(x)} - \frac{\widetilde{w}'(z)}{\widetilde{w}(z)-\widetilde{w}(0)}\right]\mathrm{d}z. \tag{2.28}$$

2. *If* $c(0) = 0$ *(when* $(-1, 1) \notin \mathcal{S}$*), then*

$$Q(0,0) = \lim_{x \to 0} \frac{1}{2i\pi c(x)} \int_{\mathcal{M}} zY_0(z) \frac{w'(z)}{w(z) - w(x)} \, \mathrm{d}z. \tag{2.29}$$

3. *If* $c(0) \neq 0$ *(when* $(-1, 1) \in \mathcal{S}$*), then for any* (x_0, y_0) *such that* $|x_0| \leq 1$, $|y_0| \leq 1$ *and* $K(x_0, y_0) = 0$*,*

$$Q(0,0) = \frac{1}{t} \left[c(x_0)Q(x_0, 0) + \widetilde{c}(y_0)Q(0, y_0) - x_0 y_0 \right]. \tag{2.30}$$

Example of the simple walk. We apply the previous theorem on the simple step set: $\mathcal{S} = \{(1,0), (0,1), (-1,0), (0,-1)\}$ (see Table 2.1). This model is symmetric ($S(x,y) = S(y,x)$) hence the polynomial $K(x,y)$ satisfies $K(x,y) = K(y,x)$. In this example, we have:

$$\begin{cases} a(x) = tx; & b(x) = tx^2 + t - x; & c(x) = tx; \\ \widetilde{a}(y) = ty; & \widetilde{b}(y) = ty^2 + t - y; & \widetilde{c}(y) = ty. \end{cases} \tag{2.31}$$

The branches of X and Y of the kernel are:

$$X(y) = \frac{1 - t(y + y^{-1}) \pm \sqrt{(1 - t(y + y^{-1}))^2 - 4t^2}}{2t} \tag{2.32}$$

and

$$Y(x) = \frac{1 - t(x + x^{-1}) \pm \sqrt{(1 - t(x + x^{-1})^2 - 4t^2}}{2t}. \tag{2.33}$$

The functional equation satisfied by the generating function is:

$$K(x,y)Q(x,y) = txQ(x,0) + tyQ(0,y) - xy. \tag{2.34}$$

The model is symmetric and $\mathcal{M}$ and $\mathcal{L}$ are both the circle $\mathcal{C}$ of center $(0,0)$ and radius 1 (see Figure 2.6b). We can take $w(z) = \widetilde{w}(z) = \frac{1}{2}\left(z + \frac{1}{z}\right)$, and w has a pole at 0. Thanks to Theorem 10, we have the following result:

$$\begin{aligned} Q(x,y) &= \frac{1}{K(x,y)} \left(-xy + \frac{1}{2i\pi} \int_{\mathcal{C}} \frac{z^2 - 1}{z} Y_0(z) \left[\frac{1}{z + z^{-1} - x - x^{-1}} + \frac{1}{z + z^{-1} - y - y^{-1}} \right] \mathrm{d}z \right) \\ &= \frac{1}{K(x,y)} \left(-xy + \frac{1}{2i\pi} \int_0^{2\pi} \left(e^{2i\theta} - 1 \right) Y_0(e^{i\theta}) \left[\frac{1}{2\cos(\theta) - x - x^{-1}} + \frac{1}{2\cos(\theta) - y - y^{-1}} \right] \mathrm{d}z \right). \end{aligned}$$

Notice that the computation of $Q(x,y)$ consists mainly to compute a trigonometric integral. After an expansion in series of this last equation in Maple (which serves to perform a consistency check

on the previous integral expression), we have:

$$Q(x,y) = 1 + (x+y)\,t + \left(x^2 + 2\,x\,y + y^2 + 2\right) t^2 + \left(x^3 + 3\,x^2 y + 3\,x\,y^2 + y^3 + 5\,x + 5\,y\right) t^3 \\ + \left(x^4 + 4\,x^3 y + 6\,x^2 y^2 + 4\,x\,y^3 + y^4 + 9\,x^2 + 16\,x\,y + 9\,y^2 + 10\right) t^4 + O\left(t^5\right),$$

which matches with a direct enumeration of walks.

2.2 Asymptotic results

Denisov and Wachtel describe in [58, Sec. 1.5] the asymptotic behavior of the number of n-excursions restricted to a d-dimensional cone. In dimension two, Bostan, Raschel and Salvy [34] made explicit the computation of the exponential growth and the critical exponent.

Theorem 11. *Let $\mathcal{S} \subset \{0, \pm 1\}^2$ be the step set of a walk in the quarter plane, which is not contained in a half-plane. Let $e(n)$ denote the number of excursions of length n with steps in $\mathcal{S}$, and let $S(x,y)$ denote the characteristic polynomial of $\mathcal{S}$ defined by $\sum_{(i,j)\in\mathcal{S}} x^i y^j$. The system*

$$\frac{\partial S}{\partial x} = \frac{\partial S}{\partial y} = 0$$

has a unique solution $(x_0, y_0) \in (0,\infty)^2$. Then, define

$$\rho := S(x_0, y_0), \quad c = \frac{\frac{\partial^2 S}{\partial x \partial y}}{\sqrt{\frac{\partial^2 S}{\partial x^2} \cdot \frac{\partial^2 S}{\partial y^2}}}(x_0, y_0), \quad \alpha = 1 + \frac{\pi}{\arccos(-c)}. \tag{2.35}$$

Then, there exists a constant $K > 0$, which depends only on $\mathcal{S}$, such that:

- *If the walk is aperiodic,*
$$e(n) \sim K \cdot \rho^n \cdot n^{-\alpha}.$$
- *If the walk is periodic (then of period p equals to 2 or 3), then $e(m) = 0$ if $m \neq pn$ and*
$$e(pn) \sim K \cdot \rho^{pn} \cdot (pn)^{-\alpha}.$$

The quantity ρ is an algebraic number called the exponential growth, and the real number α is the critical exponent. In the next paragraphs, we review the works on these two parameters in dimension two. In dimension one, formulas for walks restricted to the positive half-line are known [10]. Unrestricted walks have exponent 0 and unrestricted excursions (paths which join two given points) have exponent $\frac{1}{2}$. Dyck walks (positive walks in dimension one, see Section 1.1) have exponent $\frac{1}{2}$ and Dyck excursions have exponent $\frac{3}{2}$.

Let us give an application of Theorem 11 for Kreweras step set (see model 2.3 in Table 2.1). The inventory polynomial is defined by $S(x,y) = xy + x^{-1} + y^{-1}$. The unique positive solution to the system

$$\left\{ \begin{array}{rcccl} \frac{\partial S}{\partial x} & = & y - \frac{1}{x^2} & = & 0 \\ \frac{\partial S}{\partial y} & = & x - \frac{1}{y^2} & = & 0 \end{array} \right.$$

is $(x_0, y_0) = (1,1)$. We have then

$$\rho = S(1,1) = 4, \quad c = \left. \frac{1}{\sqrt{\frac{2}{x^3} \cdot \frac{2}{y^3}}} \right|_{(x,y)=(1,1)} = \frac{1}{2}, \quad \alpha = -1 - \frac{\pi}{\arccos(-1/2)} = -\frac{5}{2}.$$

Exponential growth. The values of ρ for small step quadrant walks are numerically conjectured by Bostan and Kauers in [30]. Theses conjectures are proved by Bousquet-Mélou and Mishna [41] and Fayolle and Raschel [74]. In dimension three, Bacher, Kauers and Yatchak [6] give experimental results about the exponential growth. Exact expressions of the exponential growth are given by Denisov and Wachtel in [58].

Critical exponent. The total number of walks for the simple walks case in a cone of opening angle η has exponent $\frac{\pi}{2\eta}$ [58]. In the same angular sector, the number of excursions for the simple walks has exponent $\frac{\pi}{\eta} + 1$ [58]. Theorem 11 gives an explicit formula for λ and is systematically computed in [34]. In the same article, the authors prove that in the case of the 51 *nonsingular walks*[9] with infinite group, the number α is not a rational number, which implies the non-D-finiteness of the generating function of walks in the quadrant. In dimension 3, the critical exponent can be expressed as a function of the smallest eigenvalue of a Dirichlet problem in a spherical triangle, which can be computed algorithmically (and easily) in terms of the model $\mathcal{S}$. This last point is developed in Chapter 5.

2.3 Classification of lattice walks

2.3.1 Group of the walk

A group structure can be defined for walks with small steps and properties of the groups induce a classification of the walks according the order of the group. This group is first defined by Malyshev in [105] for probabilistic applications (namely the study of the stationary distribution of Markov chains with small steps in the quarter plane). It has also been used to solve various enumeration problems (walks, permutations or set partitions, see [41, Sec. 1.2] and references therein) by generating

[9]These are models which differ from the following five step sets $\{\mathsf{NE}, \mathsf{NW}, \mathsf{SE}\}$, $\{\mathsf{N}, \mathsf{NW}, \mathsf{SE}\}$, $\{\mathsf{E}, \mathsf{NE}, \mathsf{N}, \mathsf{NW}, \mathsf{SE}\}$, $\{\mathsf{E}, \mathsf{N}, \mathsf{NW}, \mathsf{SE}\}$ and $\{\mathsf{NE}, \mathsf{N}, \mathsf{NW}, \mathsf{SE}\}$ (see the classification of [41]). A singular step set has each step $(i,j) \in \mathcal{S}$ satisfying$i + j \geq 0$. See the hypothesis (H) in Section 5.1 under which we do another description of a singular model.

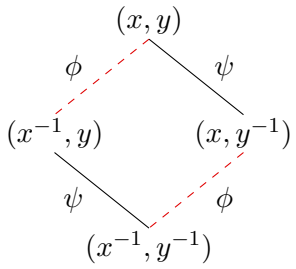

Figure 2.9 – Orbit of (x, y) under the group G in the simple walk case

multiples equations to work with. This notion of group only depends on the steps of the walks (thus not on the region of restriction). The group $G(\mathcal{S})$ of the walk is a group of bi-rational transformations generated by:

$$\begin{cases} \phi(x,y) &= \left(x^{-1}\frac{A_-(y)}{A_+(y)}, y\right), \\ \psi(x,y) &= \left(x, y^{-1}\frac{B_-(x)}{B_+(x)}\right), \end{cases} \tag{2.36}$$

where $A_-(x), A_+(x), B_-(y), B_+(y)$ are defined in (2.4). For example, consider the simple step set (see Table 2.1). The inventory polynomial $S(x, y) = x + y + x^{-1} + y^{-1}$, then $\Phi(x, y) = (x^{-1}, y)$ and $\Psi(x, y) = (x, y^{-1})$. The orbit of (x, y) under the group G gives three new elements (x^{-1}, y), (x^{-1}, y^{-1}) and (x, y^{-1}) (see Figure 2.9), then $G(\mathcal{S})$ is of order 4.

When the model is a walk in a Weyl chamber, the group of the model corresponds to the Weyl group and exists in higher dimension (see Section 5.2.2 for the dimension three). In dimension two, the group generated by ϕ and ψ is isomorphic to a dihedral group of order $2n$, with $n \in \{\mathbb{N} \setminus \{0, 1\}\} \cup \{\infty\}$. The order of the group for the 79 models is computed by Bousquet-Mélou and Mishna in [41]: there are 23 models with a finite group (16 of order 4, 5 of order 6 and 2 of order 8) and 56 models with infinite order. To find the order of a finite group, it suffices[10] to compute the orbit of (x, y) by Φ and Ψ. On the other side, showing that the orbit is infinite can be difficult. In [41, Sec. 3], Bousquet-Mélou and Mishna use a valuation argument for five step sets and a fixed point argument for the remaining case of infinite group.

Remark 12. The polynomial of the steps $S(x, y)$ is left unchanged by the action of ϕ and ψ. However, not all transformations of (x, y) that leave $S(x, y)$ unchanged are in $G(\mathcal{S})$. Indeed, let $\mathcal{S} = \{(1, 0), (0, 1), (-1, 0), (0, -1)\}$, the transformation $(x, y) \to (y, x)$ leaves $S(x, y)$ unchanged, but does not belong to $G(\mathcal{S})$.

In the case of large steps in dimension two, the notion of group does not exist anymore. However Bostan, Bousquet-Mélou and Melczer extend the small step terminology of orbit, which can be seen as the generalization of the group [28, Sec. 3] to big step models. As the group in the small-step

[10] Luckily enough, the (finite) orders are small!

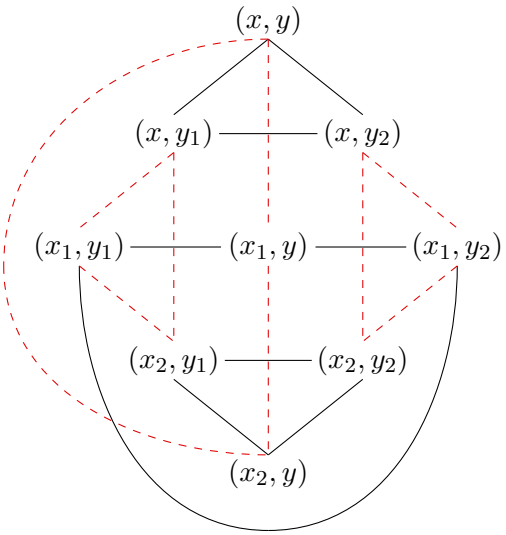

Figure 2.10 – Orbit of (x, y) when $S(x, y) = x^2 + y + x^{-1} + y^{-2}$. We have followed the convention of [28] with dashed (resp. solid) edges for 1-adjacency (resp. 2-adjacency)

case, the orbit notion allows to produce numerous variations of the functional equation which can be used to find an expression of the generating function of the walks. In the small step case, the inventory polynomial $S(x, y)$ is unchanged by the action of the group $G(\mathcal{S})$. The pairs $\phi(x, y)$, $\psi(x, y)$ are *adjacent* to (x, y): they give the same value to the inventory polynomial $S(x, y)$ and they have one coordinate in common. For example, in the simple walk case, (x^{-1}, y) and (x, y^{-1}) are adjacent to (x, y) (see Figure 2.9). The orbit of (x, y) is its equivalence class with respect to the transitive closure of the adjacency relation.

For example, let $S(x, y) = x^2 + y + x^{-1} + y^{-2}$. Solving $S(x, y) = S(X, y)$ in X gives the 1-adjacent elements (i.e., adjacent with respect to the first coordinate) to (x, y), namely (x_1, y) and (x_2, y) where $x_{1,2} = \frac{-x^2 \pm \sqrt{x^4+4x}}{2x}$. On the other side, solving $S(x, y) = S(x, Y)$ in Y gives (x, y_1) and (x, y_2), with $y_{1,2} = \frac{1 \pm \sqrt{4y^3+1}}{2y^2}$, which are the 2-adjacent elements to (x, y). Then we find the pairs (x_1, Y) adjacent to (x_1, y), and so on. We end up with an orbit sum composed of nine elements, see Figure 2.10.

The notion of group exists as well for model with small steps in higher dimension. The case of the three-dimensional walks is developed in Section 5.2.2.

2.3.2 Nature of the generating function of the walk

Generating functions of walks[11] can be classified by their nature[12]. A function can be *rational*, *algebraic*, *D-finite*[13], *D-algebraic* or *hypertranscendental*. These families have interesting closure properties and one has the following hierarchical chain

$$\text{rational} \subsetneq \text{algebraic} \subsetneq \text{D-finite} \subsetneq \text{D-algebraic}$$

The nature of a function gives some indications on the combinatorial structure it describes. For example, a subclass of algebraic functions called $\mathbb{N}$-algebraic consists of those functions which can be generated by a context-free grammar [9].

Let $F(t) = \sum_{n\geq 0} f(n)t^n$ be a formal power series. In addition to the classification of functions, knowing the nature is interesting for the properties it induces on the coefficients $f(n)$ of its series. Let p be the period of the coefficients $f(n)$.

Rational functions. The function $F(t)$ is *rational* if there exist $P(t)$ and $Q(t)$ two polynomials in t such that

$$F(t) = \frac{P(t)}{Q(t)}.$$

The coefficients $f(n)$ satisfy linear recurrence relations with constant coefficients, and for n big enough

$$f(pn) \sim \alpha \mu^{pn} (pn)^{\gamma},$$

with α and μ algebraic over $\mathbb{Q}$ and γ a non-negative integer. For example, let $f(n) = F_n$, the Fibonacci number. The function $\sum_{n\geq 0} F_n t^n = \frac{t}{1-t-t^2}$ is rational, the coefficients F_n satisfy the well-known linear recurrence $F_n = F_{n-1} + F_{n-2}$ with $F_0 = F_1 = 1$ and $F_n \sim \frac{\varphi^n}{\sqrt{5}}$, where $\varphi = \frac{1+\sqrt{5}}{2}$ is the golden ratio. The generating function of the number $f(n)$ of non-self-intersecting n-paths starting at $(0,0)$ with step set $\{(1,0),(-1,0),(0,1)\}$ is rational as well, see [120, Sec. 4.1.3].

Algebraic function. The function $F(t)$ is *algebraic* of degree d if there exist polynomials $(P_i(t))_{i=0}^{d}$ such that

$$P_0(t) + P_1(t)F(t) + \cdots + P_{d-1}(t)F^{d-1}(t) + P_d(t)F^d(t) = 0.$$

Equivalently, $F(t)$ satisfies a non trivial polynomial equation $P(t, F(t)) = 0$ with $P(t, X) \in \mathbb{C}[t, X]$ of degree d in its second variable. An algebraic function of degree 1 is rational. The coefficients

[11] or more generally, any generating functions which enumerates discrete objects (e.g., trees, words).

[12] References on this topic can be found in [120, Ch. 4], [121, Ch. 6] and in [79, Ch. IV, Ch. VII, App. B].

[13] one can also say *holonomic*.

$f(n)$ satisfy linear recurrence relations with polynomial coefficients, and

$$f(pn) \sim \alpha \mu^{pn} (pn)^{\gamma},$$

with α and μ algebraic over $\mathbb{Q}$ and $\gamma =\in \mathbb{Q} \setminus \{-1, -2, \dots\}$. For example, let $f(n) = \binom{2n}{n}$. The function $F(t) = \sum_{n \geq 0} \binom{2n}{n} t^n$ is algebraic because $(1-4t)F^2(t) - 1 = 0$. The coefficients $f(n)$ satisfy the relations $f(n+1) = \frac{2(2n+1)}{n+1} f(n)$ and thanks to the Stirling formula, we easily have $f(n) \sim \frac{4^n n^{-1/2}}{\sqrt{\pi}}$.

D-finite function. The function $F(t)$ is *D-finite* if it is solution of a linear differential equation The function $F(t)$ is D-finite of order d if there exist polynomials $(P_i(t))_{i=-1}^{d}$ such that

$$P_{-1}(t) + P_0(t)F(t) + P_1(t)F'(t) + \cdots + P_{d-1}(t)F^{(d-1)}(t) + P_d(t)F^{(d)}(t) = 0.$$

The coefficients $f(n)$ satisfy linear recurrence relations with polynomial coefficients, and a subclass of functions called G-functions [37, Sec. 1] has asymptotic behavior

$$f(pn) \sim \alpha \mu^{pn} (pn)^{\gamma} \left(\log(pn)\right)^{j},$$

where α, μ, γ are algebraic over $\mathbb{Q}$ and j is a non-negative integer. Ordinary generating functions of lattice walks are G-functions. For example, let $f(n) = n!$. The formal power series $F(t) = \sum_{n \geq 0} n! t^n$ satisfies the equation $t^2 F'(t) + (t-1)F(t) + 1 = 0$ and thus is D-finite of order 1. The coefficients $f(n)$ satisfy the relation $f(n+1) = (n+1)f(n)$ and $f(n) \sim \sqrt{2\pi n} \left(\frac{n}{e}\right)^n$ (Stirling formula).

D-algebraic function. The function $F(t)$ is *D-algebraic* if it satisfies an algebraic differential equation. The function $F(t)$ is D-algebraic of order d if there exists a polynomial $P(t, X_0, X_1, \dots, X_d)$ $\in \mathbb{C}\left[t, X_0, X_1, \dots, X_d\right]$ such that

$$P(t, F(t), F'(t), \dots, F^{(d-1)}(t), F^{d}(t)) = 0.$$

For example, the function $F(t) = \frac{1}{\cos(t)}$ is D-algebraic (but not D-finite) and satisfies the equation $F(t)F''(t) - 2\left(F'(t)\right)^2 - F(t)^2 = 0$. Less is known about this class of D-algebraic functions.

Hypertranscendental function. The function $F(t)$ is *hypertranscendental* if it is not D-algebraic. The Gamma function $\Gamma(t) = \int_0^\infty x^{t-1} e^{-x} \, \mathrm{d}x$ and the Riemann zeta function $\zeta(t) = \frac{1}{\Gamma(t)} \int_0^\infty \frac{x^{t-1}}{e^x - 1} \, \mathrm{d}x$ are famous hypertranscendental functions.

Each class of functions can be generalized to the multivariate case. For example, if F is a D-finite multivariate series, then F needs to satisfy one differential equation per variable.

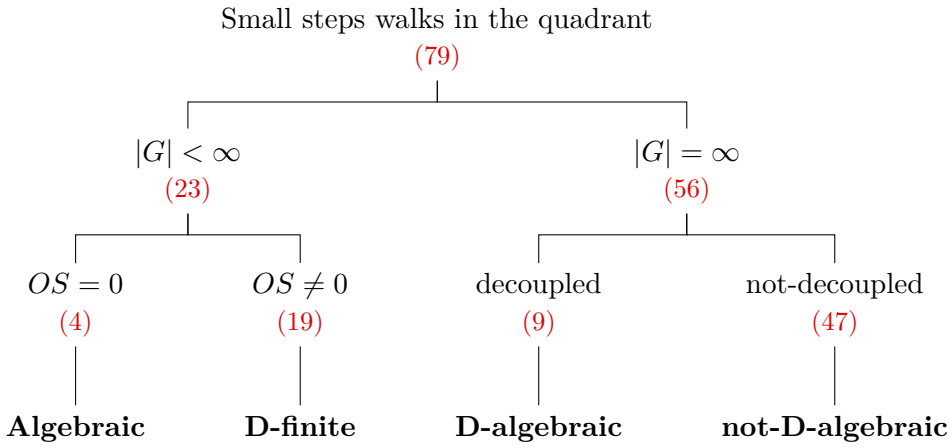

Table 2.2 – Classification of walks with small steps in the quadrant

Let us now recall results on the nature of the generating function of walks in cones. In $\mathbb{Z}^2$, the generating function is rational in the case of unrestricted walks and is algebraic for walks restricted to a half plane ([10] and [43, Prop. 2]). What about the walks restricted to the quadrant? At first sight, it is natural to think that quadrant walks have D-finite generating functions. However, Bousquet-Mélou and Petkovšek proved in [43] that the length generating function of *knight's walk* (with step set $\mathcal{S} = \{(-1,2),(2,-1)\}$) in the quarter plane starting at $(1,1)$ is not D-finite, and Mishna and Rechnitzer in [109] give two examples of non-D-finite small step walks in a quadrant.

Mishna started in [108] an algebraic classification for generating functions of walks with step set of cardinality three and conjectured the equivalence between the finiteness of the group and the D-finiteness of the generating function of walks [108, Conj. 1]. Bousquet-Mélou and Mishna [41] proved with combinatorial tools that 22 of the 23 models with finite group are D-finite and conjectured that the remaining 56 models with infinite group have a non-D-finite generating function. The missing case with finite group, known as the Gessel's walks, was more difficult than the other 22 to deal with. In parallel, using computer algebra, Bostan and Kauers [30] found again experimentally this classification of small step walks in the quadrant.

In 2001, Gessel made the conjecture that the number of excursions in the quarter plane for the Gessel step set satisfies a linear recurrence relation. Proving that the generating function of Gessel's walks is algebraic is not obvious at the first sight: the asymptotic of its coefficients is $4^n/n^{2/3}$, making the generating function non-$\mathbb{N}$-algebraic, thus not related to a nice and simple combinatorics structure. The conjecture of Gessel has been proven, using computer computations, in 2008 by Kauers, Koutschan and Zeilberger in [94]. In parallel, Kauers and Bostan in [31] get for the first time an explicit expression for the generating function of the Gessel's walks. A year later, using an analytic method, a contour-integral expression of the generating function of the walks is given by Kurkova and Raschel in [99]. The first human proof (i.e., without using a computer) has been given by Bostan, Kurkova and Raschel in 2013 [32]. In 2016, Bousquet-Mélou gives an

elementary solution of Gessel's walks in the quadrant [38] and the same year, along the study of the simple walk in the three quarter plane, Bousquet-Mélou gets another proof of Gessel's conjecture via the reflection principle [40].

Kurkova and Raschel proved in [100] that the 51 of the 56 models with infinite group have a non-D-finite trivariate generating function. An alternative proof is given by Bostan, Raschel and Salvy in [34], using the non-D-finiteness of the generating function of excursions $Q(0,0)$. The univariate generating function of the number of walks for the 5 remaining cases, called *singular walks*, has been proven to be non-D-finite by Mishna and Rechnitzer in [109] for two cases and by Melczer and Mishna in [106] for the last three cases.

Finally, quadrant-walks are D-finite if and only if the associated group is finite. In addition to Gessel's step set, three other models are algebraic, namely the Kreweras trilogy. In [101], Kurkova and Raschel show that the generating function is algebraic as long as a certain sum is zero. This sum, denoted by the *Orbit sum*[14], is obtained by the action of the group $G(\mathcal{S})$ defined in Section 2.3.1 on the functional equation (2.11). More recently, in [17], Bernardi, Bousquet-Mélou and Raschel present the notion of Tutte's invariant for proving algebraicity and can be even extended for proving D-algebraicity: the existence of a *decoupling function* is equivalent to algebraicity in the case of a finite group and to D-algebraicity in the case of an infinite group. Using Galois theory of difference equations, Dreyfus, Hardouin, Roques and Singer find back the D-algebraicity of nine cases with infinite group and prove the hypertranscendence of the 47 other models with infinite group [62]. The complete classification of walks in a quadrant is sumarized in Table 2.2.

[14]Orbit Sum is abbreviated as OS.

Chapter 3

Walks avoiding a quadrant[1]

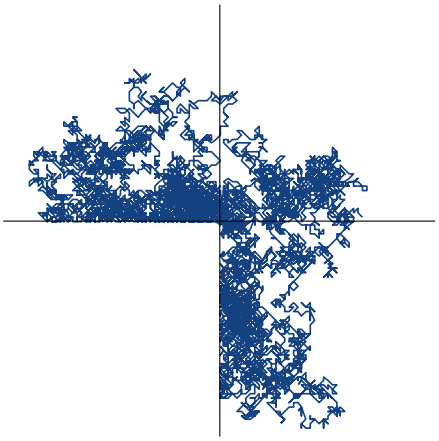

A random 10,000 step walk in the three quarter plane

3.1 Introduction

Two-dimensional (random) walks in cones are very natural both in combinatorics and probability theory: they are interesting in their own right and also in relation to other discrete structures. As we have seen in Section 1.1 and Chapter 2, most of the attention has been devoted to the case of convex cones and one now has a very good understanding of these quadrant models, most of the time via their generating function, which counts the number of walks of length n, starting from a fixed point, ending at an arbitrary point (i, j) and remaining in the cone (see (2.2)). Throughout the present chapter, all walk models will be assumed to have small steps, i.e., jumps in $\{-1, 0, 1\}^2$.

[1]This chapter is mainly from [115].

Given the vivid interest in combinatorics of walks confined to a quadrant, it is very natural to consider next the non-equivalent case of non-convex cones, as in particular the union of three quadrants

$$\mathcal{C} = \{(i,j) \in \mathbb{Z}^2 : i \geq 0 \text{ or } j \geq 0\},$$

see Figure 3.1. Following Bousquet-Mélou [40], we will also speak about walks avoiding a quadrant. Although walks avoiding a quarter plane have many common features with walks in a quarter plane, the former cited model is definitely much more complicated. To illustrate this fact, let us recall [40] that the simple walk (usually the simplest model, see model 1.1 in Table 2.1) in three quadrants has the same level of complexity as the notoriously difficult Gessel's model (see model 3.1 in Table 2.1) [31, 39] in the quadrant!

Three-quadrant walks have been approached only recently. In [40], Bousquet-Mélou solves the simple walk and the diagonal walk (see model 1.1 and model 1.2 in Table 2.1 for a representation of these step sets) starting at various points. She obtains an exact expression for the generating function and derives several combinatorial identities, among which a new proof of Gessel's conjecture via the reflection principle. Mustapha [111] computes the asymptotics of the number of walks of length n in the case of zero-drift small step sets as well as the asymptotics of the number of excursions for all small step models, following [58, 34] (interestingly and in contrast with combinatorics, the probabilistic results [58, 111] on random walks in cones do not really depend on convexity). Using an original connection with planar maps, Budd [46] obtains various enumerating formulas for planar walks, keeping track of the winding angle. These formulas can be used to enumerate simple walks in the three-quarter plane [46, 110].

In this chapter we present the analytic approach of [71, 72, 113] applied to walks in three quadrants, thereby answering a question of Bousquet-Mélou in [40, Sec. 7.2].

Strategy. Once a step set $\mathcal{S}$ is fixed, our starting point is a functional equation satisfied by the generating function

$$C(x,y) = \sum_{n \geq 0} \sum_{(i,j) \in \mathcal{C}} c_{i,j}(n) x^i y^j t^n, \tag{3.1}$$

where $c_{i,j}(n)$ counts n-step $\mathcal{S}$-walks going from $(0,0)$ to (i,j) and remaining in $\mathcal{C}$. Stated already as (2.10), this functional equation translates the step-by-step construction of three-quadrant walks and takes into account the forbidden moves which would lead the walk into the forbidden negative quadrant. At first sight, this equation is very similar to its one-quadrant analogue (we compare the equations (2.10) to (2.8) in Section 2.1.1), the only difference is that negative powers of x and y arise: this can be seen in the definition of the generating function (3.1) and on the functional equation (2.10) as well, since the right-hand side of the latter involves some generating functions in the variables $\frac{1}{x}$ and $\frac{1}{y}$. This difference is fundamental and the methodology of [41, 113] (namely,

performing algebraic substitutions or evaluating the functional equation at well-chosen complex points) breaks down, as the series are no longer convergent.

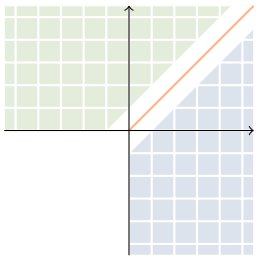

Figure 3.1 – Splitting of the three-quadrant cone in two wedges of opening angle $\frac{3\pi}{4}$

The idea in [40] is to see $\mathcal{C}$ as the union of three quarter planes, and to state for each quadrant a new equation, which is more complicated but (by construction) may be evaluated. Our strategy follows the same line: we split the three-quadrant in two convex cones (of opening angle $\frac{3\pi}{4}$, see Figure 3.1) and write a system of two functional equations, one for each domain. The drawbacks of this decomposition is that it increases the complexity:

- There are two functional equations instead of one;
- The functional equations involve more unknowns (corresponding to the diagonal and close-to-diagonal terms) in their right-hand sides, see Section 3.2.

On the other hand:

- The fundamental advantage is that the new equations may be evaluated—and ultimately will be solved;
- Unexpectedly, this splitting of the cone (see Figure 3.1) allows us to relate the combinatorial model of walks avoiding a quadrant to an interesting class of *space-inhomogeneous walks*, among which a well-known problem in queueing theory: the Join-the-Shortest-Queue (JSQ) model, see Section 3.4.1.

Main result: a contour-integral expression for the generating function. Throughout this chapter we will do the following assumption:

(H) The step set $\mathcal{S}$ is symmetric (i.e., if $(i,j) \in \mathcal{S}$ then $(j,i) \in \mathcal{S}$) and does not contain the jumps $(-1,1)$ and $(1,-1)$.

An exhaustive list of which step sets obey (H) is given on Figures 3.2a and 3.2b. We are not able to deal with asymmetric walks (as we are unable to solve the asymmetric JSQ model, see Section 3.4.1), because of the complexity of the functional equations. The jumps $(-1,1)$ and $(1,-1)$ are discarded for similar reasons: they would lead to additional terms in the functional equation (see Figure 3.6).

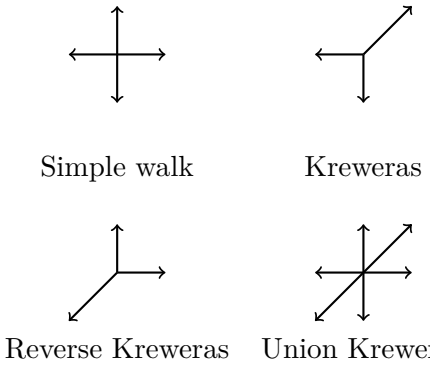

(a) Symmetric models with a finite group. The notion of group associated to a model is recalled in Section 2.3.1

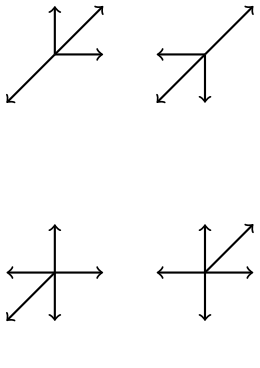

(b) Symmetric models with infinite group

Figure 3.2 – Symmetric models with no jumps $(-1,1)$ and $(1,-1)$

Our main result is a contour-integral expression for the diagonal section

$$D_\varphi(x) = \sum_{n\geq 0, i\geq 0} c_{i,i}(n) x^i t^n.$$

We shall see later that knowing $D_\varphi(x)$ actually suffices to give a complete solution to the problem (i.e., to find an expression for $C(x,y)$ in (3.1)). Let us postpone to Theorem 15 the very precise statement, and instead let us give now the main idea and the shape of the solution. We will show that

$$D_\varphi(x) = w'(x) f(w(x)) \int g(z, w(z)) \frac{w'(z)}{w(x) - w(z)} \, \mathrm{d}z, \tag{3.2}$$

where f and g are algebraic functions. The integral in (3.2) is taken over a quartic curve, constructed from the step set of the model. The function w is interpreted as a conformal mapping for the domain bounded by the quartic (see Section 2.1.2), and its algebraic nature heavily depends on the model under consideration: it can be algebraic (finite group case) or non-D-finite (otherwise).

Five consequences of our main results. Our first contribution is methodology: we show that under the symmetry condition (H), three-quadrant walk models are exactly solvable, in the sense that their generating function admits an explicit (contour-integral) expression (3.2).

The second point is that our techniques allow to compare walks in a quadrant and walks in three quadrants. More precisely, it is proved in [113] that the generating function counting quadrant walks ending on the horizontal axis can typically be expressed as

$$\widetilde{f}(x) \int \widetilde{g}(z) \frac{w'(z)}{w(x) - w(z)} \, \mathrm{d}z, \tag{3.3}$$

with the same function w as in (3.2) but different functions $\widetilde{f}$ (rational) and $\widetilde{g}$ (algebraic). Though simpler, Equation (3.3) is quite similar to (3.2). This similarity opens the way to prove combinatorial formulas relating the two models.

Our third corollary is a partial answer to two questions raised by Bousquet-Mélou in [40], that we briefly recall: first, could it be that for any step set associated with a finite group, the generating function $C(x, y)$ is D-finite? Second, could it be that for the four step sets [Kreweras, reverse Kreweras, union Kreweras (see Figure 3.2a) and Gessel (model 3.1 in Table 2.1)], for which [the quadrant generating function] is known to be algebraic, $C(x, y)$ is also algebraic?

The expression (3.2) rather easily implies that if w is algebraic (which will correspond to the finite group case, see Section 2.3.1), the generating function $D(x)$ is D-finite, being the Cauchy integral of an algebraic function. On the other hand, when the group is infinite the function w is non-D-finite by [113, Thm 2], and the expression (3.2) uses non-D-finite functions (note, this does not a priori imply that $D(x)$ itself is non-D-finite, but does provide some evidence).

Next, although we do not solve them, the expression (3.2) provides a way to attack the following questions:

- Starting from the integral (3.3), various asymptotic questions concerning quadrant models are solved in [74] (asymptotics of the excursions, of the number of walks returning to one axis, etc.). Similar arguments should lead to the asymptotics of walks in three quadrants. Remember, however, that the asymptotics of the excursion sequence is already found in [111].

- A further natural question (still unsolved in the quadrant case) is to find, in the finite group case, a concrete differential equation (or minimal polynomial in case of algebraicity) for the generating function, starting from the contour integrals (3.2) or (3.3). It seems that the technique of creative telescoping could be applied to the contour integral expressions.

- Several interesting (and sometimes surprising) combinatorial identities relating quadrant walks to three-quadrant walks are proved in [40] (in particular, a proof of the former Gessel's conjecture by means of simple walks in $\mathcal{C}$ and the reflection principle). Moreover, Bousquet-Mélou asks in [40] whether $C(x, y)$ could differ from (a simple D-finite series related to) the quadrant generating function by an algebraic series? Taking advantage of the similarity between (3.2) and (3.3) provides a starting point to answer this question.

Finally, along the way of proving our results, we develop a noteworthy concept of anti-Tutte's invariant, namely a function g such that ($\overline{y}$ denoting the complex conjugate number of $y \in \mathbb{C}$)

$$g(y) = \frac{1}{g(\overline{y})} \tag{3.4}$$

when y lies on the contour of (3.2). The terminology comes from [17], where a function g satisfying $g(y) = g(\overline{y})$ is called a Tutte invariant and is strongly used in solving the models. Originally,

Tutte introduced the notion of invariant to solve a functional equation counting colored planar triangulations, see [123]. Tutte's equation is rather close to functional equations arising in two-dimensional counting problems. Interestingly, a function g as in (3.4) appears in the book [50], which proposes an analytic approach to quadrant walk problems (the latter is more general than [72] in the sense that it works for arbitrarily large positive jumps, i.e., not only small steps). In [50] it is further assumed that $g(\overline{y}) = \overline{g(y)}$, so that with (3.4) one has $|g(y)| = 1$, and g may be interpreted as a conformal mapping from the domain bounded by contour of (3.2) onto the unit disc.

Equations with (too) many unknowns. What about asymmetric models? From a functional equation viewpoint, the latter are close to random walks with big jumps [75, 28] or random walks with catastrophes [11], in the sense that the functional equation has more than two unknowns in its right-hand side. One idea to get rid of these extra terms is to transform the initial functional equation, as in [40], where Bousquet-Mélou solves the simple and diagonal models, starting from non-symmetric points ($(-1, 0)$, for instance). Another idea, present in [28], is to extend the kernel method by computing weighted sums of several functional equations, each of them being an algebraic substitution of the initial equation. However, finding such combinations is very difficult in general.

From the complex analysis point of view [72, 113, 75], equations with many unknowns become systems of boundary value problems, which seem not to have a solution in the literature. It is also shown in [72, Chap. 10] that the asymmetric JSQ is equivalent to solving an integral Fredholm equation for the generating function, but again, no closed-form expression seems to exist.

Structure of the chapter. In *Section 3.2*, we write various functional equations in the $\frac{3\pi}{4}$-cone (Lemma 13) and present a change of variable φ (3.9) which simplifies the resolution of the problem.

In *Section 3.3*, we state a boundary value problem (BVP) satisfied by the diagonal generating function (Lemma 14) and solve this BVP (Theorems 15 and 16). We also give a list and properties of conformal mappings used in Theorems 15 and 16.

In *Section 3.4.1*, we suppose that the step set is not necessarily symmetric anymore. We set a system of functional equations and relate the problem of walks in the three quadrants to inhomomegeous walks and JSQ model.

3.2 Functional equations for the $\frac{3\pi}{4}$-cone walks

In this section and in the remainder of this chapter, we shall use two different step sets, $\mathcal{S}$ and $\mathcal{S}_\varphi$[2]. The first one, $\mathcal{S}$, will refer to the main step set, corresponding to the walks in the three-quarter

[2]For the sake of consistency throughout this thesis, notation in this chapter are slightly different from the ones in [115] where for example $\widehat{\mathcal{S}}$ stand for $\mathcal{S}$ and $\mathcal{S}$ stands for $\mathcal{S}_\varphi$.

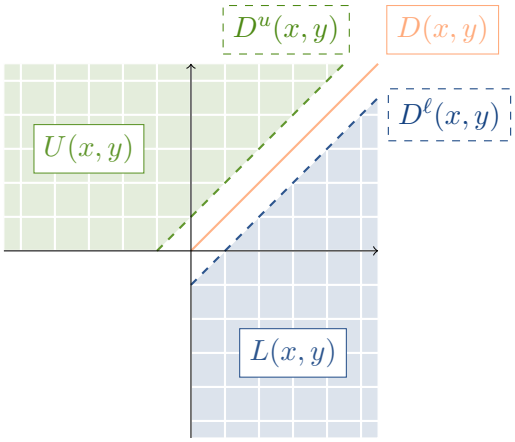

Figure 3.3 – Decomposition of the three-quarter plane and associated generating functions

plane we are counting. The second step set, $\mathcal{S}_\varphi$, is associated to $\mathcal{S}$ after the change of variable (3.9). Quantities with a φ-tag will be associated to the step set $\mathcal{S}_\varphi$, for instance the kernel $K_\varphi(x,y)$. In order not to make the notation too heavy and because in this case there is no possible ambiguity, the only exception to this rule will be the coefficients $c_{i,j}(n)$, which will always correspond to $\mathcal{S}$. Thereafter, unless explicitly mentioned, we will only consider symmetric models starting at $(0,0)$, but notice that our study can be easily generalized to arbitrary diagonal starting points.

Having said that, we start by splitting the domain of possible ends of the walks into three parts: the diagonal, the lower part $\{i \geq 0, j \leq i-1\}$ and the upper part $\{j \geq 0, i \leq j-1\}$, see Figure 3.1. We may write

$$C(x,y) = L(x,y) + D(x,y) + U(x,y), \tag{3.5}$$

where

$$L(x,y) = \sum_{\substack{i\geq 0\\ j\leq i-1\\ n\geq 0}} c_{i,j}(n)x^i y^j t^n, \quad D(x,y) = \sum_{\substack{i\geq 0\\ n\geq 0}} c_{i,i}(n)x^i y^i t^n \quad \text{and} \quad U(x,y) = \sum_{\substack{j\geq 0\\ i\leq j-1\\ n\geq 0}} c_{i,j}(n)x^i y^j t^n.$$

Let $\delta_{i,j} = 1$ if $(i,j) \in \mathcal{S}$ and 0 otherwise.

Lemma 13. *For any step set which satisfies* (H) *and walk that starts at* $(0,0)$*, one has*

$$\begin{aligned} K(x,y)L(x,y) = &-\frac{1}{2}xy + txy\left(\delta_{-1,-1}x^{-1}y^{-1} + \delta_{-1,0}x^{-1}\right)L_{0-}(y^{-1}) + \frac{1}{2}t\delta_{-1,-1}D(0,0) \\ &- xy\left(-\frac{1}{2} + t\left(\frac{1}{2}(\delta_{1,1}xy + \delta_{-1,-1}x^{-1}y^{-1}) + \delta_{0,-1}y^{-1} + \delta_{1,0}x\right)\right)D(x,y), \end{aligned} \tag{3.6}$$

with $L_{-0}(y^{-1}) = \sum_{n\geq 0, j\leq -1} c_{0,j}(n)y^j t^n$.

Proof. The decomposition in (3.5) expresses $C(x,y)$ as a sum of three generating functions. Thanks to the symmetry of the step set and the fact that the starting point lies on the diagonal, $U(x,y) = L(y,x)$ and $C(x,y)$ is written as the sum $L(x,y) + D(x,y) + L(y,x)$ of two unknowns. We further introduce the generating functions

$$D^{\ell}(x,y) = \sum_{n\geq 0, i\geq 0} c_{i,i-1}(n) x^i y^{i-1} t^n \quad \text{and} \quad D^{u}(x,y) = \sum_{n\geq 0, i\geq 0} c_{i-1,i}(n) x^{i-1} y^i t^n,$$

which respectively count walks ending on the lower (resp. upper) diagonal, see Figure 3.3.

Classically [41], one constructs a walk by adding a new step at the end of the walk at each stage. We first derive a functional equation for $L(x,y)$ by taking into account all possibilities of ending in the lower part:

- We may add a step from $\mathcal{S}$ to walks ending in the lower part, yielding below in (3.7) the term $t(\sum_{(i,j)\in\mathcal{S}} x^i y^j) L(x,y)$, see the second picture on Figure 3.4 in the particular case of the simple walk;
- Walks coming from the diagonal also need to be counted up, giving rise in (3.7) to the term $t(\delta_{1,0}x + \delta_{0,-1}y^{-1})D(x,y)$ (third picture on Figure 3.4);
- On the other hand, walks going out of the three-eighth plane need to be removed, yielding the terms $t(\delta_{-1,0}x^{-1} + \delta_{0,1}y)D^{\ell}(x,y)$ (from the lower diagonal) and $t(\delta_{-1,0}x^{-1} + \delta_{-1,-1}x^{-1}y^{-1})L_{0-}(y^{-1})$ (from the negative y-axis), see the fourth and fifth pictures on Figure 3.4;
- We finally add the term $t\delta_{-1,0}x^{-1}\sum_{n\geq 0} c_{0,-1}(n)y^{-1}t^n$ which was subtracted twice, corresponding to the rightmost picture on Figure 3.4.

We end up with a first functional equation:

$$\begin{aligned} L(x,y) = t\sum_{(i,j)\in\mathcal{S}} x^i y^j L(x,y) + t(\delta_{1,0}x + \delta_{0,-1}y^{-1})D(x,y) - t(\delta_{-1,0}x^{-1} + \delta_{0,1}y)D^{\ell}(x,y) \\ - t(\delta_{-1,0}x^{-1} + \delta_{-1,-1}x^{-1}y^{-1})L_{0-}(y^{-1}) + t(\delta_{-1,0}x^{-1})\sum_{n\geq 0} c_{0,-1}(n)y^{-1}t^n. \quad (3.7) \end{aligned}$$

Before we prove the second equation

$$\begin{aligned} D(x,y) = 1 + t(\delta_{1,1}xy + \delta_{-1,-1}x^{-1}y^{-1})D(x,y) - t\delta_{-1,-1}x^{-1}y^{-1}D(0,0) \\ + 2t(\delta_{-1,0}x^{-1} + \delta_{0,1}y)D^{\ell}(x,y) - 2t\delta_{-1,0}x^{-1}\sum_{n\geq 0} c_{0,-1}(n)y^{-1}t^n, \quad (3.8) \end{aligned}$$

let us remark that we can we can eliminate $D^{\ell}(x,y)$ from (3.7) using (3.8) and get (3.6), thereby completing the proof of Lemma 13.

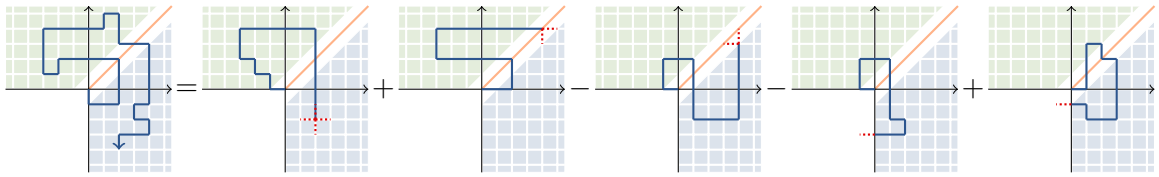

Figure 3.4 – Different ways to end in the lower part (example of the simple walk)

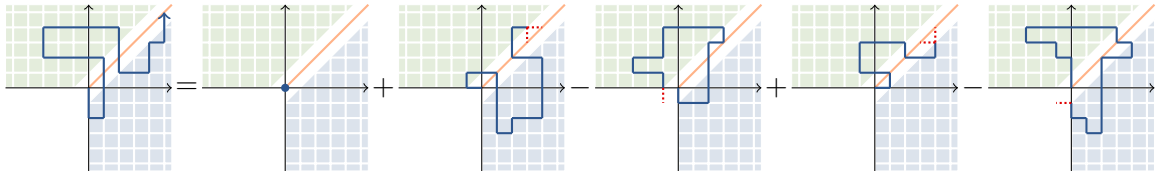

Figure 3.5 – Different ways to end on the diagonal (example of the simple walk)

This second equation (3.8) is obtained by writing all possibilities of ending on the diagonal, as illustrated on Figure 3.5 for simple walks:

- we first count the empty walk, giving the term 1;
- we add the walks remaining on the diagonal $t(\delta_{1,1}xy+\delta_{-1,-1}x^{-1}y^{-1})D(x,y)$, the walks ending on the diagonal coming from the upper part $t(\delta_{0,-1}y^{-1}+\delta_{1,0}x)D^u(x,y)$ and those coming from the lower part $t(\delta_{-1,0}x^{-1}+\delta_{0,1}y)D^\ell(x,y)$;
- finally, walks going out of the domain need to be removed, giving $t\delta_{-1,-1}x^{-1}y^{-1}D(0,0)$, $t\delta_{0,-1}y^{-1}\sum_{n\geq 0}c_{-1,0}(n)x^{-1}t^n$ and $t\delta_{-1,0}x^{-1}\sum_{n\geq 0}c_{0,-1}(n)y^{-1}t^n$.

Thanks to the symmetry of the step set, the number of walks coming from the upper part is the same as the number of walks coming from the lower part: $t(\delta_{0,-1}y^{-1}+\delta_{1,0}x)D^u(x,y) = t(\delta_{-1,0}x^{-1}+\delta_{0,1}y)D^\ell(x,y)$ and $t\delta_{0,-1}y^{-1}\sum_{n\geq 0}c_{-1,0}(n)x^{-1}t^n = t\delta_{-1,0}x^{-1}\sum_{n\geq 0}c_{0,-1}(n)y^{-1}t^n$. □

In order to simplify the functional equation (3.6), we perform the change of variable

$$\varphi(x,y) = (xy, x^{-1}). \tag{3.9}$$

Then (3.6) becomes

$$K_\varphi(x,y)L_\varphi(x,y) = c_\varphi(x)L_\varphi(x,0) - x\left(x\widetilde{a}_\varphi(y) + \frac{\widetilde{b}_\varphi(y)}{2}\right)D_\varphi(y) + \frac{1}{2}t\delta_{-1,-1}xD_\varphi(0) - \frac{1}{2}xy, \tag{3.10}$$

Model	Image under φ
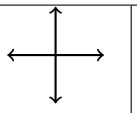	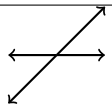
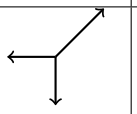	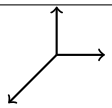
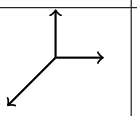	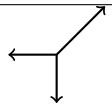
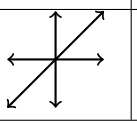	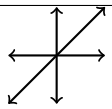

Model	Image under φ
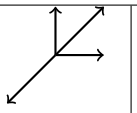	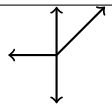
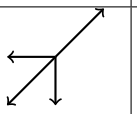	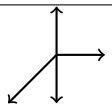
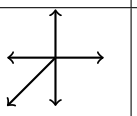	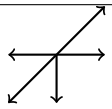
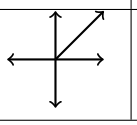	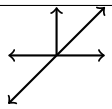

Table 3.1 – Transformation φ on the eight symmetric models (with finite group on the left and infinite group on the right) without the steps $(-1,1)$ and $(1,-1)$. In particular, the simple walk is related by φ to Gessel's model. After [40], this is another illustration that counting simple walks in three-quarter plane is related to counting Gessel walks in a quadrant

where $K_\varphi(x,y) = xy(t\sum_{(i,j)\in\varphi(\mathcal{S})} x^{i-j}y^i - 1) = xK(\varphi(x,y))$, $L_\varphi(x,0) = \sum_{n\geq 0, j\geq 1} c_{0,-j}x^j t^n$ and similarly

$$L_\varphi(x,y) = L(\varphi(x,y)) = \sum_{\substack{i\geq 1\\ j\geq 0\\ n\geq 0}} c_{j,j-i}(n)x^i y^j t^n \quad \text{and} \quad D_\varphi(y) = D(\varphi(x,y)) = \sum_{\substack{i\geq 0\\ n\geq 0}} c_{i,i}(n)y^i t^n. \quad (3.11)$$

The change of coordinates φ simplifies the resolution of the problem, as the functional equation (3.10) is closer to a (solvable) quadrant equation; compare with (2.11). We have

$$\mathcal{S}_\varphi = \varphi(\mathcal{S}) = \{(i-j,i) : (i,j) \in \mathcal{S}\}.$$

For the reader's convenience, we have represented on Table 3.1 the effect of φ on the symmetric models of Figures 3.2a and 3.2b. We also remark on Figure 3.6 that the presence of anti-diagonal jumps $(-1,1)$ or $(1,-1)$ would lead to the bigger steps $(-2,-1)$ or $(2,1)$; this is the reason why they are discarded.

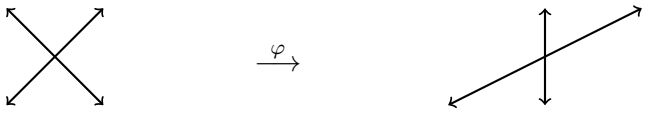

Figure 3.6 – The diagonal model is transformed by φ into a model with bigger steps

3.3 Expression for the generating functions

3.3.1 Main results and discussion

The first and crucial point is to prove that the diagonal $D_\varphi(y)$ in (3.11) satisfies a boundary value problem (BVP), in the sense of the lemma below, the proof of which is postponed to Section 3.3.3. Let $\mathcal{D}$ denote the open unit disc, $\widetilde{d}_\varphi$ be the discriminant (2.15) and $\mathcal{G}_{\mathcal{L}_\varphi}$ be the open set delimited by the curve $\mathcal{L}_\varphi$ (2.18).

Lemma 14. *The function $D_\varphi(y)$ can be analytically continued from the unit disc[3] to the domain $\mathcal{D}\cup\mathcal{G}_{\mathcal{L}_\varphi}$ and admits finite limits on $\mathcal{L}_\varphi$. Moreover, $D_\varphi(y)$ satisfies the following boundary condition, for $y \in \mathcal{L}_\varphi$:*

$$\sqrt{\widetilde{d}_\varphi(y)}D_\varphi(y) - \sqrt{\widetilde{d}_\varphi(\overline{y})}D_\varphi(\overline{y}) = y - \overline{y}. \tag{3.12}$$

In the remainder of the chapter, we prove Lemma 14 in two different ways, leading to the contour-integral expressions of $D_\varphi(y)$ given in Theorem 15 and Theorem 16 below. Let us first remark that contrary to the usual quadrant case [113], the prefactor $\sqrt{\widetilde{d}_\varphi(y)}$ in front of the unknown $D_\varphi(y)$ is not meromorphic in $\mathcal{G}_{\mathcal{L}_\varphi}$, simply because it is the square root of a polynomial, two roots of which being located in $\mathcal{G}_{\mathcal{L}_\varphi}$ (see Chapter 2, Section 2.1.2). This innocent-looking difference has strong consequences on the resolution:

- Due to the presence of a non-meromorphic prefactor in Equation (3.12), solving the BVP of Lemma 14 requires the computation of an index (in the sense of Section 3.3.4 and Definition 7). This index is an integer and will be non-zero in our case, which will increase the complexity of the solutions. In Theorem 15 we solve the BVP by taking into account this non-zero index.

- A second, alternative idea is to reduce to the case of a meromorphic boundary condition, and thereby to an index equal to 0. To do so, we will find an analytic function f_φ with the property that

$$\frac{\sqrt{\widetilde{d}_\varphi(\overline{y})}}{\sqrt{\widetilde{d}_\varphi(y)}} = \frac{f_\varphi(\overline{y})}{f_\varphi(y)} \tag{3.13}$$

  for $y \in \mathcal{L}_\varphi$, see Section 3.3.5 for more details. Such a function f_φ allows us to rewrite Equation (3.12) as

$$f_\varphi(y)D_\varphi(y) - f_\varphi(\overline{y})D_\varphi(\overline{y}) = \frac{f_\varphi(y)}{\sqrt{\widetilde{d}_\varphi(y)}}(y - \overline{y}), \tag{3.14}$$

  which by construction admits a meromorphic prefactor $f_\varphi(y)$. In Theorem 16 we solve this zero-index BVP by this technique.

[3] Because $t \in (0, 1/|\mathcal{S}|)$, we already know that $D_\varphi(y)$ is holomorphic in $\mathcal{D}$.

Although they represent the same function $D_\varphi(y)$ (and so should be equal!), it will be apparent that the expressions obtained in Theorems 15 and 16 are quite different, and that the second one is simpler. However, we decided to present the two resolutions, as we think that they offer different insights on this boundary value method, and also because it is not obvious at all to be able to solve an equation of the form (3.13) and thereby to reduce to the zero-index case. Recall (Section 2.1.2 and see Figure 3.9) that $\mathcal{L}_{\varphi,0}$ is the upper half of the curve $\mathcal{L}_\varphi$ and let w_φ be a conformal gluing function in the sense of Definition 9 for $\mathcal{G}_{\mathcal{L}_\varphi}$ [4].

Theorem 15. *Let w_φ be a conformal gluing function with a pole at $y_{\varphi,2}$. For any step set $\mathcal{S}$ satisfying* (H)*, the diagonal section* (3.11) *can be written, for $y \in \mathcal{G}_{\mathcal{L}_\varphi}$,*

$$D_\varphi(y) = \frac{\Psi(w_\varphi(y))}{2i\pi} \int_{\mathcal{L}_{\varphi,0}} \frac{z-\overline{z}}{\sqrt{\widetilde{d}_\varphi(z)}} \frac{w'_\varphi(z)}{\Psi^+(w_\varphi(z))(w_\varphi(z)-w_\varphi(y))}\,\mathrm{d}z,$$

with

$$\begin{cases} \Gamma(w_\varphi(y)) &= \dfrac{1}{2i\pi}\displaystyle\int_{\mathcal{L}_{\varphi,0}} \log\left(\frac{\sqrt{\widetilde{d}_\varphi(\overline{z})}}{\sqrt{\widetilde{d}_\varphi(z)}}\right) \frac{w'_\varphi(z)}{w_\varphi(z)-w_\varphi(y)}\,\mathrm{d}z, \\ \Psi(y) &= (y - Y_\varphi(x_{\varphi,1}))\exp\Gamma(y). \end{cases}$$

The left limits Ψ^+, Γ^+ of Ψ, Γ are related by

$$\Psi^+(y) = (y - Y_\varphi(x_{\varphi,1}))\exp\Gamma^+(y)$$

and the left limit Γ^+ can be computed with the help of Sokhotski-Plemelj formulas, that we have recalled in Proposition 6 of Section 2.1.2.

All quantities are defined relatively to the step set $\mathcal{S}_\varphi = \varphi(\mathcal{S})$ after the change of coordinates (3.9)*.*

We now turn to our second main result.

Theorem 16. *Let w_φ be a conformal gluing function with a pole at $y_{\varphi,2}$, with residue r. For any step set $\mathcal{S}$ satisfying* (H)*, the diagonal section* (3.11) *can be written, for $y \in \mathcal{G}_{\mathcal{L}_\varphi}$,*

$$D_\varphi(y) = \frac{-w'_\varphi(y)\sqrt{r}}{\sqrt{\widetilde{d}'_\varphi(y_{\varphi,2})(w_\varphi(y)-w(Y_\varphi(x_{\varphi,1})))(w_\varphi(y)-w(Y_\varphi(x_{\varphi,2})))}} \\ \frac{1}{2i\pi}\int_{\mathcal{L}_\varphi} \frac{z w'_\varphi(z)}{\sqrt{w_\varphi(z)-w_\varphi(y_{\varphi,1})}(w_\varphi(z)-w_\varphi(y))}\,\mathrm{d}z.$$

[4] Unlike the usual notation (see Definition 9), in the interest of simplification, in this chapter w is a conformal gluing function for the set $\mathcal{G}_\mathcal{L}$ (instead of $\mathcal{G}_\mathcal{M}$).

All quantities are defined according to the step set $\mathcal{S}_\varphi = \varphi(\mathcal{S})$.

Remark 17. Here are some comments about these results:

• First, it is important to notice that having an expression for $D_\varphi(y)$ is sufficient for characterizing the complete generating function $C(x,y)$. Indeed, one is easily convinced that

$$C(x,y) = L_\varphi(\varphi^{-1}(x,y)) + D_\varphi(\varphi^{-1}(x,y)) + L_\varphi(\varphi^{-1}(y,x)),$$

with

$$\begin{cases} L_\varphi(x,y) &= \dfrac{1}{K_\varphi(x,y)}\left(c_\varphi(x)L_\varphi(x,0) - x\left(x\widetilde{a}_\varphi(y) + \dfrac{1}{2}\widetilde{b}_\varphi(y)\right)D_\varphi(y) - \dfrac{1}{2}xy\right), \\ L_\varphi(x,0) &= \dfrac{x}{c_\varphi(x)}\left(\dfrac{1}{2}Y_{\varphi,0}(x) + \left(x\widetilde{a}_\varphi(Y_{\varphi,0}(x)) + \dfrac{1}{2}\widetilde{b}_\varphi(Y_{\varphi,0}(x))\right)D_\varphi(Y_{\varphi,0}(x))\right), \\ \varphi^{-1}(x,y) &= (y^{-1}, xy). \end{cases}$$

• Regarding the question of determining the algebraic nature of the diagonal series $D_\varphi(y)$, the expression in Theorem 16 is much simpler than that of Theorem 15. Indeed, the integrand as well as the prefactor of the integral of Theorem 16 are algebraic functions of y, z, t and w_φ (and its derivative) evaluated at various points. In addition, let us recall from [113, Thm 2] that w is algebraic if and only if the group is finite, and non-D-finite in the infinite group case. See Table 3.2 below for some implications. On the contrary, based on the exponential of a D-finite function, the integrand in Theorem 15 is a priori non-algebraic.

Model	Nature of w	Nature of $Q(x,y)$	Nature of $C(x,y)$
	rational [113]	D-finite [41]	D-finite by [40] and Thm 16
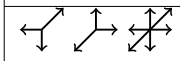	algebraic [113]	algebraic [41]	D-finite by Thm 16; algebraic?
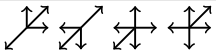	non-D-finite [113]	non-D-finite in t [34] non-D-finite in x,y [100, 61]	non-D-finite in t [111]; non-D-finite in x,y?

Table 3.2 – Algebraic nature of the conformal mapping w, the quadrant generating function $Q(x,y)$ and the three-quarter plane counting function $C(x,y)$

• Lemma 14 states that the function $D_\varphi(y)$ can be analytically continued to the domain $\mathcal{D}\cup\mathcal{G}_{\mathcal{L}_\varphi}$. This is apparent on the first statement (using properties of contour integrals). This is a little bit less explicit on Theorem 16, because of the prefactor.

• Theorem 15 (resp. Theorem 16) will be proved in Section 3.3.4 (resp. Sections 3.3.5 and 3.3.6).

3.3.2 Simplification and series expansion in the reverse Kreweras case

In this part we apply Theorem 16 to reverse Kreweras walks in the three-quarter plane: we first make explicit all quantities appearing in the statement of Theorem 16, then we explain how to deduce the series expansion

$$D_\varphi(0) = 1 + 4\,t^3 + 46\,t^6 + 706\,t^9 + 12472\,t^{12} + 239632\,t^{15} + 4869440\,t^{18} + O\left(t^{24}\right), \tag{3.15}$$

obtained here by direct enumeration. Let us recall that the coefficients in front of t^n are the $c_{0,0}(n)$, which count the numbers of reverse Kreweras walks of length n, starting and ending at $(0,0)$ and confined to the three-quarter plane.

This symmetric model has the step set $\mathcal{S} = \{(1,0),(0,1),(-1,-1)\}$, see Figure 3.2a. The change of variable φ defined in (3.9) transforms it into Kreweras step set, see Figure 3.2a and Table 3.1, with $\mathcal{S}_\varphi = \{(1,1),(-1,0),(0,-1)\}$.

Computation of various quantities. The kernel defined in (2.12) for Kreweras step set is $K_\varphi(x,y) = xy(t(xy + x^{-1} + y^{-1}) - 1)$. With the notation (2.14) and (2.15), we have

$$a_\varphi(x) = tx^2, \quad b_\varphi(x) = t - x, \quad c_\varphi(x) = tx, \quad d_\varphi(x) = (t-x)^2 - 4t^2x^3,$$

and by symmetry $\widetilde{a}_\varphi = a_\varphi$, $\widetilde{b}_\varphi = b_\varphi$, $\widetilde{c}_\varphi = c_\varphi$ and $\widetilde{d}_\varphi = d_\varphi$.

The branch points $x_{\varphi,1}$ and $x_{\varphi,2}$ (resp. $y_{\varphi,1}$ and $y_{\varphi,2}$) are the roots of d_φ (reps. $\widetilde{d}_\varphi$) in the open unit disc, such that $x_{\varphi,1} < x_{\varphi,2}$ (resp. $y_{\varphi,1} < y_{\varphi,2}$). We easily obtain

$$\begin{cases} x_{\varphi,1} \;=\; y_{\varphi,1} \;=\; t - 2\,t^{5/2} + 6\,t^4 - 21\,t^{11/2} + 80\,t^7 - \dfrac{1287}{4}t^{17/2} + O(t^{10}), \\ x_{\varphi,2} \;=\; y_{\varphi,2} \;=\; t + 2\,t^{5/2} + 6\,t^4 + 21\,t^{11/2} + 80\,t^7 + \dfrac{1287}{4}t^{17/2} + O(t^{10}). \end{cases}$$

We further have

$$\widetilde{d}'_\varphi(y_{\varphi,2}) = 2\,t^{5/4} - \frac{3}{2}\,t^{17/4} - 8\,t^{23/4} - \frac{603}{16}t^{29/4} - 174\,t^{35/4} + O\left(t^{41/4}\right).$$

We finally need to compute $Y_\varphi(x_{\varphi,1})$ and $Y_\varphi(x_{\varphi,2})$. By (2.16) these quantities may be simplified as

$$Y_\varphi(x_{\varphi,1}) = -\sqrt{\frac{c_\varphi(x_{\varphi,1})}{a_\varphi(x_{\varphi,1})}} = -\sqrt{\frac{1}{x_{\varphi,1}}} \qquad \text{and} \qquad Y_\varphi(x_{\varphi,2}) = \sqrt{\frac{c_\varphi(x_{\varphi,2})}{a_\varphi(x_{\varphi,2})}} = \sqrt{\frac{1}{x_{\varphi,2}}}.$$

Expression of the conformal gluing function. As we shall prove in Lemma 21, the following is a suitable conformal mapping:

$$w_\varphi(y) = \left(\frac{1}{y} - \frac{1}{W}\right)\sqrt{1 - yW^2},$$

where W is the unique power series solution to $W = t(2+W^3)$. In particular, $W \sim 2t$. As Theorem 16 is stated for a conformal gluing function with a pole at $y_{\varphi,2}$ and not at 0, we should consider instead $\widehat{w}_\varphi(y) = \frac{1}{w_\varphi(t)-w_\varphi(y_{\varphi,2})}$. We will further need the following expansions:

$$\begin{cases} W &= 2\,t + 8\,t^4 + 96\,t^7 + 1536\,t^{10} + O\left(t^{11}\right), \\ w_\varphi(y_{\varphi,1}) &= \frac{1}{2}t^{-1} + 2\,t^{1/2} - t^2 + 3t^{7/2} + -7\,t^5 + \frac{115}{4}\,t^{13/2} - 90\,t^8 + \frac{3247}{8}\,t^{19/2} + O\left(t^{11}\right), \\ w_\varphi(y_{\varphi,2}) &= \frac{1}{2}t^{-1} - 2\,t^{1/2} - t^2 - 3\,t^{7/2} - 7\,t^5 - \frac{115}{4}t^{13/2} - 90\,t^8 - \frac{3247}{8}t^{19/2} + O\left(t^{11}\right), \\ \widehat{w}_\varphi(Y_\varphi(x_{\varphi,1})) &= -t - 2\,t^4 - 18\,t^7 + O\left(t^{10}\right), \\ \widehat{w}_\varphi(Y_\varphi(x_{\varphi,2})) &= -t - 4\,t^{5/2} - 18\,t^4 - 86\,t^{11/2} - 418\,t^7 - \frac{4131}{2}t^{17/2} + O\left(t^{10}\right), \\ w'_\varphi(y_{\varphi,2}) &= t^{-1} - 2\,t^{1/2} - 5/2\,t^2 - 6\,t^{7/2} - \frac{169}{8}t^5 - 75\,t^{13/2} - \frac{4957}{16}t^8 - 1251\,t^{19/2} + O\left(t^{11}\right). \end{cases}$$

Explicit expression of $D_\varphi(y)$. We apply now Theorem 16 and obtain

$$D_\varphi(y) = \frac{-\widehat{w}'_\varphi(y)}{\sqrt{(\widehat{w}_\varphi(y) - \widehat{w}_\varphi(-1/\sqrt{x_{\varphi,1}}))(\widehat{w}_\varphi(y) - \widehat{w}_\varphi(1/\sqrt{x_{\varphi,2}}))\widetilde{d}'_\varphi(y_{\varphi,2})w'_\varphi(y_{\varphi,2})}} \\ \frac{1}{2i\pi}\int_{\mathcal{L}_\varphi} \frac{z\widehat{w}'_\varphi(z)}{\sqrt{\widehat{w}_\varphi(z) - \widehat{w}_\varphi(y_{\varphi,1})}(\widehat{w}_\varphi(z) - \widehat{w}_\varphi(y))}\,\mathrm{d}z,$$

where $\mathcal{L}_\varphi$ is the contour defined in (2.18), represented on Figure 3.7. Since $\widehat{w}_\varphi(0) = 0$ and $\widehat{w}'_\varphi(0) = 1$ (remember that w_φ has a pole at $y = 0$), evaluating at $y = 0$ the expression above yields

$$D_\varphi(0) = \frac{-1}{\sqrt{\widehat{w}_\varphi(-1/\sqrt{x_{\varphi,1}})\widehat{w}_\varphi(1/\sqrt{x_{\varphi,2}})\widetilde{d}'_\varphi(y_{\varphi,2})w'(y_{\varphi,2})}}\frac{1}{2i\pi}\int_{\mathcal{L}_\varphi} \frac{z\widehat{w}'_\varphi(z)}{\sqrt{\widehat{w}_\varphi(z) - \widehat{w}_\varphi(y_{\varphi,1})}\widehat{w}_\varphi(z)}\,\mathrm{d}z. \tag{3.16}$$

The integrand in the right-hand side of the above equation is analytic on $\mathcal{G}_\mathcal{L} \setminus [y_{\varphi,1}, y_{\varphi,2}]$. Hence by Cauchy's integral theorem, the contour $\mathcal{L}_\varphi$ may be replaced by the unit circle $\mathcal{C}(0,1)$, which simplifies the computations.

Expression of $D_\varphi(0)$ as a function of W. We could directly make a series expansion of $D_\varphi(0)$ in t. However, for greater efficiency of the series expansion computation, we will first express $D_\varphi(0)$ in terms of W, expand this integral in a series of W and finally get back to a series in t. The

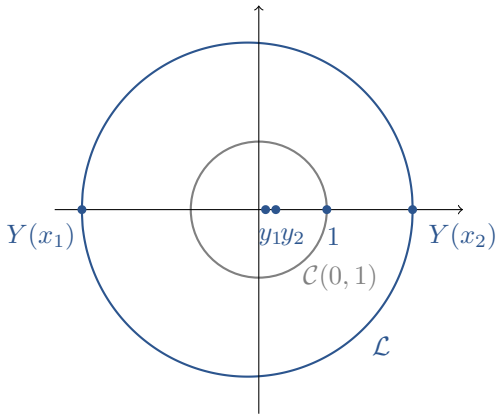

Figure 3.7 – The curve $\mathcal{L}$ for Kreweras model, for $t = 1/6$

generating function of excursions, $D_\varphi(0)$, can be written as

$$D_\varphi(0) = -\frac{\sqrt{w_\varphi(y_{\varphi,1}) - w_\varphi(y_{\varphi,2})}}{\sqrt{\widehat{w}_\varphi(-1/\sqrt{x_{\varphi,1}})\widehat{w}_\varphi(1/\sqrt{x_{\varphi,2}})\widetilde{d}'_\varphi(y_{\varphi,2})w'_\varphi(y_{\varphi,2})}} \frac{1}{2i\pi} \int_{\mathcal{L}_\varphi} \frac{z w'_\varphi(z)}{\sqrt{P - S w_\varphi(z) + w_\varphi(z)^2}} \, \mathrm{d}z, \tag{3.17}$$

with

$$\begin{cases} S &= w_\varphi(y_{\varphi,1}) + w_\varphi(y_{\varphi,2}) &= \sqrt{2P - \frac{1}{4W^2}(W^6 - 20W^3 - 8)}, \\ P &= w_\varphi(y_{\varphi,1}) w_\varphi(y_{\varphi,2}) &= \frac{(1-W^3)^{3/2}}{W^2}. \end{cases} \tag{3.18}$$

In order to derive (3.17), we start by writing the integrand of (3.16) in terms of w_φ:

$$\int_{\mathcal{L}_\varphi} \frac{z\widehat{w}'_\varphi(z)}{\sqrt{\widehat{w}_\varphi(z) - \widehat{w}_\varphi(y_{\varphi,1})}\widehat{w}_\varphi(z)} \, \mathrm{d}z = -\sqrt{w_\varphi(y_{\varphi,1}) - w_\varphi(y_{\varphi,2})} \int_{\mathcal{L}_\varphi} \frac{z w'_\varphi(z)}{\sqrt{(w_\varphi(z) - w_\varphi(y_{\varphi,1}))(w_\varphi(z) - w_\varphi(y_{\varphi,2}))}} \, \mathrm{d}z.$$

Then, note that $\widetilde{d}_\varphi(y) = -4t^2(y - y_{\varphi,1})(y - y_{\varphi,2})(y - y_{\varphi,3}) = -4t^2(y - y_{\varphi,1})(y - y_{\varphi,2})\left(y - \frac{1}{W^2}\right)$, thus we have $y_{\varphi,1} + y_{\varphi,2} = \frac{1}{4t^2} - \frac{1}{W^2}$ and $y_{\varphi,1}y_{\varphi,2} = \frac{W^2}{4}$. On the one hand, we can deduce that

$$\begin{aligned} P &= \left(\frac{1}{y_{\varphi,1}} - \frac{1}{W}\right)\left(\frac{1}{y_{\varphi,2}} - \frac{1}{W}\right)\sqrt{(1 - y_{\varphi,1}W^2)(1 - y_{\varphi,2}W^2)} \\ &= \frac{-(W - 2t)(W - 3t)}{W^5 t^2}\sqrt{W^6 t^2 - W^2 + 8t^2}. \end{aligned}$$

On the other hand,

$$S^2 = \left(1 - y_{\varphi,1}W^2\right)\left(\frac{1}{y_{\varphi,1}^2} - \frac{2}{y_{\varphi,1}W} + \frac{1}{W^2}\right) + \left(1 - y_{\varphi,2}W^2\right)\left(\frac{1}{y_{\varphi,2}^2} - \frac{2}{y_{\varphi,2}W} + \frac{1}{W^2}\right) + 2P.$$

Both equations can be simplified into (3.18), using several times the identity $t(2+W^3) - W = 0$.

Series expansion. Let us first expand in t the factor in front of the integral in (3.17); we get

$$-\frac{\sqrt{w_\varphi(y_{\varphi,1}) - w_\varphi(y_{\varphi,2})}}{\sqrt{\widehat{w}_\varphi(-1/\sqrt{x_{\varphi,1}})\widehat{w}_\varphi(1/\sqrt{x_{\varphi,2}})\widetilde{d}'_\varphi(y_{\varphi,2})w'_\varphi(y_{\varphi,2})}} = -\frac{1}{t} + O\left(t^{10}\right).$$

(One could even prove that the left-hand side of the above equation is identically equal to $-\frac{1}{t}$.) Then the factor in the integral in (3.17) may be written as

$$\begin{aligned}\frac{zw'_\varphi(z)}{\sqrt{P - Sw_\varphi(z) + w_\varphi(z)^2}} =& -\frac{1}{2z}W + \left(-\frac{1}{4z^2} + \frac{z}{4}\right)W^2 - \frac{1}{8z^3}W^3 + \left(-\frac{1}{16z^4} + \frac{3z^2}{16}\right)W^4 \\ &+ \left(-\frac{z}{32} - \frac{1}{16z^2} - \frac{1}{32z^5}\right)W^5 + \left(-\frac{3}{32\,z^3} - \frac{1}{64\,z^6} + \frac{5\,z^3}{32}\right)W^6 \\ &+ \left(-\frac{z^2}{32} + \frac{1}{64\,z} - \frac{3}{32\,z^4} - \frac{1}{128\,z^7}\right)W^7 \\ &+ \left(\frac{1}{64\,z^2} - \frac{1}{256\,z^8} - \frac{5}{64\,z^5} - \frac{z}{128} + \frac{35\,z^4}{256}\right)W^8 \\ &+ \left(-\frac{1}{512\,z^9} - \frac{15}{256\,z^6} - \frac{15\,z^3}{512}\right)W^9 + O\left(W^{10}\right)\end{aligned}$$

and then we integrate the latter on the unit circle (the only terms which contribute are the $1/z$-terms). Coming back to a series in t we obtain

$$\begin{aligned}&\frac{1}{2i\pi}\int_{\mathcal{C}(0,1)} \frac{zw'_\varphi(z)}{\sqrt{P - Sw_\varphi(z) + w_\varphi(z)^2}}\,\mathrm{d}z \\ &\qquad = -t - 4\,t^4 - 46\,t^7 - 706\,t^{10} - 12472\,t^{13} - 239632\,t^{16} - 4869440\,t^{19} + O\left(t^{21}\right).\end{aligned}$$

Finally, putting every ingredients in order, we deduce (3.15).

3.3.3 Proof of Lemma 14

We first start to prove the boundary condition (3.12) and in a second part we prove the analytic continuation.

- Assuming that $D_\varphi(y)$ may be continued as in the statement of Lemma 14, it is easy to prove the boundary condition (3.12). We evaluate the functional equation (3.10) at $Y_{\varphi,0}(x)$ for x close to $[x_{\varphi,1}, x_{\varphi,2}]$:

$$-\frac{1}{2}xY_{\varphi,0}(x) + c_\varphi(x)L_\varphi(x,0) - x\Big(x\widetilde{a}_\varphi(Y_{\varphi,0}(x)) + \frac{1}{2}\widetilde{b}_\varphi(Y_{\varphi,0}(x))\Big)D_\varphi(Y_{\varphi,0}(x)) + \frac{1}{2}txD_\varphi(0) = 0. \tag{3.19}$$

  We obtain two new equations by letting x go to any point of $[x_{\varphi,1}, x_{\varphi,2}]$ with a positive (resp. negative) imaginary part. We do the subtraction of the two equations and obtain (3.12).

- We now prove the analytic continuation. We follow the same idea as in [113, Thm 5]. Starting from (3.10) we can prove that

$$2c_\varphi(X_{\varphi,0}(y))L_\varphi(X_{\varphi,0}(y),0) + X_{\varphi,0}(y)\sqrt{\widetilde{d}_\varphi(y)}D_\varphi(y) - X_{\varphi,0}(y)y + tX_{\varphi,0}(y)D_\varphi(0) = 0$$

  for $y \in \{y \in \mathbb{C} : |X_{\varphi,0}(y)| < 1\} \cap \mathcal{D}$, and then

$$2c_\varphi(X_{\varphi,0}(y)) \sum_{n\geq 0, j\geq 0} c_{0,-j-1}(n) X_{\varphi,0}(y)^j t^n + \sqrt{\widetilde{d}_\varphi(y)}D_\varphi(y) - y + tD_\varphi(0) = 0$$

  for $y \in \{y \in \mathbb{C} : |X_{\varphi,0}(y)| < 1 \text{ and } X_{\varphi,0}(y) \neq 0\} \cap \mathcal{D}$ which can be continued in $\mathcal{G}_{\mathcal{L}_\varphi} \cup \mathcal{D}$. Being a power series, $D_\varphi(y)$ is analytic on $\mathcal{D}$ and on $(\mathcal{G}_{\mathcal{L}_\varphi} \cup \mathcal{D}) \setminus \mathcal{D}$, $D_\varphi(y)$ may have the same singularities as $X_{\varphi,0}$ and $\sqrt{\widetilde{d}_\varphi(y)}$, namely the branch cuts $[y_{\varphi,1}, y_{\varphi,2}]$ and $[y_{\varphi,3}, y_{\varphi,4}]$. But none of these segments belong to $(\mathcal{G}_{\mathcal{L}_\varphi} \cup \mathcal{D}) \setminus \mathcal{D}$, see Lemma 2. Then $D_\varphi(y)$ can be analytically continued to the domain $\mathcal{G}_{\mathcal{L}_\varphi} \cup \mathcal{D}$. Using the same idea, we can prove that $D_\varphi(y)$ has finite limits on $\mathcal{L}_\varphi$. From (3.19), it is enough to study the zeros of $x\widetilde{a}_\varphi(Y_{\varphi,0}(x)) + \frac{1}{2}\widetilde{b}_\varphi(Y_{\varphi,0}(x))$ for x in $[x_{\varphi,1}, x_{\varphi,2}]$. Using the relation $X_{\varphi,0}(Y_{\varphi,0}(x)) = x$ valid in $\mathcal{G}_{\mathcal{M}_\varphi}$ (see [72, Cor. 5.3.5]) shows that it recurs to study the zeros of $\widetilde{d}_\varphi(y)$ for $y \in (\mathcal{G}_{\mathcal{L}_\varphi} \cup \mathcal{D}) \setminus \mathcal{D}$. None of these roots $(y_{\varphi,1}, y_{\varphi,2}, y_{\varphi,3}, y_{\varphi,4})$ belong to the last set, then D_φ has finite limits on $\mathcal{L}_\varphi$.

3.3.4 Proof of Theorem 15

The function $\sqrt{\widetilde{d}_\varphi(y)}D_\varphi(y)$ satisfies a BVP of Riemann-Carleman type on $\mathcal{L}_\varphi$, see Lemma 14. Following the literature [72, 113], we use a conformal mapping to transform the latter into a more classical Riemann-Hilbert BVP. Throughout this section, we shall use notation and results of Section 2.1.2.

More precisely, let w_φ be a conformal gluing function for the set $\mathcal{G}_{\mathcal{L}_\varphi}$ in the sense of Definition 9, and let $\mathcal{U}_\varphi$ denote the real segment

$$\mathcal{U}_\varphi = w_\varphi(\mathcal{L}_\varphi).$$

(With this notation, w_φ is a conformal mapping from $\mathcal{G}_{\mathcal{L}_\varphi}$ onto the cut plane $\mathbb{C} \setminus \mathcal{U}_\varphi$.) The segment $\mathcal{U}_\varphi$ is oriented such that the positive direction is from $w_\varphi(Y_\varphi(x_{\varphi,2}))$ to $w_\varphi(Y_\varphi(x_{\varphi,1}))$, see Figure 3.9.

Define v_φ as the inverse function of w_φ. The latter is meromorphic on $\mathbb{C} \setminus \mathcal{U}_\varphi$. Following the notation of Section 2.1.2 and [72], we denote by v_φ^+ and v_φ^- the left and right limits of v_φ on $\mathcal{U}_\varphi$, see Figure 3.9.

Then (3.12) may be rephrased as the following new boundary condition on $\mathcal{U}_\varphi$:

$$D_\varphi(v_\varphi^+(u)) = \frac{\sqrt{\widetilde{d}_\varphi(v_\varphi^-(u))}}{\sqrt{\widetilde{d}_\varphi(v_\varphi^+(u))}} D_\varphi(v_\varphi^-(u)) + \frac{v_\varphi^+(u) - v_\varphi^-(u)}{\sqrt{\widetilde{d}_\varphi(v_\varphi^+(u))}}. \tag{3.20}$$

As explained in Section 2.1.2 (see in particular Definition 7), the first step in the way of solving the Riemann-Hilbert problem with boundary condition (3.20) is to compute the index of the BVP.

Proposition 18. *The index of* $\frac{\sqrt{\widetilde{d}_\varphi(v_\varphi^-(u))}}{\sqrt{\widetilde{d}_\varphi(v_\varphi^+(u))}}$ *along the curve* $\mathcal{U}_\varphi$ *is* -1.

Proof. First of all, let us recall that when $\mathcal{L}$ is a closed curve of interior $\mathcal{G}_\mathcal{L}$ and G is a non-constant, meromorphic function without zeros or poles on $\mathcal{L}$, then

$$\operatorname{ind}_\mathcal{L} G = \frac{1}{2i\pi} \int_\mathcal{L} \frac{G'(z)}{G(z)} \, \mathrm{d}z = Z - P,$$

where Z and P are respectively the numbers of zeros and poles of G in $\mathcal{G}_\mathcal{L}$, counted with multiplicity.

Applying this result to the function $d_\varphi(y)$, which in $\mathcal{G}_{\mathcal{L}_\varphi}$ has no pole and exactly two zeros (at $y_{\varphi,1}$ and $y_{\varphi,2}$ — remember that $y_{\varphi,3}$ and $y_{\varphi,4}$ are also roots of $d_\varphi(y)$ but are not in $\mathcal{G}_{\mathcal{L}_\varphi}$), we have $\operatorname{ind}_{\mathcal{L}_\varphi} \widetilde{d}_\varphi(y) = 2$, see Figure 3.8 for an illustration.

We get then

$$\begin{aligned}
\operatorname{ind}_{\mathcal{U}_\varphi} \frac{\sqrt{\widetilde{d}_\varphi(v_\varphi^-(u))}}{\sqrt{\widetilde{d}_\varphi(v_\varphi^+(u))}} &= \operatorname{ind}_{\mathcal{U}_\varphi} \sqrt{\widetilde{d}_\varphi(v_\varphi^-(u))} - \operatorname{ind}_{\mathcal{U}_\varphi} \sqrt{\widetilde{d}_\varphi(v_\varphi^+(u))} \\
&= -\operatorname{ind}_{\mathcal{L}_{\varphi,1}} \sqrt{\widetilde{d}_\varphi(y)} - \operatorname{ind}_{\mathcal{L}_{\varphi,0}} \sqrt{\widetilde{d}_\varphi(y)} \\
&= -\operatorname{ind}_{\mathcal{L}_\varphi} \sqrt{\widetilde{d}_\varphi(y)} \\
&= -\frac{1}{2} \operatorname{ind}_{\mathcal{L}_\varphi} \widetilde{d}_\varphi(y) \\
&= -1.
\end{aligned}$$

□

With Theorem 8, we deduce a contour-integral expression for the function $D_\varphi(v_\varphi(u))$, namely

$$D_\varphi(v_\varphi(u)) = \frac{\Psi(u)}{2i\pi} \int_{\mathcal{U}_\varphi} \frac{v_\varphi^+(s) - v_\varphi^-(s)}{\sqrt{\widetilde{d}_\varphi\left(v_\varphi^+(s)\right)}} \frac{1}{\Psi^+(s)(s-u)} \, \mathrm{d}s.$$

With the changes of variable $u = w_\varphi(y)$ and $s = w_\varphi(z)$, we easily have the result of Theorem 15.

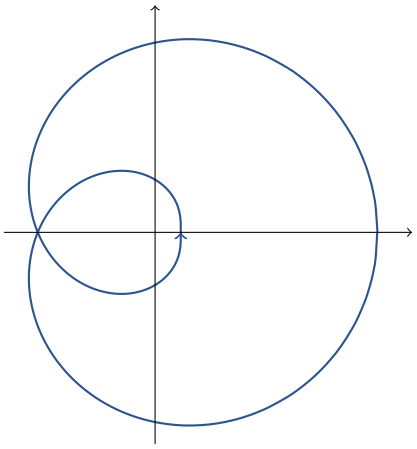

Figure 3.8 – Plot of $\widetilde{d}_\varphi(y)$ when y lies on $\mathcal{L}_\varphi$, in the case of Gessel's step set

3.3.5 Anti-Tutte's invariant

Our aim here is to find a function f_φ, analytic in $\mathcal{G}_{\mathcal{L}_\varphi}$ with finite limits on $\mathcal{L}_\varphi$, satisfying the decoupling condition (3.13), namely

$$\frac{\sqrt{\widetilde{d}_\varphi(\overline{y})}}{\sqrt{\widetilde{d}_\varphi(y)}} = \frac{f_\varphi(\overline{y})}{f_\varphi(y)}, \qquad \forall y \in \mathcal{L}_\varphi.$$

Indeed, such a function is used in a crucial way in Theorem 16.

Before giving a systematic construction of a function f_φ as above, we start by an example. For Gessel's model[5], we easily prove that the function

$$g_\varphi(y) = \frac{y}{t(y+1)^2}$$

satisfies $g_\varphi(Y_{\varphi,0})g_\varphi(Y_{\varphi,1}) = 1$, and so for $x \in [x_{\varphi,1}, x_{\varphi,2}]$ it also satisfies the condition (3.4) in Section 3.1. As in Theorem 19 below, we deduce that

$$f_\varphi(y) = \frac{g_\varphi(y)}{g'_\varphi(y)} = \frac{y(y+1)}{y-1}$$

satisfies the decoupling condition (3.13).

However, a simple rational expression of f_φ as above does not exist in general. Instead, our general construction consists in writing f_φ in terms of a conformal mapping. Our main result is the following.

[5]Let us recall that the simple model is changed into Gessel's model after the transformation φ.

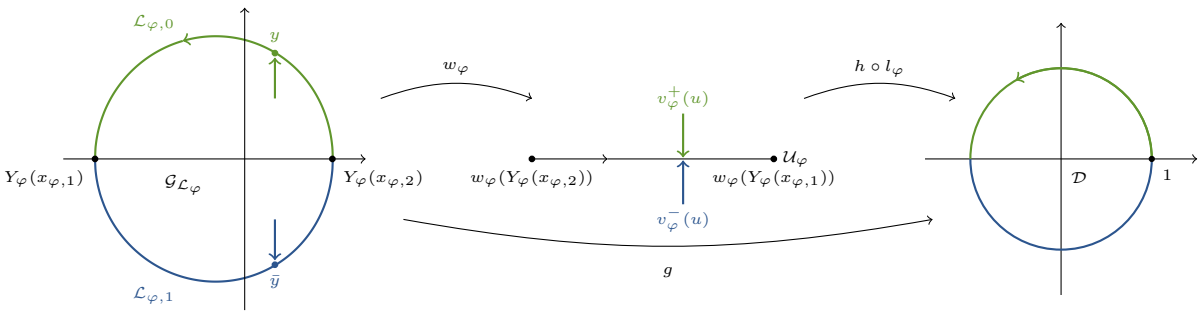

Figure 3.9 – Conformal gluing functions from $\mathcal{G}_{\mathcal{L}_\varphi}$ to $\mathbb{C} \setminus \mathcal{U}_\varphi$ and conformal mappings from $\mathcal{G}_{\mathcal{L}_\varphi}$ to the unit disc $\mathcal{D}$

Theorem 19. *Let g_φ be any conformal mapping from $\mathcal{G}_{\mathcal{L}_\varphi}$ onto the unit disc $\mathcal{D}$, with the property that $g_\varphi(\overline{y}) = \overline{g_\varphi(y)}$. Then the function f_φ defined by*

$$f_\varphi = \frac{g_\varphi}{g'_\varphi}$$

satisfies the decoupling condition (3.13)*. Moreover, f_φ is analytic in $\mathcal{G}_{\mathcal{L}_\varphi}$ and has finite limits on $\mathcal{L}_\varphi$.*

Finally, defining $h(z) = -z + \sqrt{z^2 - 1}$ and letting w_φ be a conformal gluing function as in Definition 9, one can choose

$$g_\varphi(y) = h\left(\frac{2}{w_\varphi(Y_\varphi(x_{\varphi,2})) - w_\varphi(Y_\varphi(x_{\varphi,1}))}\left(w_\varphi(y) - \frac{w_\varphi(Y_\varphi(x_{\varphi,1})) + w_\varphi(Y_\varphi(x_{\varphi,2}))}{2}\right)\right), \qquad (3.21)$$

see Figure 3.9.

To obtain the expression of g_φ in (3.21) for a given model, we refer to the list of conformal mappings w_φ provided in Section 3.3.7.

Proof. We first prove that if g_φ is a conformal mapping from $\mathcal{G}_{\mathcal{L}_\varphi}$ onto the unit disc $\mathcal{D}$ with the property that $g_\varphi(\overline{y}) = \overline{g_\varphi(y)}$, then $f_\varphi = \frac{g_\varphi}{g'_\varphi}$ satisfies the decoupling condition (3.13). First, for $x \in [x_{\varphi,1}, x_{\varphi,2}]$ one has

$$g_\varphi(Y_{\varphi,0}(x))g_\varphi(Y_{\varphi,1}(x)) = g_\varphi(Y_{\varphi,0}(x))g_\varphi(\overline{Y_{\varphi,0}(x)}) = g_\varphi(Y_{\varphi,0}(x))\overline{g_\varphi(Y_{\varphi,0}(x))} = |g_\varphi(Y_{\varphi,0}(x))|^2 = 1.$$

Differentiating the identity $g_\varphi(Y_{\varphi,0}(x))g_\varphi(Y_{\varphi,1}(x)) = 1$, one finds on $[x_{\varphi,1}, x_{\varphi,2}]$

$$\frac{f_\varphi(Y_{\varphi,0}(x))}{f_\varphi(Y_{\varphi,1}(x))} = -\frac{Y'_{\varphi,0}(x)}{Y'_{\varphi,1}(x)}.$$

To conclude the proof, we show that on $[x_{\varphi,1}, x_{\varphi,2}]$

$$\frac{\sqrt{\widetilde{d}_\varphi(Y_{\varphi,0}(x))}}{\sqrt{\widetilde{d}_\varphi(Y_{\varphi,1}(x))}} = -\frac{Y'_{\varphi,0}(x)}{Y'_{\varphi,1}(x)}. \tag{3.22}$$

To that purpose, let us first consider $x \in \mathcal{G}_{\mathcal{M}_\varphi} \setminus [x_{\varphi,1}, x_{\varphi,2}]$. Differentiating the identity $K(x, Y_{\varphi,0}(x)) = 0$ in (2.13) yields

$$Y'_{\varphi,0}(x)(2a_\varphi(x)Y_{\varphi,0}(x) + b_\varphi(x)) = -(a'_\varphi(x)Y_{\varphi,0}(x)^2 + b'_\varphi(x)Y_{\varphi,0}(x) + c'_\varphi(x)). \tag{3.23}$$

First, it follows from Section 2.1.2 that $2a_\varphi(x)Y_{\varphi,0}(x)+b_\varphi(x) = -\sqrt{d_\varphi(x)}$. Moreover, differentiating (2.13) in x and using the relation $X_{\varphi,0}(Y_{\varphi,0}(x)) = x$ valid in $\mathcal{G}_{\mathcal{M}_\varphi}$ (see [72, Cor. 5.3.5]) shows that the right-hand side of (3.23) satisfies

$$a'_\varphi(x)Y_{\varphi,0}(x)^2 + b'_\varphi(x)Y_{\varphi,0}(x) + c'_\varphi(x) = -\sqrt{\widetilde{d}_\varphi(Y_{\varphi,0}(x))}.$$

Then for $x \in \mathcal{G}_{\mathcal{M}_\varphi} \setminus [x_{\varphi,1}, x_{\varphi,2}]$, Equation (3.23) becomes

$$-\sqrt{d_\varphi(x)}Y'_{\varphi,0}(x) = \sqrt{\widetilde{d}_\varphi(Y_{\varphi,0}(x))}.$$

To complete the proof of (3.22), we let x converge to a point $x \in [x_{\varphi,1}, x_{\varphi,2}]$ from above and then from below, and we compute the ratio of the two identities so-obtained. The minus sign in (3.22) comes from that

$$\lim_{x \downarrow [x_{\varphi,1}, x_{\varphi,2}]} \sqrt{d_\varphi(x)} = -\lim_{x \uparrow [x_{\varphi,1}, x_{\varphi,2}]} \sqrt{d_\varphi(x)},$$

see Section 2.1.2.

Our second point is to show that the function g_φ in (3.21) is a conformal mapping from $\mathcal{G}_{\mathcal{L}_\varphi}$ onto the unit disc $\mathcal{D}$, which in addition is such that $g_\varphi(\overline{y}) = \overline{g_\varphi(y)}$. This is obvious from our construction (3.21), since as illustrated on Figure 3.9, $g_\varphi = h \circ l_\varphi \circ w_\varphi$ is the composition of the conformal mapping w_φ from $\mathcal{G}_{\mathcal{L}_\varphi}$ to the cut plane $\mathbb{C} \setminus [w_\varphi(Y_\varphi(x_\varphi, 2)), w_\varphi(Y_\varphi(x_\varphi, 1))]$ by the conformal mapping

$$l_\varphi(z) = \frac{2}{w_\varphi(Y_\varphi(x_{\varphi,1})) - w_\varphi(Y_\varphi(x_{\varphi,2}))} \left(z - \frac{w_\varphi(Y_\varphi(x_{\varphi,1})) + w_\varphi(Y_\varphi(x_{\varphi,2}))}{2} \right) \tag{3.24}$$

from the same cut plane to the cut plane $\mathbb{C} \setminus [-1, 1]$ and by the conformal mapping h from $\mathbb{C} \setminus [-1, 1]$ onto the unit disc.

The third item is to prove that f_φ has finite limits on $\mathcal{L}_\varphi$, for any initial choice of conformal mapping g_φ. We may propose two different proofs of this fact. First, we could prove that the function f_φ constructed from the particular function g_φ in (3.21) has the desired properties (this follows from

a direct study). Then as any two suitable conformal mappings $g_{\varphi,1}$ and $g_{\varphi,2}$ are necessarily related by a linear fractional transformation

$$g_{\varphi,1} = \frac{\alpha g_{\varphi,2} + \beta}{\gamma g_{\varphi,2} + \delta},$$

it is easily seen that all functions have indeed the good properties. We could also use a very general statement on conformal mapping. Namely, any conformal mapping which maps the unit disc onto a Jordan domain (the domain $\mathcal{G}_{\mathcal{L}_\varphi}$) with analytic boundary (our curve $\mathcal{L}_\varphi$) can be extended to a univalent function in a larger disc, see [68, Sec. 1.6]. As the extension is univalent, it becomes obvious that the derivative g'_φ in the denominator of f_φ cannot vanish. □

3.3.6 Proof of Theorem 16

Our main idea here is to reformulate the initial boundary condition (3.12) as (3.14), with the help of a function f_φ which is analytic in $\mathcal{G}_{\mathcal{L}_\varphi}$, admits finite limits on $\mathcal{L}_\varphi$ and satisfies on $\mathcal{L}_\varphi$ the decoupling condition (3.13). Using Lemma 14 and Theorem 19, we deduce that $f_\varphi(y)D_\varphi(y)$ is analytic in $\mathcal{G}_{\mathcal{L}_\varphi}$ and has finite limits on $\mathcal{L}_\varphi$. As a consequence, $f_\varphi(y)D_\varphi(y)$ satisfies a Riemann-Carleman BVP with index zero (in the sense of Definition 7). Similarly to Section 3.3.4 and using again a conformal gluing function, we transform the latter BVP into a Riemann-Hilbert BVP on an open contour, whose solution is

$$D_\varphi(y)f_\varphi(y) = \frac{1}{2i\pi}\int_{\mathcal{L}_\varphi} \frac{z f_\varphi(z)}{\sqrt{\widetilde{d}_\varphi(z)}} \frac{w'_\varphi(z)}{w_\varphi(z) - w_\varphi(y)}\,\mathrm{d}z + c, \tag{3.25}$$

where c is constant in y, but may depend on t (as recalled in Theorem 8 from Section 2.1.2, the solutions to a BVP of index zero are determined up to one constant). Notice that f_φ cancels at $y_{\varphi,2}$ (the unique pole of w_φ) and the integral in the right-hand side of (3.25) as well, it follows that $c = 0$.

We now simplify the integrand in (3.25). First, noting that h satisfies the simple differential equation $h' = \frac{-h}{\sqrt{z^2-1}}$, we obtain with our notation (3.24)

$$f_\varphi = \frac{g_\varphi}{g'_\varphi} = \frac{h(\widetilde{w}_\varphi)}{\widetilde{w}'_\varphi h'(\widetilde{w}_\varphi)} = -\frac{\sqrt{\widetilde{w}_\varphi^2 - 1}}{\widetilde{w}'_\varphi} = -\frac{\sqrt{(w_\varphi - w_\varphi(Y_\varphi(x_{\varphi,1})))(w_\varphi - w_\varphi(Y_\varphi(x_{\varphi,2})))}}{w'_\varphi}.$$

Furthermore, the conformal gluing function w_φ satisfies the following differential equation

$$\widetilde{d}_\varphi(z)w'_\varphi(z)^2 = (w_\varphi(z) - w_\varphi(Y_\varphi(x_{\varphi,1})))(w_\varphi(z) - w_\varphi(Y_\varphi(x_{\varphi,2})))(w_\varphi(z) - w_\varphi(y_{\varphi,1})), \tag{3.26}$$

see [72, Sec. 5.5.2.2]. Taking the square root of (3.26) in the neighborhood of $[y_{\varphi,2}, y_{\varphi,3}] \cap \mathcal{G}_{\mathcal{L}_\varphi}$ gives

$$-\sqrt{\widetilde{d}_\varphi(z)} w'_\varphi(z) = \sqrt{(w_\varphi(z) - w_\varphi(Y_\varphi(x_{\varphi,1})))(w_\varphi(z) - w_\varphi(Y_\varphi(x_{\varphi,2})))(w_\varphi(z) - w_\varphi(y_{\varphi,1}))},$$

as w_φ is decreasing on $[y_{\varphi,2}, y_{\varphi,3}] \cap \mathcal{G}_{\mathcal{L}_\varphi}$. It follows that

$$\frac{f_\varphi(z)}{\sqrt{\widetilde{d}_\varphi(z)}} = \frac{1}{\sqrt{w_\varphi(z) - w_\varphi\left(y_{\varphi,1}\right)}}.$$

The proof of Theorem 16 is complete.

Remark 20. The differential equation (3.26) is only true for the conformal gluing function w_φ whose expression is given in Section 3.3.7, with a pole at $y_{\varphi,2}$. If instead we have at hand a function w_φ with a pole at $y_0 \neq y_{\varphi,2}$ (for example $y_0 = 0$, as in Lemma 21), we can consider $\widehat{w}_\varphi = \frac{1}{w_\varphi - w_\varphi(y_{\varphi,2})}$, which instead of (3.26) satisfies the differential equation

$$\widetilde{d}_\varphi(z)\widehat{w}'_\varphi(z)^2 = \widetilde{d}'_\varphi(y_{\varphi,2}) w'_\varphi(y_{\varphi,2}) \left[\widehat{w}_\varphi(z) - \widehat{w}_\varphi(Y_{\varphi,0}(x_{\varphi,1}))\right] \\ \left[\widehat{w}_\varphi(z) - \widehat{w}_\varphi(Y_{\varphi,0}(x_{\varphi,2}))\right] \left[\widehat{w}_\varphi(z) - \widehat{w}_\varphi(y_{\varphi,1})\right].$$

3.3.7 Expression and properties of conformal gluing functions

A crucial ingredient in our main results (Theorems 15 and 16) is the function $w_\varphi(y)$, which we interpret as a conformal mapping from the domain $\mathcal{G}_{\mathcal{L}_\varphi}$ onto a complex plane cut along an interval, see Section 2.1.2. In this section, we recall from [113, 17] an explicit expression as well as some analytic properties of this function for the transformed models in Table 3.1, first in the finite group case, then for infinite group models.

Let us recall that if w is a suitable[6] mapping, then any $\frac{\alpha w + \beta}{\gamma w + \delta}$ is also a suitable mapping, as soon as $\alpha\delta - \beta\gamma \neq 0$. Therefore, all expressions hereafter are given up to such a fractional linear transform.

Finite group models. We start by giving an expression of the conformal mapping $w(y)$ for the Kreweras trilogy of Figure 3.2a. Let $W = W(t)$ and $Z = Z(t)$ be the unique power series satisfying

$$W = t(2 + W^3) \qquad \text{and} \qquad Z = t\frac{1 - 2Z + 6Z^2 - 2Z^3 + Z^4}{(1 - Z)^2}. \tag{3.27}$$

Lemma 21. *Let W and Z as in* (3.27)*. The function*

$$w(y) = \left(\frac{1}{y} - \frac{1}{W}\right)\sqrt{1 - yW^2}$$

[6] In the sense of Definition 9

is a conformal mapping for Kreweras model. Likewise, a conformal mapping for reverse Kreweras model is given by

$$w(y) = \frac{-ty^3 + y^2 + t}{2yt} - \frac{2y^2 - yW^2 - W}{2yW}\sqrt{1 - yW(W^3+4)/4 + y^2W^2/4}.$$

Finally, a conformal mapping for double Kreweras model is

$$w(y) = \sqrt{1 - 2yZ(1+Z^2)/(1-Z)^2 + Z^2y^2}\,\frac{(Z(1-Z) + 2yZ - (1-Z)y^2)}{2yZ(1-Z)(1+y)} + \frac{Z(1-Z)^2 - Z^2(-1+2Z+Z^2)y + (1-2Z+7Z^2-4Z^3)y^2 - Z(1-Z)^2y^3}{2y(1+y)Z(1-Z)^2}.$$

Notice that the functions w given in Lemma 21 all have a pole at $y = 0$.

Proof. Expressions for w are given in [113, Thm 3 (iii)], but some quantities in the latter statement (namely α, β, δ and γ, all depending on t) are not totally explicit. So to derive the above expressions of w, we will rather use a combination of the works [41] and [17]. Indeed, algebraic expressions of $Q(0, y)$ in terms of y and t are obtained in [41] for the three Kreweras models (see Prop. 13, Prop. 14 and Prop. 15 there). On the other hand, an alternative formulation of $Q(0, y)$ as a rational function of $w(y)$, y and t is derived in [17] (see Thm 23 and Tab. 8 there). The formulas of Lemma 21 are obtained by equating the two expressions. □

An expression for $w(y)$ for Gessel's model is obtained in [99, Thm 7].

Infinite group models. In the infinite group case, the function w is not algebraic anymore (it is even non-D-finite, see [113, Thm 2]). As $\mathcal{L}$ is a quartic curve [72, Thm 5.3.3 (i)], w can be expressed in terms of Weierstrass' elliptic functions (see [72, Sec. 5.5.2.1] or [113, Thm 6]):

Lemma 22 ([72, 113, 17])**.** *The function w defined by*

$$w(y) = \wp_{1,3}\Big(-\frac{\omega_1 + \omega_2}{2} + \wp_{1,2}^{-1}(f(y))\Big) \tag{3.28}$$

is a conformal mapping for the domain $\mathcal{G}_{\mathcal{L}}$, and has in this domain a unique (and simple) pole, located at y_2. The function w admits a meromorphic continuation on $\mathbb{C} \setminus [y_3, y_4]$. It is D-algebraic in y and in t.

The differential algebraicity is shown in [17, Thm 33]. The remaining properties stated in Lemma 22 come from [72, 113], see e.g. [113, Thm 6 and Rem. 7].

Let us now comment on the expression (3.28), following the discussion in [17, Sec. 5.2]. First, $f(y)$ is a rational function of y whose coefficients are algebraic functions of t:

$$f(y) = \begin{cases} \dfrac{\widetilde{d}''(y_4)}{6} + \dfrac{\widetilde{d}'(y_4)}{y - y_4} & \text{if } y_4 \neq \infty, \\ \dfrac{\widetilde{d}''(0)}{6} + \dfrac{\widetilde{d}'''(0)y}{6} & \text{if } y_4 = \infty, \end{cases}$$

where $\widetilde{d}(y)$ is the discriminant (2.15) and y_4 is one of its roots.

The next ingredient in (3.28) is Weierstrass' elliptic function $\wp$, with periods ω_1 and ω_2:

$$\wp(z) = \wp(z, \omega_1, \omega_2) = \frac{1}{z^2} + \sum_{(i,j) \in \mathbb{Z}^2 \setminus \{(0,0)\}} \left(\frac{1}{(z - i\omega_1 - j\omega_2)^2} - \frac{1}{(i\omega_1 + j\omega_2)^2} \right).$$

Then $\wp_{1,2}(z)$ (resp. $\wp_{1,3}(z)$) is the Weierstrass function with periods ω_1 and ω_2 (resp. ω_1 and ω_3) defined by:

$$\omega_1 = i \int_{y_1}^{y_2} \frac{\mathrm{d}y}{\sqrt{-\widetilde{d}(y)}}, \qquad \omega_2 = \int_{y_2}^{y_3} \frac{\mathrm{d}y}{\sqrt{\widetilde{d}(y)}}, \qquad \omega_3 = \int_{Y(x_1)}^{y_1} \frac{\mathrm{d}y}{\sqrt{\widetilde{d}(y)}}.$$

These definitions make sense thanks to the properties of the y_i's and $Y(x_i)$'s (see [17, Sec. 5.1]). If $Y(x_1)$ is infinite (which happens if and only if neither $(-1, 0)$ nor $(-1, 1)$ are in $\mathcal{S}$), the integral defining ω_3 starts at $-\infty$. Note that $\omega_1 \in i\mathbb{R}_+$ and $\omega_2, \omega_3 \in \mathbb{R}_+$.

Finally, as the Weierstrass function is not injective on $\mathbb{C}$, we need to clarify our definition of $\wp_{1,2}^{-1}$ in (3.28). The function $\wp_{1,2}$ is two-to-one on the fundamental parallelogram $[0, \omega_1) + [0, \omega_2)$ (because $\wp(z) = \wp(-z + \omega_1 + \omega_2)$), but is one-to-one when restricted to a half-parallelogram—more precisely, when restricted to the open rectangle $(0, \omega_1) + (0, \omega_2/2)$ together with the three boundary segments $[0, \omega_1/2]$, $[0, \omega_2/2]$ and $\omega_2/2 + [0, \omega_1/2]$. We choose the determination of $\wp_{1,2}^{-1}$ in this set.

3.4 Further objectives and perspectives

3.4.1 Asymmetric step sets, inhomogeneous walks and JSQ model

Asymmetric step sets and inhomogeneous walks. Let us consider a walk with a non-necessarily symmetric step set $\mathcal{S}$. We still require that the jumps $(-1, 1)$ and $(1, -1)$ do not belong to $\mathcal{S}$. In this case, instead of one functional equation, we will get a system of two functional equations, one for the generating function of walks ending in the lower part $L(x, y)$ and another one for the generating function ending in the upper part $U(x, y)$ (see 3.5). Both equations involve the generating function of walks ending in the diagonal $D(x, y)$. We can easily write a similar equation to (3.7) for the generating function $U(x, y)$ by taking into account all possibilities of ending in the

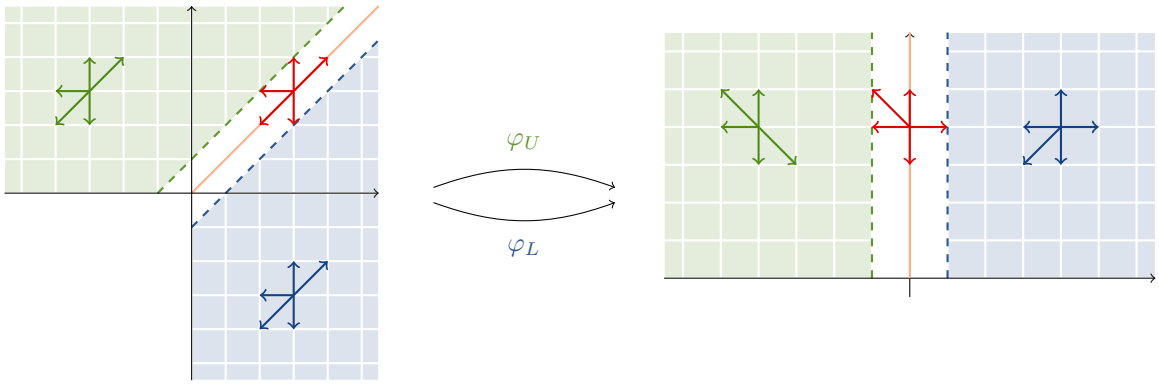

Figure 3.10 – Solving a walk model in the three-quadrant cone is equivalent to solving a space inhomogeneous model in a half-plane

upper part and get

$$\begin{aligned} U(x,y) =& t \sum_{(i,j)\in\mathcal{S}} x^i y^j U(x,y) + t(\delta_{0,1}y + \delta_{-1,0}x^{-1})D(x,y) - t(\delta_{0,-1}y^{-1} + \delta_{1,0}x)D^u(x,y) \\ & - t(\delta_{-1,-1}x^{-1}y^{-1} + \delta_{0,-1}y^{-1})U_{-0}(x) + t\delta_{0,-1}y^{-1}\sum_{n\geq 0} c_{-1,0}(n)x^{-1}t^n. \end{aligned} \tag{3.29}$$

Without the symmetry, instead of (3.8), the functional equation for $D(x,y)$ becomes

$$\begin{aligned} D(x,y) =& 1 + t(\delta_{-1,-1}x^{-1}y^{-1} + \delta_{1,1}xy)D(x,y) - t\delta_{-1,-1}x^{-1}y^{-1}D(0,0) \\ & + t(\delta_{0,-1}y^{-1} + \delta_{1,0}x)D^u(x,y) - ty^{-1}\sum_{n\geq 0} c_{-1,0}(n)x^{-1} \\ & + t(\delta_{-1,0}x^{-1} + \delta_{0,1}y)D^\ell(x,y) - tx^{-1}\sum_{n\geq 0} c_{0,-1}(n)y^{-1}t^n. \end{aligned} \tag{3.30}$$

By multiplying by xy then mixing equations (3.7) and (3.30) as well as the equations (3.29) and (3.30), we get the system of functional equations (note that is the step set is symmetric, then $U(x,y) = L(y,x)$ and both equations in (3.31) are the same)

$$\begin{cases} L(x,y)K(x,y) &= -xy - \left[t\left(\delta_{-1,-1} + \delta_{1,0}x^2y + \delta_{0,-1}x + \delta_{1,1}x^2y^2\right) - xy\right] D(x,y) \\ & \quad + t\left(\delta_{-1,-1} + \delta_{-1,0}y\right) L_{0-}(y) - t\left(\delta_{0,-1}x + \delta_{1,0}x^2y\right) D^u(x,y) \\ & \quad + t\delta_{0,-1}\textstyle\sum_{n\geq 0} c_{-1,0}(n)t^n + t\delta_{-1,-1}D(0,0). \\ U(x,y)K(x,y) &= -xy - \left[t\left(\delta_{-1,-1} + \delta_{0,1}xy^2 + \delta_{-1,0}y + \delta_{1,1}x^2y^2\right) - xy\right] D(x,y) \\ & \quad + t\left(\delta_{-1,-1} + \delta_{0,-1}x\right) U_{-0}(x) - t\left(\delta_{-1,0}y + \delta_{0,1}xy^2\right) D^\ell(x,y) \\ & \quad + t\delta_{-1,0}\textstyle\sum_{n\geq 0} c_{0,-1}(n)t^n + t\delta_{-1,-1}D(0,0). \end{cases} \tag{3.31}$$

To simplify the system (3.31), we apply a change of variable as follows: every section above the diagonal will have the change of variable φ_U and we apply φ_L to every section below the diagonal

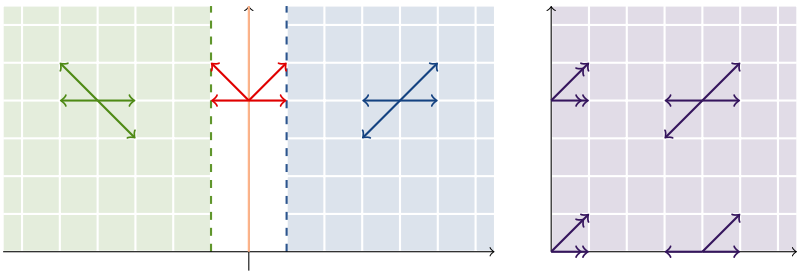

(a) Solving a symmetric walk model in the three-quadrant cone is equivalent to solving a walk in the quarter plane reflected on the y-axis

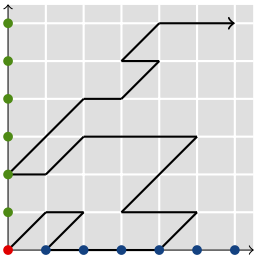

(b) Walks in the quarter plane with weights on the boundary

Figure 3.11 – Symmetric walk in the three-quadrant and walk with weights on the boundary

such that φ_U transforms the upper part $\{j \geq 1, i \leq j-1\}$ into the left quadrant $\{i \leq -1, j \geq 0\}$ and φ_L transforms the lower part $\{i \geq 1, j \leq i-1\}$ into the right quadrant $\{i \geq 1, j \geq 0\}$ (see Figure 3.10). Thanks to these changes of variable, walks in the three-quadrant can be seen as walks in the half plane with two different step sets in each quadrant (see again Figure 3.10). On the y-axis, the step set is composed of mixed steps from the step sets of the left and right quadrants. We are not able to solve yet this asymmetric case, which has in fact the same issues and level of complexity as the non-symmetric JSQ, model still unresolved [1]. This difficulty of asymmetric step sets appears as well in the study of discrete harmonic functions in the three-quarter plane which we present in Section 4.6.1.

In particular, starting with a symmetric step set in the three-quarter plane, say the simple walk, one obtains (with the terminology of Table 2.1) Gouyou-Beauchamps' model in the left quadrant and Gessel's model in the right one, see Figure 3.11a on the left[7]. This model is equivalent to study Gessel's step set in the quadrant reflected on the y-axis, see Figure 3.11a on the right. A related model is studied in [12, 127]: in these articles, the authors work on walks in the quadrant with different weights on the boundary, see Figure 3.11b, and give some results on the nature of the generating function of such walks.

[7]The symmetry condition implies compatibility between the groups of the two models after changes of variables. Indeed, if $\mathcal{S}$ and $\mathcal{S}'$ are two step sets differing by one of the eight symmetry of the square (in your case, the models are symmetric with respects to the y-axis), then the groups $G(\mathcal{S})$ and $G(\mathcal{S}')$ are isomorphic [41, Lem. 2].

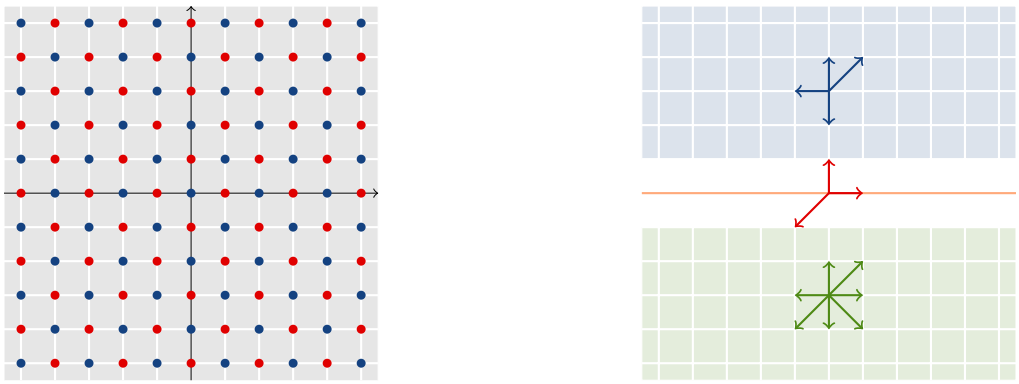

(a) An example of spatially inhomogeneous model studied in [35, 111, 45]

(b) Block inhomogeneous model in the plane

Figure 3.12 – Various kinds of inhomogeneous models

A related, simpler model (that we do not solve in the present chapter) would be to split the full plane into two half-planes and a boundary axis, to consider in each of the three regions a (different) step set, and to solve the associated walk model, see Figure 3.12b.

Some other space inhomogeneous walk models have been investigated in [35, 111, 45], but this notion of inhomogeneity does not match with ours. Indeed, a simple but typical example in [35, 111, 45] consists in dividing $\mathbb{Z}^2$ into the odd and even lattices, and assigning to each point of the even (resp. odd) lattice a certain step set $\mathcal{S}$ fixed a priori (resp. another step set $\mathcal{S}'$), see Figure 3.12a.

Join-the-Shortest-Queue model. Suppose that there are two lines (see Figure 3.13), each of them with a service time exponentially distributed of rate r_1 and r_2 and that the customers arrive according to a Poisson process. The clients choose the shortest queue and if both lines happen to have the same length, the costumers pick one or the other with probability p_1 or p_2. A common question in queuing theory is to obtain closed-form expression for the stationary distribution.

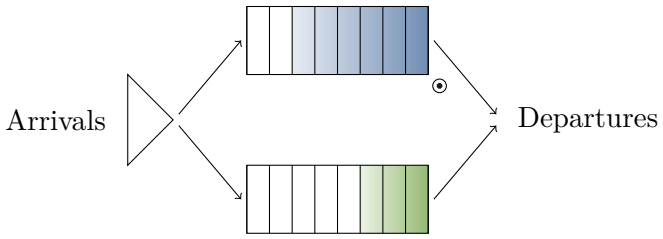

Figure 3.13 – The JSQ model can be represented as a system of two queues, in which the customers choose the shortest one (the green one, on the picture)

This JSQ problem can be modeled by random walks in the quarter plane split into two octants (cones of opening angle $\frac{\pi}{4}$), each axis representing the length of a line. The JSQ is called symmetric

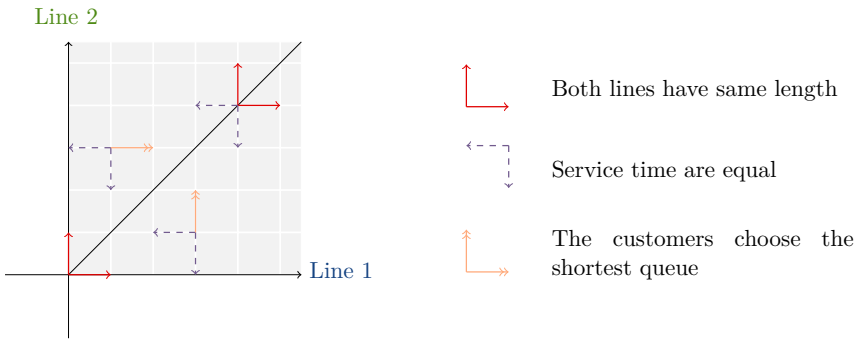

(a) Walk model for symmetric JSQ

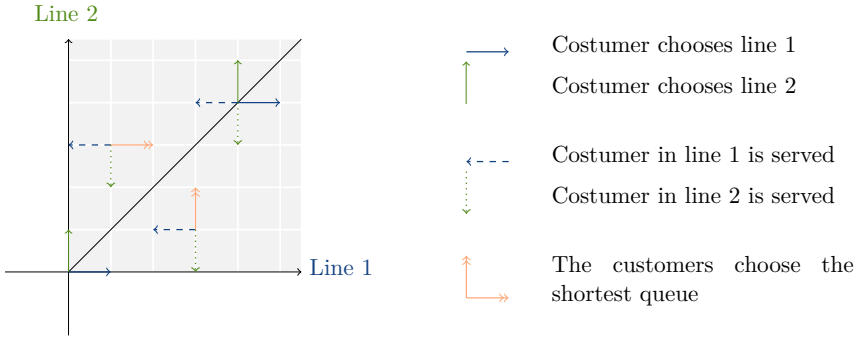

(b) Walk model for asymmetric JSQ

Figure 3.14 – Walk model for JSQ

when the service times are equal and the probability to pick one or the other line is the same (that is, when $r_1 = r_2$ and $p_1 = p_2 = 1/2$). With a random walk point of view, it means that the walk is symmetric and homogeneous (see Figure 3.14a). This symmetric case is solvable, see [1, 82, 102] and [72, Chap. 10] for references. However, in general, the service times depend on the servers ($r_1 \neq r_2$) and the transition probabilities are different in the upper and lower octants. In this case, one speaks about spatially inhomogeneous random walks, and of the general asymmetric JSQ (see Figure 3.14b). Surprisingly, the non-symmetric JSQ is still an open problem. Let us briefly notice that quadrant walks could also be treated with a JSQ approach, by decomposing the quarter plane into two octants as on Figure 3.14a, see e.g. [102] for asymptotic results and Section 4.5.

3.4.2 Nature of the generating functions of walks avoiding a quadrant

As mentioned previously, there is a complete classification of the nature of the generating functions of walks in the quadrant (see Table 2.2). It is therefore natural to get interested in the nature of the generating functions of walks avoiding a quadrant and continue the classification. Let us emphasize that to prove that the generating function $C(x, y)$ is algebraic, it suffices to prove the algebraicity of $D_\varphi(y)$. Indeed, thanks to the functional equation (3.6), if the generating function

$D_\varphi(y) = D(x, y)$ is algebraic, then $L(x, y)$ and $U(x, y)$ by symmetry are algebraic as well. Finally, $C(x, y)$ is also algebraic (see the decomposition (3.5)).

Conjecture 23. The generating function of walks for the Kreweras trilogy (see Figure 3.2a) in three quadrants is algebraic.

The algebraic nature of $D_\varphi(0)$ (see (3.16) for the example of Reverse Kreweras) can be proven using the creative telescoping, which can provide the minimal polynomial. This is an ongoing project with A. Bostan and K. Raschel.

An other complementary ongoing work with T. Dreyfus, M. Mishna and K. Raschel consists in extending the analytical approach of [101] to walks in the three-quadrant. This method has been applied in [32] to the Gessel step set in the quadrant and has given the first *human proof* of the algebraicity of this model. The general idea is to make an analytic version of the orbit sum in [41]. In this case, we can directly remark that a zero orbit sum is equivalent to an algebraic generating function. Furthermore, this method systematically gives an infinite series expression for the generating function of the walks [101, Thm 1.2], in both case of a finite and infinite group. Furthermore, the strategy and the tools developed in [62] allow us to make the following conjecture

Conjecture 24. The generating function of walks with infinite group in Figure 3.2b in the three-quadrant are D-transcendental.

Although it is not directly inspired by our work, let us end this chapter with one last conjecture related to the starting point of the walks avoiding a quadrant.

Conjecture 25. Consider an arbitrary finite group step set $\mathcal{S}$ (not necessarily satisfying (H) but with small steps). The generating function for walks in three quadrants $C(x, y)$ is algebraic as soon as the starting point $(i_0, j_0) \in \mathcal{C}$ is such that $i_0 = -1$ or $j_0 = -1$.

This conjecture is motivated by an analogy with the quarter plane, in which the following result holds: a finite group model (having group G) with starting point at (i, j) is algebraic if and only if the orbit-sum

$$\sum_{g \in G} (-1)^g g(x^{i+1} y^{j+1})$$

is identically zero, see [41, 31, 100]. Taking $i = -1$ in the sum above (which obviously is not possible in the quadrant case!) yields a zero orbit-sum—more generally, the orbit-sum of any function depending on only one of the two variables x, y is zero.

Chapter 4

Discrete harmonic functions in three quadrants[1]

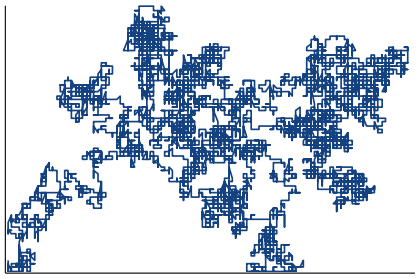

A simple random 10,000 step walk in the quarter plane

4.1 Introduction

As we have discussed in Chapter 1, discrete harmonic functions appear naturally in the study of random walks in cone. For instance, harmonic functions arise in the asymptotic behavior of excursions in a cone. Let $e_{0\to x}(n)$ be the number of n-walks with step set $\mathcal{S}$, starting at the origin

[1]This chapter is mainly from [122].

and ending at x within a given cone. Then [58, Eq. (12)][2]

$$e_{0\to x}(n) \sim \kappa \cdot V(x) \cdot \rho^n \cdot n^{-\alpha}, \quad n \longrightarrow \infty$$

where V is a discrete harmonic function, ρ and α are respectively the exponential growth and the critical exponent, both defined in Section 2.2. Furthermore, the growth of the harmonic function V turns out to be directly related to the critical exponent α, thus studying and understanding harmonic functions allows us to get information on the asymptotic behavior of walks restricted to a cone.

In the two-dimensional continuous case, a continuous harmonic function is a function for which the standard Laplacian $\Delta = \frac{\partial^2}{\partial x^2} + \frac{\partial^2}{\partial y^2}$ is zero (see Section 1.2). For example, the function $\ln(x^2+y^2)$, which appears in potential analysis, is harmonic in $\mathbb{R}^2 \setminus (0,0)$. With polar coordinates, in the cone $\{r\exp(it) : 0 \le r < \infty, 0 \le t \le \eta\}$ of opening angle η, $u(r,t) = r^{\pi/\eta}\sin\left(\frac{\pi}{\eta}t\right)$ is the unique (up to multiplicative constants) positive harmonic function equal to zero on the boundary.

In the two-dimensional discrete case, consider the simplest Laplacian operator

$$f(i+1,j) + f(i,j+1) + f(i-1,j) + f(i,j-1) - 4f(i,j).$$

The function $f(i,j) = i$ is positive harmonic in the right half plane and equal to zero on y-axis. In the positive quadrant, the function $f(i,j) = ij$ is positive harmonic with Dirichlet boundary conditions. What about harmonic functions in the three-quarter plane? Surprisingly, harmonic functions in the three-quarter plan have more complex expressions, see Equations (41) and (42). Unlike the two last examples, the three quadrants is not a convex cone and finding positive harmonic functions is more complicated. Although the difference between the intersection of two half-planes (the quarter plane) and union of two half-planes (the three-quarter plane) seems geometrically insignificant at first sight, this is not in any way the same in a combinatorial and probabilistic point of view (see Chapter 3). In this chapter, we present a systematic approach to find positive discrete harmonic functions in the three-quarter plane with Dirichlet conditions[3].

Context. In the discrete case, planar lattice random walks in cones occupy a central position in probability and combinatorics. Harmonic functions play an important role in probability theory. Doob h-transform is a way to build conditioned random processes in cones from a random process and a positive harmonic function vanishing on the boundary of the cone. Finding positive harmonic functions for random processes is therefore a natural objective in the study of confined random

[2]In our case of bounded step set, the following identity holds for any arbitrary starlike cone.

[3]In this chapter, the discrete harmonic functions vanishe on the boundary.

walks. There are very few ways to compute discrete harmonic functions (see [114] and references therein).

Most of walks studies have been done on the quadrant, or more generally in convex cones. A natural generalization is to consider other domains of restriction and determine how the framework of (random) walks is different from the quarter plane to this region. Recently, non-convex cones, in particular the three-quarter plane

$$\mathcal{C} = \{(i,j) \in \mathbb{Z}^2 : i \geq 0 \text{ or } j \geq 0\}, \tag{4.1}$$

have been examined, see Chapter 3. Unlike the quarter plane, where generating functions involve only positive powers of the variables, in the three-quarter plane we face both positive and negative powers of the variables, giving rise to convergence issues. A natural strategy consists of cutting the three quadrants in some convex cones in which the generating functions are convergent. In [40], Bousquet-Mélou sees the three-quarter plane as the union of three quadrants and obtains results for the simple and diagonals walks avoiding a quadrant. Integral expressions for the generating function of walks avoiding a quadrant with symmetric step sets are derived (see again Chapter 3), where the three-quarter plane is seen as the union of two symmetric convex cones of opening angle $3\pi/4$. Asymptotics of the number of excursions of walks with small steps in the three-quadrant is computed in [111] by Mustapha. In that article, Mustapha expresses the critical exponent of harmonic functions in three quadrants as a function of the critical exponent of harmonic functions in a quadrant. When this exponent is not rational, then the generating function of walks is not D-finite and [111, Thm 1.3] proves that the generating function of the walks of the 51 non-singular step sets with infinite group are not D-finite in the three-quarter plane (recall that neither are they in the quadrant).

In this chapter, we find an explicit expression for generating functions of discrete harmonic functions associated to random walks avoiding a quadrant with a mixed approach of [114] and Chapter 3. We focus on the analytic approach developed in [114], which consists in writing a functional equation for the generating function for a fixed harmonic function, transforming this functional equation into a boundary value problem and finally solving this problem, which results in an explicit expression for the generating function. We begin by making some assumptions on both the random walks and discrete harmonic functions for these random walks.

(H1) The walk is homogeneous inside the cone with transition probabilities $\{p_{i,j}\}_{-1\leq i,j\leq 1}$ to the nearest neighbors;

(H2) The transition probabilities are symmetric ($p_{i,j} = p_{j,i}$) and $p_{0,0} = p_{-1,1} = p_{1,-1} = 0$;

(H3) In the list $p_{1,1}$, $p_{1,0}$, $p_{1,-1}$, $p_{0,-1}$, $p_{-1,-1}$, $p_{-1,0}$, $p_{-1,1}$, $p_{0,1}$, there are no three consecutive zeros;

(H4) The drifts are zero: $\sum_{-1\leq i,j\leq 1} ip_{i,j} = 0$ and $\sum_{-1\leq i,j\leq 1} jp_{i,j} = 0$.

We first suppose with (H1) the random walks to be homogeneous with small steps, which therefore provide us techniques and tools developed in [72]. Moreover, with assumption (H2)[4], we suppose the walks to be symmetric with no anti-diagonal jumps. The third hypothesis (H3) is not essential in the study, but automatically excludes degenerate cases which could have been studied with easier methods. Finally, we assume the walks to have zero drifts with (H4). Note that the zero and non-zero drifts are two very different frameworks [66], and most results are given in the non-zero drift case. Furthermore, (H4) makes the random walks hit the negative axes almost surely. Figure 4.1 illustrates a possible transition probabilities set which satisfies (H1), (H2) and (H3). We will use the combinatorial step set terminology (see Table 2.1): the simple model is when $p_{1,0} = p_{1,0} = p_{-1,0} = p_{0,-1} = 1/4$, Gouyou-Beauchamps model (see Figure 4.11) has $p_{1,0} = p_{-1,1} = p_{-1,0} = p_{1,-1} = 1/4$ and Gessel model (see Figure 4.9) has $p_{1,0} = p_{1,1} = p_{-1,0} = p_{-1,-1} = 1/4$. In addition, we ask the associated discrete harmonic functions $f = (f(i,j))_{(i,j)\in\mathcal{C}}$ to satisfy four properties:

(P1) For all $i \geq 1$ or $j \geq 1$, $f(i,j) = \sum_{-1\leq i_0,j_0\leq 1} p_{i_0,j_0} f(i+i_0, j+j_0)$;

(P2) If $i \leq 0$, $f(i,0) = 0$ and if $j \leq 0$, then $f(0,j) = 0$;

(P3) If $i > 0$ or $j > 0$ then $f(i,j) > 0$.

We also make the hypothesis (P4) which, as we shall see (Remark 33), will be automatically satisfied for *positive* harmonic functions associated to symmetric step sets.

(P4) For all $(i,j) \in \mathcal{C}$, $f(i,j) = f(j,i)$.

The first property (P1) is the harmonicity condition, the second one (P2) is the zero condition on the boundary, the third one (P3) is the positivity condition within the cone and the last one (P4) is a symmetry condition (coming then from (H2)). In other words, we are interested in symmetric positive discrete harmonic functions for symmetric random walks with small steps constrained to the boundary of $\mathcal{C}$. Thereafter, for such a fixed harmonic function f, we consider its generating function

$$H(x,y) = \sum_{(i,j)\in\mathcal{C}} f(i,j) x^{i-1} y^{j-1}. \tag{4.2}$$

We observe here one of the main difficulties of the three quadrants: the series $H(x,y)$ is not convergent. Thereafter, we may see this object as a formal series.

Method. Working in non-convex cones, here in particular in the three-quarter plane, raises convergence problems. Indeed, it is not difficult to write a functional equation from the properties of

[4]Note that the hypothesis $p_{0,0} = 0$ is not restrictive.

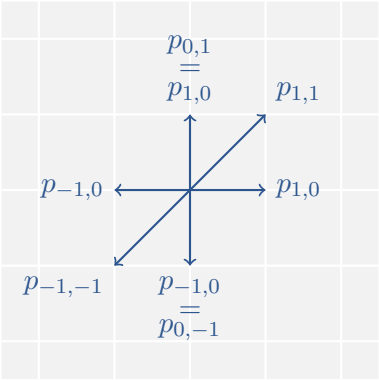

Figure 4.1 – Models satisfying (H1), (H2) and (H3)

harmonicity (P1) and vanishing conditions on the boundary (P2). However, even if this functional equation (4.19) seems close to the quarter plane case (4.16) solved in [114], it is in fact fundamentally different: the three quadrants case involves negative powers of x and y making the series not convergent anymore. To remedy this difficulty, we follow the same strategy as in Chapter 3: we divide the three quadrants into two symmetric convex cones and the diagonal (see Figure 3.3) and write a system of two functional equations (one for each cone). At first sight, this cut increases even more the level of difficulty: we have now two functional equations and more unknowns to deal with, but in the particular case of symmetric harmonic functions and symmetric transition probabilities, the system is composed of twice the same equation and the problem can be seen as a slightly different variation of the quadrant case (see Figure 4.8). In this symmetric case, we are able to use the tools and methods of [114]: transform the functional equation into a boundary value problem, solve it and write an explicit expression for the generating function. Finally, let us point out that this method of splitting the domain in two octants can also be applied in the quadrant in the symmetric case, and allows us to give alternative proofs of [114].

Main results. Our main result is an expression for the diagonal section

$$D(x,y) = D_\varphi(xy) = \sum_{i\geq 1} f(i,i)x^{i-1}y^{i-1},$$

in Lemma 44. Let $\widetilde{w}_\varphi$ be a conformal mapping (see Section 4.4.1, $\widetilde{w}_\varphi$ depends on the step set and satisfies an algebraic differential equation and can be simply expressed in terms of sine and arcsine functions) and G_φ an explicit algebraic function defined from $\widetilde{w}_\varphi$. The generating function $D(x,y)$ of discrete harmonic functions *not necessarily positive* (satisfying (P1) and (P2)) can be expressed as

$$D(x,y) = \frac{P(\widetilde{w}_\varphi(xy))}{G_\varphi(xy)}, \quad P \in \mathbb{R}[y]. \tag{4.3}$$

In particular, taking P of degree 1, we get the *unique positive* discrete harmonic function (satisfying (P1), (P2) and (P3)), see Theorem 41.

This expression of $D_\varphi(y)$ suffices to get a complete solution to the problem and Theorem 42 gives a formal explicit expression for $H(x,y)$. This formal series is expressed with the kernel $K(x,y)$, a polynomial in x and y, and two conformal mappings $W_\varphi(x)$ and $\widetilde{W}_\varphi(y)$. Each quantity depends on the transition probabilities of the random walk.

As mentioned earlier (see Section 1.2), for the simple step set, the positive discrete harmonic function in the half-plane is given by $f(i,j) = i$ with critical exponent 1. In the quadrant, the positive discrete harmonic function is given by $f(i,j) = ij$ with critical exponent 2. In this case, the value of the critical exponent in the quadrant (intersection of two half-planes) is twice the value of the critical exponent in the half-plane. Along our study, we find similar relations on harmonic functions in various quadrants (see Lemma 38 and Equation (4.66)) and the critical exponent. The growth of harmonic functions can be expressed from the angle θ defined by [73, Sec. 1.2]

$$\theta = \arccos\left(-\frac{\displaystyle\sum_{-1\le i,j\le 1} ijp_{i,j}}{\sqrt{\left(\displaystyle\sum_{-1\le i,j\le 1} i^2 p_{i,j}\right)\cdot\left(\displaystyle\sum_{-1\le i,j\le 1} j^2 p_{i,j}\right)}}\right). \tag{4.4}$$

For example, the growth of the positive harmonic function in the quadrant is π/θ. In the three-quarter plane, Mustapha [111, Eq. 1.4] proves that the critical exponent of the harmonic function is $\pi/(2\pi-\theta) = \pi/(2\theta_\varphi)$. In this chapter, we show that after the decomposition of the three quadrants and the changes of variables, the random walk in the three quadrants is equivalent to an inhomogeneous random walk in the half-plane (see Figure 4.14), with associated angle $\theta_\varphi = \pi - \theta/2$ in each quadrant (see Figure 4.2a). We also recover the factor two between walks in the quadrant and walks in the half plane: in the quarter plane, the critical exponent is $\pi/\theta = \pi/(2\theta_\psi)$. With the same reasoning as the three quadrants case, a random walk associated with angle θ can be seen as an inhomogeneous random walk in the half-plane, with associated angle $\theta_\psi = \theta/2$ in each quadrant (see Figure 4.2b).

Structure of the chapter. In *Section 4.2*, we start with underlining an important tool used in this analytic study of harmonic functions of random walks with small steps. This object, denominated by $K(x,y)$, is called the kernel of the walks and is a polynomial of degree 2 in x and y which encodes the transition probabilities of the walk. In the second part, we review results on discrete harmonic functions in the quarter plane.

In *Section 4.3*, we set up various functional equations for generating series of harmonic functions in the three-quarter plane involving the kernel $K(x,y)$.

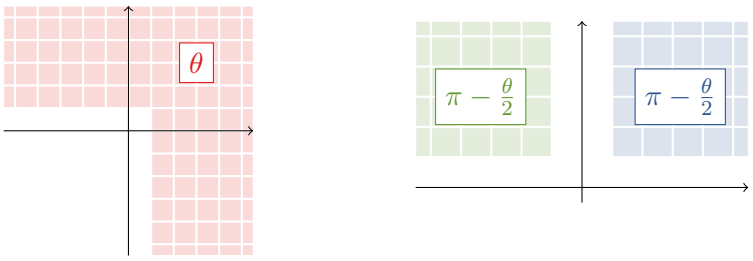

(a) Three-quarter plane case

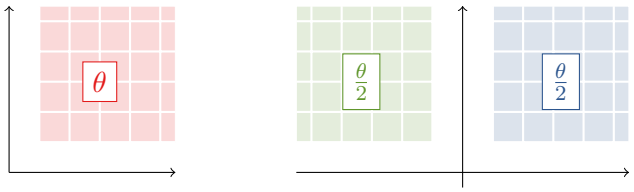

(b) Quarter plane case

Figure 4.2 – A random walk with a step set of associated angle θ in the three quadrants (resp. the quadrant) has critical exponent $\frac{\pi}{2\pi-\theta}$ (resp $\frac{\pi}{\theta}$). Such a walk can be seen as an inhomogeneous random walk in the half-plane with a step set of associated angle $\pi - \frac{\theta}{2}$ (resp. $\frac{\theta}{2}$) in each quadrant.

In *Section 4.4*, we express explicitly generating functions of harmonic functions for some models of random walks. To come to these results, we transform a functional equation (built in the previous section) into a boundary value problem in Subsection 4.4.2, and the solution process of this problem can be found in Subsection 4.4.3. The resolution of the boundary value problem involves conformal gluing functions, introduced in Subsection 4.4.1. We end this part with the application of the results to the example of the simple random walks (Subsection 4.4.4).

In *Section 4.5*, we apply this decomposition of the domain into two convex cones to symmetric harmonic functions of symmetric random walks in the quadrant and find partially the same results as [114].

In *Section 4.6*, we suppose that we do not have the symmetry of the transition probabilities of the walks. We are still able to build kernel functional equations, but unfortunately there are too many unknowns and we are not able to solve this difficult problem yet.

4.2 Preliminaries

The objects introduced in the following Section 4.2.1 may seem similar to Section 2.1.2. However, in Section 2.1.2 the Riemann surface defined by the zeros of the kernel is of genus 1 whereas in Section 4.2.1 it is of genus 0. The properties of the kernel are then slightly different in both cases.

4.2.1 Kernel of the random walks

The kernel of the random walks, denoted by $K(x,y)$, is an important object of the study. It appears in the various functional equations of this section, and we use it later to transform a functional equation into a boundary value problem. The kernel is characterized by the transition probabilities of the associated random walk by

$$K(x,y) = xy\left[\sum_{-1\le i,j\le 1} p_{i,j}x^{-i}y^{-j} - 1\right]. \tag{4.5}$$

The kernel is a polynomial of degree two in x and y (consequence of (H1) and (H3)) and can be written as[5]

$$K(x,y) = \alpha(x)y^2 + \beta(x)y + \gamma(x) = \widetilde{\alpha}(y)x^2 + \widetilde{\beta}(y)x + \widetilde{\gamma}(y), \tag{4.6}$$

where

$$\begin{cases} \alpha(x) = p_{-1,-1}x^2 + p_{0,-1}x; & \beta(x) = p_{-1,0}x^2 - x + p_{1,0}; & \gamma(x) = p_{0,1}x + p_{1,1}; \\ \widetilde{\alpha}(y) = p_{-1,-1}y^2 + p_{-1,0}y; & \widetilde{\beta}(y) = p_{0,-1}y^2 - y + p_{0,1}; & \widetilde{\gamma}(y) = p_{1,0}y + p_{1,1}. \end{cases} \tag{4.7}$$

We also define the discriminants in the x-plane and in the y-plane:

$$\widetilde{\delta}(y) = \widetilde{\beta}(y)^2 - 4\widetilde{\alpha}(y)\widetilde{\gamma}(y), \qquad \delta(x) = \beta(x)^2 - 4\alpha(x)\gamma(x). \tag{4.8}$$

The discriminant $\delta(x)$ (resp. $\widetilde{\delta}(y)$) is a polynomial of degree three or four (this is a consequence of (H2)). Hence there are four branch points x_1, x_2, x_3, x_4 (resp. y_1, y_2, y_3, y_4), with $x_4 = \infty$ (resp. $y_4 = \infty$) when $\delta(x)$ (resp. $\widetilde{\delta}(y)$) is of degree 3.

Example 26. *For the simple random walk (model with transition probabilities $p_{1,0} = p_{0,1} = p_{-1,0} = p_{0,-1} = \frac{1}{4}$), the kernel is $K(x,y) = xy\left[\frac{1}{4}\left(x + y + x^{-1} + y^{-1}\right) - 1\right]$.*

Lemma 27 (Sec. 2.3 in [72] and Sec. 2.5 in [114])**.** *The branch points x_i are real and*

$$|x_1| \le x_2 = 1 = x_3 \le |x_4| \le \infty. \tag{4.9}$$

More precisely, we have $x_1 \in [-1,1)$ and $x_4 \in (1,\infty) \cup \{\infty\} \cup (-\infty,-1]$. Furthermore, on the real line, $\delta(x)$ is negative if and only if $x \in (x_1,x_4) \setminus \{1\}$. Symmetric results hold for the y_i, roots of $\widetilde{\delta}(y)$.

[5] We follow the notations of [114] which are slightly different from the usual ones in [72]. Indeed, [114] points out that the kernel in (4.5) is the reciprocal one of the kernel $Q(x,y)$ in [72]: $K(x,y) = x^2y^2Q(1/x,1/y)$.

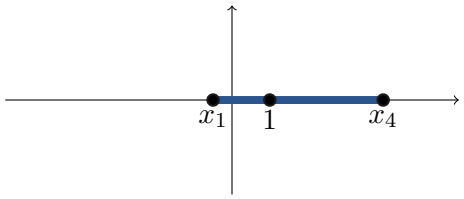

Figure 4.3 – Cut plane $\mathbb{C} \setminus [x_1, x_4]$

Let $Y(x)$ (resp. $X(y)$) be the multivalued solution to $K(x, Y(x)) = 0$ (resp. $K(X(y), y) = 0$). These algebraic functions can be written as

$$Y(x) = \frac{-\beta(x) \pm \sqrt{\delta(x)}}{2\alpha(x)} \quad \text{and} \quad X(y) = \frac{-\widetilde{\beta}(y) \pm \sqrt{\widetilde{\delta}(y)}}{2\widetilde{\alpha}(y)}. \tag{4.10}$$

Over the x-plane, the function Y has two branches Y_0 and Y_1, both meromorphic on $\mathbb{C} \setminus [x_1, x_4]$ (see Figure 4.3). We fix the notation by choosing $Y_0 = Y_-$ and $Y_1 = Y_+$. On the whole of $\mathbb{C}$ (see [72, Thm 5.3.3]),

$$|Y_0| \leq |Y_1|. \tag{4.11}$$

On the segment $[x_1, 1]$, $Y_0(x)$ and $Y_1(x)$ are complex conjugate and at the branch points x_i, we have $Y_0(x_i) = Y_1(x_i)$ (when finite), and this common value is denoted by $Y(x_i)$. We introduce the curve $\mathcal{L}$ by

$$\mathcal{L} = Y_0([x_1, 1]) \cup Y_1([x_1, 1]) = \{y \in \mathbb{C} : K(x, y) = 0 \text{ and } x \in [x_1, 1]\}. \tag{4.12}$$

We denote by $\mathcal{G}_{\mathcal{L}}$ the domain bounded by $\mathcal{L}$ which contains y_1. Figure 4.4 presents examples of the curve $\mathcal{L}$ for the simple ($p_{1,0} = p_{0,1} = p_{-1,0} = p_{0,-1} = 1/4$) and Gouyou-Beauchamps ($p_{1,0} = p_{-1,1} = p_{0,-1} = p_{1,-1} = 1/4$) case.

Lemma 28 (Lem. 6.5.1 in [72])**.** *The curve $\mathcal{L}$ in* (4.12) *is symmetric with respect to the horizontal axis, smooth except at $Y(1) = 1$ where it may have a corner point. At this point, the angle between the curve and the segment $[y_1, 1]$ is given by* (4.4)*.*

Remark 29. The quotient

$$c = \frac{\sum\limits_{-1 \leq i,j \leq 1} ijp_{i,j}}{\sqrt{\left(\sum\limits_{-1 \leq i,j \leq 1} i^2 p_{i,j}\right) \cdot \left(\sum\limits_{-1 \leq i,j \leq 1} j^2 p_{i,j}\right)}} \tag{4.13}$$

is the coefficient of correlation of the walk (compare with Section 2.2) and is related to the angle *theta* given in (4.4) by $\theta = \arccos(-c)$.

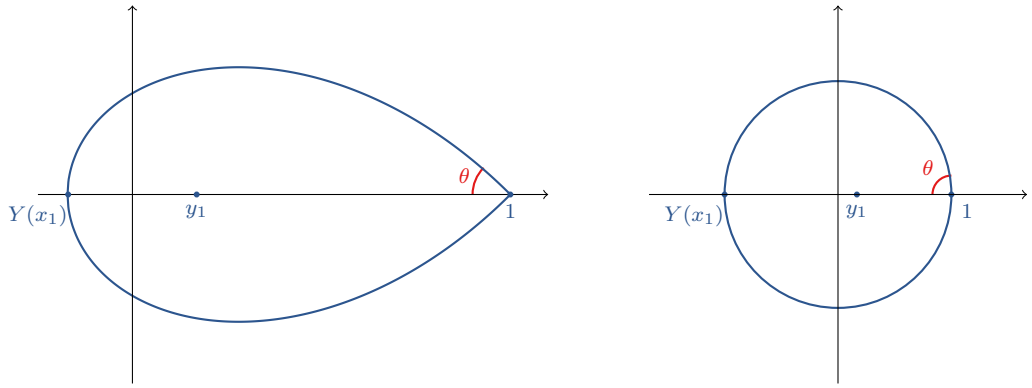

Figure 4.4 – The curve $\mathcal{L}$ for Gouyou-Beauchamps model (on the left) and for the simple model (on the right). In the case of Gouyou-Beauchamps model $\theta = \pi/4$, and in the case of the simple model, the curve is simply the unit circle and $\theta = \pi/2$

Similarly, we define the curve $\mathcal{M} = X_0([y_1, 1]) \cup X_1([y_1, 1])$, and the same symmetric results and notations hold. One has the following automorphism relations (see [72, Sec. 5.3]):

$$X_0 : \mathcal{G}_{\mathcal{L}} \setminus [y_1, 1] \to \mathcal{G}_{\mathcal{M}} \setminus [x_1, 1] \qquad \text{and} \qquad Y_0 : \mathcal{G}_{\mathcal{M}} \setminus [x_1, 1] \to \mathcal{G}_{\mathcal{L}} \setminus [y_1, 1]$$

are conformal and inverse of one another. In particular, we have then $X_0(Y(x_1)) = x_1$ and $Y_0(X(y_1)) = y_1$.

4.2.2 Previous results on discrete harmonic functions in the quarter plane

In this section we review results [114] on discrete harmonic functions in the first quadrant

$$\mathcal{Q} = \{(i, j) \in \mathbb{Z}^2 : i \geq 1 \text{ and } j \geq 1\}. \tag{4.14}$$

In this case, we assume that random walks satisfy the hypotheses (H1), (H3), (H4). We also ask the associated discrete harmonic functions to have the properties ($\tilde{\text{P}}$1), ($\tilde{\text{P}}$2), ($\tilde{\text{P}}$3) where

($\tilde{\text{P}}$1) For all $i \geq 1$ and $j \geq 1$, $\widetilde{f}(i, j) = \sum_{-1 \leq i_0, j_0 \leq 1} p_{i_0, j_0} \widetilde{f}(i + i_0, j + j_0)$;

($\tilde{\text{P}}$2) If $i \leq 0$ or $j \leq 0$, then $\widetilde{f}(i, j) = 0$;

($\tilde{\text{P}}$3) If $i > 0$ and $j > 0$ then $\widetilde{f}(i, j) > 0$.

Functional equation. The generating function of such harmonic functions $\widetilde{f}$

$$\widetilde{H}(x, y) = \sum_{i,j \geq 1} \widetilde{f}(i, j) x^{i-1} y^{j-1} \tag{4.15}$$

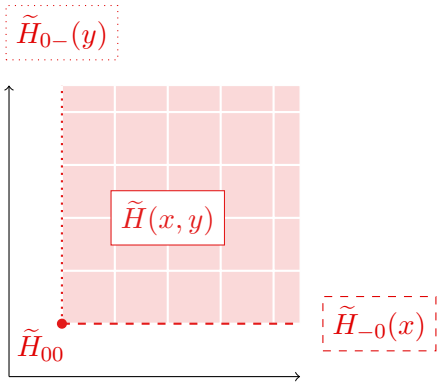

Figure 4.5 – First quadrant and associated generating functions

satisfies the functional equation equation [114, Sec. 2.3]

$$K(x,y)\widetilde{H}(x,y) = K(x,0)\widetilde{H}_{-0}(x) + K(0,y)\widetilde{H}_{0-}(y) - K(0,0)\widetilde{H}_{00}, \tag{4.16}$$

where

$$\widetilde{H}_{-0}(x) = \sum_{i\geq 1} \widetilde{f}(i,1)x^{i-1}, \qquad \widetilde{H}_{0-}(y) = \sum_{j\geq 1} \widetilde{f}(1,j)y^{j-1} \qquad \text{and} \qquad \widetilde{H}_{0,0} = \widetilde{f}(1,1). \tag{4.17}$$

Example 30. *Let us check the previous functional equation* (4.16) *with the simple random walk and it associated harmonic function* $f(i,j) = ij$ *[112]. The kernel in Example 26 can be factored into* $K(x,y) = \frac{y}{4}(x-1)^2 + \frac{x}{4}(y-1)^2$ *and we check*

$$\begin{aligned} K(x,y)\widetilde{H}(x,y) &= \left[\frac{y}{4}(1-x)^2 + \frac{x}{4}(1-y)^2\right] \frac{1}{(1-x)^2(1-y)^2} \\ &= \frac{y}{4(1-y)^2} + \frac{x}{4(1-x)^2} = K(x,0)\widetilde{H}_{-0}(x) + K(0,y)\widetilde{H}_{0-}(y). \end{aligned}$$

Boundary value problem. Using the properties of the kernel in Section 4.2.1, the functional equation (4.16) satisfied by the generating function $\widetilde{H}(x,y)$ (4.15) can be transformed into a boundary value problem. The function $\widetilde{H}_{-0}(x)$ satisfies the following boundary value problem [114, Sec. 2.4]

(i) $H_{-0}(x)$ is analytic in $\mathcal{G}_{\mathcal{M}}$;

(ii) $H_{-0}(x)$ is continuous on $\overline{\mathcal{G}_{\mathcal{M}}} \setminus \{1\}$;

(iii) For all $x \in \mathcal{M} \setminus \{1\}$, $K(x,0)\widetilde{H}_{-0}(x) - K(\bar{x},0)\widetilde{H}_{-0}(\bar{x}) = 0$.

Explicit expression for the generating function. The function $\widetilde{H}_{-0}(x)$ has the following explicit expression

$$\widetilde{H}_{-0}(x) = \mu \frac{w(x)+\nu}{K(x,0)}, \tag{4.18}$$

where w is a conformal mapping vanishing at 0 (see Section 4.4.1), and the constants ν and μ are defined by

$$\nu = -w\left(X_0(0)\right), \qquad \mu = \widetilde{f}(1,1) \times \begin{cases} \frac{2p_{-1,1}}{w''(0)} & \text{if } \ p_{1,1}=0 \text{ and } p_{0,1}=0, \\ \frac{p_{0,1}}{w'(0)} & \text{if } \ p_{1,1}=0 \text{ and } p_{0,1}\neq 0, \\ -\frac{p_{1,1}}{w(X_0(0))} & \text{if } \ p_{1,1}\neq 0. \end{cases}$$

Example 31. *For the simple random walk case,* $w(x) = \frac{-2x}{(1-x)^2}$, $\nu = 0$, *and* $\mu = \widetilde{f}(1,1) \times \frac{1/4}{-2}$. *Finally*

$$\widetilde{H}_{-0}(x) = \frac{\widetilde{f}(1,1)}{(1-x)^2}.$$

In the following sections we apply the three-step method of [114]– write a functional equation for the generating function of harmonic functions; transform this equation into a boundary value problem; and finally solve this boundary value problem and get an explicit expression of the generating function – to harmonic functions in the three-quarter plane.

4.3 Kernel functional equations

4.3.1 A first functional equation

From the properties (P1) and (P2), we deduce a functional equation satisfied by the generating function $H(x,y)$ defined in (4.2) for random walks under the hypothesis (H1)

$$K(x,y)H(x,y) = K(x,0)H_{-0}(x^{-1}) + K(0,y)H_{0-}(y^{-1}) - K(0,0)H_{0,0}, \tag{4.19}$$

where

$$H_{-0}(x^{-1}) \ = \ \sum_{i\leq 0} f(i,1)x^{i-1}, \quad H_{0-}(y^{-1}) \ = \ \sum_{j\leq 0} f(1,j)y^{j-1} \quad \text{and} \quad H_{0,0} \ = \ f(1,1). \tag{4.20}$$

This equation looks similar to the functional equation for discrete harmonic functions of random walks in a quadrant (4.16). As noted above, the structure of equations (4.19) and (4.16) is the same except that in the case of (4.19) there are infinitely many terms with positive and negative powers of x and y. As noticed in Chapter 3, this difference is not anecdotal, the series are not convergent anymore (for instance, it is not possible to evaluate them) and almost all the methodology of [41, 113] can no longer be performed.

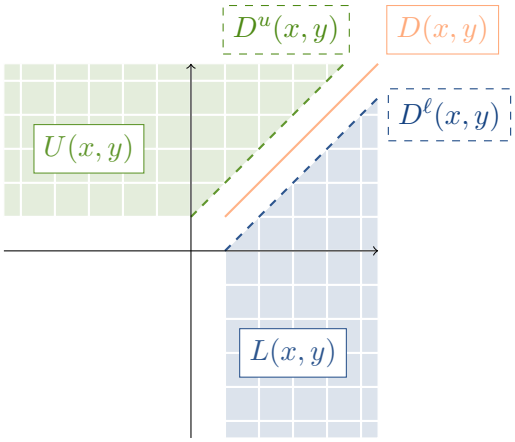

Figure 4.6 – Decomposition of the three-quarter plane and associated generating functions

This difficulty appears as well in the study of counting walks avoiding a quadrant and in order to avoid this situation, in [40] Bousquet-Mélou views the three-quarter plane as the union of three quadrants and with a combinatorial approach, gets results on the simple and the diagonal walks. In Chapter 3, the three quadrants are split in two symmetric convex cones of opening angle $\frac{3\pi}{4}$. In this chapter, we follow the same strategy as in Chapter 3.

4.3.2 Functional equations in the $\frac{3\pi}{4}$-cones

The cone $\mathcal{C}$ is cut into three parts: the lower part $\{i \geq 1, j \leq i-1\}$, the diagonal $\{i = j\}$ and the upper part $\{j \geq 1, i \geq j-1\}$. Let $L(x,y)$ (resp. $D(x,y)$ and $U(x,y)$) be the generating function of harmonic functions evaluated in the lower part (resp. diagonal and upper part), see Figure 4.6. By construction, we have

$$H(x,y) = L(x,y) + D(x,y) + U(x,y), \tag{4.21}$$

where

$$L(x,y) = \sum_{\substack{i\geq 1\\ j\leq i-1}} f(i,j)x^{i-1}y^{j-1}, \quad D(x,y) = \sum_{i\geq 1} f(i,i)x^{i-1}y^{i-1}$$
$$\text{and} \quad U(x,y) = \sum_{\substack{j\geq 1\\ i\leq j-1}} f(i,j)x^{i-1}y^{j-1}.$$

Lemma 32. *For any random walks with properties (H1) and (H2), the generating function $L(x,y)$ satisfies the following functional equation*

$$K(x,y)L(x,y) = -\left(p_{0,1}x + p_{-1,0}x^2y + \frac{1}{2}\left(p_{1,1} + p_{-1,-1}x^2y^2 - xy\right)\right) D(x,y)$$
$$+ \left(p_{1,0}y + p_{1,1}\right) L_{0-}(y^{-1}) + \frac{1}{2}p_{1,1}f(1,1), \tag{4.22}$$

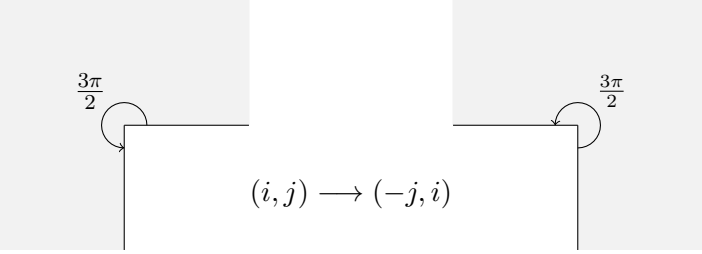

Figure 4.7 – Various cones of opening angle $\frac{3\pi}{2}$, see Remark 33. On the left the cone $\{R\exp(is) : 0 \le R < \infty, 0 \le s \le \frac{3\pi}{2}\}$ and the right the cone $\{R\exp(is) : 0 \le R < \infty, -\frac{\pi}{2} \le s \le \pi\}$

with $L_{0-}(y^{-1}) = \sum_{j\le -1} f(1,j)y^{j-1}$.

Remark 33. The symmetry of both the random walks (H2) and the harmonic function (P4) are crucial. In fact, we can directly observe the symmetry of the positive discrete harmonic function in the case of a symmetric random walk.

Let $S(n)$ be a symmetric random walk in the three quadrants and $\tau_{(i,j)}$ the exit time of the random walk starting at (i,j) from $\mathcal{C}$. Writing $(p,q) = (r\cos(t), r\sin(t))$, the harmonic function for the Brownian motion in the cone $\{R\exp(is) : 0 \le R < \infty, 0 \le s \le \frac{3\pi}{2}\}$ of opening angle $\frac{3\pi}{2}$ (see Figure 4.7) is

$$u_{\frac{3\pi}{2}}(r,t) = r^{2/3}\sin\left(\frac{2}{3}t\right), \quad t \in \left[0, \frac{3\pi}{2}\right].$$

After the change of variable $(i,j) \mapsto (-j,i) = \left(r\cos\left(t+\frac{\pi}{2}\right), r\sin\left(t+\frac{\pi}{2}\right)\right)$ (see again Figure 4.7), the harmonic function for the Brownian motion avoiding the negative quadrant is

$$u(r,t) = r^{2/3}\sin\left(\frac{2}{3}\left(t+\frac{\pi}{2}\right)\right), \quad t \in \left[-\frac{\pi}{2}, \pi\right].$$

This harmonic function is symmetric in the left cone of Figure 4.7 with respect to the diagonal $\left(u\left(r, \frac{\pi}{4} - t\right) = u\left(r, \frac{\pi}{4} + t\right)\right)$. Moreover, there is a direct link between the positive discrete harmonic function V and the harmonic function u for the Brownian motion (see [58, Lem. 12]):

$$V(i,j) = \lim_{n\to\infty} \mathbb{E}\left[u((i,j) + S(n)); \tau_{(i,j)} > n\right], \qquad (i,j) \in \mathcal{C}.$$

The exit time $\tau_{(i,j)}$ and the harmonic function u are both symmetric in the symmetric cone $\mathcal{C}$. Therefore the positive discrete harmonic function V is symmetric as well.

The positivity of the harmonic function is crucial to deduce its symmetry from the symmetry of the random walk. Let us give the following counter-example, again in the three quadrants: the *non-symmetric* function $f(i,j) = i^2 - j^2$ is harmonic for the *symmetric* simple walks. Note that this function is *not positive* everywhere in the three quadrants.

Proof of Lemma 32. Thanks to (P1) and (P2), we can easily write a functional equation for $L(x,y)$ and $D(x,y)$. Let $D^u(x,y)$ (resp. $D^\ell(x,y)$) be the generating function of a harmonic function eval-

uated in the upper (resp. lower) diagonal:

$$D^u(x,y) = \sum_{i\geq 1} f(i-1,i)x^{i-2}y^{i-1} \qquad \text{and} \qquad D^\ell(x,y) = \sum_{i\geq 1} f(i,i-1)x^{i-1}y^{i-2}.$$

We have

$$\begin{aligned} L(x,y) = &\left(\sum_{-1\leq i,j\leq 1} p_{i,j}x^{-i}y^{-j}\right) L(x,y) + \left(p_{0,1}y^{-1} + p_{-1,0}x\right) D(x,y) \\ &- \left(p_{0,-1}y + p_{1,0}x^{-1}\right) D^\ell(x,y) - \left(p_{1,0}x^{-1} + p_{1,1}x^{-1}y^{-1}\right) L_{0-}(y^{-1}) + p_{1,0}x^{-1}f(1,0)y^{-1}, \quad (4.23) \end{aligned}$$

$$\begin{aligned} D(x,y) = &\left(p_{1,1}x^{-1}y^{-1} + p_{-1,-1}xy\right) D(x,y) - p_{1,1}x^{-1}y^{-1}f(1,1) + \left(p_{1,0}x^{-1} + p_{0,-1}y\right) D^\ell(x,y) \\ &- p_{1,0}x^{-1}f(1,0)y^{-1} + \left(p_{0,1}y^{-1} + p_{-1,0}x\right) D^u(x,y) - p_{0,1}y^{-1}f(0,1)x^{-1}. \quad (4.24) \end{aligned}$$

Due to the symmetry of the cut and the random walks ($p_{i,j} = p_{j,i}$, hypothesis (H2)), we can simplify the last equation and get

$$\begin{aligned} D(x,y) = &\left(p_{1,1}x^{-1}y^{-1} + p_{-1,-1}xy\right) D(x,y) - p_{1,1}x^{-1}y^{-1} \\ &+ 2\left(p_{1,0}x^{-1} + p_{0,-1}y\right) D^\ell(x,y) - 2p_{1,0}x^{-1}f(1,0)y^{-1}. \quad (4.25) \end{aligned}$$

Plugging (4.25) into (4.23) and multiplying by xy, we get (4.22). □

In Equation (4.22), the bivariate generating function $L(x,y)$ is related to the bivariate generating function $D(x,y)$ and the univariate generating function $L_{0-}(y^{-1})$. In order to simplify the functional equation (4.22), we perform the following change of variable (introduced as well in Chapter 3)

$$\varphi(x,y) = (xy, x^{-1}). \quad (4.26)$$

Equation (4.22) is transformed into

$$K_\varphi(x,y)L_\varphi(x,y) = -\left[x\widetilde{\alpha}_\varphi(y) + \frac{1}{2}\widetilde{\beta}_\varphi(y)\right] D_\varphi(y) + K_\varphi(x,0)L_\varphi(x,0) + \frac{1}{2}p_{1,1}f(1,1), \quad (4.27)$$

with

$$\left\{ \begin{array}{lcll} K\left(\varphi(x,y)\right) & = & \frac{1}{x}K_\varphi(x,y), & \\ L\left(\varphi(x,y)\right) & = & xL_\varphi(x,y) & = \; x\sum_{i,j\geq 1} f(j,j-i)x^{i-1}y^{j-1}, \\ D\left(\varphi(x,y)\right) & = & D_\varphi(y) & = \; \sum_{i\geq 1} f(i,i)y^{i-1}, \end{array} \right. \quad (4.28)$$

and

$$K_\varphi(x,y) = \alpha_\varphi(x)y^2 + \beta_\varphi(x)y + \gamma_\varphi(x) = \widetilde{\alpha}_\varphi(y)x^2 + \widetilde{\beta}_\varphi(y)x + \widetilde{\gamma}_\varphi(y),$$
$$\widetilde{\delta}_\varphi(y) = \widetilde{\beta}_\varphi(y)^2 - 4\widetilde{\alpha}_\varphi(y)\widetilde{\gamma}_\varphi(y), \quad \delta_\varphi(x) = \beta_\varphi(x)^2 - 4\alpha_\varphi(x)\gamma_\varphi(x). \quad (4.29)$$

Example 34. *The function $f(i,j) = ij$ is harmonic (non positive) in the three quarter plane for the simple random walks case. We have*

$$K_\varphi(x,y) = \frac{y}{4}(1-x)^2 + \frac{1}{4}(1-xy)^2, \quad \widetilde{\alpha}_\varphi(y) = \frac{y(1+y)}{4}, \quad \widetilde{\beta}_\varphi(y) = -y.$$

Moreover,

$$L_\varphi(x,y) = -\frac{x+(x-2)y}{(1-y)^3(1-x)^2}, \quad \textit{and} \quad D_\varphi(y) = \frac{1+y}{(1-y)^3}.$$

The functional equation (4.27) *is satisfied*

$$K_\varphi(x,y)L_\varphi(x,y) = -\frac{(1+x^2y^2+(x^2-4x+1)y)((x-2)y+x)}{4(1-y)^3(1-x)^2}$$
$$= -\left[x\widetilde{\alpha}_\varphi(y) + \frac{1}{2}\widetilde{\beta}_\varphi(y)\right] D_\varphi(y) + K_\varphi(x,0)L_\varphi(x,0).$$

The functional equation (4.27) now has a closer structure to the functional equation in the quadrant (4.16) (see Figure 4.8), and to solve this problem, we can use some tools stated in [114]. The significant difference is the mixed factor in x and y in front of $D_\varphi(y)$, whereas in the quarter plane case, see Equation (2.11), the generating function $\widetilde{H}(x,y)$ is decomposed into a sum of two univariate functions: one section on the x-axis, namely $K(x,0)\widetilde{H}(x,0)$, and the other on the y-axis, namely $K(0,y)\widetilde{H}(0,y)$. This functional equation (4.27) holds at least for $|x|<1$ and $|y|<1$. Indeed, in [114, Sec. 2], it is proved that for any positive discrete harmonic function $\widehat{f}$ in the quarter plane, $\sum_{i\geq 1}\widehat{f}(i,1)x^{i-1}$, $\sum_{j\geq 1}\widehat{f}(1,j)y^{j-1}$ and further $K(x,y)\sum_{(i,j)\in\mathcal{Q}}\widehat{f}(i,j)x^{i-1}y^{j-1}$ are bounded at least on $\{(x,y)\in\mathbb{C}^2 : |x|<1, |y|<1\}$. We can finally deduce that $K_\varphi(x,y)L_\varphi(x,y)$, $D_\varphi(y)$ and $L_\varphi(x,0)$ are bounded at least for $|x|<1$ and $|y|<1$ as well.

Remark 35. Note that in (H2), we exclude non-zero probabilities $p_{-1,1}$ and $p_{1,-1}$. Indeed, as noted in Section 3.2, after the change of variable φ, we would end up with random walks with non-zero probabilities $p_{-2,-1}$ and $p_{2,1}$ respectively for big jumps of vector $(-2,-1)$ and $(2,1)$. Note that the analytic theory for walks with big steps is still incomplete [50, 49].

4.4 Expression for the generating functions

We start this section with the introduction of an important conformal gluing function $W(x)$ that maps the domain $\mathcal{G}_\mathcal{M}$ to the complex plane cut along a segment. We use a similar method to the one in Chapter 3 and transform the functional equation (4.27) into a boundary value problem, which is a problem involving both regularity and boundary conditions. Finally we solve this problem

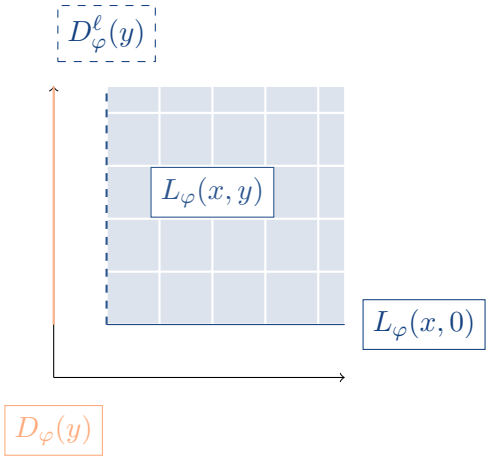

Figure 4.8 – Lower convex cone after the change of variable

and end up with an explicit expression for the generating function $H(x,y)$. The boundary value problem satisfied by the generating function $D_{\varphi}(y)$ and ultimately the generating function $H(x,y)$ will be both expressed in terms of W. Further, all quantities with a φ-tag are objects defined from the changed random walks with kernel $K_{\varphi}(x,y)$, as in Section 4.3.2.

4.4.1 Conformal gluing function

Let W be a conformal gluing function for the set $\mathcal{G}_{\mathcal{M}}$. By Definition 9, the function W is injective in $\mathcal{G}_{\mathcal{M}}$, analytic on $\mathcal{G}_{\mathcal{M}}$ and satisfies $W(x) = W(\overline{x})$ for $x \in \mathcal{M}$, as soon as $W(x)$ is defined and finite. Moreover, W has an infinite value at least on one point of $\mathcal{M}$ (or else W would be constant, see [114, Lem. 4]). In this chapter, we choose W to be infinite at 1 (if W_m is a conformal gluing function taking the value ∞ anywhere else on $\mathcal{M}$, then we can consider $W = 1/(W_m - W_m(1))$). The expression of such a function is computed in [73, Sec. 2.2]. Let

$$T(x) = \frac{1}{\sqrt{\frac{1}{3} - \frac{2f(x)}{\delta''(1)}}}, \qquad f(x) = \begin{cases} \frac{\delta''(x_4)}{6} + \frac{\delta'(x_4)}{x - x_4} & \text{if } x_4 \neq \infty, \\ \frac{\delta''(0)}{6} + \frac{\delta'''(0)x}{6} & \text{if } x_4 = \infty. \end{cases} \tag{4.30}$$

Then

$$W(x) = \left[\sin\left(\frac{\pi}{\theta}\left[\arcsin(T(x)) - \frac{\pi}{2}\right]\right)\right]^2, \tag{4.31}$$

with θ defined in (4.4). Moreover, there exists $c \neq 0$ such that for x in the neighborhood of 1,

$$W(x) = \frac{c + o(1)}{(1-x)^{\pi/\theta}}. \tag{4.32}$$

As in [73, Sec. 2.2] and [114, Sec. 3.4], the expression of $W(x)$ in (4.31) is valid only for $|T(x)| \leq 1$. When $|T(x)| \geq 1$, writing $\arcsin(T) = \pi/2 \pm i \ln(T + \sqrt{T^2 - 1})$, we can write

$$W(x) = -\frac{1}{4}\left[\left(T(x) + \sqrt{T(x)^2 - 1}\right)^{2\pi/\theta} - 2 + \left(T(x) - \sqrt{T(x)^2 - 1}\right)^{2\pi/\theta}\right]. \tag{4.33}$$

Lemma 36. *The function W defined in* (4.31) *has a zero at x_1 and is equal to* 1 *at $X(y_1)$. Moreover, for $x \in \mathcal{G}_{\mathcal{M}}$, it satisfies the following non-linear differential equation*

$$\delta(x)W'(x)^2 = \left(\frac{\pi}{\theta}\right)^2 \left(\frac{-\delta''(1)}{2}\right) W(x)(1 - W(x)). \tag{4.34}$$

Proof. We start from (4.31). After differentiation and squaring, we can write

$$W'(x)^2 = \left(\frac{\pi}{\theta}\right)^2 \frac{4T'(x)^2}{1 - T(x)^2} W(x)(1 - W(x)). \tag{4.35}$$

The strategy now is to write $\delta(x)$ in its factored form (remember that δ has four roots x_1, 1, 1, and x_4 if δ is of degree 4). If $x_4 = \infty$, then $T(x)^2 = \frac{1-x_1}{1-x}$ and if $x_4 \neq \infty$, then $T(x)^2 = \frac{(1-x_1)(x_4-x)}{(x_4-x_1)(1-x)}$. In both cases, $\frac{4T'(x)^2}{1-T(x)^2} = -\frac{\delta''(1)}{2\delta(x)}$ (and $\delta''(1) < 0$). We also note that $T(x_1) = 1$ which implies that $W(x_1) = 0$ (and because W is injective, it is the only zero). The only zero of W' is at $X(y_1)$ (see [17, Sec. 5.3]), and from (4.35), we deduce that $W(X(y_1)) = 1$. □

Similarly, we define $\widetilde{W}$ a conformal gluing for $\mathcal{G}_{\mathcal{L}}$. We show that W and $\widetilde{W}$ are strongly related as

$$\widetilde{W}(Y_0(x)) = -W(x) + 1.$$

Indeed, see [113, Thm 6 and Rem. 6][6], $\widetilde{W}(Y(x))$ is a conformal gluing for $\mathcal{G}_{\mathcal{M}}$ but may not be the one defined by (4.31). However, we know for sure that $\widetilde{W}(Y(x)) = aW(x) + b$, with $a, b \in \mathbb{C}$. By plugging in $x = x_1$ and $x = X(y_1)$, we deduce $a = -1$ and $b = 1$.

Thereafter, we are interested in a conformal gluing function which vanishes at 0. We consider w defined by

$$w(x) = W(x) - W(0). \tag{4.36}$$

The function w is a conformal gluing function in the sense of Definition 9 with a pole at 1, vanishes at 0, and satisfies the differential equation (which can be easily derived from (4.34))

$$\delta(x)w'(x)^2 = \left(\frac{\pi}{\theta}\right)^2 \left(-\frac{\delta''(1)}{2}\right) (w(x) + W(0)) (w(X(y_1)) - w(x)). \tag{4.37}$$

[6] In fact, in [113, Rem. 6], it is said that if W is a suitable mapping, then any $\frac{aW(x)+b}{cW(x)+d}$ with $a, b, c, d \in \mathbb{C}$ such that $ad - bc \neq 0$ is also a suitable mapping. In our case, we are interested in a mapping with a pole at 1. As $Y(1) = 1$, by letting x go to 1, we get $c = 0$. Hence we only need to find a and b such that $\widetilde{W}(Y(x)) = aW(x) + b$.

Remark 37. Let $\widetilde{w}$ (resp. w_φ and $\widetilde{w}_\varphi$) be a conformal gluing function for $\mathcal{G}_\mathcal{L}$ (resp. $\mathcal{G}_{\mathcal{M}_\varphi}$ and $\mathcal{G}_{\mathcal{L}_\varphi}$) which vanishes at 0. Similar results and properties hold for those functions.

The conformal gluing functions w_φ and $\widetilde{w}_\varphi$ are defined from θ_φ which can be computed with (4.4) and transition probabilities $\varphi(p_{i,j}) = p_{i-j,i}$. The angles θ_φ and θ are simply related (see Figure 4.2a), as stated in the following lemma. Relations between θ and θ_φ will be ultimately interpreted as relations between the growths of harmonic functions.

Lemma 38. *The angle between the curve $\mathcal{L}_\varphi$ and the segment $[y_{\varphi,1}, 1]$ is given by*

$$\theta_\varphi = \pi - \frac{\theta}{2}, \tag{4.38}$$

with θ defined in (4.4)*.*

Proof. With c defined in (29), we have $\theta = \arccos(-c)$. Similarly, we write $\theta_\varphi = \arccos(-c_\varphi)$. Thanks to hypotheses (H2) (symmetry condition) and (H4) (zero-drift condition), we have $p_{1,0} + p_{1,1} = p_{-1,0} + p_{-1,-1}$ and the coefficient c can be simplified as

$$c = \frac{p_{1,1} + p_{-1,-1}}{2(p_{1,0} + p_{1,1})}.$$

On the other side, the coefficient c_φ can be written as

$$c_\varphi = \frac{\sum_{-1\le i,j\le 1}(i-j)ip_{i,j}}{\sqrt{\left(\sum_{-1\le i,j\le 1}(i-j)^2 p_{i,j}\right)\cdot\left(\sum_{-1\le i,j\le 1} i^2 p_{i,j}\right)}} = \frac{1}{2}\sqrt{\frac{p_{1,0}+p_{-1,0}}{p_{1,0}+p_{1,1}}}.$$

We have then

$$c_\varphi = \sqrt{\frac{1-c}{2}} \Rightarrow \theta_\varphi = \arccos\left(-\sqrt{\frac{1-c}{2}}\right) = \pi - \frac{1}{2}\arccos(-c) = \pi - \frac{\theta}{2}. \qquad \square$$

4.4.2 Boundary value problem

Lemma 39. *The generating function $D_\varphi(y)$ can be analytically continued from the unit disc $\mathcal{D}$ to the domain $\mathcal{G}_{\mathcal{L}_\varphi} \cup \mathcal{D}$ and is continuous on $\overline{\mathcal{G}_{\mathcal{L}_\varphi}} \setminus \{1\}$. Moreover, for all $y \in \mathcal{L}_\varphi \setminus \{1\}$, $D_\varphi(y)$ satisfies the following boundary condition*

$$\frac{g_\varphi(y)}{g'_\varphi(y)} D_\varphi(y) - \frac{g_\varphi(\bar{y})}{g'_\varphi(\bar{y})} D_\varphi(\bar{y}) = 0, \tag{4.39}$$

where g_φ is defined below in (4.42) *and $\widetilde{w}_\varphi$ is a conformal gluing function defined in Section 4.4.1.*

Remark 40. The boundary condition (4.39) is the homogeneous version of the boundary condition for the enumeration of walks avoiding a quadrant (3.14). However, unlike the boundary value

problem for the enumeration case, in Lemma 39 the function $D_\varphi(y)$ has a pole at $y = 1$ (which is a point of the curve $\mathcal{L}_\varphi$) making Theorem 8 not usable.

Note also that the structure of the boundary value problem in Lemma 39 is very close to the boundary value problem stated in the quarter plane case, see Section 4.2.2.

Proof. We first assume the analyticity and continuity of $D_\varphi(y)$ and we begin to prove the boundary condition (4.39). We start to evaluate the functional equation (4.27) at $Y_{0,\varphi}(x)$ for x close to $[x_{\varphi,1}, 1)$:

$$0 = -\left[x\widetilde{\alpha}_\varphi(Y_{\varphi,0}(x)) + \frac{1}{2}\widetilde{\beta}_\varphi(Y_{\varphi,0}(x))\right] D_\varphi(Y_{\varphi,0}(x)) + K_\varphi(x,0)L_\varphi(x,0) + \frac{1}{2}p_{1,1}f(1,1). \tag{4.40}$$

By letting x go to any point of $[x_{\varphi,1}, 1]$ with a positive (resp. negative) imaginary part, we obtain two new equations. After making the difference between these two equations, we get:

$$\left[X_0(y)\widetilde{\alpha}(y) + \frac{1}{2}\widetilde{\beta}(y)\right] D_\varphi(y) - \left[X_0(\bar{y})\widetilde{\alpha}(\bar{y}) + \frac{1}{2}\widetilde{\beta}(\bar{y})\right] D_\varphi(\bar{y}), \quad y \in \mathcal{L}_\varphi \setminus \{1\}.$$

With (4.10) this last equation can be simplified as

$$\sqrt{\widetilde{\delta}_\varphi(y)}D_\varphi(y) - \sqrt{\widetilde{\delta}_\varphi(\bar{y})}D_\varphi(\bar{y}) = 0, \quad y \in \mathcal{L}_\varphi \setminus \{1\}. \tag{4.41}$$

This boundary condition is the homogeneous equation of the boundary condition in Lemma 14 with the same difficulty, which does not appear in previous works, to deal with a non-meromorphic prefactor in $\mathcal{G}_{\mathcal{L}_\varphi}$, namely $\sqrt{\widetilde{d}(y)}$ in (4.41). Therefore we follow the same strategy as in Section 3.3.5 and introduce the function g_φ defined in $\mathcal{G}_{\mathcal{L}_\varphi}$ by

$$g_\varphi(y) = h\left(\frac{2\widetilde{w}_\varphi\left(Y_\varphi(x_{\varphi,1})\right)}{\widetilde{w}_\varphi(y)} - 1\right), \tag{4.42}$$

with $h(y) = -y + \sqrt{y^2 - 1}$ and $\widetilde{w}_\varphi$ defined in Section 4.4.1. The function g_φ/g'_φ is analytic in $\mathcal{G}_{\mathcal{L}_\varphi}$, has finite limits on $\mathcal{L}_\varphi$ and the condition $\frac{\sqrt{\widetilde{\delta}_\varphi(y)}}{\sqrt{\widetilde{\delta}_\varphi(\bar{y})}} = \frac{g_\varphi(y)/g'_\varphi(y)}{g_\varphi(\bar{y})/g'_\varphi(\bar{y})}$ (the argumentation is very closed to Section 3.3.5 then we refer the reader to this section for the details). Finally, the boundary condition (4.41) can be rewritten as (4.39).

With the same reasoning as Section 3.3.3, we can prove that $D_\varphi(y)$ is analytic in $\mathcal{G}_{\mathcal{L}_\varphi}$, has finite limits on $\mathcal{L}_\varphi \setminus \{1\}$ and then is continuous on $\overline{\mathcal{G}_{\mathcal{L}_\varphi}} \setminus \{1\}$. We start with proving the analytic continuation of $D_\varphi(y)$ from the unit disc $\mathcal{D}$ to $\mathcal{G}_{\mathcal{L}_\varphi}$. From the functional equation (4.27), for $y \in \{y \in \mathbb{C} : |X_{\varphi,0}(y)| \leq 1\} \cap \mathcal{D}\}$,

$$2K_\varphi\left(X_{\varphi,0}(y), 0\right) L_\varphi\left(X_{\varphi,0}, 0\right) + \sqrt{\widetilde{\delta}(y)}D_\varphi(y) + p_{1,1}f(1,1) = 0.$$

The latter equation defined on $\mathcal{G}_{\mathcal{L}_\varphi} \cap \mathcal{D}$ can be continued in $\mathcal{G}_{\mathcal{L}_\varphi} \cup \mathcal{D}$. The generating function $D_\varphi(y)$ is analytic on $\mathcal{D}$, and on $(\mathcal{G}_{\mathcal{L}_\varphi} \cup \mathcal{D}) \setminus \mathcal{D}$, $D_\varphi(y)$ has the same singularities as $\sqrt{\widetilde{\delta}_\varphi(y)}$ and $X_{\varphi,0}(y)$, namely the branch cut $[y_1, y_4]$. However, this segment does not belong to $(\mathcal{G}_{\mathcal{L}_\varphi} \cup \mathcal{D} \backslash \mathcal{D})$, then $D_\varphi(y)$ can be analytically continued to $\mathcal{G}_{\mathcal{L}_\varphi}$. Then we prove that $D_\varphi(y)$ has finite limits on $\mathcal{L}_\varphi \setminus \{1\}$. From equation (4.40), we only need to study the zeros of $x\widetilde{\alpha}_\varphi\left(Y_{\varphi,0}(x)\right) + \frac{1}{2}\widetilde{\beta}_\varphi\left(Y_{\varphi,0}\right)$ for x in $[x_{\varphi,1}, x_{\varphi,2}]$. Thanks to the relation $X_{\varphi,0}(Y_{\varphi,0}(x)) = x$ valid in $\mathcal{G}_{\mathcal{M}_\varphi}$ (see [72, Cor. 5.3.5]), it recurs to study the zeros of $\widetilde{\delta}_\varphi$ for y in $(\mathcal{G}_{\mathcal{L}_\varphi} \cup \mathcal{D}) \setminus \mathcal{D}$. The discriminant $\widetilde{\delta}_\varphi$ vanishes at $y_{\varphi,1}, 1, y_{\varphi,4}$ and only 1 belongs to the last set. Then $D_\varphi(y)$ has finite limits on $\mathcal{L}_\varphi \setminus \{1\}$. □

4.4.3 Solution of the boundary value problem

In this section we solve the boundary value problem stated in Lemma 39 and obtain in Theorem 41 an explicit expression for the generating function $D_\varphi(y) = \sum_{i\geq 1} f(i,i)y^{i-1}$. Finally, Theorem 42 gives a formal expression of the generating function $H(x,y) = \sum_{(i,j)\in\mathcal{C}} f(i,j)x^{i-1}y^{j-1}$. Along the proof of Theorem 41, we also state Lemma 44 which gives an expression for $D_\varphi(y)$ for a family of harmonic function non necessarily positive.

Theorem 41. *The generating function $D_\varphi(y)$ can be written as*

$$D_\varphi(y) = -\frac{f(1,1)}{\widetilde{w}'_\varphi(0)}\frac{\pi}{\theta_\varphi}\sqrt{-\frac{\widetilde{\delta}''_\varphi(1)}{2\widetilde{\delta}_\varphi(y)}}\sqrt{1-\widetilde{W}_\varphi(0)}\sqrt{\widetilde{W}_\varphi(y)}, \tag{4.43}$$

with θ_φ, $\widetilde{w}_\varphi(y)$ and $\widetilde{W}_\varphi$ defined in Subsection 4.4.1 and $\widetilde{\delta}_\varphi$ in (4.29).

Theorem 42. *Let f be a harmonic function associated to a random walk in the three-quarter plane with hypotheses (H1), (H2), (H3) and (H4). The generating function $H(x,y)$ of f can be formally written as the finite sum of convergent generating functions (see* (4.21)*)*

$$\begin{aligned} H(x,y) = -\frac{f(1,1)}{\widetilde{w}'_\varphi(0)}\frac{\pi}{\theta_\varphi}\sqrt{1-\widetilde{W}_\varphi(0)}\sqrt{-\frac{\widetilde{\delta}''_\varphi(1)}{2}}\left[\frac{1}{K(x,y)}\left(\frac{\sqrt{1-W_\varphi(y^{-1})}+\sqrt{1-W_\varphi(x^{-1})}}{2}\right.\right. \\ \left.\left.-\frac{\sqrt{\widetilde{W}_\varphi(xy)}}{\sqrt{\widetilde{\delta}_\varphi(xy)}}\left(\left(x^{-1}+y^{-1}\right)\widetilde{\alpha}_\varphi(xy)+\widetilde{\beta}_\varphi(xy)\right)\right)+\frac{\sqrt{\widetilde{W}_\varphi(xy)}}{\sqrt{\widetilde{\delta}(xy)}}\right]. \end{aligned} \tag{4.44}$$

Remark 43. In equation (4.44), up to the multiplicative constant $-\frac{f(1,1)}{\widetilde{w}'_\varphi(0)}\frac{\pi}{\theta_\varphi}\sqrt{1-\widetilde{W}_\varphi(0)}\sqrt{-\frac{\widetilde{\delta}''_\varphi(1)}{2}}$, the terms

$$\frac{1}{K(x,y)}\left[\frac{-\left(y^{-1}\widetilde{\alpha}_\varphi(xy)+\frac{1}{2}\widetilde{\beta}_\varphi(xy)\right)}{\sqrt{\widetilde{\delta}_\varphi(xy)}}\sqrt{\widetilde{W}_\varphi(xy)}+\frac{\sqrt{1-W_\varphi(y^{-1})}}{2}\right], \quad \frac{\sqrt{\widetilde{W}_\varphi(xy)}}{\sqrt{\widetilde{\delta}_\varphi(xy)}},$$

$$\text{and} \quad \frac{1}{K(x,y)}\left[\frac{-\left(x^{-1}\widetilde{\alpha}_\varphi(xy)+\frac{1}{2}\widetilde{\beta}_\varphi(xy)\right)}{\sqrt{\widetilde{\delta}_\varphi(xy)}}\sqrt{\widetilde{W}_\varphi(xy)}+\frac{\sqrt{1-W_\varphi(x^{-1})}}{2}\right],$$

contribute respectively for the generating functions $L(x,y)$ in the lower cone $\{i \geq 1, j \leq i-1\}$, the diagonal $D(x,y)$ and the generating function $U(x,y)$ in the upper cone $\{j \geq 1, i \leq j-1\}$.

Lemma 44. *Let g_φ and D_φ be as in Lemma 39. Then there exists a polynomial $P \in \mathbb{R}[y]$ such that*

$$\frac{g_\varphi(y)}{g'_\varphi(y)}D_\varphi(y) = P(\widetilde{w}_\varphi(y)). \tag{4.45}$$

Proof of Lemma 44. The conformal gluing function $\widetilde{w}_\varphi(y)$ defined in Subsection 4.4.1 transforms the domain $\mathcal{G}_{\mathcal{L}_\varphi}$ into the complex plane cut by the segment $I_\varphi = [\widetilde{w}_\varphi(Y_\varphi(x_{\varphi,1})), 1)$. Let $\widetilde{w}_\varphi^{-1}$ be the inverse function of $\widetilde{w}_\varphi$. We denote by $\widetilde{w}_\varphi^{-1}(z)^+$ and $\widetilde{w}_\varphi^{-1}(z)^-$ the left and right limits of $\widetilde{w}_\varphi^{-1}$ on I_φ. The latter are complex conjugate on I. Let

$$\Delta_\varphi(y) = \frac{1}{\frac{g_\varphi(y)}{g'_\varphi(y)}D_\varphi(y)} \qquad \text{and} \qquad Z_\varphi = \left\{ z \in I_\varphi : \frac{g_\varphi}{g'_\varphi}D_\varphi \circ \widetilde{w}^{-1}(z) = 0 \right\}.$$

The set Z_φ is finite, otherwise by the principle of isolated zeros, $\frac{g_\varphi(y)}{g'_\varphi(y)}D_\varphi(y)$ would be equal to zero on the whole of $\overline{\mathcal{G}_{\mathcal{L}_\varphi}}$. Let N_φ be the cardinal of Z_φ. Thanks to Lemma 39, we have

$$\begin{cases} \Delta_\varphi \circ \widetilde{w}^{-1}(z)^+ - \Delta_\varphi \circ \widetilde{w}^{-1}(z)^- = 0 \quad \forall z \in I_\varphi, \\ \Delta_\varphi \circ \widetilde{w}^{-1} \quad \text{is analytic on } \mathbb{C} \setminus I_\varphi, \end{cases}$$

which implies that $\Delta_\varphi \circ \widetilde{w}^{-1}$ is holomorphic in $\mathbb{C}$. Furthermore, as $\Delta_\varphi \circ \widetilde{w}_\varphi^{-1}(z) - \sum_{z_0 \in Z_\varphi} \frac{1}{(z-z_0)}$ is bounded in $\mathbb{C}$, then by Liouville's theorem, the latter is constant in the whole complex plane. In addition there exists a polynomial P of degree N_φ such that $\left(\frac{g_\varphi}{g'_\varphi}D_\varphi\right) \circ \widetilde{w}_\varphi^{-1}(z) = P(z)$, hence (4.45). □

Proof of Theorem 41. In particular take P of degree one in (4.45), the generating function $D_\varphi(y)$ can be written as

$$D_\varphi(y) = \mu \frac{\widetilde{w}_\varphi(y) + \nu}{g_\varphi(y)/g'_\varphi(y)}. \tag{4.46}$$

The expression of $\frac{g_\varphi(y)}{g'_\varphi(y)}$ where the function g is defined in (4.42) can be simplified into $\frac{g_\varphi(y)}{g'_\varphi(y)} = \frac{\widetilde{w}_\varphi(y)\sqrt{\widetilde{w}_\varphi(Y_\varphi(x_{\varphi,1}))-\widetilde{w}_\varphi(y)}}{\widetilde{w}'_\varphi(y)\sqrt{\widetilde{w}_\varphi(Y_\varphi(x_{\varphi,1}))}}$. Furthermore, as the function w_φ is decreasing[7] on $(X_\varphi(y_{\varphi,1}), 1)$, taking

[7]Indeed, w_φ is injective on $(X_\varphi(y_{\varphi,1}), 1)$ and $w_\varphi(X_\varphi(y_{\varphi,1})) = 1 > 0 = w_\varphi(1)$.

the square root of (4.37) gives

$$\sqrt{\widetilde{\delta}_\varphi(y)}\widetilde{w}'_\varphi(y) = -\frac{\pi}{\theta}\sqrt{-\frac{\widetilde{\delta}''_\varphi(1)}{2}}\sqrt{\widetilde{w}_\varphi(Y_\varphi(x_{\varphi,1})) - \widetilde{w}_\varphi(y)}\sqrt{\widetilde{w}_\varphi(y) + \widetilde{W}_\varphi(0)}.$$

Then, thanks to equation (4.32), there exists a $c_g \neq 0$ such that for y in the neighborhood of 1,

$$\frac{g_\varphi(y)}{g'_\varphi(y)} = -\frac{\widetilde{w}_\varphi(y)}{\widetilde{w}_\varphi\left(Y_\varphi(x_{\varphi,1})\right)}\frac{\theta_\varphi}{\pi}\frac{\sqrt{\widetilde{d}_\varphi(y)}}{\sqrt{-\frac{\widetilde{d}''_\varphi(1)}{2}}\sqrt{\widetilde{w}_\varphi(y) + \widetilde{W}_\varphi(0)}} = \frac{c_g + o(1)}{(1-y)^{\pi/(2\theta_\varphi)-1}}.$$

and finally, there exists a $c'_D \neq 0$ such that

$$D_\varphi(y) = \frac{c'_D + o(1)}{(1-y)^{\pi/\theta_\varphi - \pi/(2\theta_\varphi)+1}} = \frac{c'_D + o(1)}{(1-y)^{\pi/(2\theta_\varphi)+1}} = \frac{c'_D + o(1)}{(1-y)^{\pi/(2\pi-\theta)+1}}. \tag{4.47}$$

If P is a polynomial of degree $n \neq 1$, then $D_\varphi(y) = \frac{c'_D+o(1)}{(1-y)^{(2n-1)\pi/(2\pi-\theta)+1}}$ thus the asymptotics of the coefficients of $D_\varphi(y)$ do not match [111, Eq. (1.4)]. Therefore, by uniqueness of the positive harmonic function, P is a polynomial of degree one.

Going back to (4.46) and noticing that $g_\varphi(0)/g'_\varphi(0) = 0$, we deduce $\nu = -\widetilde{w}_\varphi(0) = 0$. Then, computing the first term in the expansion of (4.46) at $y = 0$, we find $\mu = \frac{f(1,1)}{\widetilde{w}'_\varphi(0)}$. □

Remark 45. In [111], Mustapha computes the asymptotics of the number of small steps walks excursions in the three-quarter plane. In particular, his Equation (1.4) shows that the polynomial exponent $\alpha_{\mathcal{C}}$ in the three quadrants can be easily expressed as a function of the critical exponent $\alpha_{\mathcal{Q}}$ in the quadrant. From this equation we have for y close to 1, a constant $c_H \neq 0$ such that $H(x,0) = \frac{c_H+o(1)}{(1-x)^{\pi/(2\pi-\theta)}}$, and we deduce that there exists $c_D \neq 0$ such that $D_\varphi(y) = \frac{c_D+o(1)}{(1-y)^{\pi/(2\pi-\theta)+1}}$. Let us point out that the positivity of the harmonic function (property (P3)) is crucial in the proof of asymptotic results in [111].

Proof of Theorem 42. The expression of $D_\varphi(y)$ in Theorem 41 suffices to calculate $H(x,y)$. Indeed, to have an expression of $H(x,y)$, we only need to have one of $D(x,y)$ and $L(x,y)$ (thanks to the symmetry of the problem we have $U(x,y) = L(y,x)$). We begin by plugging in $Y_{\varphi,0}(x)$ to the functional equation (4.27) and get

$$\begin{aligned} K_\varphi(x,0)L_\varphi(x,0) &= -\frac{1}{2}\left(\sqrt{\widetilde{\delta}_\varphi(Y_{\varphi,0}(x))}D_\varphi(Y_{\varphi,0}(x)) + p_{1,1}f(1,1)\right) \\ &= -\frac{f(1,1)}{2}\left(\frac{1}{\widetilde{w}'_\varphi(0)}\frac{\pi}{\theta_\varphi}\sqrt{-\frac{\widetilde{\delta}''_\varphi(1)}{2}}\sqrt{1-\widetilde{W}_\varphi(0)}\sqrt{1-W_\varphi(x)} + p_{1,1}\right). \end{aligned} \tag{4.48}$$

Together with (4.27), we can write an expression of $L_\varphi(x,y)$ and thanks to the symmetry, we get for free an expression of $U_\varphi(x,y) = L_\varphi(x^{-1},y)$, and with a series expansion of $L_\varphi(x,y)$, $U_\varphi(x,y)$ and

$D_\varphi(y)$, the value of $f(i,j)$ for all $(i,j) \in \mathcal{C}$. In order to write a formal expression of the generating function $H(x,y)$ defined in (4.2), we can use the following relations

$$K_\varphi\left(y^{-1},0\right) L_\varphi(y^{-1},0) = K(0,y) L_{0,-}(y^{-1}) \qquad \text{and} \qquad D_\varphi(xy) = D(x,y),$$

and from them we can write

$$K(x,y)L(x,y) = -\frac{f(1,1)}{\widetilde{w}'_\varphi(0)} \frac{\pi}{\theta_\varphi} \sqrt{1-\widetilde{W}_\varphi(0)} \sqrt{-\frac{\widetilde{\delta}''_\varphi(1)}{2}} \left[\frac{-\left(y^{-1}\widetilde{\alpha}_\varphi(xy) + \frac{1}{2}\widetilde{\beta}_\varphi(xy)\right)}{\sqrt{\widetilde{\delta}_\varphi(xy)}} \sqrt{\widetilde{W}_\varphi(xy)} + \frac{\sqrt{1-W_\varphi(y^{-1})}}{2} \right]. \quad (4.49)$$

We have now all the ingredients to write an expression of $H(x,y)$ as in (4.44). □

4.4.4 Example of the simple random walk

In this subsection, we apply the results of Subsection 4.4.3 to the simple random walk. The change of variable φ defined in (4.26) transforms the simple random walk into the Gessel random walk (see Figure 4.9). We first need to compute the angle θ_φ and the conformal gluing functions W_φ, $\widetilde{W}_\varphi$ and $\widetilde{w}_\varphi$. Then we get an expression for $D_\varphi(y)$ and $L_\varphi(x,0)$ and end up with a series expansion of $H(x,y)$.

The simple walk is defined by $p_{1,0} = p_{-1,0} = p_{0,-1} = p_{0,1} = \frac{1}{4}$. We easily have $\theta = \frac{\pi}{2}$ and together with (4.38), we deduce $\theta_\varphi = \frac{3\pi}{4}$. From Equations (4.5) and (4.28), the kernel after the change of variable is defined by

$$K_\varphi(x,y) = xy\left(\frac{1}{4}x + \frac{1}{4}x^{-1} + \frac{1}{4}xy + \frac{1}{4}x^{-1}y^{-1} - 1\right), \quad (4.50)$$

$$\begin{cases} \alpha_\varphi(x) = \frac{x^2}{4}; & \beta_\varphi(x) = \frac{1}{4}x^2 - x + \frac{1}{4}; & \gamma_\varphi(x) = \frac{1}{4}; \\ \widetilde{\alpha}_\varphi(y) = \frac{1}{4}y(y+1); & \widetilde{\beta}_\varphi(y) = -y; & \widetilde{\gamma}_\varphi(y) = \frac{1}{4}(1+y). \end{cases} \quad (4.51)$$

Conformal gluing functions. On one side, we have

$$\begin{cases} \delta_\varphi(x) &= \frac{(x^2-6x+1)(x-1)^2}{16}, \\ x_4 &= 3+2\sqrt{2}, \\ \delta'_\varphi(x_4) &= 3\sqrt{2}+4, \\ \delta''_\varphi(x_4) &= \frac{11}{2}+3\sqrt{2}, \\ \delta''_\varphi(1) &= -1/2, \end{cases}$$

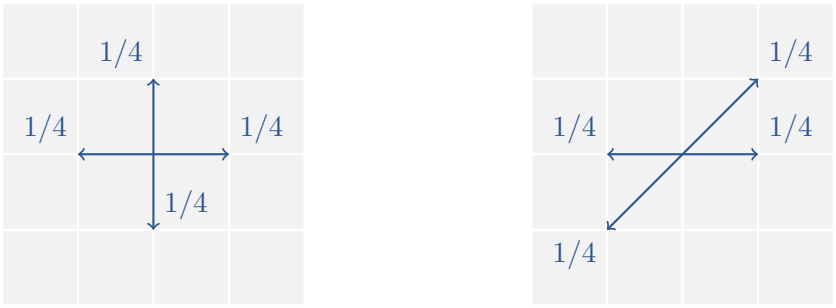

Figure 4.9 – Simple random walk (left) and Gessel random walk (right)

we have then $T_\varphi(x) = \sqrt{\dfrac{3+2\sqrt{2}-x}{1-x}}\dfrac{\sqrt{2}}{2\sqrt{2+\sqrt{2}}}$, and finally

$$W_\varphi(x) = \frac{1}{4} - \frac{(\sqrt{2}-1)^{4/3}}{16} \frac{\left(\sqrt{3+2\sqrt{2}-x}+\sqrt{x(3+2\sqrt{2})-1}\right)^{8/3} + \left(\sqrt{3+2\sqrt{2}-x}-\sqrt{x(3+2\sqrt{2})-1}\right)^{8/3}}{(1-x)^{4/3}}. \quad (4.52)$$

On the other side,

$$\begin{cases} \widetilde{\delta}_\varphi(y) &= -\frac{y(y-1)^2}{4}, \\ y_4 &= \infty, \\ \widetilde{\delta}''_\varphi(0) &= 1, \\ \widetilde{\delta}'''_\varphi(0) &= -3/2, \\ \widetilde{\delta}''_\varphi(1) &= -1/2, \end{cases}$$

we have then $\widetilde{T}_\varphi(y) = \dfrac{1}{\sqrt{1-y}}$, and finally

$$\widetilde{W}_\varphi(y) = -\frac{(y-2\sqrt{y}+1)(1-\sqrt{y})^{2/3} + (2y-2)\sqrt[3]{1-y} + (\sqrt{y}+1)^{2/3}(y+2\sqrt{y}+1)}{4(1-y)^{4/3}} \quad (4.53)$$

$$\widetilde{w}_\varphi(y) = \widetilde{W}_\varphi(y). \quad (4.54)$$

Series expansion of $D_\varphi(y)$ and $L_\varphi(x,0)$. Noticing that $\widetilde{w}_\varphi(0) = -16/9$, $\widetilde{W}_\varphi(0) = 0$, thanks to Theorem 41, we have

$$D_\varphi(y) = f(1,1)\frac{3}{8}\frac{\sqrt{\widetilde{W}_\varphi(y)}}{\sqrt{\widetilde{\delta}_\varphi(y)}} = f(1,1)\left(1 + \frac{44}{27}y + \frac{523}{243}y^2 + \frac{17168}{6561}y^3 + O\left(y^4\right)\right). \quad (4.55)$$

Thanks to (4.48) with $K_\varphi(x,0) = 1/4$, we have

$$\begin{aligned} L_\varphi(x,0) &= f(1,1)\frac{3}{4}\sqrt{1-W_\varphi(x)} \\ &= f(1,1)\left(\frac{3\sqrt{3}}{8} + \frac{1}{2}x + \left(1-\frac{\sqrt{3}}{3}\right)x^2 + \left(\frac{145}{54} - \frac{4\sqrt{3}}{3}\right)x^3 + O\left(x^4\right)\right). \end{aligned} \tag{4.56}$$

Series expansion of $L_\varphi(x,y)$. To begin with, we write an expression of $K_\varphi(x,y)L_\varphi(x,y)$. With (4.27), we get

$$\begin{aligned} L_\varphi(x,y) &= \frac{1}{K_\varphi(x,y)}\left(-\left[x\frac{1}{4}y(y+1) - \frac{1}{2}y\right]D_\varphi(y) + K_\varphi(x,0)L_\varphi(x,0)\right) \\ &= f(1,1)\left[\frac{3\sqrt{3}}{8} + \left(2 - \frac{3\sqrt{3}}{8}\right)y + \left(\frac{34}{27} + \frac{3\sqrt{3}}{8}\right)y^2 + O\left(y^3\right)\right. \\ &+ \left(\frac{1}{2} + \left(-\frac{3}{2} + \frac{3\sqrt{3}}{2}\right)y + \left(\frac{371}{54} - 3\sqrt{3}\right)y^2 + O\left(y^3\right)\right)x \\ &\left.+ \left(1 - \frac{\sqrt{3}}{3} + \left(1 - \frac{\sqrt{3}}{24}\right)y + \left(\frac{145\sqrt{3}}{24} - 9\right)y^2 + O\left(y^3\right)\right)x^2 + O\left(x^3\right)\right]. \end{aligned} \tag{4.57}$$

Remark 46. More generally, for any polynomial P of degree n in Lemma 44, we get harmonic functions satisfying (P1) and (P2) (but not necessarily (P3)). Let us give an example with a polynomial P of degree 3.

The harmonic function $f(i,j) = ij$ is a positive harmonic function for the simple walk in the quarter plane. In the three-quarter plane, this function is still harmonic, but does not satisfy (P3). However, there exists a polynomial P as in (4.45) such that $D_\varphi(y) = \sum_{i\geq 1} f(i,i)y^{i-1} = \frac{1+y}{(1-y)^3}$. A quick study of exponent in the same idea of Section 4.4.3 shows that P should be of degree 2. Then there exists $(a,b,c) \in \mathbb{R}^3$ such that

$$\frac{g_\varphi(y)}{g'_\varphi(y)}D_\varphi(y) = a\widetilde{w}_\varphi(y)^2 + b\widetilde{w}_\varphi(y) + c. \tag{4.58}$$

We have $\frac{g_\varphi(y)}{g'_\varphi(y)} = \frac{\widetilde{w}_\varphi(y)\sqrt{1-\widetilde{w}_\varphi(y)}}{\widetilde{w}'_\varphi(y)}$, and evaluating this last equation at $y = 0$ gives $c = 0$. Then, dividing by $\widetilde{w}_\varphi(y)$ and letting y go to 0 gives $b = -\frac{9}{16}$. Finally, examining the first and second term of the expansion of (4.58) at $y = 0$ gives $a = \frac{3}{4}$. Vice versa, letting $P(y) = \frac{3}{4}y^2 - \frac{9}{16}y$, when we develop $D_\varphi(y)$ in series, we find

$$D_\varphi(y) = 1 + 4\,y + 9\,y^2 + 16\,y^3 + 25\,y^4 + O\left(y^5\right), \tag{4.59}$$

which matches with $\sum_{i\geq 1} i^2 y^{i-1}$.

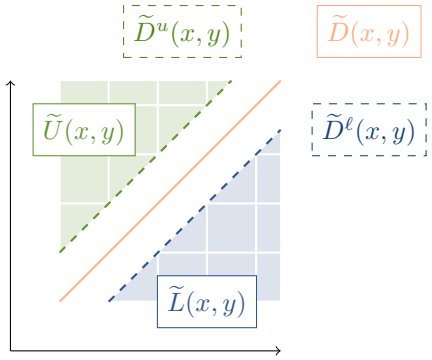

Figure 4.10 – Decomposition of the quadrant and associated generating functions

4.5 Discrete harmonic functions in the split quadrant

Even if discrete harmonic functions of random walks in the quarter plane are already studied in [114], we want to point out that the strategy of splitting the domain into three parts (the upper part, the diagonal and the lower part) can also be performed in the quarter plane $\mathcal{Q}$ defined in (4.14) to get explicit expressions of harmonic functions. We suppose that random walks satisfy the hypotheses (H1), (H2), (H3), (H4), and associated discrete harmonic functions $\widetilde{f}$ the properties ($\tilde{\text{P}}1$), ($\tilde{\text{P}}2$), ($\tilde{\text{P}}3$). The generating function of such harmonic functions is defined in (4.15). We split the quadrant $\mathcal{Q}$ in three parts: the lower part $\{i \geq 2, 1 \leq j \leq i-1\}$, the diagonal and the upper part $\{j \geq 2, 1 \leq i \leq j-1\}$. As in (4.21), by construction we have

$$\widetilde{H}(x,y) = \widetilde{L}(x,y) + \widetilde{D}(x,y) + \widetilde{U}(x,y), \tag{4.60}$$

where $\widetilde{L}(x,y) = \sum_{\substack{i\geq 2\\ 1\leq j\leq i-1}} \widetilde{f}(i,j)x^{i-1}y^{j-1}$ denotes the generating function of harmonic functions evaluated in the lower part, $\widetilde{D}(x,y) = \sum_{i\geq 1} \widetilde{f}(i,i)x^{i-1}y^{i-1}$ for harmonic functions evaluated in the diagonal and $\widetilde{U}(x,y) = \sum_{\substack{j\geq 2\\ 1\leq i\leq j-1}} \widetilde{f}(i,j)x^{i-1}y^{j-1}$ for harmonic functions evaluated in the upper part (see Figure 4.10).

We can write a functional equation for each section and finally get a functional equation in terms of $\widetilde{L}(x,y)$, $\widetilde{L}_{-0}$ and $\widetilde{D}(x,y)$.

Lemma 47. *For any random walks with properties (H1) and (H2), the generating function $\widetilde{L}(x,y)$ satisfies the following functional equation*

$$K(x,y)\widetilde{L}(x,y) = -\left(p_{0,1}x + p_{-1,0}x^2y + \frac{1}{2}\left(p_{1,1} + p_{-1,-1}x^2y^2 - xy\right)\right)\widetilde{D}(x,y) + \left(p_{0,1}x + p_{1,1}\right)\widetilde{L}_{-0}(x) + \left(p_{0,1}x + \frac{1}{2}p_{1,1}\right)\widetilde{f}(1,1), \tag{4.61}$$

with $\widetilde{L}_{-0}(x) = \sum_{i\geq 2} \widetilde{f}(i,1)x^{i-1}$.

In order to simplify the last functional equation (4.61), we apply the following change of variables

$$\psi(x,y) = (x, x^{-1}y). \tag{4.62}$$

The equation (4.61) is changed into

$$K_\psi(x,y)\widetilde{L}_\psi(x,y) = -\left[x\widetilde{\alpha}_\psi(y) + \frac{1}{2}\widetilde{\beta}_\psi(y)\right]\widetilde{D}_\psi(y) + K_\psi(x,0)\widetilde{L}_\psi(x,0) + \left(p_{0,1}x + \frac{1}{2}p_{1,1}\right)\widetilde{f}(1,1), \tag{4.63}$$

with

$$\begin{cases} K\left(\psi(x,y)\right) &=& \dfrac{1}{x}K_\psi(x,y), & & \\ \widetilde{L}\left(\psi(x,y)\right) &=& x\widetilde{L}_\psi(x,y) &=& x\displaystyle\sum_{i,j\geq 1}\widetilde{f}(i+j,j)x^{i-1}y^{j-1}, \\ \widetilde{D}\left(\psi(x,y)\right) &=& \widetilde{D}_\psi(y) &=& \displaystyle\sum_{i\geq 1}\widetilde{f}(i,i)y^{i-1}, \end{cases} \tag{4.64}$$

and

$$K_\psi(x,y) = \alpha_\psi(x)y^2 + \beta_\psi(x)y + \gamma_\psi(x) = \widetilde{\alpha}_\psi(y)x^2 + \widetilde{\beta}_\psi(y)x + \widetilde{\gamma}_\psi(y),$$
$$\widetilde{\delta}_\psi(y) = \widetilde{\beta}_\psi(y)^2 - 4\widetilde{\alpha}_\psi(y)\widetilde{\gamma}_\psi(y), \quad \delta_\psi(x) = \beta_\psi(x)^2 - 4\alpha_\psi(x)\gamma_\psi(x). \tag{4.65}$$

The angle θ_ψ is also simply related to θ (see Figure 4.2b) as

$$\theta_\psi = \frac{\theta}{2}. \tag{4.66}$$

The scheme of the proof is the same as the proof of Lemma 38. Writing $\theta_\psi = \arccos(-c_\psi)$, we have $c_\psi = -\sqrt{\frac{1-c}{2}}$, hence (4.66). The functional equation (4.63) is very close to the functional equation in the three-quarter plane (4.27), the only difference is the additional term $p_{0,1}x$. We can then write a similar boundary value problem as Lemma 39.

Lemma 48. *The generating function* $\widetilde{D}_\psi(y)$ *is analytic in* $\mathcal{G}_{\mathcal{L}_\psi}$ *and continuous on* $\overline{\mathcal{G}_{\mathcal{L}_\psi}} \setminus \{1\}$. *Moreover, for all* $y \in \mathcal{L}_\psi \setminus \{1\}$, $\widetilde{D}_\psi(y)$ *satisfies the following boundary condition*

$$\frac{g_\psi(y)}{g'_\psi(y)}\widetilde{D}_\psi(y) - \frac{g_\psi(\bar{y})}{g'_\psi(\bar{y})}\widetilde{D}_\psi(\bar{y}) = 0, \tag{4.67}$$

where $\frac{g_\psi(y)}{g'_\psi(y)} = \frac{\widetilde{w}_\psi(y)\sqrt{\widetilde{w}_\psi(Y_\varphi(x_{\psi,1}))-\widetilde{w}_\psi(y)}}{\widetilde{w}'_\psi(y)\sqrt{\widetilde{w}_\psi(Y_\psi(x_{\psi,1}))}}$ *and* $\widetilde{w}_\psi$ *is a conformal gluing function defined in Subsection 4.4.1.*

Figure 4.11 – Simple random walk (left) and Gouyou-Beauchamps random walk (right)

Moreover, the expression of $\widetilde{D}_\psi(y)$ is the same as in the three-quarter plane and we have the following theorem, which is a quarter plane equivalent to Theorem 41.

Theorem 49. *The generating function $D_\psi(y)$ can be written as*

$$\widetilde{D}_\psi(y) = \frac{\widetilde{f}(1,1)}{\widetilde{w}'_\psi(0)}\frac{\pi}{\theta_\psi}\sqrt{-\frac{\widetilde{\delta}''_\psi(1)}{2\widetilde{\delta}_\psi(y)}}\sqrt{\widetilde{w}_\psi(Y_\psi(x_{\psi,1}))\left(\widetilde{w}_\psi(y)+\widetilde{W}_\psi(0)\right)}, \tag{4.68}$$

with θ_ψ, $\widetilde{w}_\psi(y)$ and $\widetilde{W}_\psi$ defined in Subsection 4.4.1 and $\widetilde{\delta}_\psi$ in (4.65).

From the expression of $\widetilde{D}_\psi$ in (4.68) and the functional equation (4.63), we get an expression for $\widetilde{L}_\psi(x,0)$:

$$K_\psi(x,0)\widetilde{L}_\psi(x,0) = -\frac{1}{2}\frac{\widetilde{f}(1,1)}{\widetilde{w}'_\psi(0)}\frac{\pi}{\theta_\psi}\sqrt{-\frac{\widetilde{\delta}''_\psi(1)}{2}}\sqrt{1-\widetilde{W}_\psi(0)}\sqrt{1-W_\psi(x)} - (p_{0,1}x+\frac{1}{2}p_{1,1})\widetilde{f}(1,1), \tag{4.69}$$

and from (4.32) there exists $k\neq 0$ such that, for x in the neighborhood of 1,

$$K_\psi(x,0)\widetilde{L}_\psi(x,0) = K(x,0)\widetilde{L}(x,0) = \frac{k+o(1)}{(1-x)^{\pi/(2\theta_\psi)}} = \frac{k+o(1)}{(1-x)^{\pi/\theta}}. \tag{4.70}$$

This asymptotic results matches that in [114].

We end this section with the example of the simple random walk. The application ψ changes the simple random walk into the Gouyou-Beauchamps random walk (see Figure 4.11). In order to compute $\widetilde{L}(x,0)$, we need to calculate θ_ψ, $\widetilde{\delta}_\psi$, $\widetilde{w}_\psi$ and W_ψ. We easily have $\theta_\psi = \frac{\pi}{4}$ and

$$\begin{cases} \widetilde{\delta}_\psi(y) &= -\frac{y(y-1)^2}{4}, \\ y_4 &= \infty, \\ \widetilde{\delta}''_\psi(0) &= 1, \\ \widetilde{\delta}'''_\psi(0) &= -3/2, \\ \widetilde{\delta}''_\psi(1) &= -1/2, \end{cases} \qquad \text{we have then } \widetilde{W}_\psi(y) = -\frac{16y(y+1)^2}{(1-y)^4}.$$

On the other side, we have

$$\begin{cases} \delta_\psi(x) &= \frac{(x^2-6x+1)(x-1)^2}{16}, \\ x_4 &= 3+2\sqrt{2}, \\ \delta'_\psi(x_4) &= 3\sqrt{2}+4, \\ \delta''_\psi(x_4) &= \frac{11}{2}+3\sqrt{2}, \\ \delta''_\psi(1) &= -1/2, \end{cases} \qquad \text{we have then } W_\psi(x) = 1 - \frac{64x^2}{4(x-1)^4}.$$

Finally, noticing that $K(x,0) = \frac{x}{4}$ and that $\widetilde{H}(x,0) = \widetilde{f}(1,1) + \widetilde{L}(x,0)$, from (4.69) we get

$$\widetilde{H}(x,0) = \frac{\widetilde{f}(1,1)}{(1-x)^2}, \tag{4.71}$$

and this result matches the computation in [114, Eq. 2.6].

4.6 Further objectives and perspectives

4.6.1 Non-symmetric case

In this section (except clearly stated) we suppose that the probability transitions of the random walks we consider are not symmetric and a priori neither is the harmonic function. In other words, the random walks satisfy hypotheses (H1), ($\hat{\text{H}}$2), (H3) and (H4) with

($\hat{\text{H}}$2) We assume that the transition probabilities $p_{0,0}$, $p_{-1,1}$, and $p_{1,-1}$ are all equal to zero.

and discrete harmonic functions associated to these random walks satisfy the properties (P1), (P2), (P3) but not necessarily (P4).

Like in Section 4.3.2, we split the three-quadrant into two symmetric convex cones of opening angle $\frac{3\pi}{4}$, and split the generating function $H(x,y)$ into three generating functions: $L(x,y)$ for harmonic functions in the lower part, $D(x,y)$ for harmonic functions on the diagonal and $U(x,y)$ for the ones in the upper part (see (4.21)). Since we do not have the symmetry condition anymore, instead of one functional equation as in Lemma 32, we end up with a system of two functional equations.

Lemma 50. *For any random walks with property (H1), the generating functions $L(x,y)$ and $U(x,y)$ satisfy the following system of functional equations*

$$\begin{cases} K(x,y)U(x,y) &= -\left(p_{1,0}y + p_{0,-1}xy^2 + p_{1,1} + p_{-1,-1}x^2y^2 - xy\right) D(x,y) \\ &\quad + \left(p_{0,1}x + p_{1,1}\right) U_{-0}(x^{-1}) - \left(p_{1,0}y + p_{0,-1}xy^2\right) D^\ell(x,y) \\ &\quad + p_{1,1}f(1,1) + p_{1,0}f(1,0), \\ K(x,y)L(x,y) &= -\left(p_{0,1}x + p_{-1,0}x^2y + p_{1,1} + p_{-1,-1}x^2y^2 - xy\right) D(x,y) \\ &\quad + \left(p_{1,0}y + p_{1,1}\right) L_{0-}(y^{-1}) - \left(p_{0,1}x + p_{-1,0}x^2y\right) D^u(x,y) \\ &\quad + p_{1,1}f(1,1) + p_{0,1}f(0,1). \end{cases} \tag{4.72}$$

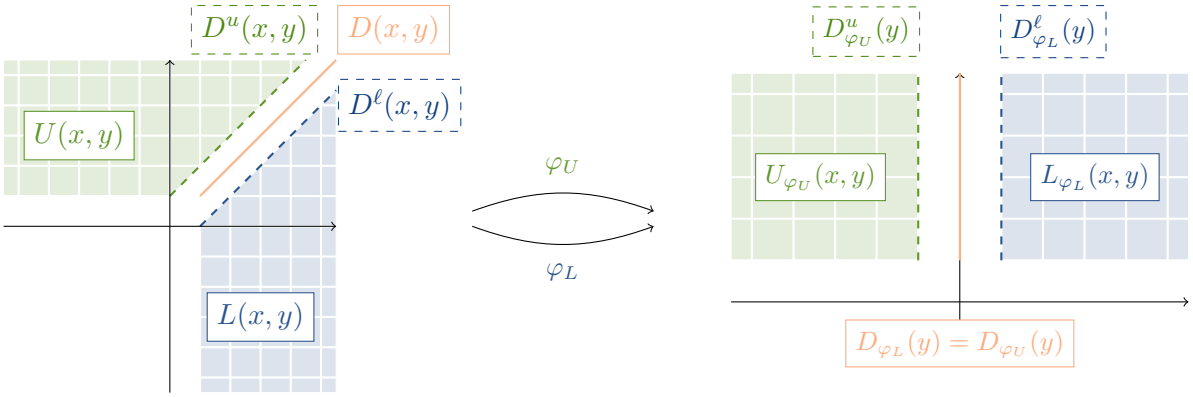

Figure 4.12 – Decomposition of the three-quarter plane, associated generating functions and changes of variable

Remark 51. Notice the symmetry between x and y in (4.72). In the case of a symmetric random walk (i.e., if $p_{i,j} = p_{j,i}$) the two functional equations are the same. Indeed, in this case, the positive harmonic function is symmetric as well (see Remark 33) and in particular we also have $U(x,y) = L(y,x)$. The first equation of the system of equations (4.72) becomes then

$$\begin{aligned} K(y,x)L(y,x) = &- \left(p_{0,1}y + p_{-1,0}xy^2 + p_{1,1} + p_{-1,-1}x^2y^2 - xy\right) D(y,x) \\ &+ (p_{1,0}x + p_{1,1})\, L_{0-}(x^{-1}) - \left(p_{0,1}y + p_{-1,0}xy^2\right) D^u(y,x) \\ &+ p_{1,1}f(1,1) + p_{0,1}f(0,1). \end{aligned}$$

Proof. The strategy of the proof is similar to the proof of Lemma 32. In addition to the functional equations for $L(x,y)$ and $D(x,y)$, see (4.23) and (4.24), we can write a functional equation for $U(x,y)$:

$$\begin{aligned} U(x,y) = &\left(\sum_{-1\le i,j\le 1} p_{i,j}x^{-i}y^{-j}\right) U(x,y) + \left(p_{1,0}x^{-1} + p_{0,-1}y\right) D(x,y) \\ &- \left(p_{-1,0}x + p_{0,1}y^{-1}\right) D^u(x,y) - \left(p_{0,1}y^{-1} + p_{1,1}x^{-1}y^{-1}\right) U_{-0}(x^{-1}) + p_{0,1}y^{-1}f(0,1)x^{-1}. \end{aligned} \quad (4.73)$$

Mixing equations (4.23), (4.73) and (4.24) and multiplying by xy, we get (4.72). □

In this system of two functional equations, the bivariate generating function $U(x,y)$ (resp. $L(x,y)$) is related to the bivariate generating functions $D(x,y)$, $D^\ell(x,y)$ (resp. $D^u(x,y)$) and the univariate generating function $U_{-0}(x^{-1})$ (resp. $L_{0-}(y^{-1})$). In order to simplify this system of functional equations, we perform two changes of variables, φ_L for the lower part and φ_U for the upper part with

$$\varphi_U(x,y) = (x, x^{-1}y) \qquad \text{and} \qquad \varphi_L(x,y) = (xy, x^{-1}).$$

These changes of variables transforms the upper part $\{j \geq 1, i \leq j-1\}$ into the left quadrant $\{i \leq -1, j \geq 0\}$ and the lower part $\{i \geq 1, j \leq i-1\}$ into the right quadrant $\{i \geq 1, j \geq 0\}$ (see Figure 4.12). Note that the diagonal is changed by both φ_L and φ_U into the positive y-axis (see again Figure 4.12). The step set is changed as well, and walks in the three-quadrant can be seen as inhomogeneous walks in the half plane with two different step sets in each quadrant and a mixed step set on the positive y-axis (see Figure 4.13). Other type of inhomogeneous walks are studied in [35, 45], see Section 3.4.1.

After the changes of variables, the generating functions become

$$\begin{cases} K\left(\varphi_U(x,y)\right) = \dfrac{1}{x} K_{\varphi_U}(x,y), \\ U(\varphi_U(x,y)) = xU_{\varphi_U}(x,y) = x \displaystyle\sum_{i_0 \leq -1, j_0 \geq 1} f(i_0+j_0, j_0) x^{i_0-1} y^{j_0-1}, \\ D^u(\varphi_U(x,y)) = x^{-1} D^u_{\varphi_U}(y) = x^{-1} \displaystyle\sum_{i_0 \geq 1} f(i_0-1, i_0) y^{i_0-1}, \\ D\left(\varphi_U(x,y)\right) = D_{\varphi_U}(y) = \displaystyle\sum_{i_0 \geq 1} f(i_0,i_0) y^{i_0-1} = D_{\varphi_L}(y) = D(\varphi_L(x,y)), \\ K\left(\varphi_L(x,y)\right) = \dfrac{1}{x} K_{\varphi_L}(x,y), \\ L\left(\varphi_L(x,y)\right) = xL_{\varphi_L}(x,y) = x \displaystyle\sum_{i_0, j_0 \geq 1} f(j_0, j_0-i_0) x^{i_0-1} y^{j_0-1}, \\ D^\ell(\varphi_L(x,y)) = xD^\ell_{\varphi_L}(y) = x \displaystyle\sum_{i_0 \geq 1} f(i_0, i_0-1) y^{i_0-1}, \end{cases} \tag{4.74}$$

with the following relations

$$D^\ell(\varphi_U(x,y)) = xy^{-1} D^\ell_{\varphi_L}(y) \qquad \text{and} \qquad D^u(\varphi_L(x,y)) = x^{-1}y^{-1} D^u_{\varphi_U}(y). \tag{4.75}$$

We apply these changes of variables to the system of functional equations (4.72) and get

$$\begin{cases} K_{\varphi_U}(x,y) U_{\varphi_U}(x,y) &= -\left(p_{1,0}x^{-1}y + p_{0,-1}x^{-1}y^2 + p_{1,1} + p_{-1,-1}y^2 - y\right) D_{\varphi_U}(y) \\ &\quad + \left(p_{0,1}x^2 + p_{1,1}x\right) U_{\varphi_U}(x,0) - \left(p_{1,0} + p_{0,-1}y\right) D^\ell_{\varphi_L}(y) \\ &\quad + p_{1,1}f(1,1) + p_{1,0}f(1,0), \\ K_{\varphi_L}(x,y) L_{\varphi_L}(x,y) &= -\left(p_{0,1}xy + p_{-1,0}xy^2 + p_{1,1} + p_{-1,-1}y^2 - y\right) D_{\varphi_L}(y) \\ &\quad + \left(p_{1,0} + p_{1,1}x\right) L_{\varphi_L}(x,0) - \left(p_{0,1} + p_{-1,0}y\right) D^u_{\varphi_U}(y) \\ &\quad + p_{1,1}f(1,1) + p_{0,1}f(0,1). \end{cases} \tag{4.76}$$

Writing

$$K_{\varphi_U}(x,y) = \alpha_{\varphi_U}(x)y^2 + \beta_{\varphi_U}(x)y + \gamma_{\varphi_U}(x) = \widetilde{\alpha}_{\varphi_U}(y) + \widetilde{\beta}_{\varphi_U}(y) + \widetilde{\gamma}_{\varphi_U}(y),$$
$$\widetilde{\delta}_{\varphi_U}(y) = \widetilde{\beta}_{\varphi_U}(y)^2 - 4\widetilde{\alpha}_{\varphi_U}(y)\widetilde{\gamma}_{\varphi_U}(y), \quad \delta_{\varphi_U}(x) = \beta_{\varphi_U}(x)^2 - 4\alpha_{\varphi_U}(x)\gamma_{\varphi_U}(x),$$

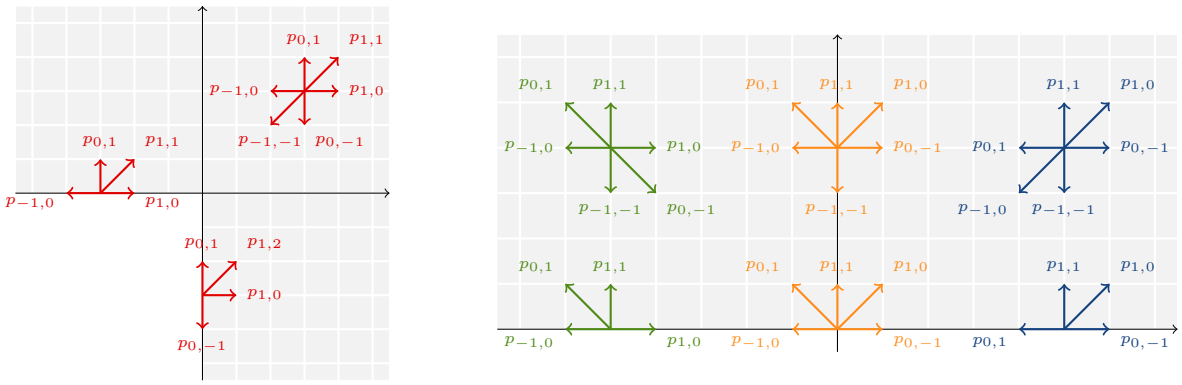

Figure 4.13 – Random walks avoiding a quadrant (on the left) can be seen as walks in the half plane with probability transitions $\varphi_U((p_{i,j})_{-1\le i,j\le 1})$ in the left quadrant and $\varphi_L((p_{i,j})_{-1\le i,j\le 1})$ on the right quadrant (on the right)

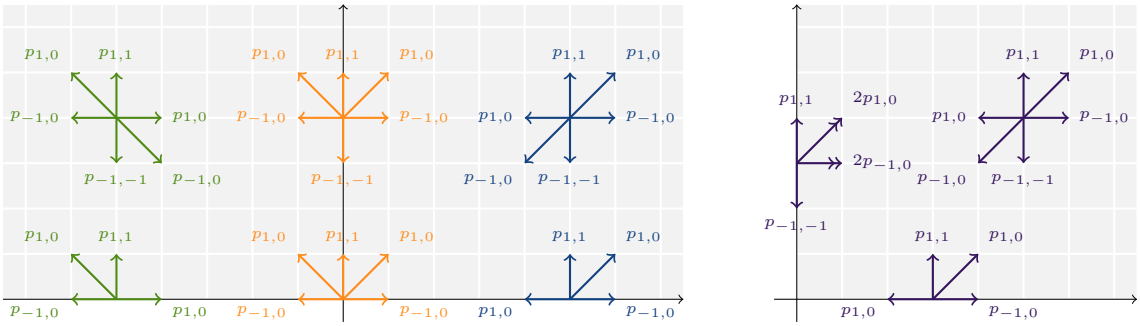

Figure 4.14 – Random walks with symmetric probability transitions avoiding a quadrant can be seen as random walks reflected on the y-axis and constrained by the x-axis

$$K_{\varphi_L}(x,y)=\alpha_{\varphi_L}(x)y^2+\beta_{\varphi_L}(x)y+\gamma_{\varphi_L}(x)=\widetilde{\alpha}_{\varphi_L}(y)+\widetilde{\beta}_{\varphi_L}(y)+\widetilde{\gamma}_{\varphi_L}(y),$$
$$\widetilde{\delta}_{\varphi_L}(y)=\widetilde{\beta}_{\varphi_L}(y)^2-4\widetilde{\alpha}_{\varphi_L}(y)\widetilde{\gamma}_{\varphi_L}(y),\quad \delta_{\varphi_L}(x)=\beta_{\varphi_L}(x)^2-4\alpha_{\varphi_L}(x)\gamma_{\varphi_L}(x),$$

the previous system can be written as

$$\begin{cases} K_{\varphi_U}(x,y)U_{\varphi_U}(x,y) &= -\left(x^{-1}\widetilde{\gamma}_{\varphi_U}(y)+\widetilde{\beta}_{\varphi_U}(y)\right)D_{\varphi_U}(y)+\gamma_{\varphi_U}(x)U_{\varphi_U}(x,0)\\ &\quad -\widetilde{\gamma}_{\varphi_L}(y)D^{\ell}_{\varphi_L}(y)+p_{1,1}f(1,1)+p_{1,0}f(1,0),\\ K_{\varphi_L}(x,y)L_{\varphi_L}(x,y) &= -\left(x\widetilde{\alpha}_{\varphi_L}(y)+\widetilde{\beta}_{\varphi_L}(y)\right)D_{\varphi_L}(y)+\gamma_{\varphi_L}(x)L_{\varphi_L}(x,0)\\ &\quad -\widetilde{\alpha}_{\varphi_U}(y)D^{u}_{\varphi_U}(y)+p_{1,1}f(1,1)+p_{0,1}f(0,1). \end{cases} \tag{4.77}$$

Unfortunately, due to number of unknown functions, we are not able to solve this system of functional equations yet. Let us end this section by pointing out that the split cone along the diagonal can also be related to the Join-the-Shortest-Queue model, see Section 3.4.1.

In the symmetric case (symmetry of the random walks and hence symmetry of the unique positive harmonic function), the study of harmonic functions of random walks in the three quadrants

is then equivalent to the study of harmonic functions of random walks reflected on the y-axis and constrained by the x-axis in the positive quadrant (see Figure 4.14). Articles [12, 127] work on problem in the same vein: their authors study walks in the quadrant with different weights on the boundary, see Figure 3.11b.

4.6.2 Non-positive harmonic functions

As we have seen in this chapter, lots of work have been done on positive discrete harmonic functions. In the non-zero drift case (when (H4) is not satisfied), there are infinitely many positive harmonic functions whereas in the zero drift case there exists exactly one (up to a multiplicative constant) non-zero positive harmonic function. In the quadrant and the three-quadrant, the generating function of the harmonic function can be written as a polynomial P of a conformal gluing function w (see [114, Sec. 3.1] and Lemma 44). When the degree of P is minimal (of degree 1 then), we can determine the unique positive harmonic function. When the polynomial P is of degree more than 1, we get a set of non-positive (or signed) harmonic function (see Remark 46). It is therefore natural to get interested in non-positive harmonic functions. Let us give a (non-exhaustive and non-hierarchical) list of some reasonable questions:

Question 52. Is every harmonic function (not necessarily positive) completely determined by the polynomial P?

Question 53. What is the structure of non-positive harmonic functions and how many are they?

Question 54. Every harmonic function in the quadrant is harmonic in the three-quadrant. How does the cone of restriction affect the structure of signed harmonic functions?

Question 55. What are the properties of non-positive harmonic functions?

This is an ongoing project with É. Fusy, K. Raschel and P. Tarrago.

Chapter 5

3-Dimensional positive lattice walks and spherical triangles[1]

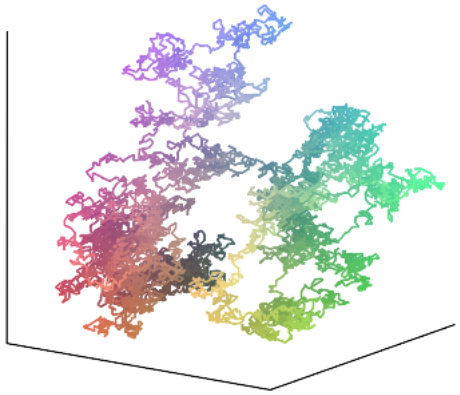

A random 10,000 step walk in the positive octant

5.1 Introduction

As we have seen in Chapter 1, the enumeration of lattice walks is an important topic in combinatorics. In addition to having various applications, it is connected to other mathematical fields such as probability theory. Recently, lots of consideration have been given to the enumeration of walks confined to cones. We will typically be considering walks on $\mathbb{Z}^d$ that start at the origin and consist of steps taken from $\mathcal{S}$, a finite subset of $\mathbb{Z}^d$. Most of the time we will constrain the walks in the orthant $\mathbb{N}^d$, with $\mathbb{N}$ denoting the set of non-negative integers $\{0, 1, 2, \ldots\}$.

[1]This chapter is mainly from [26].

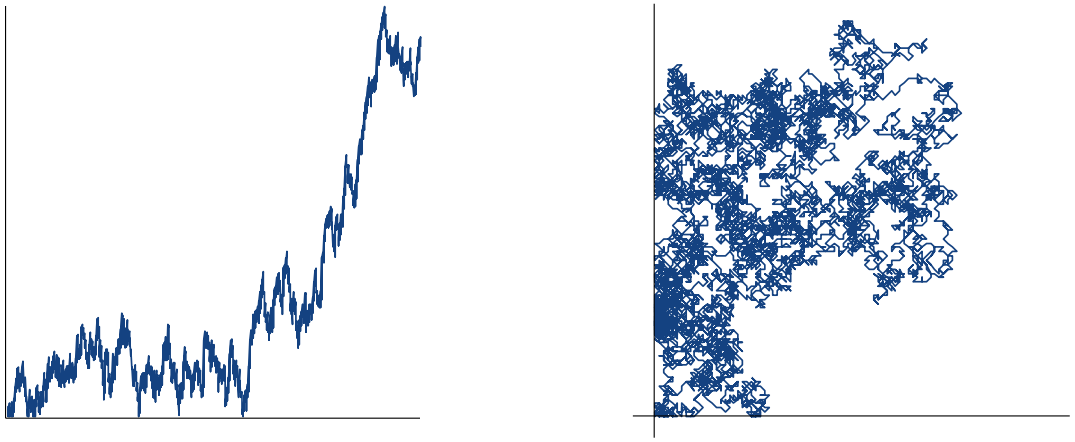

(a) Motzkin paths in $\mathbb{N}$
$\mathcal{S} = \{(1,1),(1,0),(1,-1)\}$

(b) Random walk in $\mathbb{N}^2$
$\mathcal{S} = \{(\pm 1,0)\}^2 \setminus \{(0,0)\}$

Figure 5.1 – Walks in $\mathbb{N}$ and $\mathbb{N}^2$

In dimension one (Figure 5.1a) there is essentially one unique cone (the positive half-line), and positive (random) walks are very well understood, see in particular [18, 10].

Following the seminal works [72, 41], many recent papers deal with the enumeration of 2D walks with prescribed steps confined to the positive quadrant (Figure 5.1b). In the case of small steps ($\mathcal{S}$ included in $\{0,\pm 1\}^2$), various results have been obtained: exact and asymptotic expressions [41, 30, 34] (see Section 2.2), classification of the generating function according to the classes rational, algebraic, D-finite [41], non-D-finite [100, 34], and even non-differentially algebraic [62] (see Section 2.3).

In dimension three, determining whether the equivalence of the dimension two (see Table 2.2) between D-finiteness of the generating function and finiteness of the symmetry group holds or not remains an open problem. More generally, much less is known on 3D lattice walks confined to the non-negative octant $\mathbb{N}^3$. An intrinsic difficulty lies in the number of models to handle: more than 11 million [27] (compare with 79 quadrant models). The first work is an empirical classification by Bostan and Kauers [30] of the models with at most five steps. Then in [27], Bostan, Bousquet-Mélou, Kauers and Melczer study models of cardinality at most six. They introduce key concepts: the dimensionality (1D, 2D or 3D) of a model, the group of the model, the Hadamard structure (roughly speaking, it is a generalization of Cartesian products of lower dimensional models). These notions will be made precise in Section 5.2.2. Furthermore, the authors of [27] classify the models with respect to these concepts and compute, in various cases (but only in presence of a finite group), the generating function

$$O(x,y,z) = \sum_{i,j,k,n\geq 0} o_{i,j,k}(n) x^i y^j z^k t^n, \tag{5.1}$$

(a) From left to right: the simple walk, Kreweras 3D model, a $(1,2)$-type Hadamard model and a $(2,1)$-type Hadamard model. The models are the same ones as in Figure 5.2b. These pictures are courtesy of Alin Bostan

(b) For each model, the first diagram shows steps of the form $(i,j,-1)$, the second the steps $(i,j,0)$, and the third the steps $(i,j,1)$. The models are the same ones as in Figure 5.2a. These cross-section views were first proposed in [30, 27]

Figure 5.2 – Various 3D step sets. As these perspective drawings of Figure 5.2a might be difficult to read, we will prefer the cross-section views of the step sets as in Figure 5.2b

where $o_{i,j,k}(n)$ is the number of n-step walks in the octant starting at the origin $(0,0,0)$ and ending at position (i,j,k). The techniques used in [27] to solve finite group models are the algebraic kernel method and computer algebra (using the guessing-and-proving paradigm).

The classification (in particular with respect to the finiteness of the group and the Hadamard structure) of the 3D small step models with arbitrary cardinality is pursued in the articles [6, 64, 128, 95]. Table 5.2 reproduces this classification.

Asymptotics of the excursion sequence. Let us finally recall (see Section 2.2) a result of Denisov and Wachtel [58], which is fundamental to our study. It proves in a great level of generality the following asymptotics for the excursion sequence $e_{A\to B}(n)$, i.e., the number of n-step walks in the octant starting (resp. ending) at $A \in \mathbb{N}^3$ (resp. $B \in \mathbb{N}^3$). If A and B are far enough from the boundary, as $n \to \infty$,

$$e_{A\to B}(pn) = \varkappa(A,B) \cdot \rho^{pn} \cdot n^{-\alpha} \cdot (1 + o(1)), \tag{5.2}$$

where $\varkappa(A,B) > 0$ is some constant, $\rho \in (0, |\mathcal{S}|]$ is the exponential growth, $\alpha > 0$ is the critical exponent and $p \in \mathbb{N}$ is the period of the model, i.e.,

$$p = \gcd\{n \in \mathbb{N} : o_{A\to B}(n) > 0\}. \tag{5.3}$$

The asymptotics expression (5.2) is proved in [58] in the aperiodic case ($p = 1$) and commented in [67, 28] for periodic models ($p > 1$). For exact hypotheses and a discussion, see Theorem 58 in Section 5.2.3 and the comments following the statement.

Most of the time we shall assume that

(H) The step set $\mathcal{S}$ is not included in any half-space $\{y \in \mathbb{R}^d : \langle x, y\rangle \geq 0\}$ with $x \in \mathbb{R}^d \setminus \{0\}$, $\langle \cdot, \cdot \rangle$ denoting the classical Euclidean inner product. In this case, we say that the walks are non-singular.

The quantities ρ and α in (5.2) are computed in [58]. First, ρ is the global minimum on $\mathbb{R}^d_+$ of the inventory (or characteristic polynomial)

$$\chi_{\mathcal{S}}(x, y, z) = \chi(x, y, z) = \sum_{(i,j,k)\in\mathcal{S}} x^i y^j z^k \tag{5.4}$$

and is thus well understood and easily computed (it is an algebraic number). On the other hand, the computation of α is much more elaborate: applying the results of [58] (see in particular Equation (12) there) readily gives, under the hypothesis (H), an expression for the critical exponent. Let λ_1 be the smallest eigenvalue Λ of the Dirichlet problem for the Laplace-Beltrami operator $\Delta_{\mathbb{S}^2}$ on the sphere $\mathbb{S}^2 \subset \mathbb{R}^3$

$$\begin{cases} -\Delta_{\mathbb{S}^2} m &= \Lambda m \quad \text{in } T, \\ m &= 0 \quad \text{in } \partial T, \end{cases} \tag{5.5}$$

$T = T(\alpha, \beta, \gamma)$ being a spherical triangle (see Figure 5.3 for an illustration). Then, the critical exponent have the following expression

$$\alpha = \sqrt{\lambda_1 + \frac{1}{4}} + 1. \tag{5.6}$$

Note that the spherical triangle T can be computed algorithmically (and easily) in terms of the model $\mathcal{S}$, see Theorem 58 for a precise statement.

Concerning the algebraic nature of the 3D generating function (5.1), a few results are known: in the finite group cases solved in [27], the generating function is always D-finite. On the other hand, the article [64] proves that for some degenerate (in the sense of the dimensionality) 3D models, the excursion generating function $O(0, 0, 0)$ is non-D-finite, by looking at the asymptotic behavior of the excursion sequence and showing that α in (5.2) is irrational, extending the work [34]. Does there exist a non-degenerate 3D finite group model with a non-D-finite generating function (5.1)? The 3D Kreweras model of Figure 5.2a could provide such an example. The 3D simple walk in the complement of an octant is also conjectured to admit a non-D-finite generating function, see [111, Sec. 4].

Structure of the chapter and main contributions. In *Section 5.2* we start by presenting all needed definitions and first properties of 3D models. In particular, we associate to each model a spherical triangle, which captures a lot of combinatorial information. Results in that section come from [58, 27, 6, 95].

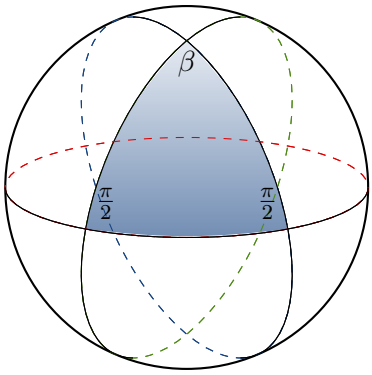

(a) A particular spherical triangle with two right angles (these triangles will eventually correspond to Hadamard models)

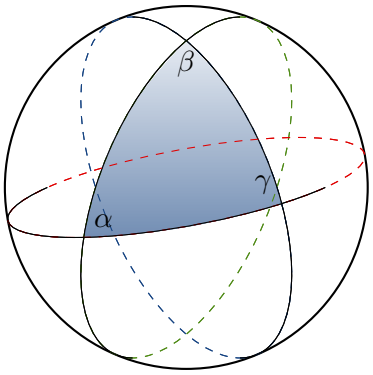

(b) A generic triangle with angles α, β, γ

Figure 5.3 – Spherical triangles

In *Section 5.3* we first recall properties of spherical triangles and the principal eigenvalue of a Dirichlet problem. This section gathers also some elementary facts on spherical geometry.

In *Section 5.4* we give the exact value of the angles of a spherical triangle. We also present further features of the covariance matrix as well as the construction of a walk model from a given spherical triangle.

Section 5.5 is at the heart of this chapter. Our result deals with Hadamard models (mostly with infinite group, as finite group Hadamard walks are solved in [27]). They have birectangular triangles, as in Figure 5.3a. Finite (resp. infinite) group Hadamard models correspond to angles β such that $\frac{\pi}{\beta} \in \mathbb{Q}$ (resp. $\frac{\pi}{\beta} \notin \mathbb{Q}$). Hadamard models are quite special for combinatorial reasons, as explained in [27], but also for the Laplacian: to the best of our knowledge, their birectangular triangles are the only triangles (with the exception of the tiling triangles described in Lemma 64) for which one can compute the spectrum. We deduce the critical exponent α and show that (most of) infinite group Hadamard models are non-D-finite. This is the first result on the non-D-finiteness of truly 3D models.

In *Section 5.6* we classify the models with respect to their triangle and the associated principal eigenvalue, and compare our results with the classification in terms of the group and the Hadamard property obtained in [27, 95]. Finite group models correspond to triangular tilings of the sphere $\mathbb{S}^2$. The simplest example is the simple walk with steps

$$\mathcal{S} = \{(\pm 1, 0, 0), (0, \pm 1, 0), (0, 0, \pm 1)\},$$

see Figure 5.2b (leftmost). Its triangle has three right angles, namely $\alpha = \beta = \gamma = \frac{\pi}{2}$ in Figures 5.3 and 5.4a. A second example is 3D Kreweras model, with step set

$$\mathcal{S} = \{(-1, 0, 0), (0, -1, 0), (0, 0, -1), (1, 1, 1)\},$$

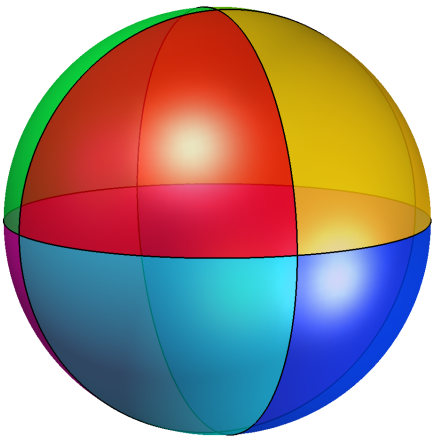

(a) Tiling of the sphere by equilateral triangles with right angles. It is associated to the simple walk

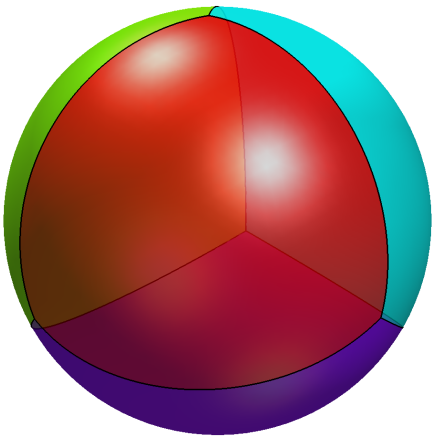

(b) The tetrahedral partition of the sphere. It corresponds to Kreweras 3D model

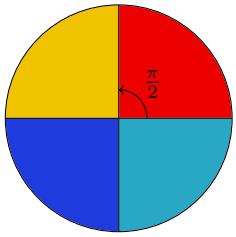

(c) Decomposition of the circle by regions of opening angle $\pi/2$, associated to the simple model. This is a 2D version of Figure 5.4a.

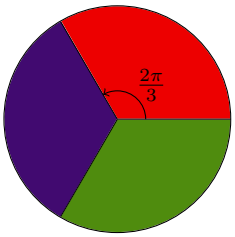

(d) Decomposition of the circle by of regions opening angle $2\pi/3$, associated to the Kreweras model. This is a 2D version of Figure 5.4b.

Figure 5.4 – Various tilings of the sphere and the circle. See Figure 5.13 for further examples of tilings

see Figure 5.2b (left). The associated triangle is also equilateral, with angles $\frac{2\pi}{3}$, this corresponds to the tetrahedral tiling of the sphere, see Figure 5.4b. Let us recall that in dimension two, the coefficient $\arccos(-c)$ (see (2.35)) is rational in the case of finite groups models, which correspond to partition the circle in circular sector (see Figures 5.4c and 5.4d).

We exhibit some exceptional models, which do not have the Hadamard property but for which, remarkably, one can compute an explicit form for the eigenvalue; this typically leads to non-D-finiteness results.

Although we will not consider these issues here, let us mention that we can also see the dimensionality on the triangle. In the case of 2D models, the triangles degenerate into a spherical digon, see Section 5.8.4 (in particular Figure 5.20).

In *Section 5.7* we present our last result which is about generic infinite group models. Even if no closed-form formula exists for λ_1, we may consider λ_1 as a *special function* of the triangle T (or equivalently of its angles α, β, γ, as in spherical geometry a triangle is completely determined by its angles), and with numerical analysis methods, obtain approximations of this function when

evaluated at particular values. The techniques developed in Section 5.7 are completely different from the rest of the paper. Notice that for some cases, approximate values of the critical exponents have been found by Bostan and Kauers [30], Bacher, Kauers and Yatchak [6], Bogosel [25], Guttmann [88], Dahne and Salvy [53]. See Section 5.7.1 for more details.

Finally, the *Section 5.8* proposes various extensions and remarks.

5.2 Preliminaries

In this section we introduce key concepts to study 3D walks. We are largely inspired by the paper [27], which gives a functional equation of walks in the positive octant (Section 5.2.1) and classifies three-dimensional walks according to the dimension of a model, the group of a model, or the Hadamard structure (Section 5.2.2). The thorough classification presented in Section 5.2.2 is done in the papers [6, 95] and the fundamental asymptotic results of Section 5.2.3 can be found in [58]. We follow the notations of [27].

5.2.1 Functional equation

With the same strategy as for 2D walks (see Section 2.1.1), a functional equation for the generating function $O(x,y,z)$ (5.1) can be easily derived describing how a 3D walk in the positive octant can be built. The inventory Laurent polynomial of $\mathcal{S}$ defined in (5.4) can be written as

$$\begin{aligned}\chi(x,y,z) &= A_-(y,z)x^{-1} + A_0(y,z) + A_+(y,z)x \\ &= B_-(x,z)y^{-1} + B_0(x,z) + B_+(x,z)y \\ &= C_-(x,y)z^{-1} + C_0(x,y) + C_+(x,y)z.\end{aligned} \tag{5.7}$$

The term $A_-(y,z)x^{-1}$ (resp. $B_-(x,z)y^{-1}$ and $C_-(x,y)z^{-1}$) represents the steps in the negative x-direction (resp. y-direction and z-direction), $A_0(y,z)$ (resp. $B_0(x,z)$ and $C_0(x,y)$) is for steps without x-direction (resp. y-direction and z-direction) and $A_+(y,z)x$ (resp. $B_+(x,z)y$ and $C_+(x,y)z$) stands for steps with positive x-direction (resp. y-direction and z-direction). Let us introduce

$$D_-(z) = \sum_{(-1,-1,k)\in\mathcal{S}} z^k, \qquad E_-(y) = \sum_{(-1,j,-1)\in\mathcal{S}} y^j, \qquad F_-(x) = \sum_{(i,-1,-1)\in\mathcal{S}} x^i,$$

which represent respectively the steps with negative xy-direction, xz-direction and yz-direction. We also define $\varepsilon = 1$ when $(-1,-1,-1) \in \mathcal{S}$ and 0 otherwise.

Walks in the 3D octant can be empty with generating function 1, or can be walks in the octant to which we add a step from $\mathcal{S}$, that is $t\chi(x,y,z)O(x,y,z)$. We need to remove the walks going out from the plane yz (resp. xz and xy) with generating function $tx^{-1}A_-(y,z)O(0,y,z)$ (resp. $ty^{-1}B_-(x,z)O(x,0,z)$ and $tz^{-1}C_-(x,y)O(x,y,0)$). However, we have removed twice some walks going out from the z-axis (resp. y-axis and x-axis) and thus we need to add $tx^{-1}y^{-1}D_-(z)O(0,0,z)$

(resp. $tx^{-1}z^{-1}E_-(y)O(0,y,0)$ and $ty^{-1}z^{-1}F_-(x)O(x,0,0)$). Finally, we remove the walks out of the octant with generating function $\varepsilon t x^{-1}y^{-1}z^{-1}O(0,0,0)$. This construction is also known as the inclusion-exclusion principle. The generating function $O(x,y,z)$ satisfies then the following functional equation [27, Sec. 4.1].

$$\begin{aligned} O(x,y,z) = 1 &+ t\chi(x,y,z)O(x,y,z) \\ &- tx^{-1}A_-(y,z)O(0,y,z) - ty^{-1}B_-(x,z)O(x,0,z) - tz^{-1}C_-(x,y)O(x,y,0) \\ &+ tx^{-1}y^{-1}D_-(z)O(0,0,z) + tx^{-1}z^{-1}E_-(y)O(0,y,0) + ty^{-1}z^{-1}F_-(x)O(x,0,0) \\ &- \varepsilon t x^{-1}y^{-1}z^{-1}O(0,0,0). \end{aligned} \tag{5.8}$$

5.2.2 Classification of three-dimensional walks

Dimension of a model. Let $w = w_1 w_2 \dots w_n$ be a walk of length n with increments w_i in $\mathcal{S}$. The walk w ends in the positive octant if and only if the following three linear inequalities hold:

$$\sum_{s\in\mathcal{S}} a_s s_x \geq 0, \qquad \sum_{s\in\mathcal{S}} a_s s_y \geq 0, \qquad \sum_{s\in\mathcal{S}} a_s s_z \geq 0, \tag{5.9}$$

where a_s is the multiplicity of $s = (s_x, s_y, s_z)$ in w. Notice that the walk w remains in the octant if the multiplicities observed in each of its prefixes satisfy these inequalities.

Definition 56 ([27])**.** Let $d \in \{0,1,2,3\}$. A model $\mathcal{S}$ is said to have dimension at most d if there exist d inequalities in (5.9) such that any $|\mathcal{S}|$-tuple $(a_s)_{s\in\mathcal{S}}$ of non-negative integers satisfying these d inequalities satisfies in fact the three ones. We define accordingly models of dimension (exactly) d.

(a) $d = 0$ (b) $d = 1$ (c) $d = 2$ (d) $d = 3$

Figure 5.5 – Four-step models of various dimensions [27, Fig. 1]

See Figure 5.5 for an illustration of Definition 56. Models of dimension 0 have a step set $\mathcal{S} \subset \{0,1\}^3 \setminus \{(0,0,0)\}$ making the positive octant restriction removable (A_-, B_-, C_-, D_-, E_- and F_- are all equal to zero in (5.8)). In this case, the generating function of the walk is rational and $O(x,y,z) = \frac{1}{1-tS(x,y,z)}$. Models of dimension 1 are in fact walks confined to a half-space. These models are characterized in [27, Sec. 2.1] and the generating function of the walk is algebraic. Less is known for models of dimension 2 (walks confined to the intersection of two half-spaces) and of dimension 3. Proposition 2.5 of [27] gives the number of models having dimension 2 or 3, with no unused step (that is, a step that is never used in a walk confined to the octant), and counted up to permutations of the coordinates, ending up with the number 11,074,225 in Table 5.2. In what

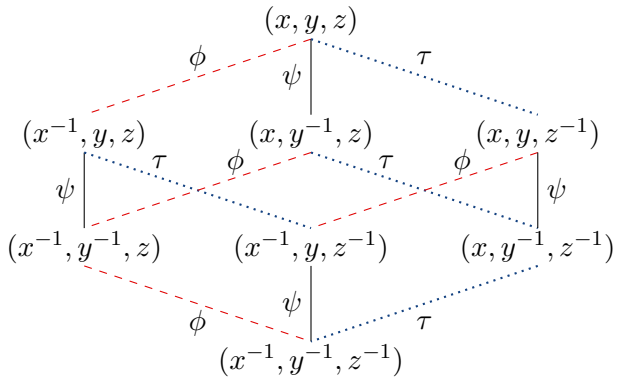

Figure 5.6 – Orbit of (x,y,z) under the group G in the simple walk case

follows we will be principally considering models of dimension 3, and in fact only a subclass of them: most of the time we will assume the hypothesis (H) stated in Section 5.1.

Group of the model. This group was first introduced in the context of 2D walks, see Section 2.3.1 and turns out to be very useful. If $\mathcal{S}$ is 3-dimensional then it has a positive step in each direction and A_+, B_+ and C_+ defined in (5.7) are all non-zero. The group of $\mathcal{S}$ is the group $G = \langle \phi, \psi, \tau \rangle$ of birational transformations of the variables (x,y,z) generated by the following three involutions:

$$\begin{cases} \phi(x,y,z) &= \left(x^{-1}\frac{A_-(y,z)}{A_+(y,z)}, y, z\right), \\ \psi(x,y,z) &= \left(x, y^{-1}\frac{B_-(x,z)}{B_+(x,z)}, z\right), \\ \tau(x,y,z) &= \left(x, y, z^{-1}\frac{C_-(x,y)}{C_+(x,y)}\right), \end{cases} \tag{5.10}$$

where $A_\pm(y,z), B_\pm(x,z), C_\pm(x,y)$ are defined in (5.7). For example, consider the simple step set with $S(x,y,z) = x+y+z+x^{-1}+y^{-1}z^{-1}$. Then $\Phi(x,y,z) = (x^{-1},y,z)$, $\Psi(x,y,z) = (x,y^{-1},z)$ and $\tau(x,y,z) = (x,y,z^{-1})$ and the group $G(\mathcal{S})$ is of order 8 (see Figure 5.6). We refer to [27, Sec. 2.4] for more details on the group.

The classification of the models according to the (in)finiteness of the group is known, see Table 5.2. Let us also reproduce [95, Tab. 1].

Hadamard structure. Hadamard models are introduced in [27] (see in particular Section 5 there). These are 3-dimensional models which can be reduced to the study of a pair of models, one in $\mathbb{Z}$ and one in $\mathbb{Z}^2$, using a Hadamard product of generating functions.

There are two types of Hadamard models: the $(1,2)$-type and the $(2,1)$-type. More generally, in arbitrary dimension d there is the notion of (D,δ)-Hadamard model, with $D+\delta = d$, see [27,

[2] A Coxeter group is a group generated by reflections. For instance, Weyl groups and the dihedral group are Coxeter group.

Group	Number of models	Group	Number of models
$G_1 = \langle \mathtt{a}, \mathtt{b}, \mathtt{c} \mid \mathtt{a}^2, \mathtt{b}^2, \mathtt{c}^2 \rangle$	10,759,449	$G_7 = \langle \mathtt{a}, \mathtt{b}, \mathtt{c} \mid \mathtt{a}^2, \mathtt{b}^2, \mathtt{c}^2, (\mathtt{ab})^4 \rangle$	82
$G_2 = \langle \mathtt{a}, \mathtt{b}, \mathtt{c} \mid \mathtt{a}^2, \mathtt{b}^2, \mathtt{c}^2, (\mathtt{ab})^2 \rangle$	84,241	$G_8 = \langle \mathtt{a}, \mathtt{b}, \mathtt{c} \mid \mathtt{a}^2, \mathtt{b}^2, \mathtt{c}^2, (\mathtt{ab})^3, (\mathtt{bc})^3 \rangle$	30
$G_3 = \langle \mathtt{a}, \mathtt{b}, \mathtt{c} \mid \mathtt{a}^2, \mathtt{b}^2, \mathtt{c}^2, (\mathtt{ac})^2, (\mathtt{ab})^2 \rangle$	58,642	$G_9 = \langle \mathtt{a}, \mathtt{b}, \mathtt{c} \mid \mathtt{a}^2, \mathtt{b}^2, \mathtt{c}^2, \mathtt{acbacbcabc} \rangle$	20
$G_4 = \langle \mathtt{a}, \mathtt{b}, \mathtt{c} \mid \mathtt{a}^2, \mathtt{b}^2, \mathtt{c}^2, (\mathtt{ac})^2, (\mathtt{ab})^3 \rangle$	1,483	$G_{10} = \langle \mathtt{a}, \mathtt{b}, \mathtt{c} \mid \mathtt{a}^2, \mathtt{b}^2, \mathtt{c}^2, (\mathtt{ab})^3, (\mathtt{cbca})^2 \rangle$	8
$G_5 = \langle \mathtt{a}, \mathtt{b}, \mathtt{c} \mid \mathtt{a}^2, \mathtt{b}^2, \mathtt{c}^2, (\mathtt{ab})^3 \rangle$	1,426	$G_{11} = \langle \mathtt{a}, \mathtt{b}, \mathtt{c} \mid \mathtt{a}^2, \mathtt{b}^2, \mathtt{c}^2, (\mathtt{ca})^3, (\mathtt{ab})^4, (\mathtt{babc})^2 \rangle$	8
$G_6 = \langle \mathtt{a}, \mathtt{b}, \mathtt{c} \mid \mathtt{a}^2, \mathtt{b}^2, \mathtt{c}^2, (\mathtt{ac})^2, (\mathtt{ab})^4 \rangle$	440	$G_{12} = \langle \mathtt{a}, \mathtt{b}, \mathtt{c} \mid \mathtt{a}^2, \mathtt{b}^2, \mathtt{c}^2, (\mathtt{ab})^4, (\mathtt{ac})^4 \rangle$	4

Table 5.1 – Various infinite groups associated to 3D models. Notice that the presentations of the groups are not certified: it is not excluded [95] that further relations exist, but then involving more than 400 generators. With the exception of G_9, G_{10} and G_{11}, all groups are Coxeter groups[2]. Most of the time, but not systematically, one can take $\mathtt{a} = \phi$, $\mathtt{b} = \psi$ and $\mathtt{c} = \tau$

(a) A $(1,2)$-type Hadamard model

(b) A $(2,1)$-type Hadamard model

Figure 5.7 – Hadamard models

Sec. 5.2]. Back to the dimension 3, the $(1,2)$-type corresponds to models for which the inventory (5.4) can be written under the form

$$\chi(x,y,z) = U(x) + V(x)T(y,z). \tag{5.11}$$

The $(2,1)$-type corresponds to

$$\chi(x,y,z) = U(x,y) + V(x,y)T(z). \tag{5.12}$$

The number of Hadamard models (with the additional information on the type) can be found in Table 5.2.

For each type, an example is presented in Figure 5.7: for the $(1,2)$-type we have $\chi(x,y,z) = U(z) + V(z)T(x,y)$ (permutation of the variables in the definition (5.11)), with $U(z) = z + z^{-1}$, $V(z) = z + 1 + z^{-1}$ and $T(x,y) = x + xy^{-1} + x^{-1}y^{-1} + x^{-1}y + y$ (scarecrow 1 model, see Figure 5.8). For the $(2,1)$-type we have taken $U(x,y) = x + x^{-1} + y + y^{-1}$ (the 2D simple walk, see Figure 5.8), $V(x,y) = x + xy^{-1} + x^{-1}y^{-1} + x^{-1}y + y$ (scarecrow 1 model, see again Figure 5.8) and $T(z) = z + z^{-1}$.

Hadamard models extend Cartesian products of walks: Cartesian products (or equivalently independent random walks in the probabilistic framework) correspond to taking $U(x) = 0$ in (5.11) or $U(x,y) = 0$ in (5.12). Notice that Hadamard models in dimension 2 are always D-finite [28], even with large steps.

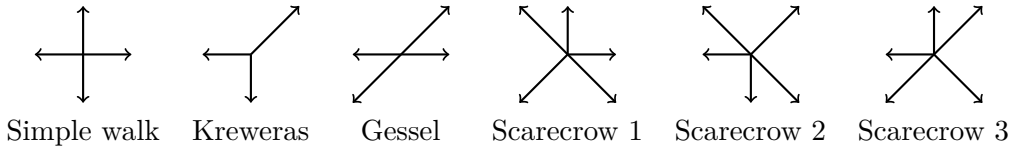

Figure 5.8 – Some 2D models. The three scarecrows are named after [34, Fig. 1]

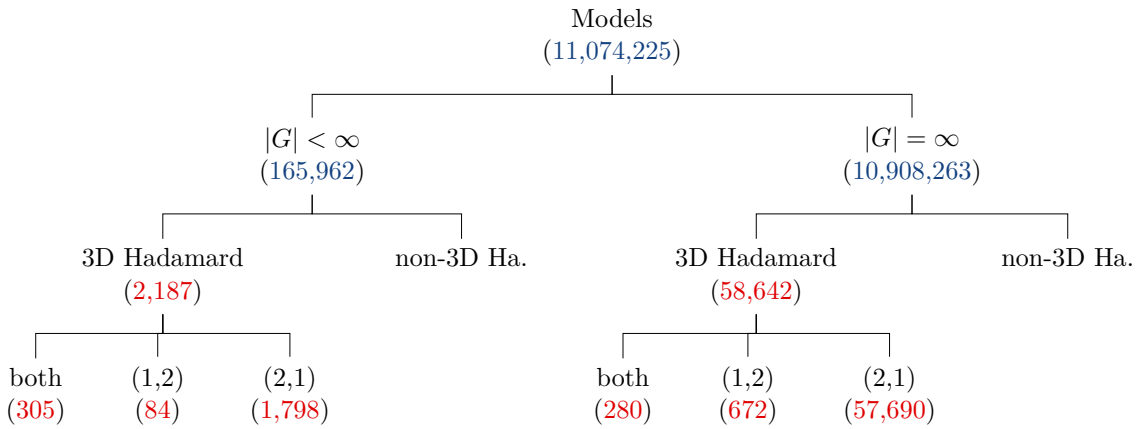

Table 5.2 – Classification of 3D walks (of dimension 2 and 3) according to the finiteness of the group and the Hadamard property [95]. The numbers of (non-)Hadamard models refer exclusively to dimension 3 models. Hence among the non-3D Hadamard models one can find models of dimensionality 2 having a (degenerate) Hadamard decomposition. A model labeled "both" is simultaneously $(1,2)$-type and $(2,1)$-type Hadamard. The total number of models is computed in [27], the number of (in)finite groups in [27, 64, 95] and the refined statistics on 3D Hadamard models in [93]

5.2.3 Formula for the exponent of the excursions

We now explain that the exponent α in (5.2) is directly related to the smallest eigenvalue of a certain Dirichlet problem on a spherical triangle. Let us start with a simple definition:

Definition 57 ([15])**.** A spherical triangle on $\mathbb{S}^2$ is a triple (x, y, z) of points of $\mathbb{S}^2$ that are linearly independent as vectors in $\mathbb{R}^3$. We denote it by $\langle x, y, z\rangle$.

See examples in Figures 5.3 and 5.4. The points x, y, z are the vertices of $\langle x, y, z\rangle$. By the sides of $\langle x, y, z\rangle$ we mean the arcs of great circle determined by (x, y), (y, z) and (z, x).

The following result gives a method to compute the critical exponent; several explanatory remarks may be found below the statement.

Theorem 58 ([58]). *Consider an irreducible walk*[3] *with step set $\mathcal{S}$ satisfying* (H) *and let χ be its inventory* (5.4)*. The system of equations*

$$\frac{\partial \chi}{\partial x} = \frac{\partial \chi}{\partial y} = \frac{\partial \chi}{\partial z} = 0 \tag{5.13}$$

admits a unique solution in $(0,\infty)^3$, denoted by (x_0, y_0, z_0). Define

$$a = \frac{\frac{\partial^2 \chi}{\partial x \partial y}}{\sqrt{\frac{\partial^2 \chi}{\partial x^2} \cdot \frac{\partial^2 \chi}{\partial y^2}}}(x_0, y_0, z_0), \quad b = \frac{\frac{\partial^2 \chi}{\partial x \partial z}}{\sqrt{\frac{\partial^2 \chi}{\partial x^2} \cdot \frac{\partial^2 \chi}{\partial z^2}}}(x_0, y_0, z_0), \quad c = \frac{\frac{\partial^2 \chi}{\partial y \partial z}}{\sqrt{\frac{\partial^2 \chi}{\partial y^2} \cdot \frac{\partial^2 \chi}{\partial z^2}}}(x_0, y_0, z_0) \tag{5.14}$$

and introduce the covariance matrix

$$\mathrm{cov} = \begin{pmatrix} 1 & a & b \\ a & 1 & c \\ b & c & 1 \end{pmatrix}. \tag{5.15}$$

Let S denote a square root of the covariance matrix, namely

$$\mathrm{cov} = SS^{\intercal}. \tag{5.16}$$

Consider the spherical triangle $T = (S^{-1}\mathbb{R}^3_+) \cap \mathbb{S}^2$. Let λ_1 be the smallest eigenvalue of the Dirichlet problem (5.5) *on T. Then for A and B far enough from the boundary ∂T, the asymptotics* (5.2) *of the number of excursions going from A to B holds, where the exponential growth*

$$\rho = \min_{(0,\infty)^3} \chi \tag{5.17}$$

and the critical exponent α in (5.2) *is given by* (5.6)*.*

Before sketching the proof of Theorem 58, let us comment its hypotheses. First, under (H) the characteristic polynomial is strictly convex and coercive[4] on $(0,\infty)^3$ and hence there is a unique global minimizing point (x_0, y_0, z_0), which satisfies (5.13).

The covariance matrix (5.15) is positive definite, this is a direct consequence of (H) (the rank of the covariance matrix describes the dimension of the subspace in which the random walk evolves).

The matrix S^{-1} has full rank and hence $T = (S^{-1}\mathbb{R}^3_+) \cap \mathbb{S}^2$ is a spherical triangle (see our Definition 57), bounded by the three great-circle arcs $(S^{-1}e_i) \cap \mathbb{S}^2$, with e_i denoting the ith vector of the canonical basis.

[3] This irreducibility hypothesis means that for any two points in the space $\mathbb{Z}^3$, there exists a path connecting these points.

[4] A function $f : \mathbb{R}^n \to \mathbb{R}$ is coercive if $\lim_{\|x\|\to\infty} f(x) = +\infty$

The choice of the square root in (5.16) is not relevant: if $\mathrm{cov} = S_1 S_1^\intercal = S_2 S_2^\intercal$ then obviously $S_1 = M S_2$, where M is an orthogonal matrix, and the two associated spherical triangles are isometric (and in particular they have the same angles).

The boundary of the spherical triangle is piecewise infinitely differentiable. Under this assumption, the spectrum of the Laplacian for the Dirichlet problem (5.5) is discrete (see [48, p. 169]), of the form $0 < \lambda_1 < \lambda_2 \leq \lambda_3 \leq \cdots$.

The asymptotics (5.2) is proved in [58] under the assumption that the walk is strongly aperiodic (see the lattice assumption in [58, p. 999]), i.e., irreducible and aperiodic in the sense of the Markov chains. The aperiodicity is defined by $p = 1$ in (5.3). Two remarks should be made:

- As explained in [28], an extra-assumption (namely, a reachability condition) has to be made. There is indeed in [28] the example of a 2D walk which is strongly aperiodic but such that no excursion to the origin is possible, due to the (ad hoc) particular configuration of the steps. We could easily construct a 3D analogue such that $o(0,0,0;n) = 0$ for all n.

- The second point is about periodic models ($p > 1$ in (5.3)), which stricto sensu are not covered by [58]. It is briefly mentioned in [67] that the main asymptotics (5.2) still holds true. A detailed discussion of the periodic case may be found in [28].

As our point is not to state Theorem 58 at the greatest level of generality, we have stated it under rather strong hypotheses, namely that A and B are far enough from the boundary (this is sufficient for the reachability condition).

Sketch of the proof of Theorem 58. This proof follows a certain number of steps that we now briefly recall. For more details we refer to the presentation of [34] (see Section 2.3 there, see also [58]). Following Denisov and Wachtel [58, Sec. 1.5], the main idea is to write the number of excursions (see (5.1)) as a local probability for a random walk[5], namely,

$$o(i,j,k;n) = |\mathcal{S}|^n \mathbb{P}\left[\sum_{\ell=1}^{n} (X(\ell), Y(\ell), Z(\ell)) = (i,j,k), \tau > n\right], \tag{5.18}$$

where $\{(X(\ell), Y(\ell), Z(\ell))\}$ are i.i.d copies of a random variable (X,Y,Z) having uniform law on the step set $\mathcal{S}$, i.e., for each $s \in \mathcal{S}$, $\mathbb{P}[(X,Y,Z) = s] = 1/|\mathcal{S}|$, and where τ is the first hitting time of the translated cone $(\mathbb{N} \cup \{-1\})^3$. At the end we shall apply the local limit theorem [58, Thm 6] for random walks in cones. The latter theorem gives the asymptotics of (5.18) for normalized random walks, in the sense that the increments of the random walks should have no drift, i.e., $\sum_{s \in \mathcal{S}} \mathbb{P}[(X,Y,Z) = s] \cdot s = 0$, and a covariance matrix (5.15) equal to the identity.

[5] where $\mathbb{P}[A,B]$ stands for $\mathbb{P}[A \cap B]$.

If the model we consider has a non-zero drift, it is rather standard to perform an exponential change of measure so as to remove the drift (this is known as the Cramér transform). Let $s = (s_1, s_2, s_3) \in \mathcal{S}$. Define the triplet (X_1, Y_1, Z_1) by

$$\mathbb{P}[(X_1, Y_1, Z_1) = s] = \frac{x_0^{s_1} y_0^{s_2} z_0^{s_3}}{\chi(x_0, y_0, z_0)}.$$

Under our hypothesis (H), the drift of (X_1, Y_1, Z_1) is zero if and only if (x_0, y_0, z_0) is solution to (5.13), which we now assume.

To have a model with a covariance matrix equal to the identity, we first normalize the variables by

$$(X_2, Y_2, Z_2) = \left(\frac{X_1}{\sqrt{\mathbb{E}[X_1^2]}}, \frac{Y_1}{\sqrt{\mathbb{E}[Y_1^2]}}, \frac{Z_1}{\sqrt{\mathbb{E}[Z_1^2]}} \right),$$

so that the variances of the coordinates are 1, and more generally the covariance matrix of (X_2, Y_2, Z_2) is given by (5.15). Writing $\mathrm{cov} = SS^\intercal$ as in (5.16) and

$$\begin{pmatrix} X_3 \\ Y_3 \\ Z_3 \end{pmatrix} = S^{-1} \begin{pmatrix} X_2 \\ Y_2 \\ Z_2 \end{pmatrix},$$

we obtain that (X_3, Y_3, Z_3) has an identity covariance matrix, since $S^{-1} \cdot \mathrm{cov} \cdot (S^{-1})^\intercal$ is the identity. If (X, Y, Z) is defined in the octant $\mathbb{R}_+^3$, then (X_3, Y_3, Z_3) takes its values in the cone $S^{-1}\mathbb{R}_+^3$.

Remarkably, the probability on the right-hand side of (5.18) can be expressed in terms of the random walk with increments (X_3, Y_3, Z_3). For instance, for (i, j, k) equal to the origin,

$$\mathbb{P}\left[\sum_{\ell=1}^{n} (X(\ell), Y(\ell), Z(\ell)) = (0,0,0), \tau > n \right] = \left(\frac{\chi(x_0, y_0, z_0)}{|\mathcal{S}|} \right)^n \mathbb{P}\left[\sum_{\ell=1}^{n} (X_3(\ell), Y_3(\ell), Z_3(\ell)) = (0,0,0), \tau_3 > n \right],$$

with τ_3 denoting the exit time from the cone $S^{-1}\mathbb{R}_+^3$. Using (5.18) and applying [58, Thm 6] finally gives the result stated in Theorem 58. □

5.3 Spherical triangles and Dirichlet eigenvalues

5.3.1 Computing the principal eigenvalue of a spherical triangle

There are very few spherical triangles (and more generally, few domains on the sphere, see Section 5.3.3 and Section 5.3.4) for which we can explicitly compute the first eigenvalue λ_1 of the Dirichlet problem (5.5). As a matter of comparison, let us recall that (to our knowledge, see also

[14]) there does not exist in general a closed-form expression for the analogous problem for flat triangles.

Back to spherical triangles, there essentially exists a unique case for which an explicit expression for λ_1 is known: the case of two angles $\frac{\pi}{2}$ as in Figure 5.3 (these triangles are called birectangular). Then according to [125, Eq. (36)] (or [124, Sec. IV]) the smallest eigenvalue is

$$\lambda_1 = \left(\frac{\pi}{\beta} + 1\right)\left(\frac{\pi}{\beta} + 2\right). \tag{5.19}$$

Let us give three relevant cases in the range of application of formula (5.19):

- The 3D simple random walk (Figure 5.2b): then $\beta = \frac{\pi}{2}$ and $\lambda_1 = 12$, which with (5.6) corresponds to $\alpha = \frac{9}{2}$ (in accordance with the intuition $3 \times \frac{3}{2}$, i.e., three independent positive 1D excursions).
- More generally, finite group Hadamard models. They correspond to $\beta \in \pi\mathbb{Q}$. They represent tiling groups of the sphere. See Section 5.6 for more details.
- Last but not least, all Hadamard models, even with infinite group (typically $\beta \notin \pi\mathbb{Q}$); see Section 5.5.

Let us continue this section with interesting properties and facts about spherical triangles and the principal eigenvalue of a Dirichlet problem.

5.3.2 Elementary spherical geometry

Our main source is the book [15] by Berger. Spherical triangles have been introduced in Definition 57. A spherical digon is a domain bounded by two great arcs of circles, see Figure 5.20 and [15, 18.3.8.2].

A natural operation in spherical geometry is to take the polar spherical triangle; see [15, 18.3.8.2] and [15, 18.6.12] for more details that we briefly recall below.

Definition 59 (polar triangle)**.** Let $\langle x, y, z\rangle$ be a spherical triangle in the sense of Definition 57. Define the triplet (x', y', z') by the conditions

$$\begin{cases} \langle x', y\rangle = \langle x', z\rangle = 0, & \langle x', x\rangle > 0, \\ \langle y', z\rangle = \langle y', x\rangle = 0, & \langle y', y\rangle > 0, \\ \langle z', x\rangle = \langle z', y\rangle = 0, & \langle z', z\rangle > 0. \end{cases}$$

Then $\langle x', y', z'\rangle$ is a spherical triangle, called the polar triangle of $\langle x, y, z\rangle$.

The polar transformation is involutive, and the equilateral right triangle is invariant. There is no simple formula relating the eigenvalues of a spherical triangle to that of its polar triangle. See Figure 5.9 for examples.

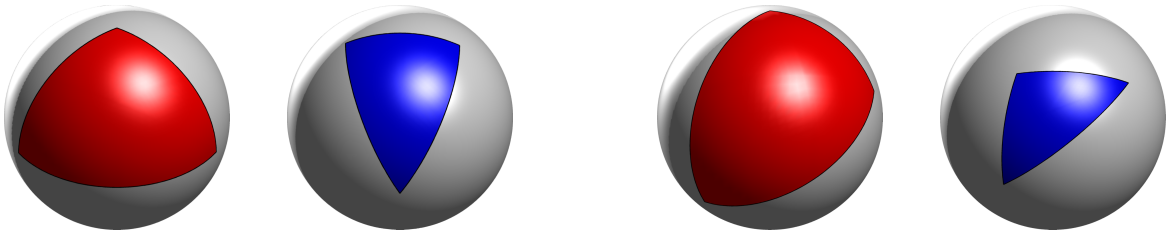

Figure 5.9 – Two triangles (color red) and their polar triangles (in blue), see Definition 59

Interestingly, polar cones already appear in [85] (resp. [84]) to compute the exponential decay of the survival probability of random walks (resp. the exponential decay and the critical exponent of the Brownian survival probability) in cones.

5.3.3 Some properties of the principal eigenvalue

Our main reference here is the book [54] of Dauge.

Monotonicity and regularity of the eigenvalues.

Lemma 60 (Lemma 18.5 in [54])**.** *Let T_1 and T_2 be two simply connected domains on $\mathbb{S}^2$. If $T_1 \subset T_2$ then*

$$\lambda_1(T_1) \geq \lambda_1(T_2).$$

In particular, as any spherical triangle is included in a half-sphere (whose principal eigenvalue equals 2), one has the universal lower bound

$$\lambda_1(T) \geq 2$$

for any spherical triangle T. (By (5.6), this implies that the critical exponent α should be bigger than $\frac{5}{2}$.)

Classical arguments in perturbation theory for operators [92] state that analytic perturbations of the operator induce analytic perturbations of the eigenvalues, see in particular [90, Lem. 2.1] in our context.

Lemma 61. *The function $\lambda_1(T) = \lambda_1(\alpha, \beta, \gamma)$ is analytic in the angles α, β, γ.*

A consequence of Lemma 61 is that a generic triangle has an irrational (and even transcendental) principal eigenvalue λ_1.

Lemma 62. *As one of the angles goes to 0, λ_1 goes to infinity.*

Proof. Lemma 62 is a simple consequence of Lemma 60 and the fact that each spherical triangle can be included in any of the digons determined by its angles. Indeed, suppose the triangle T has

an angle equal to α. Then T is included in the digon D_α with angle α and

$$\lambda_1(T) \geq \lambda_1(D_\alpha) = \frac{\pi}{\alpha}\left(\frac{\pi}{\alpha} + 1\right).$$

We can notice immediately that if $\alpha \to 0$ then the first eigenvalue of T goes to infinity. □

Revolution cones. We now compute the spectrum of a revolution cone (or solid angle) in arbitrary dimension $d \geq 2$. Let us introduce some notation. We fix a half-axis A in $\mathbb{R}^d$ and for any $x \neq 0$ denote by $\theta(x) \in [0, \pi]$ the angle between the axes A and $\vec{x}$. By definition, the revolution cone with apex angle ζ is (see Figure 5.10)

$$K(\zeta) = \{x \in \mathbb{R}^d \setminus \{0\} : \theta(x) \in [0, \zeta)\}. \tag{5.20}$$

Its section on the sphere is the disc $C(\zeta) = K(\zeta) \cap \mathbb{S}^2$.

Lemma 63 (Proposition 18.10 in [54])**.** *The spectrum of $C(\zeta)$ is the set of positive $\nu(\nu + d - 2)$ for which there is $m \in \mathbb{N}$ such that $\mathsf{P}_\nu^m(\cos\zeta) = 0$, where P_ν^m denotes the mth Legendre function of the first kind.*

Notice that [54, Prop. 18.10] computes the spectrum of the cone $K(\zeta)$, not of its section $C(\zeta)$. However the eigenvalues $\lambda_i(K)$ of a cone K are directly related to the eigenvalues of its section $C = K \cap \mathbb{S}^2$, namely (see, e.g., [54, 18.3])

$$\lambda_i(K) = \sqrt{\lambda_i(C) + \left(1 - \frac{d}{2}\right)^2} + \left(1 - \frac{d}{2}\right). \tag{5.21}$$

A few remarkable spherical triangles. Consider triangles with angles

$$\left(\frac{\pi}{p}, \frac{\pi}{q}, \frac{\pi}{r}\right), \quad \text{with } (p, q, r) \in (\mathbb{N} \setminus \{0, 1\})^3.$$

As recalled in [13, 54], the only possible triplets are

- $(2, 3, 3)$ tetrahedral group;
- $(2, 3, 4)$ octahedral group;
- $(2, 3, 5)$ icosahedral group;
- $(2, 2, r)$ dihedral group or order $2r \geq 4$

Each triplet above corresponds to a tiling of the sphere. See Figures 5.4 and 5.13 for a few examples. Denote by $T_{(p,q,r)}$ the associated triangle when it exists.

Lemma 64 (Theorem 6 in [13]). *The eigenvalues of $T_{(p,q,r)}$ have the form $\nu_{(p,q,r)}(\nu_{(p,q,r)}+1)$, with $(\ell_1, \ell_2 \in \mathbb{N})$*

- $\nu_{(2,3,3)} = 6 + 3\ell_1 + 4\ell_2$;
- $\nu_{(2,3,4)} = 9 + 6\ell_1 + 6\ell_2$;
- $\nu_{(2,3,5)} = 15 + 6\ell_1 + 10\ell_2$;
- $\nu_{(2,2,r)} = r + 1 + 2\ell_1 + r\ell_2$.

5.3.4 Other cones

As we have seen in Theorem 58, computing critical exponents for walks in $\mathbb{N}^3$ (or in any cone formed by an intersection of three half-spaces, by a linear transform) requires the computation of the principal eigenvalue of a spherical triangle. More generally, we could consider walks confined to an arbitrary cone K in dimension 3 or more (even so the natural combinatorial interpretation of positive walks is lost), and ask whether there exists a closed-form expression for the principal eigenvalue. However, only very few domains seem to admit such closed-form eigenvalues. Besides spherical digons and birectangle triangles, there are for instance the revolution cones, see Figure 5.10. The first eigenvalue (and in fact the whole spectrum) is described in Lemma 63. From an analytic viewpoint, the domains leading to explicit eigenvalues have typically the property of separation of the variables, see [117, 116] for more details.

5.4 The covariance matrix

5.4.1 Expression for the angles of the spherical triangle

The angles of the spherical triangle appearing in the main Theorem 58 are totally explicit in terms of the correlation coefficients a, b and c defined in (5.14).

Lemma 65. *Let α, β, γ be the angles of the spherical triangle T defined in Theorem 58, and a, b, c as in* (5.14). *One has*

$$\alpha = \arccos(-a), \quad \beta = \arccos(-b), \quad \gamma = \arccos(-c). \tag{5.22}$$

Three remarks should be made.

- It is easily seen that the correlation coefficients a, b and c of Lemma 65 are algebraic numbers. We can use the exact same algorithmic computations as in [34, Sec. 2.4.1] to deduce their minimal polynomials.

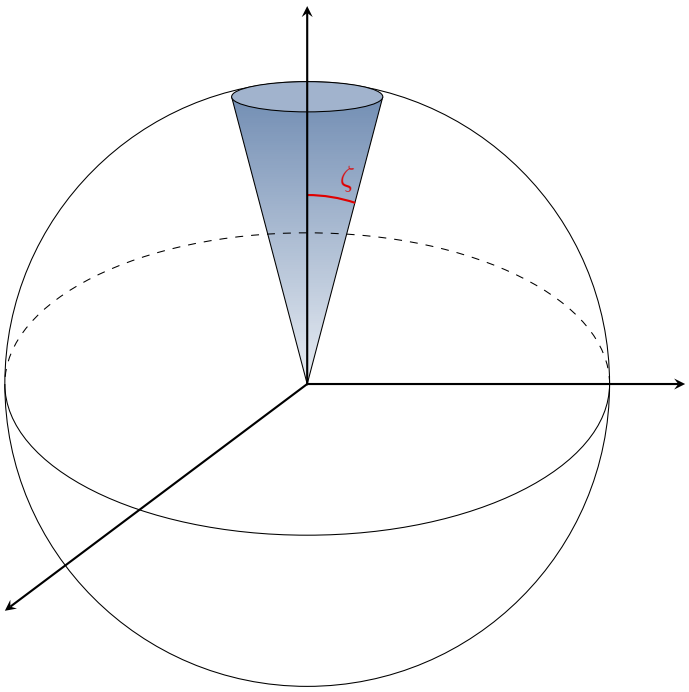

Figure 5.10 – The revolution cone (or spherical cap) $K(\zeta)$ of apex angle ζ

- The formulas given in Lemma 65 are the most natural generalization of the 2D situation, where by [34] the spherical triangle is replaced by a wedge of opening angle $\arccos(-c)$, see Figure 5.11.
- If (at least) two of the three correlation coefficients a, b and c are equal to 0, then the spherical triangle is birectangular and conversely.

Proof of Lemma 65. Let cov be the matrix defined in (5.15). We easily obtain the Cholesky decomposition $\text{cov} = LL^\intercal$, with

$$L = \begin{pmatrix} 1 & 0 & 0 \\ a & \sqrt{1-a^2} & 0 \\ b & \frac{c-ab}{\sqrt{1-a^2}} & \frac{\sqrt{1-a^2-b^2-c^2+2abc}}{\sqrt{1-a^2}} \end{pmatrix}. \tag{5.23}$$

One deduces that

$$L^{-1} = \begin{pmatrix} 1 & 0 & 0 \\ \frac{-a}{\sqrt{1-a^2}} & \frac{1}{\sqrt{1-a^2}} & 0 \\ \frac{ac-b}{\sqrt{1-a^2}\sqrt{1-a^2-b^2-c^2+2abc}} & \frac{ab-c}{\sqrt{1-a^2}\sqrt{1-a^2-b^2-c^2+2abc}} & \frac{\sqrt{1-a^2}}{\sqrt{1-a^2-b^2-c^2+2abc}} \end{pmatrix}. \tag{5.24}$$

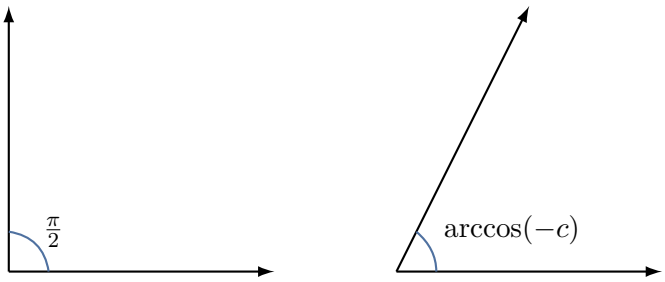

Figure 5.11 – After decorrelation of a 2D random walk, the quarter plane (left) becomes a wedge of opening $\arccos(-c)$ (right), where c is the correlation coefficient of the driftless model

Denoting by (e_1, e_2, e_3) the canonical basis of $\mathbb{R}^3$, the three points defining the triangle are

$$x = \frac{L^{-1}e_1}{\|L^{-1}e_1\|}, \quad y = \frac{L^{-1}e_2}{\|L^{-1}e_2\|}, \quad z = \frac{L^{-1}e_3}{\|L^{-1}e_3\|},$$

see the third comment following Theorem 58 or its proof (Section 5.2.3). Setting

$$x_y = \frac{y - \langle x, y\rangle x}{\|y - \langle x, y\rangle x\|}$$

and x_z, y_x, y_z, z_x, z_y similarly, we have by [15, 18.6.6] (giving the formulas for the angles of the triangle $\langle x, y, z\rangle$)

$$\alpha = \arccos\langle x_y, x_z\rangle, \quad \beta = \arccos\langle y_z, y_x\rangle, \quad \gamma = \arccos\langle z_x, z_y\rangle.$$

To conclude the proof it is enough to do the above computations in terms of a, b and c. □

Notice that the above expression of L in terms of a, b and c is particularly simple, and thus the proof of Lemma 65 is easily obtained. On the other hand, solving the equation $\mathrm{cov} = SS^\intercal$ with the constraint of taking a symmetric square root S happens to be much more complicated and less intrinsic.

We end this section with further aspects and properties of the covariance matrix. We establish a strong relationship between the cosine matrix of the angles and the Coxeter matrix of the group, we then interpret the covariance matrix as a Gram matrix, and finally we show that it is possible to realize any spherical triangle as a walk triangle.

5.4.2 Relation with the Coxeter matrix

Assume that there exists a presentation of the group G of Section 5.2.2 as

$$G = \langle \mathtt{a}, \mathtt{b}, \mathtt{c} \mid \mathtt{a}^2, \mathtt{b}^2, \mathtt{c}^2, (\mathtt{ab})^{m_{\mathtt{ab}}}, (\mathtt{ac})^{m_{\mathtt{ac}}}, (\mathtt{bc})^{m_{\mathtt{bc}}}\rangle,$$

with $m_{\mathtt{ab}} = \infty$ if there is no relation between $\mathtt{a}$ and $\mathtt{b}$, and similarly for $m_{\mathtt{ac}}$ and $m_{\mathtt{bc}}$. (It is not always possible to present the group G as above, see Table 5.1.) Following Bourbaki [36] we introduce the two matrices

$$\begin{pmatrix} 1 & m_{\mathtt{ab}} & m_{\mathtt{ac}} \\ m_{\mathtt{ab}} & 1 & m_{\mathtt{bc}} \\ m_{\mathtt{ac}} & m_{\mathtt{bc}} & 1 \end{pmatrix} \quad \text{and} \quad \begin{pmatrix} 1 & -\cos\left(\frac{\pi}{m_{\mathtt{ab}}}\right) & -\cos\left(\frac{\pi}{m_{\mathtt{ac}}}\right) \\ -\cos\left(\frac{\pi}{m_{\mathtt{ab}}}\right) & 1 & -\cos\left(\frac{\pi}{m_{\mathtt{bc}}}\right) \\ -\cos\left(\frac{\pi}{m_{\mathtt{ac}}}\right) & -\cos\left(\frac{\pi}{m_{\mathtt{bc}}}\right) & 1 \end{pmatrix}. \tag{5.25}$$

The first one is called the Coxeter matrix, see Definition 4 in [36, Ch. IV]. The second one is used in [36] to define a quadratic form, whose property of being non-degenerate characterizes the finiteness of the group G, see Theorem 2 in [36, Ch. V].

Our point here is to remark the strong link between the matrix on the right-hand side of (5.25) and the covariance matrix, which by Lemma 65 may be rewritten as the cosine matrix

$$\begin{pmatrix} 1 & -\cos(\gamma) & -\cos(\beta) \\ -\cos(\gamma) & 1 & -\cos(\alpha) \\ -\cos(\beta) & -\cos(\alpha) & 1 \end{pmatrix}. \tag{5.26}$$

There are, however, two differences between the matrices (5.26) and (5.25). The first one is that in the infinite group case, all non-diagonal coefficients of the matrix (5.26) are in the open interval $(-1, 1)$, while if there is no relation between $\mathtt{a}$ and $\mathtt{b}$ (say), then $m_{\mathtt{ab}} = \infty$ and $-\cos(\frac{\pi}{m_{\mathtt{ab}}}) = -1$. See [56] for a rather general study of cosine matrices (5.26).

The second difference is about the finite group case. Take any two step sets which are obtained from one another by a reflection (see Figure 5.12 below for an example). Then the group has the exact same structure and thus the matrix of [36] is unchanged. On the other hand, the matrix (5.26) changes after a reflection (Kreweras on the left, reflected Kreweras on the right):

$$\begin{pmatrix} 1 & \frac{1}{2} & \frac{1}{2} \\ \frac{1}{2} & 1 & \frac{1}{2} \\ \frac{1}{2} & \frac{1}{2} & 1 \end{pmatrix} \quad \text{and} \quad \begin{pmatrix} 1 & -\frac{1}{2} & -\frac{1}{2} \\ -\frac{1}{2} & 1 & \frac{1}{2} \\ -\frac{1}{2} & \frac{1}{2} & 1 \end{pmatrix}.$$

Figure 5.12 – On the left, Kreweras 3D model. On the right, the reflection of Kreweras 3D with respect to the x-axis, which can be thought of as a 3D tandem model

5.4.3 Polar angles and Gram matrix

It is possible to compute the angles between the three segments connecting the origin to the vertices of the triangle $\langle x, y, z\rangle$. These angles may also be interpreted as the lengths $A = \overline{yz}$, $B = \overline{xz}$ and $C = \overline{xy}$ of the sides of the triangle. By [15, 18.6.12.2] they are the complements to π of the polar angles (see Definition 59).

Lemma 66. *Let O denote the origin $(0, 0, 0)$. The angles between the vectors $\vec{Ox}$, $\vec{Oy}$ and $\vec{Oz}$ are given by*

$$A = \arccos\left(\frac{bc - a}{\sqrt{1-b^2}\sqrt{1-c^2}}\right), \quad B = \arccos\left(\frac{ac - b}{\sqrt{1-a^2}\sqrt{1-c^2}}\right),$$
$$C = \arccos\left(\frac{ab - c}{\sqrt{1-a^2}\sqrt{1-b^2}}\right).$$

As it should be, the quantity $\frac{bc-a}{\sqrt{1-b^2}\sqrt{1-c^2}}$ (and its cyclic permutations as well) in Lemma 66 belongs to $(-1, 1)$. Indeed if $bc \geq a$ then

$$\frac{bc - a}{\sqrt{1-b^2}\sqrt{1-c^2}} < 1 \text{ iff } (bc-a)^2 < (1-b^2)(1-c^2) \text{ iff } 1 - a^2 - b^2 - c^2 + 2abc > 0.$$

The quantity $1 - a^2 - b^2 - c^2 + 2abc$ is positive because it is the determinant of the covariance matrix (5.15), which is assumed positive definite. In the case $bc \leq a$ we would prove similarly that $\frac{bc-a}{\sqrt{1-b^2}\sqrt{1-c^2}} > -1$.

Proof of Lemma 66. The angles are easily computed: if e_1, e_2 and e_3 are the vectors of the canonical basis and L^{-1} is as in (5.24),

$$\langle L^{-1}e_1, L^{-1}e_2\rangle = \|L^{-1}e_1\| \cdot \|L^{-1}e_j\| \cdot \cos C, \tag{5.27}$$

and cyclic permutations of the above identities hold. The formulas stated in Lemma 66 follow from (5.27), after having computed the norms and the dot products of the columns of L^{-1}.

An alternative proof is to invert the covariance matrix (5.15) and to use the orthogonality relations between the angles and their polar angles, see Definition 59. □

Finally, we stress that the covariance matrix may be interpreted as the Gram matrix

$$\begin{pmatrix} \langle u, u\rangle & \langle u, v\rangle & \langle u, w\rangle \\ \langle u, v\rangle & \langle v, v\rangle & \langle v, w\rangle \\ \langle u, w\rangle & \langle v, w\rangle & \langle w, w\rangle \end{pmatrix},$$

where u, v, w are the three vectors on the sphere which are the columns of the matrix

$$\begin{pmatrix} \frac{\sqrt{1-a^2-b^2-c^2+2abc}}{\sqrt{1-c^2}} & 0 & 0 \\ \frac{bc-a}{\sqrt{1-c^2}} & -\sqrt{1-c^2} & 0 \\ b & c & 1 \end{pmatrix}.$$

5.4.4 The reverse construction

Our general construction consists in associating to every model of walks the covariance matrix (5.15), and thereby a spherical triangle with angles α, β, γ as in Lemma 65. It is natural to ask about the converse: is it possible to realize any spherical triangle as a walk triangle? The answer turns out to be positive, if we allow weighted walks.

More specifically, let $\langle x, y, z\rangle$ be an arbitrary spherical triangle, having angles $\alpha, \beta, \gamma \in (0, \pi)$. Introduce $a, b, c \in (-1, 1)$ such that (5.22) holds. Let finally (U, V, W) be a triplet of independent random variables (actually, having non-correlated variables is enough) in $\mathbb{R}^3$ with unit variances. Introduce the random variables

$$\begin{pmatrix} Z \\ Y \\ X \end{pmatrix} = L \begin{pmatrix} U \\ V \\ W \end{pmatrix}, \tag{5.28}$$

where L is the matrix (5.23) appearing in the Cholesky decomposition of the matrix cov. Then by construction the covariance matrix of $(X, Y, Z) \in \mathbb{R}^3$ is (5.15) and its spherical triangle has angles α, β, γ. In conclusion, the random walk model whose increment distribution is the same as the distribution of (X, Y, Z) given by (5.28) has a spherical triangle with generic angles α, β, γ.

5.5 Analysis of Hadamard models

We consider Hadamard models in the sense of Section 5.2.2. Let us briefly recall that these models are characterized by the existence of a decomposition of their inventory (5.4) as follows:

$$\chi(x, y, z) = U(x) + V(x)T(y, z) \qquad \text{or} \qquad \chi(x, y, z) = U(x, y) + V(x, y)T(z).$$

As will be shown in Lemmas 67 and 71, such models admit a quite simple covariance matrix

$$\mathrm{cov} = \begin{pmatrix} 1 & 0 & 0 \\ 0 & 1 & c \\ 0 & c & 1 \end{pmatrix},$$

allowing us to perform explicitly many computations. (Notice, however, that the above form for the covariance matrix does not characterize Hadamard models, we construct counterexamples in Section 5.6.4. These examples lead to the notion of exceptional models.)

In particular, spherical triangles associated to Hadamard models are birectangular, i.e., two (or three) angles are equal to $\frac{\pi}{2}$, see Figure 5.3. These triangles are remarkable because they are the only ones (with the exception of a few sporadic cases) for which a closed-form expression for the principal eigenvalue is known. Finally, the exponent (5.6) of the excursion sequence is computed in Propositions 68 and 72 below. Using similar techniques as in [34], one can rather easily study the rationality of this exponent.

In the $(1,2)$-type (Section 5.5.1), the 2D model associated to $T(y,z)$ dictates the exponent, see Proposition 68. In particular, we will see in Corollary 69 that if the 2D model has an irrational exponent, then the 3D model is necessarily non-D-finite. To our knowledge, this is the first proof ever of the non-D-finiteness of truly 3D models, making the Hadamard case remarkable. On the other hand, $(2,1)$-type Hadamard models (Section 5.5.2) are more subtle. Their exponents can be computed from exponents of mixtures of two 2D models.

Although we will not do such considerations here, let us emphasize that most of the results in this section hold for weighted walks with arbitrarily big steps: the only crucial point is the existence of a Hadamard decomposition.

5.5.1 (1,2)-Hadamard models

Lemma 67. *For any $(1,2)$-type Hadamard model, the matrix* cov *in* (5.15) *takes the form*

$$\mathrm{cov} = \begin{pmatrix} 1 & 0 & 0 \\ 0 & 1 & c \\ 0 & c & 1 \end{pmatrix}, \quad \textit{with} \quad c = \frac{\frac{\partial^2 T}{\partial y \partial z}}{\sqrt{\frac{\partial^2 T}{\partial y^2} \cdot \frac{\partial^2 T}{\partial z^2}}}(y_0, z_0), \tag{5.29}$$

where y_0, z_0 are defined in (5.13)*. (Notice in particular that c does not depend on the components U and V in the Hadamard decomposition* (5.11)*.)*

Proof. Using the decomposition (5.11) in the last two equations of the system (5.13) gives

$$V(x)\frac{\partial T}{\partial y}(y,z) = V(x)\frac{\partial T}{\partial z}(y,z) = 0. \tag{5.30}$$

As $V(x)$ cannot be equal to 0, we obtain the autonomous system $\frac{\partial T}{\partial y} = \frac{\partial T}{\partial z} = 0$. Let (y_0, z_0) be its unique solution. Moreover, the first equation in (5.13) leads to

$$U'(x) + V'(x)T(y_0, z_0) = 0$$

which (as $T(y_0, z_0) > 0$) has a unique solution x_0. Using once again (5.11) as well as (5.30), we deduce that

$$V'(x_0)\frac{\partial T}{\partial y}(y_0, z_0) = 0,$$

whence $a = 0$ and similarly $b = 0$ in the general formula for cov. The formula (5.29) for c is a direct consequence of (5.14) and (5.11). □

Our aim now is to compute the spherical angles in the Hadamard case. We use Lemma 65 to deduce Proposition 68 below.

Proposition 68. *The spherical triangles associated to* $(1,2)$*-type Hadamard models have angles* $\frac{\pi}{2}, \frac{\pi}{2}, \arccos(-c)$ *(as in Figure 5.3, left), with* c *defined in* (5.29)*. The smallest eigenvalue* λ_1 *of the Dirichlet problem and the exponent* α *are respectively given by*

$$\lambda_1 = \left(\frac{\pi}{\arccos(-c)} + 1\right)\left(\frac{\pi}{\arccos(-c)} + 2\right), \qquad \alpha = \frac{\pi}{\arccos(-c)} + \frac{5}{2}.$$

In order to completely characterize the excursion exponent we now compute c and α. This happens to be done in [34]: for the 2D unweighted models under consideration, c is always algebraic (possibly rational), and minimal polynomials in the infinite group case are provided in [34, Tab. 2].

For instance, for the first and second scarecrows in Figure 5.8 one has $c = -\frac{1}{4}$, while $c = \frac{1}{4}$ for the last scarecrow. Moreover, by [34, Cor. 2], α is irrational for all infinite group models. This leads to the following corollary.

Corollary 69. *For any* $(1,2)$*-type Hadamard 3D model such that the group associated to the step set* T *is infinite, the series* $O(0,0,0)$ *(and thus also* $O(x,y,z)$*) is non-D-finite.*

We list below important comments on Corollary 69.

- First of all, Corollary 69 is (to the best of our knowledge) the first non-D-finiteness result on truly 3D models (the 3D models considered in [64] have dimensionality 2 in the sense of Definition 56, and thus do not satisfy the main hypothesis (H), which guarantees the existence of a non-degenerate spherical triangle, see Section 5.8.4). It answers an open question raised in [27, Sec. 9] (concerning the possibility of extending the techniques of [34] to octant models).

- In order to give a concrete application of Corollary 69, consider a model with arbitrary U and V (provided that the model is truly 3D), and with T one scarecrow of Figure 5.8. This 3D model is non-D-finite since the 2D model associated with T has an infinite group by [41].

- Note that Corollary 69 can be extended to models with weights and arbitrarily big steps, provided that the hypothesis on the infiniteness of the group be replaced by the assumption that $\frac{\pi}{\arccos(-c)}$ is irrational. An algorithmic proof of the irrationality of such quantities is proposed in [34, Sec. 2.4], and further applied to some weighted models in [64].

- Corollary 69 is a direct consequence of [34, Cor. 2], which states that for the 51 unweighted non-singular step sets with infinite group in the quarter plane, the excursion exponent is irrational. By [34, Thm 3] this implies that the series is non-D-finite.

Remark 70 (Combinatorial interpretation of the exponent). For $(1,2)$-type models, 3D excursions may be decomposed as products of two lower dimensional excursions: a first excursion in the (y,z)-plane with the inventory T and a second, 1D excursion in x. This can easily be read on the formula of Proposition 68: writing

$$\alpha = \left(\frac{\pi}{\arccos(-c)} + 1\right) + \frac{3}{2},$$

the exponent is interpreted as the sum of the exponent of the 2D model (see [34, Thm 4]) and of the universal exponent $\frac{3}{2}$ of a 1D excursion.

5.5.2 (2,1)-Hadamard models

Lemma 71. *For any $(2,1)$-type Hadamard model, the matrix* cov *in* (5.15) *takes the form*

$$\mathrm{cov} = \begin{pmatrix} 1 & a & 0 \\ a & 1 & 0 \\ 0 & 0 & 1 \end{pmatrix}, \quad \textit{with} \quad a = \frac{\frac{\partial^2 \chi|_{z_0}}{\partial x \partial y}}{\sqrt{\frac{\partial^2 \chi|_{z_0}}{\partial x^2} \cdot \frac{\partial^2 \chi|_{z_0}}{\partial y^2}}}(x_0, y_0), \tag{5.31}$$

where x_0, y_0, z_0 are defined in (5.13) *and $\chi|_{z_0}(x,y) = \chi(x,y,z_0)$.*

Proof. We solve the system (5.13) in the z-variable first and obtain the point z_0 characterized by $T'(z_0) = 0$. We have then $b = c = 0$ in the covariance matrix cov. The first two equations of this system read

$$\frac{\partial U}{\partial x}(x,y) + T(z_0)\frac{\partial V}{\partial x}(x,y) = \frac{\partial U}{\partial y}(x,y) + T(z_0)\frac{\partial V}{\partial y}(x,y) = 0.$$

The pair (x_0, y_0) is the critical point associated to the *mixture of models* defined below in (5.32). □

The following result is derived similarly as Proposition 68.

Proposition 72. *The spherical triangles associated to $(2,1)$-type Hadamard models have angles $\frac{\pi}{2}, \frac{\pi}{2}, \arccos(-a)$ (as in Figure 5.3, left), with a defined in* (5.31). *The smallest eigenvalue λ_1 of the Dirichlet problem and the exponent α are respectively given by*

$$\lambda_1 = \left(\frac{\pi}{\arccos(-a)} + 1\right)\left(\frac{\pi}{\arccos(-a)} + 2\right), \qquad \alpha = \frac{\pi}{\arccos(-a)} + \frac{5}{2}.$$

(2,1)-type Hadamard walks and mixing of 2D models. From a probabilistic point of view, the $(2,1)$-type is slightly more interesting than the $(1,2)$-type. Many computations are indeed related to the concept of mixtures of two 2D probability laws.

More precisely, the polynomials $U(x,y)$ and $V(x,y)$ in (5.12) both induce a law (or a model) in 2D, which are *mixed* as below:

$$\chi|_{z_0}(x,y) = U(x,y) + T(z_0)V(x,y), \tag{5.32}$$

the parameter z being specialized at z_0, the latter being defined by $T'(z_0) = 0$.

In the combinatorial case, for a 3D model we must have $T(z) = z + z^{-1}$, hence $z_0 = 1$ and $T(z_0) = 2$. Equation (5.32) becomes $U(x, y)+2V(x, y)$, which is the inventory of a 2D weighted walk (with possible weights $0, 1, 2, 3$). Remark that it is not the first appearance of weighted 2D walks in the theory of (unweighted) 3D walks: in [27, Sec. 7] (see in particular Figure 5), 2D projections of 3D models are analyzed, and these projections are typically weighted 2D walks; see also [96].

Computing a in (5.31). From a technical point of view, computing a and studying the rationality of $\frac{\pi}{\arccos(-a)}$ requires the same type of computations as above for c and $\frac{\pi}{\arccos(-c)}$ (see Section 5.5.1). For an illustration see Example 74 below. However, some difficulties may occur from the fact that weighted steps are allowed:

- It is not possible to exclude that a model with infinite group has a rational exponent α (this does not happen in the unweighted case [34], but may happen in the weighted case, see examples in [28]).
- Knowing the critical exponents associated to U and V does not give much information on the exponent of the mixture (5.32).

Applications and examples. We start with a result on non-D-finiteness, for a subclass of $(2, 1)$-type Hadamard models.

Corollary 73. *For any $(2, 1)$-type Hadamard 3D model such that the group associated to the step set V is infinite, and $U = V$ or $U = 0$, the series $O(0, 0, 0)$ (and thus also $O(x, y, z)$) is non-D-finite.*

Corollary 73 applies for several models, but the constraint of taking either $U = V$ or $U = 0$ is quite strong. We now construct a more elaborate example.

Example 74. *Let U, V be any of the first two scarecrows of Figure 5.8 (possibly the same ones). These models have zero drift (meaning that the sum of the steps over the step set is zero), and thus critical point $(1, 1)$, and an easy computation shows that they have the same covariance matrices. Then for any $T(x) = t_1x+t_0+t_{-1}x^{-1}$, the associated $(2, 1)$-type Hadamard model defined by (5.12) is non-D-finite.*

5.6 Triangle and principal eigenvalue classifications of the models

5.6.1 Motivations and presentation of the results

In this section we would like to classify the $11,074,225$ models with respect to their triangle and the associated principal eigenvalue. The central idea is that there is a strong link between the group (as defined in Section 5.2.2) and the triangle. To understand this connection, we propose a

novel, natural and manipulable geometric interpretation of the group, as a reflection group on the sphere. More precisely, we will interpret the three generators of the group as the three reflections with respect to the sides of the spherical triangle. We shall present three main features:

- *Finite group case* (Section 5.6.2): we interpret the group G as a tiling group of the sphere, see Table 5.3 as well as Figures 5.4 and 5.13. We also explain a few remarkable facts observed in the tables of [6], on the number of different asymptotic behaviors.

- *Infinite group case* (Section 5.6.3): the existence of a relation between the generators of the group can be read off on the angles. The simplest example is the relation $(\mathtt{ab})^m = 1$, which on the triangle will correspond to an angle equal to $k\pi/m$ for some integer k. In particular, all triangles from the group

$$G_3 = \langle \mathtt{a}, \mathtt{b}, \mathtt{c} \mid \mathtt{a}^2, \mathtt{b}^2, \mathtt{c}^2, (\mathtt{ac})^2, (\mathtt{ab})^2 \rangle$$

  of Table 5.1 (Hadamard models) will have two right angles.

- *Exceptional models* (Section 5.6.4): for some infinite group models (a few hundreds of thousands), some unexpected further identities on the angles hold—*unexpected* means not implied by a relation between the generators, as explained above.

  The most interesting case is given by some models in G_1 and G_2, which have a triangle with exactly 2 right angles. Although these models do not have a Hadamard structure, their triangle has the same type as classical Hadamard models, and the principal eigenvalue (and hence the critical exponent) can be computed in a closed form.

  There are also models with infinite group and three right angles (in this case, the exponent is $\frac{9}{2}$ and cannot be used to detect non-D-finiteness). Let us finally mention that there are two models with infinite group and having the same triangle as Kreweras 3D. See Theorem 77.

To summarize, classifying the triangles is close to, but different from classifying the groups. The latter task has already been achieved in [6] (finite group case; we have reproduced their results in Table 5.4) and [95] (infinite groups; see our Table 5.1), using a heavy computer machinery. However, the group classification is more precise, in the sense that the spherical triangle does not determine everything: infinite group models can have a tiling triangle, and Hadamard models are not the only ones to have birectangular triangles.

5.6.2 Finite group case

Some aspects of the group. Let us recall a few applications of the concept of the group:

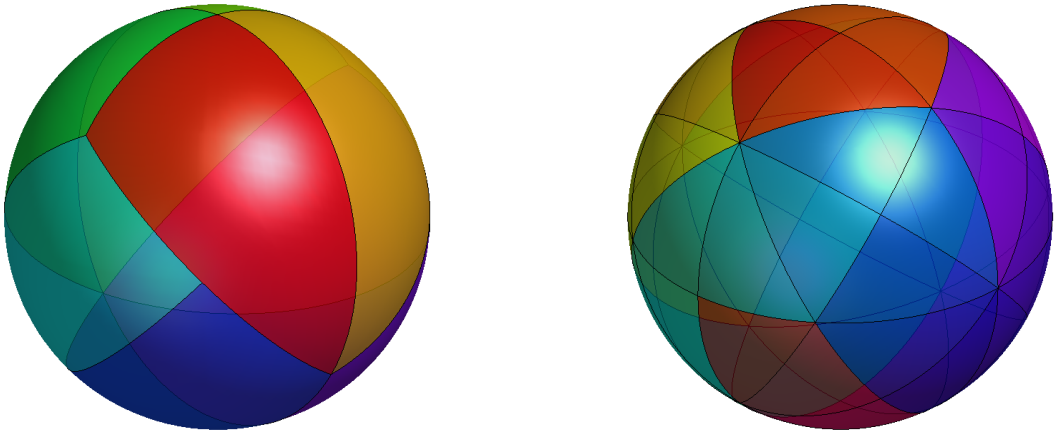

(a) Tilings associated to the triangles with angles $\frac{\pi}{3}, \frac{\pi}{2}, \frac{2\pi}{3}$

(b) Tilings associated to the triangles with angles $\frac{\pi}{4}, \frac{\pi}{3}, \frac{\pi}{2}$

Figure 5.13 – Various tilings of the sphere. These triangles correspond to the lines 9 and 17 in Table 5.3

- When the group is finite and if in addition the orbit-sum of the monomial $x_1 \times \cdots \times x_d$ under the group G, namely

$$\mathrm{OS}(x_1, \ldots, x_d) = \sum_{g \in G} \mathrm{sign}\,(g) \cdot g(x_1 \times \cdots \times x_d), \tag{5.33}$$

  is non-zero, one may obtain closed-form expressions for the generating function (as positive part extractions). See [41] for the initial application of this technique, called the orbit-sum method; it was further used in [96, 28].

- When the group is finite but the orbit-sum (5.33) is zero, it is still possible, in a restricted number of cases, to derive an expression for the generating function, see [41, 96, 28] for examples. The applicability of this technique is not completely clear.

- Last but not least, in dimension 2 there is an equivalence between the finiteness of the group and the D-finiteness of the generating functions (this is a consequence of the papers [41, 31, 100] altogether).

Let us now examine each of the above applications in dimension 3. The first item is still valid, as shown in [27, 128]. As in the 2D case, the second item only works for a few cases. For instance, Figure 4 in [27] gives a list of 19 non-Hadamard 3D models with finite group and zero orbit-sum, which are not solved at the moment. Finally, the third item is an open question. As an illustration, all 19 previous models (including Kreweras 3D model) have a finite group, but as explained in [27, Sec. 6.2], these models do not seem D-finite. In this case, the equivalence in the third item would not be satisfied.

	Eigenvalue	Exponent	Nb tri.	Angles	Hadamard	Order	Group
1	4.261,734	3.124,084	2	$\left[\frac{2\pi}{3}, \frac{3\pi}{4}, \frac{3\pi}{4}\right]$	no	48	$\mathbb{Z}_2 \times S_4$
2	5.159,145	3.325,756	7	$\left[\frac{2\pi}{3}, \frac{2\pi}{3}, \frac{2\pi}{3}\right]$	no	24	S_4
3	6.241,748	3.547,890	2	$\left[\frac{\pi}{2}, \frac{2\pi}{3}, \frac{3\pi}{4}\right]$	no	48	$\mathbb{Z}_2 \times S_4$
4	6.777,108	3.650,869	5	$\left[\frac{\pi}{2}, \frac{2\pi}{3}, \frac{2\pi}{3}\right]$	no	24	S_4
5	70/9	23/6	41	$\left[\frac{\pi}{2}, \frac{\pi}{2}, \frac{3\pi}{4}\right]$	yes	16	$\mathbb{Z}_2 \times D_8$
6	35/4	4	279	$\left[\frac{\pi}{2}, \frac{\pi}{2}, \frac{2\pi}{3}\right]$	yes/no	12	D_{12}
7	12	9/2	1,852	$\left[\frac{\pi}{2}, \frac{\pi}{2}, \frac{\pi}{2}\right]$	yes	8	$\mathbb{Z}_2 \times \mathbb{Z}_2 \times \mathbb{Z}_2$
8	12.400,051	4.556,691	2	$\left[\frac{\pi}{3}, \frac{\pi}{2}, \frac{3\pi}{4}\right]$	no	48	$\mathbb{Z}_2 \times S_4$
9	13.744,355	4.740,902	7	$\left[\frac{\pi}{3}, \frac{\pi}{2}, \frac{2\pi}{3}\right]$	no	24	S_4
10	20	11/2	172	$\left[\frac{\pi}{3}, \frac{\pi}{2}, \frac{\pi}{2}\right]$	yes/no	12	D_{12}
11	20.571,973	5.563,109	2	$\left[\frac{\pi}{4}, \frac{\pi}{2}, \frac{2\pi}{3}\right]$	no	48	$\mathbb{Z}_2 \times S_4$
12	21.309,407	5.643,211	7	$\left[\frac{\pi}{3}, \frac{\pi}{3}, \frac{2\pi}{3}\right]$	no	24	S_4
13	24.456,913	5.970,604	2	$\left[\frac{\pi}{4}, \frac{\pi}{3}, \frac{3\pi}{4}\right]$	no	48	$\mathbb{Z}_2 \times S_4$
14	30	13/2	41	$\left[\frac{\pi}{4}, \frac{\pi}{2}, \frac{\pi}{2}\right]$	yes	16	$\mathbb{Z}_2 \times D_8$
15	42	15/2	5	$\left[\frac{\pi}{3}, \frac{\pi}{3}, \frac{\pi}{2}\right]$	no	24	S_4
16	49.109,945	8.025,663	2	$\left[\frac{\pi}{4}, \frac{\pi}{4}, \frac{2\pi}{3}\right]$	no	48	$\mathbb{Z}_2 \times S_4$
17	90	21/2	2	$\left[\frac{\pi}{4}, \frac{\pi}{3}, \frac{\pi}{2}\right]$	no	48	$\mathbb{Z}_2 \times S_4$

Table 5.3 – Characterization of triangles and exponents associated to models with finite group. One can see some eigenvalues appearing in Lemma 64 (the integers eigenvalues)

Our contribution. The following result is summarized in Table 5.3:

Theorem 75. *Under the hypothesis* (H)*, there are exactly* 17 *triangles that are associated to finite groups. Each triangle corresponds to a particular eigenvalue computed in Table 5.3.*

Proof. The proof of the above result of the triangles angles is computational (all computations are done using symbolic tools and are exact) and is based on Theorem 58. In each case, the critical point of the inventory function is found by solving (5.13). Once the critical point is found, we compute the covariance matrix (5.15) and we use Lemma 65 to find the angles of the associated spherical triangle. □

Numerical tools related to this chapter are available on the webpage of the article [26].

Comments on Theorem 75. We have computed the critical exponents for each one of the models corresponding to a finite group, using the fundamental eigenvalue of the associated spherical triangles. In some cases the eigenvalues are known explicitly and are written in rational form in Table 5.3. The computation procedure is described in Section 5.7. We believe that all digits shown are accurate.

Group	Hadamard	Non-Hadamard OS $\neq 0$	Non-Hadamard OS $= 0$
$\mathbb{Z}_2 \times \mathbb{Z}_2 \times \mathbb{Z}_2$	1,852	0	0
D_{12}	253	66	132
$\mathbb{Z}_2 \times D_8$	82	0	0
S_4	0	5	26
$\mathbb{Z}_2 \times S_4$	0	2	12

Table 5.4 – Number of models with finite group. Note that OS refers to the orbit-sum defined in (5.33). The original version of this table may be found in [6, Tab. 1]

It is remarkable that among all possible 17 exponents, each one is uniquely assigned to a particular spherical triangle. Moreover, each group can be realized as a reflection group for the associated triangles, giving a connection between combinatorial and geometric aspects. More precisely, we notice that all triangles associated to models with finite groups are *Schwarz triangles*, which means that they can be used to tile the sphere, possibly overlapping, through reflection in their edges. They are classified in [118] and a nice theoretical and graphical description can be seen on the associated Wikipedia page [52]. The classification of Schwarz triangles also includes information about their symmetry groups, which are seen to coincide with the combinatorial groups.

The triangle on the ninth line of Table 5.3 is exactly half of Kreweras triangle. Accordingly (and this was confirmed by our numerical approximations) the principal eigenvalue of the models with half Kreweras triangle equals the second smallest eigenvalue of Kreweras model.

Some remarks on the tables of [6]. In this paragraph we explain a few conjectural comments which appear in the captions of Tables 2, 3 and 4 of [6].

First, Table 2 of [6] gives the guessed asymptotic behavior of the 12 models with group $\mathbb{Z}_2 \times S_4$ and zero orbit-sum (see our Table 5.4). The first remark of [6] is that the critical exponent β of the generating function $O(1,1,1)$ seems to be related to the excursion exponent α by the formula

$$\beta = \frac{\alpha}{2} - \frac{3}{4}. \tag{5.34}$$

(Notice that the remark in [6] is stated with $+\frac{3}{4}$ and not $-\frac{3}{4}$; the reason is that our critical exponents are opposite to the ones in [6].) Let us briefly mention that (5.34) is indeed true and is a consequence of Denisov and Wachtel results: by (5.6) (resp. [58, Thm 1]) one has

$$\alpha = \sqrt{\lambda_1 + \frac{1}{4}} + 1 \quad \text{and} \quad \beta = \frac{1}{2}\left(\sqrt{\lambda_1 + \frac{1}{4}} - \frac{1}{2}\right), \tag{5.35}$$

for zero-drift models (which is the case of these models under consideration). This remark also applies to [6, Tab. 3], giving the excursion asymptotics for the 26 models whose group is S_4 and orbit-sum zero (see again our Table 5.4).

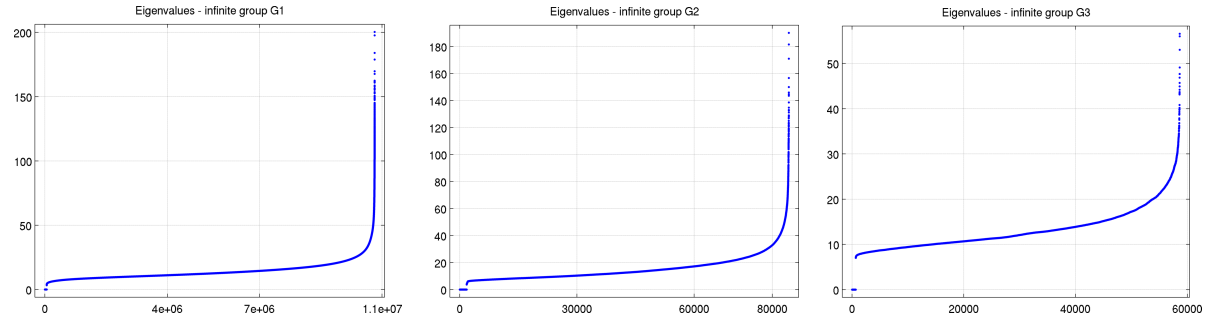

Figure 5.14 – Distribution of eigenvalues for triangles associated to the infinite groups G_1, G_2 and G_3 from Table 5.1

The second comment of [6] that we can easily explain is about the number of different critical exponents. It is remarked in [6] that each exponent α seems to appear for exactly two models in their Table 2, and that in their Table 3 there are only four different exponents (namely, $-5.643{,}21$, $-4.740{,}90$, $-3.650{,}86$ and $-3.325{,}75$). This simply follows from the fact that in [6, Tab. 2] (resp. [6, Tab. 3]) there are only six (resp. four) types of spherical triangles, which appear twice for the second table.

5.6.3 Infinite group case

We have numerically computed for each model corresponding to an infinite group its associated spherical triangle, the eigenvalue and thus the exponent. Details about numerical computations can be found in Section 5.7.

As expected, the behavior is irregular (much more than in the finite group case) and the number of distinct eigenvalues, leading to distinct exponents, is more important. Therefore, we do not attempt to classify the models by the associated eigenvalues. In order to illustrate their repartition, we show in Figure 5.14 the distribution of the eigenvalues for triangles associated to the models in G_1, G_2 and G_3. Points having y-coordinate zero represent the cases where the hypothesis (H) is not satisfied.

As in the finite group case (Table 5.3), we may wonder if there is a connection between the triangles associated to the models and their combinatorial group. The remark shown below strongly indicates that the analogous proposition holds. In some cases, like for example when the triangle has two angles equal to $\pi/2$, the realization of the infinite group as a symmetry group for the triangle is more obvious.

Remark 76. All triangles associated to non-degenerate models with infinite groups satisfy the following property: the combinatorial group can be realized as a symmetry group of the triangle. We have two possibilities:

- The generators $\mathtt{a}, \mathtt{b}, \mathtt{c}$ are the reflections with respect to the three sides of the triangle.

- In cases where the first possibility does not hold, it suffices to replace one of the reflections by its conjugate with respect to one of the other two (for example replace $\mathtt{a}$ by $\mathtt{bab}$).

Remark 76 is justified using numerical computations made in Section 5.7. We notice that only information on the angles is needed here (which can eventually be obtained using elementary functions and algebraic numbers). Therefore the arguments below can be justified using symbolic computations.

Summary of numerical observations justifying Remark 76. Every relation for the combinatorial group of the model can be seen on the associated triangle.

For G_1 there is nothing to prove: we may choose $\mathtt{a}, \mathtt{b}, \mathtt{c}$ to be the three reflections with respect to the sides of the triangle, and no additional relation is required.

Among the 82,453 triangles associated to non-degenerate models of type G_2, exactly 79,219 have (at least) one right angle. Therefore, if $\mathtt{a}$ and $\mathtt{b}$ are reflections with respect to the sides adjacent to the right angle, then $(\mathtt{ab})^2 = 1$. The remaining 3,234 triangles have the property that for one particular labeling $\mathtt{a}, \mathtt{b}, \mathtt{c}$ of the symmetries associated to the sides of the triangles, the composition $\mathtt{cacb}$ is a rotation of angle π and therefore $(\mathtt{cacb})^2 = 1$. Therefore, after a transformation of the type $\mathtt{a} \leftarrow \mathtt{cac}$ described in [95], G_2 is represented as a group of symmetries of the associated triangles.

All triangles associated to non-degenerate models in G_3 have at least two angles equal to $\pi/2$, and 40 among these have three right angles. Therefore, there is a labeling $\mathtt{a}, \mathtt{b}, \mathtt{c}$ of the reflections for which $(\mathtt{ab})^2 = 1$ and $(\mathtt{ac})^2 = 1$.

For triangles associated to groups among $G_4, \ldots, G_{11}$ (all models in G_{12} turn out to be included in a half-space) the relations are not always immediately identifiable with geometric aspects related to angles. One may find triangles with angles π/k for groups having relations of the type $(\mathtt{ab})^k = 1$, but this is not always the case. In order to validate these cases we use the following procedure:

(i) For a triangle T associated to a group G_n, $n = 4, \ldots, 11$, for every one of the six permutations of the reflections $\mathtt{a}, \mathtt{b}, \mathtt{c}$, we construct the result of the transformations $\mathcal{R}(\mathtt{a}, \mathtt{b}, \mathtt{c})(T)$, where $\mathcal{R}$ varies among the relations of the group G_n. We test if the resulting triangle after the above transformations coincides with the initial triangle. If this is the case for every relation $\mathcal{R}$ of G_n then we have found a representation of G_n as a group of reflections.

(ii) If the above step fails, then we consider transformations of the type $\mathcal{R}(\mathtt{cac}, \mathtt{b}, \mathtt{c})$ where, as before, $\mathtt{a}, \mathtt{b}, \mathtt{c}$ are reflections along the sides of the triangles and $\mathcal{R}$ varies among the relations of G_n.

For $G_5, G_7, G_8, G_9, G_{10}, G_{11}$ the step (i) of the above procedure finds a permutation of basic symmetries which satisfies the group relations. This also works partially for G_4 and G_6. For all remaining cases, the step (ii) finds a combination of reflections with one modification of the type $\mathtt{a} \leftarrow \mathtt{cac}$ such that G_n is represented again as a symmetry group of the triangle. □

5.6.4 Exceptional models

In this section we are interested in a family of models, which is remarkable in the sense that the triangle has additional symmetries than those implied by the relations between the generators. We identify models which are non-Hadamard and which have two right angles, providing additional examples where we may compute exponents explicitly. Moreover, we identify triangles associated to infinite groups with three right angles or three angles equal to $2\pi/3$. Numerical investigations show that:

- 200 models in G_6, 837 in G_4, 77,667 in G_2 and 31,005 in G_1 have exactly one right angle;
- 57,935 models in G_3, 1,552 in G_2 and 28,893 in G_1 have exactly two right angles;
- 40 models in G_3 and 563 models in G_1 have three right angles (see Figure 5.15);
- 2 models in G_4 and 3 models in G_1 have three $2\pi/3$ angles (see Figure 5.15).

We have used numerical tools to find the numbers of models in each category: we inspect the triangles by using methods described in Section 5.7 and use a tolerance of 10^{-8} in order to classify the angles of the triangle. Lists with steps corresponding to each one of the cases presented in the above numerical result can be accessed on the web page of the article [26].

Some of these results are validated using symbolic computations, as underlined below.

Theorem 77. *Among infinite group 3D models, there exist models for which the triangles have exactly one, two or three right angles. There also exist models having three* $2\pi/3$ *angles.*

Proof. The cases of three right angles and three angles equal to $2\pi/3$ are completely proved using symbolic computations (using the same approach as in the proof of Theorem 75), i.e., 40 models in G_3 and 563 models in G_1 have three right angles, and 2 models in G_4 and 3 models in G_1 have three $2\pi/3$ angles. Figure 5.15 provides a few examples. The existence of triangles with exactly one right angle in G_1, G_2, G_4 and G_6 and triangles with exactly two right angles in G_1, G_2 and G_3 is validated symbolically. □

Figure 5.15 – Left: two models with a group G_3 and three right angles. Right: two models from G_4 with three angles of measure $\frac{2\pi}{3}$

A first consequence of Theorem 77 is to illustrate that the spherical triangle does not determine everything:

- infinite group models can have triangles which tile the sphere,

- Hadamard models are not the only ones to admit birectangular triangles.

Note that the first phenomenon already appears in 2D: it is indeed possible to construct two-dimensional models with infinite group and rational exponent, see, e.g., [28]. All known examples have either small steps and weights (not only 0 and 1), or admit at least one big step. However, restricted to the unweighted case there is equivalence between the infiniteness of the group and the irrationality of the exponent [34].

A second consequence of Theorem 77 is the following:

Corollary 78. *For all models with exactly two right angles (and $a = b = 0$), the exponent is given by*

$$\alpha = \frac{\pi}{\arccos(-c)} + \frac{5}{2}.$$

In particular if $\frac{\pi}{\arccos(-c)} \notin \mathbb{Q}$ then the model is non-D-finite.

Figure 5.16 – Two models having a group G_2 (Table 5.1). Although these models do not have the Hadamard structure, they admit birectangular triangles and thus explicit eigenvalues, providing examples of application to Corollary 78

As an example, we prove that the two models of Figure 5.16 admit irrational exponents. We present an alternative approach to the irrationally proof given in [34, Sec. 2.4].

Proof. Assume that $\arccos(-c) = \frac{p}{q}\pi$. Then obviously $\cos(q \arccos(-c)) - (-1)^p = 0$, and thus c is a root of

$$f(x) = \cos(q \arccos(-x)) - (-1)^p, \tag{5.36}$$

which is (up to an additive constant) a Chebychev polynomial. For the first (resp. second) model in Figure 5.16, one has $c = \sqrt{7}/3$ (resp. $\sqrt{7/10}$), having respective minimal polynomials

$$P(X) = 9X^2 - 7 \quad \text{and} \quad P(X) = 10X^2 - 7. \tag{5.37}$$

Since Chebychev polynomials have leading coefficient equal to powers of 2, this is the same for $f(x)$.

We recall that a polynomial in $\mathbb{Z}[X]$ is called *primitive* if its coefficients have no common factor. We also recall that the product of two primitive polynomials is again primitive, by Gauss' lemma.

Suppose that P is a primitive polynomial and that P divides, in $\mathbb{Q}[X]$, the polynomial f defined in (5.36). Then there exists another polynomial $Q \in \mathbb{Q}[X]$ such that $f = PQ$. Suppose that Q does not have integer coefficients. Then, let c_Q be the least common multiple of the denominators of the

coefficients of Q. In this way, the polynomial $c_Q Q$ has integer coefficients and is primitive. Therefore

$$P \cdot (c_Q Q) = c_Q f,$$

and since P and $c_Q Q$ are both primitive, it follows that $c_Q f$ is also primitive. This leads to a contradiction if $c_Q > 1$. Therefore $Q \in \mathbb{Z}[X]$.

We can now finish the proof and give the following general result: if $P \in \mathbb{Z}[X]$ is a primitive polynomial and the leading coefficient of P is greater than 2 and is not a power of 2, then P cannot divide f. Using the argument given in the previous paragraph we can conclude that f admits a factorization of the type $f = PQ$ with $Q \in \mathbb{Z}[X]$. Therefore the leading coefficient of f is a product of the leading coefficients of P and Q. Since the leading coefficient of P is greater than 2 and is not a power of 2, it cannot divide the leading coefficient of f, which is a power of 2.

In particular, both polynomials in (5.37) are primitive and have leading coefficient greater than 2, but not a power of 2. Therefore they cannot divide f, and the exponent cannot be rational in these cases. □

5.6.5 Equilateral triangles

In spherical geometry, there exists an equilateral triangle with angles α for any $\alpha \in (\pi/3, \pi)$. The limit case $\alpha = \pi/3$ (resp. $\alpha = \pi$) is the empty triangle (resp. the half-sphere).

Among the 11 million of models, we have numerically found 279 different equilateral triangles. The most remarkable ones admit the angles $\pi/2$ (the simple walk), $2\pi/3$ (Kreweras), $\arccos(1/3)$ (polar triangle for Kreweras), $\arccos(\sqrt{2}-1)$ (the smallest equilateral triangle), $2\pi/5$, $3\pi/5$. It seems that only the first one admits an eigenvalue in closed-form.

Except for the equilateral triangles with angles $\pi/2$ and $2\pi/3$, which exist in G_3 and G_4, all other equilateral triangles come from G_1. The list of equilateral triangles in G_1 and the list of all possible angles observed can be consulted on the webpage of the article [26].

5.7 Numerical approximation of the critical exponent

5.7.1 Literature

In lattice walk problems (and more generally in various enumerative combinatorics problems), it is rather standard to generate many terms of a series and to try to predict the behavior of the model, as the algebraicity or D-finiteness of the generating function, or the asymptotic behavior of the sequence. Having a large number of terms allows further to derive estimates of the exponential growth or of the critical exponent. More specifically, in the context of walks confined to cones, it is possible to make use of a functional equation to generate typically a few thousands of terms (the functional equation corresponds to a step-by-step construction of a walk, see [27, Eq. (4.1)] for a precise statement).

One can find in [30, 6, 88] various estimates of critical exponents (contrary to the results presented here, the estimates of [30, 6, 88] also concern the total numbers of walks—and not only the numbers of excursions). In [30], Bostan and Kauers consider 3D step sets of up to five elements, and guess various asymptotic behaviors using convergence acceleration techniques. Bacher, Kauers and Yatchak go further in [6], computing more terms and considering all 3D models (with no restriction on the cardinality of the step set). In [88], Guttmann analyses the coefficients of a few models by either the method of differential approximants or the ratio method. The methods of [88] for generating the coefficients and for analyzing the resulting series are given in Chapters 7 and 8 of [87].

We present here a finite element method which computes approximation of the critical exponent. As we have previously seen, this critical exponent can be related to the smallest eigenvalue of a Dirichlet problem in a spherical triangle associated to the step set of the walk. Some other techniques of eigenvalue computation have the advantage of being applicable to any spherical triangle, not necessarily related to a 3D model. Using the stereographic projection, the 3D eigenvalue problem (5.5) can be rewritten as a 2D eigenvalue problem for a different operator. Since the stereographic projection maps circles onto circles, the new domain is bounded by three arcs of circles and is thus rather simple. However, as expected, the eigenvalue problem becomes more complicated and is a priori not exactly solvable. See [78, 77] for more details (in particular [77, Eq. (2.12) and Fig. 3]). In [53], the authors present a method for enclosing the principal eigenvalue of any triangle using validated numerical techniques.

Finally, the authors of [103] describe a Monte Carlo method for the numerical computation of the first Dirichlet eigenvalue of the Laplace operator in a bounded domain. It is based on the estimation of the speed of absorption of Brownian motion by the boundary of the domain. Theoretically this could certainly be used in our situation, but as in many probabilistic methods, it is hard to expect a precision such as ours (typically, ten digits). In [103], the speed of convergence is of order $1/\sqrt(n)$ by the Kolmogorov-Smirnov theorem.

5.7.2 Finite element method

We perform here a finite element method and compute precise approximations of the eigenvalue (typically, 10 digits of precision). We make available our codes on the webpage of the article [26]. The finite element computation consists in a few standard steps (triangulation of the domain, see Figure 5.17, assembly and the resolution of the discretized problem). For general aspects regarding finite element spaces defined on surfaces, we refer to [69]. We underline the fact that the method described below can be applied to general subsets of the sphere, not only for triangles. The precision of the computation of the eigenvalue depends on the size of the triangulation. For example, we found that the eigenvalue of the triangle associated to the Kreweras model is

$$\lambda_1 = 5.159{,}145{,}642{,}470,$$

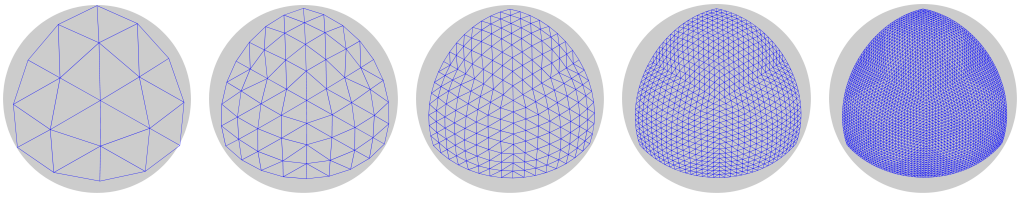

Figure 5.17 – Triangulation of a spherical triangle using successive refinements

where we believe that all digits present are correct. This is very close to the result of Guttmann [88]. A method for computing eigenvalues of spherical regions using fundamental solutions was recently proposed in [3] for smooth domains on the sphere. The singular behavior generated by the corners of the triangles renders this method is not directly adapted to our needs. For more details on the numerical method for the computation of the critical exponent we refer to [26].

5.8 Further objectives and perspectives

5.8.1 Walks avoiding an octant and complements of spherical triangles

Rather than counting walks confined to an octant, one could aim at counting walks *avoiding* an octant (or equivalently, walks confined to the union of seven octants). This model is briefly presented in [111, Sec. 4]. It is inspired by the dimension two case, where the model of walks avoiding a quadrant has started to be studied (see Chapters 3 and 4, as well as [40, 111]). As we have seen, the (geometric) difference between quarter plane and three-quarter plane first seems anecdotal. However, the combinatorial complexity is much higher in the three quadrants; this is well illustrated by the fact that the simple walk model in the three-quarter plane has the same level of difficulty as quadrant Gessel walks, as shown by Bousquet-Mélou in [40].

Going back to walks in dimension three, we consider walks confined to the union of seven octants

$$\mathcal{R} = \{(i,j,k) \in \mathbb{Z}^3 : i \geq 0 \text{ or } j \geq 0 \text{ or } k \geq 0\},$$

see Figure 5.18 for an example of such a walk. With the usual strategy of constructing the walk step-by-step (see Section 2.1.1 and Section 5.2.1), we can write a functional equation for the generating function of walks avoiding the negative octant

$$R(x,y,z) = \sum_{n \geq 0} \sum_{(i,j,k) \in \mathcal{R}} r_{i,j,k}(n) x^i y^j z^k t^n,$$

where $r_{i,j,k}(n)$ is the number of path from $(0,0,0)$ to (i,j,k) within $\mathcal{R}$.

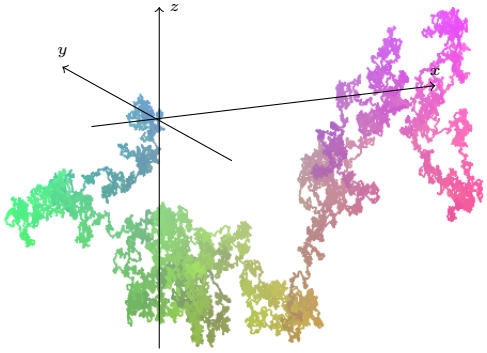

(a) 3D representation of a walk

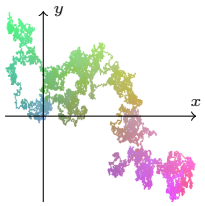

(b) Projection on the xy-plane

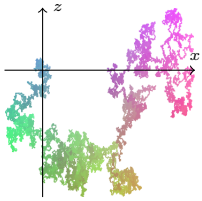

(c) Projection on the xz-plane

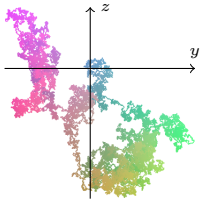

(d) Projection on the yz-plane

Figure 5.18 – A 3D walk avoiding the negative octant

Let $R_{0--}(y^{-1},z^{-1}) = \sum_{n\geq 0}\sum_{j\leq -1,k\leq -1} r_{0,j,k}(n)y^j z^k t^n$ be the generating function of walks ending in the negative yz-plane[6] and $R_{00-}(z^{-1}) = \sum_{n\geq 0}\sum_{k\leq -1} r_{0,0,k}(n)z^k t^n$ be the generating function of walks ending on the negative z-axis. We define similarly $R_{-0-}(x^{-1},z^{-1})$, $R_{--0}(x^{-1},y^{-1})$, $R_{0-0}(y^{-1})$ and $R_{-00}(x^{-1})$.

Walks avoiding the negative 3D octant can be empty with generating function 1 or can be walks in $\mathcal{R}$ to which we add a step from $\mathcal{S}$, that is $t\chi(x,y,z)R(x,y,z)$. Walks going out of $\mathcal{R}$ from the negative yz-plane with generating function $tx^{-1}A_-(y,z)R_{0--}(y^{-1},z^{-1})$ need to be removed, as well as walks going out of $\mathcal{R}$ from the negative xz-plane and negative xy-plane with generating functions $ty^{-1}B_-(x,z)R_{-0-}(x^{-1},z^{-1})$ and $tz^{-1}C_-(x,y)R_{--0}(x^{-1},y^{-1})$. But we have removed twice some walks going out from the negative z-axis (resp. negative y-axis and negative x-axis) and thus we need to add $tx^{-1}y^{-1}D_-(z)R_{00-}(z^{-1})$ (resp. $tx^{-1}z^{-1}E_-(y)R_{0-0}(y^{-1})$ and $ty^{-1}z^{-1}F_-(x)R_{-00}(x^{-1})$). We end this construction with removing the walks out of $\mathcal{R}$ with gener-

[6]The negative yz-plane denotes points with negative y and z coordinates.

ating function $\varepsilon t x^{-1}y^{-1}z^{-1}R(0,0,0)$. We get then

$$\begin{aligned} R(x,y,z) =& 1 + t\chi(x,y,z)R(x,y,z) - tx^{-1}A_-(y,z)R_{0--}(y^{-1},z^{-1}) \\ & - ty^{-1}B_-(x,z)R_{-0-}(x^{-1},z^{-1}) - tz^{-1}C_-(x,y)R_{--0}(x^{-1},y^{-1}) \\ & + tx^{-1}y^{-1}D_-(z)R_{00-}(z^{-1}) + tx^{-1}z^{-1}E_-(y)R_{0-0}(y^{-1}) + ty^{-1}z^{-1}F_-(x)R_{-00}(x^{-1}) \\ & - \varepsilon t x^{-1}y^{-1}z^{-1}O(0,0,0). \end{aligned} \tag{5.38}$$

This functional equation (5.38) seems similar to the octant case (5.8). However, we face here the same difficulties as the two-dimensional case: the functional involves both positive and negative powers of x, y and z giving rise to convergence issues. On the other side, it is clear from our construction that the critical exponent α of the excursion sequence is given by the same formula (5.6), where λ_1 is now the principal eigenvalue of the Dirichlet problem (5.5) on the *complement of a spherical triangle*.

We were not able to identify any non-degenerate spherical triangle for which the principal eigenvalue of its complement is known to admit a closed form. A fortiori, we did not find any model whose exponent of the excursion sequence in the seven octants has an explicit form. From that point of view, one notices the same complexification phenomenon as in dimension 2.

Take the example of the simple walk, for which one should compute the principal eigenvalue of the complement of the equilateral right triangle. Even for this very simple case, no closed-form expression for λ_1 seems to exist, and the exponent α is conjectured to be irrational, see Conjecture 4.1 in [111]. Numerical computations show that α is approximatively equal to 0.660,44.

5.8.2 Walks avoiding a wedge

Let us now mention the combinatorial model of 3D walks avoiding a wedge[7], see for example Figure 5.19, which is a higher dimensional analogue of walks in the slit plane [44]. 3D walks avoiding a wedge also appear as a degenerate case of the previous model of Section 5.8.1, when the triangle collapses into a single great arc of circle.

From a spherical geometry viewpoint, the problem becomes that of computing the first eigenvalue for the Dirichlet problem on the complement of a portion of great arc of circle of some given length in $[0,\pi]$. Such a problem is analyzed in [124, Sec. 6]. The extremal cases π and 0 are solved in [124, Sec. 4], they correspond to $\lambda_1 = \frac{3}{4}$ (exponent 2) and $\lambda_1 = 0$ (exponent $\frac{3}{2}$), respectively. Tables 7 and 8 of [124] provide approximate values of the fundamental eigenvalue for other values of the arc length.

[7]That is walks avoiding a planar cone.

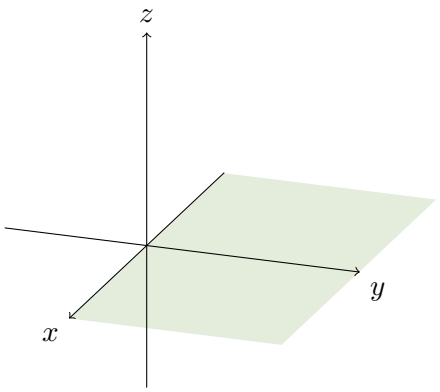

Figure 5.19 – We can study 3D walks avoiding the half-plane $(i, j, 0)$ where $j \geq 0$.

5.8.3 Total number of walks

Throughout the article we have considered the asymptotics of the number of excursions (essentially, the coefficients of $O(0,0,0)$, see (5.1) and (5.2)), but other questions are relevant from an enumerative combinatorics viewpoint, as the asymptotics of the total number of walks (regardless of the ending position), or equivalently the coefficients of the series $O(1,1,1)$.

Let us recall that it is still an open problem to determine, in general, the asymptotics as $n \to \infty$ of the coefficients of $O(1,1,1)$. Assume that it has the form

$$[t^n]O(1,1,1) = \varkappa \cdot \rho^n \cdot n^{-\beta} \cdot (1 + o(1)). \tag{5.39}$$

Recall from [85] that under the hypothesis (H), there exists $(x^*, y^*, z^*) \in [1, \infty)^3$ such that

$$\min_{[1,\infty)^3} \chi = \chi(x^*, y^*, z^*),$$

and then the exponential growth ρ in (5.39) is given by $\rho = \chi(x^*, y^*, z^*)$; compare with (5.17). There are essentially three cases for which the critical exponent β in (5.39) is known:

- Case of a drift in the interior of $\mathbb{N}^3$ ($\beta = 0$);
- Zero drift (then $\beta = \frac{\alpha}{2} - \frac{3}{4}$, α being the critical exponent of the excursions (5.2));
- Case when the point (x^*, y^*, z^*) is in the interior of the domain $[1, \infty)^3$, i.e., $x^* > 1$, $y^* > 1$ and $z^* > 1$ (in that case $\beta = \alpha$).

In the first case (drift with positive entries), the exponent is obviously 0 by the law of large numbers. In the second case the exponent β is given by the formula (5.35) proved in [58]. As recalled in (5.34), β is a simple affine combination of α, namely $\beta = \frac{\alpha}{2} - \frac{3}{4}$. The last case is proved by Duraj in [66]. The original statement of Duraj is in terms of the minimum of the Laplace transform of the step set on the dual cone, but it is equivalent to the one presented above, after an exponential

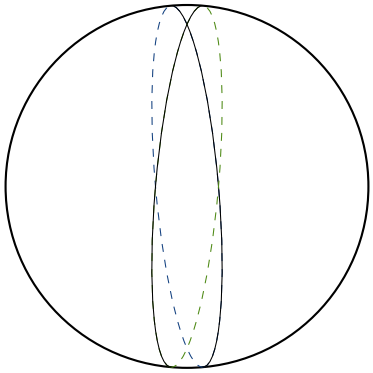

Figure 5.20 – A spherical digon is the domain bounded by two great arcs of circles

change of variables and using the self-duality of the octant $\mathbb{N}^3$. The hypothesis that the point (x^*, y^*, z^*) is an interior point cannot be easily translated in terms of the drift; note, however, that it contains the case of a drift with three negative coordinates. The intuition of the formula $\beta = \alpha$ is that the drift being directed towards the vertex of the cone, a typical walk will end at a point close to the vertex, and thus asymptotically the total number of walks is comparable to the number of excursions.

5.8.4 Walks in the quarter plane and spherical digons

In this paragraph we briefly explain how the more classical model of walks in the quarter plane enters into the framework of spherical geometry. In one sentence, spherical triangles become degenerate and should be replaced by spherical digons, see Figure 5.20, for which the principal eigenvalue (and in fact the whole spectrum) is known.

Indeed, given a 2D positive random walk $\{(X(n), Y(n))\}$, we can choose an arbitrary 1D random walk $\{Z(n)\}$ and embed the 2D model as a 3D walk $\{(X(n), Y(n), Z(n))\}$, with no positivity constraint on the last coordinate. The natural cone is therefore $\mathbb{N}^2 \times \mathbb{Z}$, or after the decorrelation of the coordinates, the cartesian product of a wedge of opening α and $\mathbb{Z}$. On the sphere $\mathbb{S}^2$, the section of the latter domain is precisely a spherical digon of angle α.

The smallest eigenvalue λ_1 of a spherical digon is easily computed, see, e.g., [124, Sec. 5]:

$$\lambda_1 = \frac{\pi}{\alpha}\left(\frac{\pi}{\alpha} + 1\right).$$

The formula (5.6) relating the smallest eigenvalue to the critical exponent gives an exponent equal to $\frac{\pi}{\alpha} + \frac{3}{2}$. To find the exponent of the initial planar random walk we have to subtract $\frac{1}{2}$ (exponent of an unconstrained excursion in the z-coordinate), which by [58, 34] is the correct result.

5.8.5 Exit time from cones for Brownian motion

All results that we obtain for discrete random walks admit continuous analogues and can be used to estimate exit times from cones of Brownian motion. In the literature, one can find applications of these estimates to the Brownian pursuit [117, 116]. As shown in [57, 5] (see in particular [5, Cor. 1]), the exit time of a standard d-dimensional Brownian motion from a cone K behaves when $t \to \infty$ as

$$\mathbb{P}_x[\tau > t] = B_1 \cdot m_1\left(\frac{x}{|x|}\right) \cdot \left(\frac{|x|^2}{2}\right)^{\lambda_1(K)/2} \cdot t^{-\lambda_1(K)/2}, \tag{5.40}$$

where $\lambda_1(K)$ is equal to

$$\lambda_1(K) = \sqrt{\lambda_1(C) + \left(1 - \frac{d}{2}\right)^2} + \left(1 - \frac{d}{2}\right)$$

and $\lambda_1(C)$ is the principal eigenvalue of the Dirichlet problem on the section $C = K \cap \mathbb{S}^{d-1}$:

$$\begin{cases} -\Delta_{\mathbb{S}^{d-1}} m &= \Lambda m \quad \text{in } C, \\ m &= 0 \quad \text{in } \partial C. \end{cases} \tag{5.41}$$

In the asymptotics (5.40), m_1 is the (suitably normalized) eigenfunction associated to λ_1.

In the particular case of 3D Brownian motion, if the cone K is an intersection of three half-spaces, the section C becomes a spherical triangle and the exponent in (5.40) is directly related to the principal eigenvalue of a spherical triangle, which is the main object of investigation studied in this paper.

Let us finally comment on the case of non-standard Brownian motion (in arbitrary dimension $d \geq 2$). First, the case of non-identity covariance matrices is easily reduced to the standard case, by applying a simple linear transform (notice, however, that this implies changing the initial cone, and therefore the domain of the Dirichlet problem). The situation is more subtle in the case of drifted Brownian motion: various asymptotic regimes exist, depending on the position of the drift with respect to the cone and the polar cone [84]. In some regimes the exponent in (5.40) involves the principal eigenvalue λ_1; in some other cases (e.g., a drift which belongs to the interior of the cone) the exponent is independent of the geometry of the cone.

5.8.6 Further open problems

Besides the open problems listed in [27, Sec. 9], let us mention the following:

Singularity analysis. Is it possible to obtain similar results on non-D-finiteness of Hadamard models using the Hadamard product of generating functions? This would mean to prove Corollaries 69 and 73 directly, at the level of generating functions.

3D Kreweras model. This is clearly the model for which we can find the greatest number of estimations in the literature; its triangle is equilateral with angle $2\pi/3$. Let us quickly give a chronological list (probably non-exhaustive):

- $[5.15, 5.16]$ by Costabel (2008, [55])
- 5.159 by Ratzkin and Treibergs (2009, [117, 116])
- 5.1589 by Bostan, Raschel and Salvy (2012, [33])
- 5.162 by Balakrishna (2013, [7])
- 5.1606 by Balakrishna (2013, [8])
- 5.1591452 by Bacher, Kauers and Yatchak (2016, [6])
- 5.159145642466 Guttmann (2017, [88])
- 5.159145642470 by our result with a finite element method (see Section 5.7)

What is the exact value? Is it a rational number? The triangle associated to Kreweras model, which corresponds to the tetrahedral partition of the sphere, is also related to minimal 4-partitions of $\mathbb{S}^2$, see [89].

Bibliography

[1] I. Adan, J. Wessels, and W. Zijm. Analysis of the asymmetric shortest queue problem. *Queueing Systems Theory Appl.*, 8(1):1–58, 1991.

[2] M. Albert and M. Bousquet-Mélou. Permutations sortable by two stacks in parallel and quarter plane walks. *European J. Combin.*, 43:131–164, 2015.

[3] C. Alves and P. Antunes. The method of fundamental solutions applied to boundary value problems on the surface of a sphere. *Comput. Math. Appl.*, 75(7):2365–2373, 2018.

[4] D. André. Solution directe du problème résolu par M. Bertrand. *C. R. Acad. Sci. Paris*, 105:436–437, 1887.

[5] R. Bañuelos and R. Smits. Brownian motion in cones. *Probab. Theory Related Fields*, 108(3):299–319, 1997.

[6] A. Bacher, M. Kauers, and R. Yatchak. Continued classification of 3d lattice models in the positive octant. In *Proceedings of FPSAC'16*, pages 95–106. DMTCS, 2016.

[7] B. Balakrishna. Heat equation on the cone and the spectrum of the spherical Laplacian. *arXiv*, 1301.6202v3:1–16, 2013.

[8] B. Balakrishna. On multi-particle brownian survivals and the spherical Laplacian. 2013. *Preprint* available at this http url.

[9] C. Banderier and M. Drmota. Formulae and asymptotics for coefficients of algebraic functions. *Combin. Probab. Comput.*, 24(1):1–53, 2015.

[10] C. Banderier and P. Flajolet. Basic analytic combinatorics of directed lattice paths. *Theoret. Comput. Sci.*, 281(1-2):37–80, 2002. Selected papers in honour of Maurice Nivat.

[11] C. Banderier and M. Wallner. Lattice paths with catastrophes. *Discrete Math. Theor. Comput. Sci.*, 19(1):Paper No. 23, 32, 2017.

[12] N. R. Beaton, A. L. Owczarek, and A. Rechnitzer. Exact solution of some quarter plane walks with interacting boundaries. *Electron. J. Combin.*, 26(3):Paper 3.53, 38, 2019.

[13] P. Bérard. Remarques sur la conjecture de Weyl. *Compositio Math.*, 48(1):35–53, 1983.

[14] P. Bérard and G. Besson. Spectres et groupes cristallographiques. II. Domaines sphériques. *Ann. Inst. Fourier (Grenoble)*, 30(3):237–248, 1980.

[15] M. Berger. *Geometry. II.* Universitext. Springer-Verlag, Berlin, 1987. Translated from the French by M. Cole and S. Levy.

[16] O. Bernardi. Bijective counting of Kreweras walks and loopless triangulations. *J. Combin. Theory Ser. A*, 114(5):931–956, 2007.

[17] O. Bernardi, M. Bousquet-Mélou, and K. Raschel. Counting quadrant walks via Tutte's invariant method. *arXiv*, 1708.08215:1–54, 2017.

[18] J. Bertoin and R. A. Doney. On conditioning a random walk to stay nonnegative. *Ann. Probab.*, 22(4):2152–2167, 1994.

[19] J. Bertrand. Solution d'un problème. *C. R. Acad. Sci. Paris*, 105:369, 1887.

[20] P. Biane. Some properties of quantum Bernoulli random walks. In *Quantum probability & related topics*, QP-PQ, VI, pages 193–203. World Sci. Publ., River Edge, NJ, 1991.

[21] P. Biane. Équation de Choquet-Deny sur le dual d'un groupe compact. *Probab. Theory Related Fields*, 94(1):39–51, 1992.

[22] P. Biane. Frontière de Martin du dual de SU(2). In *Séminaire de Probabilités, XXVI*, volume 1526 of *Lecture Notes in Math.*, pages 225–233. Springer, Berlin, 1992.

[23] P. Biane. Minuscule weights and random walks on lattices. In *Quantum probability & related topics*, QP-PQ, VII, pages 51–65. World Sci. Publ., River Edge, NJ, 1992.

[24] S. Billiard and V. C. Tran. A general stochastic model for sporophytic self-incompatibility. *J. Math. Biol.*, 64(1-2):163–210, 2012.

[25] B. Bogosel. The method of fundamental solutions applied to boundary eigenvalue problems. *J. Comput. Appl. Math.*, 306:265–285, 2016.

[26] B. Bogosel, V. Perrollaz, K. Raschel, and A. Trotignon. 3D positive lattice walks and spherical triangles. *arXiv*, 1804.06245:1–41, 2018. Webpage: `https://bit.ly/2J4Vf3X`.

[27] A. Bostan, M. Bousquet-Mélou, M. Kauers, and S. Melczer. On 3-dimensional lattice walks confined to the positive octant. *Ann. Comb.*, 20(4):661–704, 2016.

[28] A. Bostan, M. Bousquet-Mélou, and S. Melczer. On walks with large steps in an orthant. *arXiv*, 1806.00968, 2018.

[29] A. Bostan, F Chyzak, M. Van Hoeij, M. Kauers, and L. Pech. Hypergeometric expressions for generating functions of walks with small steps in the quarter plane. *European J. Combin.*, 61:242–275, 2017.

[30] A. Bostan and M. Kauers. Automatic classification of restricted lattice walks. In *21st International Conference on Formal Power Series and Algebraic Combinatorics (FPSAC 2009)*, Discrete Math. Theor. Comput. Sci. Proc., AK, pages 201–215. Assoc. Discrete Math. Theor. Comput. Sci., Nancy, 2009.

[31] A. Bostan and M. Kauers. The complete generating function for Gessel walks is algebraic. *Proc. Amer. Math. Soc.*, 138(9):3063–3078, 2010. With an appendix by Mark van Hoeij.

[32] A. Bostan, I. Kurkova, and K. Raschel. A human proof of Gessel's lattice path conjecture. *Trans. Amer. Math. Soc.*, 369(2):1365–1393, 2017.

[33] A. Bostan, K. Raschel, and B. Salvy. Unpublished notes. 2012.

[34] A. Bostan, K. Raschel, and B. Salvy. Non-D-finite excursions in the quarter plane. *J. Combin. Theory Ser. A*, 121:45–63, 2014.

[35] A. Bouaziz, S. Mustapha, and M. Sifi. Discrete harmonic functions on an orthant in $\mathbb{Z}^d$. *Electron. Commun. Probab.*, 20:no. 52, 13, 2015.

[36] N. Bourbaki. *Éléments de mathématique. Fasc. XXXIV. Groupes et algèbres de Lie. Chapitre IV: Groupes de Coxeter et systèmes de Tits. Chapitre V: Groupes engendrés par des réflexions. Chapitre VI: systèmes de racines.* Actualités Scientifiques et Industrielles, No. 1337. Hermann, Paris, 1968.

[37] M. Bousquet-Mélou. Algebraic generating functions in enumerative combinatorics and context-free languages. In *STACS 2005*, volume 3404 of *Lecture Notes in Comput. Sci.*, pages 18–35. Springer, Berlin, 2005.

[38] M. Bousquet-Mélou. An elementary solution of Gessel's walks in the quadrant. *Adv. Math.*, 303:1171–1189, 2016.

[39] M. Bousquet-Mélou. An elementary solution of Gessel's walks in the quadrant. *Adv. Math.*, 303:1171–1189, 2016.

[40] M. Bousquet-Mélou. Square lattice walks avoiding a quadrant. *J. Combin. Theory Ser. A*, 144:37–79, 2016.

[41] M. Bousquet-Mélou and M. Mishna. Walks with small steps in the quarter plane. In *Algorithmic probability and combinatorics*, volume 520 of *Contemp. Math.*, pages 1–39. Amer. Math. Soc., Providence, RI, 2010.

[42] M. Bousquet-Mélou and M. Petkovšek. Linear recurrences with constant coefficients: the multivariate case. *Discrete Math.*, 225(1-3):51–75, 2000. Formal power series and algebraic combinatorics (Toronto, ON, 1998).

[43] M. Bousquet-Mélou and M. Petkovšek. Walks confined in a quadrant are not always D-finite. *Theoret. Comput. Sci.*, 307(2):257–276, 2003. Random generation of combinatorial objects and bijective combinatorics.

[44] M. Bousquet-Mélou and G. Schaeffer. Walks on the slit plane. *Probab. Theory Related Fields*, 124(3):305–344, 2002.

[45] M. Buchacher and M. Kauers. Inhomogeneous restricted lattice walks. In *Proceedings of FPSAC 2019*, pages 1–12, 2019. (to appear).

[46] T. Budd. Winding of simple walks on the square lattice. *arXiv*, 1709.04042:1–33, 2017.

[47] N. Champagnat, P. Diaconis, and L. Miclo. On Dirichlet eigenvectors for neutral two-dimensional Markov chains. *Electron. J. Probab.*, 17:no. 63, 41, 2012.

[48] I. Chavel. *Eigenvalues in Riemannian geometry*, volume 115 of *Pure and Applied Mathematics*. Academic Press, Inc., Orlando, FL, 1984. Including a chapter by Burton Randol, With an appendix by Jozef Dodziuk.

[49] J. Cohen. *Analysis of random walks*, volume 2 of *Studies in Probability, Optimization and Statistics*. IOS Press, Amsterdam, 1992.

[50] J. Cohen and O. Boxma. *Boundary value problems in queueing system analysis*, volume 79 of *North-Holland Mathematics Studies*. North-Holland Publishing Co., Amsterdam, 1983.

[51] R. Cont and A. de Larrard. Price dynamics in a Markovian limit order market. *SIAM J. Financial Math.*, 4(1):1–25, 2013.

[52] Wikipedia contributors. Schwarz triangle. `https://en.wikipedia.org/w/index.php?title=Schwarz_triangle&oldid=858916728`, September 2018. Online; accessed 07-September-2019.

[53] J. Dahne and B. Salvy. Enclosing the first eigenvalue of the Laplacian on a spherical triangle. *In preparation*, 2019.

[54] M. Dauge. *Elliptic boundary value problems on corner domains*, volume 1341 of *Lecture Notes in Mathematics*. Springer-Verlag, Berlin, 1988. Smoothness and asymptotics of solutions.

[55] M. Dauge. Private communication. 2017.

[56] A. I. Davydychev and R. Delbourgo. A geometrical angle on Feynman integrals. *J. Math. Phys.*, 39(9):4299–4334, 1998.

[57] R. Dante DeBlassie. Exit times from cones in $\mathbf{R}^n$ of Brownian motion. *Probab. Theory Related Fields*, 74(1):1–29, 1987.

[58] D. Denisov and V. Wachtel. Random walks in cones. *Ann. Probab.*, 43(3):992–1044, 2015.

[59] Y. Doumerc and N. O'Connell. Exit problems associated with finite reflection groups. *Probab. Theory Related Fields*, 132(4):501–538, 2005.

[60] T. Dreyfus and C. Hardouin. Length derivative of the generating series of walks confined in the quarter plane. *arXiv*, 1902.10558, 2019.

[61] T. Dreyfus, C. Hardouin, J. Roques, and M. Singer. Walks in the quarter plane, genus zero case. *arXiv*, 1710.02848, 2017.

[62] T. Dreyfus, C. Hardouin, J. Roques, and M. Singer. On the nature of the generating series of walks in the quarter plane. *Invent. Math.*, 213(1):139–203, 2018.

[63] T. Dreyfus and K. Raschel. Differential transcendence and algebraicity criteria for the series counting weighted quadrant walks. *Publications mathématiques de Besançon*, 1:41–80, 2017.

[64] D. Du, Q. Hou, and R. Wang. Infinite orders and non-D-finite property of 3-dimensional lattice walks. *Electron. J. Combin.*, 23(3):Paper 3.38, 15, 2016.

[65] R. J. Duffin. Basic properties of discrete analytic functions. *Duke Math. J.*, 23:335–363, 1956.

[66] J. Duraj. Random walks in cones: the case of nonzero drift. *Stochastic Process. Appl.*, 124(4):1503–1518, 2014.

[67] J. Duraj and V. Wachtel. Invariance principles for random walks in cones. *arXiv*, 1508.07966:1–17, 2015.

[68] P. Duren. *Univalent functions*, volume 259 of *Grundlehren der Mathematischen Wissenschaften*. Springer-Verlag, New York, 1983.

[69] G. Dziuk and C. Elliott. Finite element methods for surface PDEs. *Acta Numer.*, 22:289–396, 2013.

[70] A. Elvey Price and A. Guttmann. Permutations sortable by deques and by two stacks in parallel. *European J. Combin.*, 59:71–95, 2017.

[71] G. Fayolle and R. Iasnogorodski. Two coupled processors: the reduction to a Riemann-Hilbert problem. *Z. Wahrsch. Verw. Gebiete*, 47(3):325–351, 1979.

[72] G. Fayolle, R. Iasnogorodski, and V. Malyshev. *Random walks in the quarter plane*, volume 40 of *Probability Theory and Stochastic Modelling*. Springer, Cham, second edition, 2017. Algebraic methods, boundary value problems, applications to queueing systems and analytic combinatorics.

[73] G. Fayolle and K. Raschel. Random walks in the quarter-plane with zero drift: an explicit criterion for the finiteness of the associated group. *Markov Process. Related Fields*, 17(4):619–636, 2011.

[74] G. Fayolle and K. Raschel. Some exact asymptotics in the counting of walks in the quarter plane. In *23rd Intern. Meeting on Probabilistic, Combinatorial, and Asymptotic Methods for the Analysis of Algorithms (AofA'12)*, Discrete Math. Theor. Comput. Sci. Proc., AQ, pages 109–124. Assoc. Discrete Math. Theor. Comput. Sci., Nancy, 2012.

[75] G. Fayolle and K. Raschel. About a possible analytic approach for walks in the quarter plane with arbitrary big jumps. *C. R. Math. Acad. Sci. Paris*, 353(2):89–94, 2015.

[76] J. Ferrand. Fonctions préharmoniques et fonctions préholomorphes. *Bull. Sci. Math. (2)*, 68:152–180, 1944.

[77] G. Fichera. Comportamento asintotico del campo elettrico e della densità elettrica in prossimità dei punti singolari della superficie conduttore. *Rend. Sem. Mat. Univ. e Politec. Torino*, 32:111–143 (1975), 1973/74.

[78] G. Fichera and Sneider L. Distribution de la charge électrique dans le voisinage des sommets et des arêtes d'un cube. *C. R. Acad. Sci. Paris Sér. A*, 278:1303–1306, 1974.

[79] P. Flajolet and R. Sedgewick. *Analytic combinatorics*. Cambridge University Press, Cambridge, 2009.

[80] L. Flatto. Two parallel queues created by arrivals with two demands. II. *SIAM J. Appl. Math.*, 45(5):861–878, 1985.

[81] L. Flatto and S. Hahn. Two parallel queues created by arrivals with two demands. I. *SIAM J. Appl. Math.*, 44(5):1041–1053, 1984.

[82] R. Foley and D. McDonald. Join the shortest queue: stability and exact asymptotics. *Ann. Appl. Probab.*, 11(3):569–607, 2001.

[83] F. D. Gakhov. *Boundary value problems*. Dover Publications, Inc., New York, 1990. Translated from the Russian, Reprint of the 1966 translation.

[84] R. Garbit and K. Raschel. On the exit time from a cone for Brownian motion with drift. *Electron. J. Probab.*, 19:no. 63, 27, 2014.

[85] R. Garbit and K. Raschel. On the exit time from a cone for random walks with drift. *Rev. Mat. Iberoam.*, 32(2):511–532, 2016.

[86] D. Gouyou-Beauchamps. Chemins sous-diagonaux et tableaux de Young. In *Combinatoire énumérative (Montreal, Que., 1985/Quebec, Que., 1985)*, volume 1234 of *Lecture Notes in Math.*, pages 112–125. Springer, Berlin, 1986.

[87] A. Guttmann, editor. *Polygons, polyominoes and polycubes*, volume 775 of *Lecture Notes in Physics*. Springer, Dordrecht, 2009. [Editor name on title page: Anthony J. Guttman].

[88] T. Guttmann. Private communication. 2017.

[89] B. Helffer, T. Hoffmann-Ostenhof, and S. Terracini. On spectral minimal partitions: the case of the sphere. In *Around the research of Vladimir Maz'ya. III*, volume 13 of *Int. Math. Ser. (N. Y.)*, pages 153–178. Springer, New York, 2010.

[90] L. Hillairet and C. Judge. Generic spectral simplicity of polygons. *Proc. Amer. Math. Soc.*, 137(6):2139–2145, 2009.

[91] I. Ignatiouk-Robert and C. Loree. Martin boundary of a killed random walk on a quadrant. *Ann. Probab.*, 38(3):1106–1142, 2010.

[92] T. Kato. *Perturbation theory for linear operators*. Springer-Verlag, Berlin-New York, second edition, 1976. Grundlehren der Mathematischen Wissenschaften, Band 132.

[93] M. Kauers. Private communication. 2017.

[94] M. Kauers, C. Koutschan, and D. Zeilberger. Proof of Ira Gessel's lattice path conjecture. *Proc. Natl. Acad. Sci. USA*, 106(28):11502–11505, 2009.

[95] M. Kauers and R.-H. Wang. Lattice walks in the octant with infinite associated groups. *Proceedings of EUROCOMB 2017, Electronic Notes in Discrete Mathematics*, pages 703–709, 2017.

[96] M. Kauers and R. Yatchak. Walks in the quarter plane with multiple steps. In *Proceedings of FPSAC 2015*, Discrete Math. Theor. Comput. Sci. Proc., pages 25–36. Assoc. Discrete Math. Theor. Comput. Sci., Nancy, 2015.

[97] G. Kreweras. Sur une classe de problèmes de dénombrement liés au treillis des partitions des entiers. In *Cahiers du B.U.R.O.*, volume 6, pages 5–105. 1965.

[98] I. Kurkova and V. Malyshev. Martin boundary and elliptic curves. *Markov Process. Related Fields*, 4(2):203–272, 1998.

[99] I. Kurkova and K. Raschel. Explicit expression for the generating function counting Gessel's walks. *Adv. in Appl. Math.*, 47(3):414–433, 2011.

[100] I. Kurkova and K. Raschel. On the functions counting walks with small steps in the quarter plane. *Publ. Math. Inst. Hautes Études Sci.*, 116:69–114, 2012.

[101] I. Kurkova and K. Raschel. New steps in walks with small steps in the quarter plane: series expressions for the generating functions. *Ann. Comb.*, 19(3):461–511, 2015.

[102] I. Kurkova and Y. Suhov. Malyshev's theory and JS-queues. Asymptotics of stationary probabilities. *Ann. Appl. Probab.*, 13(4):1313–1354, 2003.

[103] A. Lejay and S. Maire. Computing the principal eigenvalue of the Laplace operator by a stochastic method. *Math. Comput. Simulation*, 73(6):351–363, 2007.

[104] J. Lu. *Boundary value problems for analytic functions*, volume 16 of *Series in Pure Mathematics*. World Scientific Publishing Co., Inc., River Edge, NJ, 1993.

[105] V. A. Malyshev. Wiener-Hopf equations in the quarter-plane, discrete groups and automorphic functions. *Mat. Sb. (N.S.)*, 84 (126):499–525, 1971.

[106] S. Melczer and M. Mishna. Singularity analysis via the iterated kernel method. *Combin. Probab. Comput.*, 23(5):861–888, 2014.

[107] S. Melczer and M. Mishna. Asymptotic lattice path enumeration using diagonals. *Algorithmica*, 75(4):782–811, 2016.

[108] M. Mishna. Classifying lattice walks restricted to the quarter plane. *J. Combin. Theory Ser. A*, 116(2):460–477, 2009.

[109] M. Mishna and A. Rechnitzer. Two non-holonomic lattice walks in the quarter plane. *Theoret. Comput. Sci.*, 410(38-40):3616–3630, 2009.

[110] M. Mishna and S. Simon. Private communication. 2018.

[111] S. Mustapha. Non-D-Finite Walks in a Three-Quadrant Cone. *Ann. Comb.*, 23(1):143–158, 2019.

[112] M. Picardello and W. Woess. Martin boundaries of Cartesian products of Markov chains. *Nagoya Math. J.*, 128:153–169, 1992.

[113] K. Raschel. Counting walks in a quadrant: a unified approach via boundary value problems. *J. Eur. Math. Soc. (JEMS)*, 14(3):749–777, 2012.

[114] K. Raschel. Random walks in the quarter plane, discrete harmonic functions and conformal mappings. *Stochastic Process. Appl.*, 124(10):3147–3178, 2014. With an appendix by S. Franceschi.

[115] K. Raschel and A. Trotignon. On walks avoiding a quadrant. *Electronic Journal of Combinatorics*, 26(P3.31):1–34, 2019.

[116] J. Ratzkin and A. Treibergs. A capture problem in Brownian motion and eigenvalues of spherical domains. *Trans. Amer. Math. Soc.*, 361(1):391–405, 2009.

[117] J. Ratzkin and A. Treibergs. A Payne-Weinberger eigenvalue estimate for wedge domains on spheres. *Proc. Amer. Math. Soc.*, 137(7):2299–2309, 2009.

[118] H. A. Schwarz. Ueber diejenigen Fälle, in welchen die Gaussische hypergeometrische Reihe eine algebraische Function ihres vierten Elementes darstellt. *J. Reine Angew. Math.*, 75:292–335, 1873.

[119] S. Smirnov. Conformal invariance in random cluster models. I. Holomorphic fermions in the Ising model. *Ann. of Math. (2)*, 172(2):1435–1467, 2010.

[120] R. Stanley. *Enumerative combinatorics. Vol. 1*, volume 49 of *Cambridge Studies in Advanced Mathematics*. Cambridge University Press, Cambridge, 1997. With a foreword by Gian-Carlo Rota, Corrected reprint of the 1986 original.

[121] R. Stanley. *Enumerative combinatorics. Vol. 2*, volume 62 of *Cambridge Studies in Advanced Mathematics*. Cambridge University Press, Cambridge, 1999. With a foreword by Gian-Carlo Rota and appendix 1 by Sergey Fomin.

[122] A. Trotignon. Discrete harmonic functions in the three-quarter plane. *arXiv*, 1906.08082:1–26, 2019.

[123] W. Tutte. Chromatic sums revisited. *Aequationes Math.*, 50(1-2):95–134, 1995.

[124] H. Walden. Solution of an eigenvalue problem for the laplace operator on a spherical surface. *Document No. X-582-74-41, NASA/Goddard Space Flight Center*, 1974.

[125] H. Walden and R. B. Kellogg. Numerical determination of the fundamental eigenvalue for the Laplace operator on a spherical domain. *J. Engrg. Math.*, 11(4):299–318, 1977.

[126] W. Woess. *Random walks on infinite graphs and groups*, volume 138 of *Cambridge Tracts in Mathematics*. Cambridge University Press, Cambridge, 2000.

[127] R. Xu, N. R. Beaton, and A. L. Owczarek. Quarter-plane lattice paths with interacting boundaries: Kreweras and friends. In *Proceedings of FPSAC 2019*, pages 1–12, 2019. (to appear).

[128] R. Yatchak. Automated positive part extraction for lattice path generating functions in the octant. *Proceedings of EUROCOMB 2017, Electronic Notes in Discrete Mathematics*, 61:1061–1067, 2017.

Index